



ExxonMobil Canada Ltd Flemish Pass Exploratory Drilling Operations

Soundscape Characterization, Marine Mammal Occurrence, and Potential Effects of Underwater Noise Emissions on Cetaceans

Submitted to:

Kevin Baldwin

Wood PLC

Contract: TA1978314-005

Authors:

Julien, J-Y. Delarue

Colleen C. Wilson

Katie Kowarski

Carmen Lawrence

S. Bruce Martin

2 May 2021

P001503-001

Document 02151

Version 3.1

JASCO Applied Sciences (Canada) Ltd

Suite 202, 32 Troop Ave.

Dartmouth, NS B3B 1Z1 Canada

Tel: +1-902-405-3336

Fax: +1-902-405-3337

www.jasco.com



Suggested citation:

Delarue, J. J-Y., C.C. Wilson, Kowarski, K., Lawrence, C, and S.B Martin. 2021. *ExxonMobil Canada Ltd Flemish Pass Exploratory Drilling Operations: Soundscape Characterization, Marine Mammal Occurrence, and Potential Effects of Underwater Noise Emissions on Cetaceans*. Document 02151, Version 3.1. Technical report by JASCO Applied Sciences for Wood PLC.

Disclaimer:

The results presented herein are relevant within the specific context described in this report. They could be misinterpreted if not considered in the light of all the information contained in this report. Accordingly, if information from this report is used in documents released to the public or to regulatory bodies, such documents must clearly cite the original report, which shall be made readily available to the recipients in integral and unedited form.

Contents

EXECUTIVE SUMMARY	1
1. INTRODUCTION	3
1.1. Program Overview and Contextual Information	3
1.2. Marine Mammal Acoustic Monitoring	5
1.3. Ambient Ocean Soundscape	9
1.4. Anthropogenic Contributors to the Soundscape	10
2. METHODS.....	11
2.1. Acoustic Data Acquisition.....	11
2.2. Automated Data Analysis.....	13
2.2.1. Total Ocean Sound Levels.....	13
2.2.2. Vessel Noise Detection	15
2.2.3. Seismic Survey Event Detection	16
2.3. Detection Range Modelling.....	16
2.4. Available Listening Range.....	18
2.5. Computing MODU Underwater Radiated Noise	19
2.6. Marine Mammal Detection Overview	20
2.6.1. Odontocete Click Detection	20
2.6.2. Tonal Signal Detection	22
2.6.3. Automated Detector Validation	23
3. RESULTS.....	24
3.1. Soundscape Characterization	24
3.2. Detection Range Modelling	31
3.3. MODU Underwater Radiated Noise	44
3.4. Marine Mammal Detections	45
3.4.1. Detector Performance	45
3.4.2. Blue Whales	48
3.4.3. Fin Whales	50
3.4.4. Sei Whales	52
3.4.5. Humpback Whales	54
3.4.6. Killer Whales	55
3.4.7. Pilot Whales	56
3.4.8. Delphinids	58
3.4.9. Sperm Whales.....	62
3.4.10. Harbour Porpoises	64
3.4.11. Northern Bottlenose Whales	65
3.4.12. Sowerby's Beaked Whales	67
3.4.13. Cuvier's Beaked Whales	69
4. DISCUSSION AND CONCLUSION	71
4.1. Dependence of measured sound levels on wind conditions.....	71
4.2. Comparison of Median Power Spectral Densities	73
4.3. Measuring MODU Underwater Radiated Noise with Fixed Recorders	74

4.4. Marine Mammal Occurrence..... 76

4.5. Effects of underwater noise on Marine Mammals..... 78

 4.5.1. Comparisons to Regulatory Thresholds and Environmental Assessment Assumptions..... 78

 4.5.2. Available Listening Range 80

4.6. Conclusion..... 82

GLOSSARY 84

LITERATURE CITED 89

APPENDIX A. SOUND LEVEL TERMINOLOGY.....A-1

APPENDIX B. MARINE MAMMAL AUDITORY FREQUENCY WEIGHTINGB-1

APPENDIX C. DETECTION RANGE MODELLING C-1

APPENDIX D. MARINE MAMMAL DETECTION METHODS D-1

Figures

Figure 1. Overview of the project area, existing acoustic data sets and acoustic monitoring locations.	5
Figure 2. Wenz curves	9
Figure 3. Vessel traffic off the coast of Newfoundland in 2017.....	10
Figure 4. Mooring design used at each of the four stations.....	12
Figure 5. Wind speeds measured at Harp (EL 1165B) well site.....	13
Figure 6. Significant wave height measured at the Harp (EL 1165B) well site.....	14
Figure 7. Example of broadband and 40–315 Hz band sound pressure level (SPL), as well as the number of tonals detected per minute as a vessel approached a recorder, stopped, and then departed.....	16
Figure 8. (Top) In-band sound pressure level (SPL) and (bottom) spectrogram (or long-term spectral average; LTSA) of underwater sound for each station.....	24
Figure 9. Percentiles and mean of decidecade sound pressure level (SPL) and exceedance percentiles and probability density (grayscale) of 1-min power spectral density levels	25
Figure 10. Auditory Frequency Weighted as well as 10 Hz and above daily sound exposure levels (SEL) for each station	26
Figure 11. Annotated summary of the sound levels measured at (A) Harp (EL 1165B) and (B) Hampden (EL 1165A) from September 2019 to May 2020.....	28
Figure 12. Ten seconds of data from 24 Oct 2019 at Harp (EL 1165B) showing the presumed pulses from the ultra-short-baseline (USBL) system as well as a series of echolocation clicks from a sperm whale.....	29
Figure 13. Comparison of the spectra measured at Harp (EL 1165B) (A) without and (B) with the MODU present.....	30
Figure 14. Five seconds of data from the Hampden (EL 1165A) site during seismic surveying.....	30
Figure 15. Blue whale infrasonic A-B calls: Detection ranges associated with various probability of detection under noise conditions recorded in March at Hampden (EL 1165A) (top left), Harp (EL 1165B) (top right), Mid (bottom left) and Stn 19 (bottom right), shown at the centre of each figure.	33
Figure 16. Fin whale 20-Hz calls: Detection ranges associated with various probability of detection under noise conditions recorded in March at Hampden (EL 1165A) (top left), Harp (EL 1165B) (top right), Mid (bottom left) and Stn 19 (bottom right), shown at the centre of each figure.....	34
Figure 17. Sei whale downsweeps: Detection ranges associated with various probability of detection under noise conditions recorded in March at Hampden (EL 1165A) (top left), Harp (EL 1165B) (top right), Mid (bottom left) and Stn 19 (bottom right), shown at the centre of each figure.....	35
Figure 18. Humpback whale song unit: Detection ranges associated with various probability of detection under noise conditions recorded in March at Hampden (EL 1165A) (top left), Harp (EL 1165B) (top right), Mid (bottom left) and Stn 19 (bottom right), shown at the centre of each figure.	36
Figure 19. Killer whale tonal calls: Detection ranges associated with various probability of detection under noise conditions recorded in March at Hampden (EL 1165A) (top left), Harp (EL 1165B) (top right), Mid (bottom left) and Stn 19 (bottom right), shown at the centre of each figure.....	37
Figure 20. Dolphin whistles: Detection ranges associated with various probability of detection under noise conditions recorded in March at Hampden (EL 1165A) (top left), Harp (EL 1165B) (top right), Mid (bottom left) and Stn 19 (bottom right), shown at the centre of each figure.....	38
Figure 21. Delphinid clicks: Detection ranges associated with various probability of detection under noise conditions recorded in March at Hampden (EL 1165A) (top left), Harp (EL 1165B) (top right), Mid (bottom left) and Stn 19 (bottom right), shown at the centre of each figure.....	39
Figure 22. Sperm whale clicks: Detection ranges associated with various probability of detection under noise conditions recorded in March at Hampden (EL 1165A) (top left), Harp (EL 1165B) (top right), Mid (bottom left) and Stn 19 (bottom right), shown at the centre of each figure.....	40

Figure 23. Harbour porpoise clicks: Detection ranges associated with various probability of detection under noise conditions recorded in March at Harp (EL 1165B) (left) and Mid (right). 41

Figure 24. Northern bottlenose whale clicks: Detection ranges associated with various probability of detection under noise conditions recorded in March at Hampden (EL 1165A) (top left), Harp (EL 1165B) (top right), Mid (bottom left) and Stn 19 (bottom right), shown at the centre of each figure. 42

Figure 25. Sowerby’s beaked whale clicks: Detection ranges associated with various probability of detection under noise conditions recorded in March at Hampden (EL 1165A) (top left), Harp (EL 1165B) (top right), Mid (bottom left) and Stn 19 (bottom right), shown at the centre of each figure. 43

Figure 26. Computing the West Aquarius (WAQ) Source Factor: (A) modeled sound propagation loss for October 2019 to February 2020; (B) distribution of received SPL at Harp (EL 1165B); and (C) sum of (A) and (B) to obtain the distribution of the source factor. 44

Figure 27. Spectrogram of blue whale arch calls recorded at Hampden (EL 1165A) on 13 Sep 2019..... 48

Figure 28. Spectrogram of blue whale infrasonic A-B vocalizations recorded at Stn 19 on 18 Sep 2019 48

Figure 29. Daily and hourly occurrence of automatically and manually detected blue whale song notes. 49

Figure 30. Spectrogram showing fin whale 20-Hz and the 130-Hz song notes recorded at Hampden (EL 1165A) on 30 Nov 2019 50

Figure 31. Daily and hourly occurrence of automatically and manually detected fin whale 20-Hz calls. ... 51

Figure 32. Spectrogram of a sei whale paired downsweep recorded at Mid on 8 Nov 2019 52

Figure 33. Daily and hourly occurrence of automatically and manually detected sei whale downsweeps. 53

Figure 34. Spectrogram of humpback whale vocalizations (song) recorded at Stn 19 on 16 Jan 2020 54

Figure 35. Daily and hourly occurrence of automatically and manually detected humpback whale song notes. 54

Figure 36. Spectrogram showing killer whale vocalizations recorded at Mid on 4 Mar 2020 55

Figure 37. Spectrogram showing pilot whale vocalizations recorded at Hampden (EL 1165A) on 17 Apr 2020..... 56

Figure 38. Daily and hourly occurrence of automatically and manually detected pilot whale tonal calls. 57

Figure 39. Spectrogram showing unidentified dolphin whistles recorded at Hampden (EL 1165A) on 18 Oct 2019 58

Figure 40. Spectrogram of unidentified delphinid click trains recorded at Hampden (EL 1165A) on 21 Sep 2019..... 58

Figure 41. Spectrogram of unidentified dolphin click recorded at Stn 19 on 7 Feb 2020 59

Figure 42. Daily and hourly occurrence of automatically and manually detected dolphin whistles. 60

Figure 43. Daily and hourly occurrence of automatically and manually detected delphinid clicks. 61

Figure 44. Spectrogram showing sperm whale clicks recorded at Mid on 19 Nov 2019 62

Figure 45. Daily and hourly occurrence of automatically and manually detected sperm whale. 63

Figure 46. Spectrogram of harbour porpoise clicks recorded at Mid on 28 Jan 2020 64

Figure 47. Spectrogram of a harbour porpoise click recorded at Harp (EL 1165B) on 5 Sep 2019..... 64

Figure 48. Daily and hourly occurrence of automatically and manually detected harbour porpoise clicks. 65

Figure 49. Spectrogram of northern bottlenose whale clicks recorded at Stn 19 on 17 Jan 2020 66

Figure 50. Spectrogram of a northern bottlenose whale click recorded at Stn 19 on 14 Sep 2019 66

Figure 51. Daily and hourly occurrence of automatically and manually detected northern bottlenose whale clicks. 67

Figure 52. Spectrogram of Sowerby’s beaked whale clicks recorded at Hampden (EL 1165A) on 9 Mar 2020..... 68

Figure 53. Spectrogram of a Sowerby’s beaked whale click recorded at Mid on 19 Nov 2019 68

Figure 54. Daily and hourly occurrence of automatically and manually detected Sowerby’s beaked whale clicks..... 68

Figure 55. Spectrogram of Cuvier’s beaked whale clicks recorded at Stn 19 on 6 Feb 2020 (64 Hz frequency resolution, 0.01 s time window, 0.005 s time step, Hamming window). The window length is 15 seconds. 69

Figure 56. Spectrogram of a Cuvier’s beaked whale click recorded at Stn 19 on 6 Feb 2020 (512 Hz frequency resolution, 0.266 ms time window, 0.02 ms time step). 70

Figure 57. Weekly correlation coefficient between decidecade bands at 20, 80, 630, and 3150 Hz and wind speeds measured at Harp (EL 1165B) well site..... 72

Figure 58. Comparison of the median power spectral densities in six conditions: the full duration at the Mid and Stn 19 recorders as well as the Harp (EL 1165B) and Hampden (EL 1165A) sites with the MODU nearby and for time without the MODU..... 73

Figure 59. Recommended geometry for making underwater radiated noise measurements..... 74

Figure 60. Summary of the underwater radiated noise (URN) of the West Aquarius Mobile Offshore Drilling Unit (MODU) measured at (A) Hampden (EL 1165A) and (B) Harp (EL 1165B). 76

Figure 61. Comparison of the median underwater radiated noise (URN) computed from 10 days of data at Hampden (EL 1165A) and 5 months of data at Harp (EL 1165B). Since there were large amounts of data to work with at Harp (EL 1165B), the months with uninterrupted data (Oct 19 – Feb 20, inclusive) were chosen for this analysis. 76

Figure 62. Detection count per km² by month as a function of distance from the MODU for blue (left) and fin (right) whales. The detection area was calculated as a circular area around each recorder with a radius equal to the minimum detection ranges across all modelled azimuths for a 50% probability of detection under median noise conditions for average source levels (see Table 7). The September detection ranges were used for September. The March detection ranges were used for all other months. There were not enough detections after February to include in this figure. The dots represents measurements at (from left to right) Harp, Mid and Hampden..... 77

Figure 63. Comparison of the estimated daily sound exposure levels for the full spectrum (10 Hz and above) as well as weighted for each of the NMFS (2018) marine mammal hearing groups..... 79

Figure 64. Comparison of broadband (10-16000 Hz) SPL for Oct 2019 - Feb 2020 as measured by the recorders at the seabed. The gray shape in the background is the prediction interval for the SPL as a function of range. The dark blue line shows the maximum range to the sound levels for an FPSO and support vessel in winter from Zykov (2016). The light blue line are the maximum range to the sound levels for the MODU and support vessel at a shallow water site near Harp from Zykov (2018). 80

Figure 65. Available Listening Range for low-frequency cetaceans..... 81

Figure 66. Available Listening Range for mid-frequency cetaceans. 82

Figure A-1. Decidecade frequency bands (vertical lines) shown on a linear frequency scale and a logarithmic scale.A-3

Figure A-2. A power spectrum and the corresponding decidecade sound pressure levels of example ambient noise shown on a logarithmic frequency scale.A-4

Figure B-1. Auditory weighting functions for the functional marine mammal hearing groups as recommended by NMFS (2018).B-2

Figure C-1. The N×2-D and maximum-over-depth modelling approach used by MONM. C-1

Figure C-2. The sound speed profiles for March (left) and September (right) at Hampden (EL 1165A).. C-4

Figure D-1. The click detector/classifier block diagram. D-2

Figure D-2. The click train detector/classifier block diagram. D-3

Figure D-3. Illustration of the search area used to connect spectrogram bins. D-4
 Figure D-4. Divergence curves for Hampden (EL 1165A), 32 kHz data (top) and 512 kHz data (bottom)..... D-8
 Figure D-5. Divergence curves for Harp (EL 1165B), 32 kHz data (top) and 512 kHz data (bottom). D-9
 Figure D-6. Divergence curves for Mid, 32 kHz data (top) and 512 kHz data (bottom)..... D-10
 Figure D-7. Divergence curves for Stn 19, 32 kHz data (top) and 512 kHz data (bottom). D-11

Tables

Table 1. List of cetacean and pinniped species known to occur (or possibly occurring) in the study area 7
 Table 2. Acoustic signals used for identification and automated detection of the species expected in the study area and supporting references. 8
 Table 3. Operation period, location, and depth of the Autonomous Multichannel Acoustic Recorders..... 11
 Table 4. Decade bands analyzed for the Available Listening Range..... 19
 Table 5. List of automated detectors used to identify clicks produced by odontocetes..... 21
 Table 6. List of automated detectors used to identify tonal signals produced by baleen whales and delphinids. 22
 Table 7. Detection ranges (kilometers) for species and signals most likely to be encountered near the four monitored stations and for background noise conditions recorded in March and September at each station..... 32
 Table 8. Hampden (EL 1165A): Detector performance metrics for all detectors with Precision >0.75. 45
 Table 9. Harp (EL 1165B): Detector performance metrics for all detectors with Precision >0.75. 46
 Table 10. Mid: Detector performance metrics for all detectors with Precision >0.75. 46
 Table 11. Stn 19: Detector performance metrics for all detectors with Precision >0.75..... 47
 Table 12. Blue whales: Percent days with detections (manual or automated) and number of automated detections by month at Hampden (EL 1165A), Harp (EL 1165B), Mid and Stn 19. 49
 Table 13. Fin whales: Percent days with detections (manual or automated) and number of automated detections by month at Hampden (EL 1165A), Harp (EL 1165B), Mid and Stn 19. 52
 Table 14. Sei whales: Percent days with detections (manual or automated) and number of automated detections by month at Hampden (EL 1165A), Harp (EL 1165B), Mid and Stn 19. 53
 Table 15. Humpback whales: Percent days with detections (manual or automated) and number of automated detections by month at Hampden (EL 1165A), Mid and Stn 19. 55
 Table 16. Pilot whale: Percent days with detections (manual or automated) and number of automated detections by month at Hampden (EL 1165A), Harp (EL 1165B), Mid and Stn 19. 57
 Table 17. Dolphin whistles: Percent days with detections (manual or automated) and number of automated detections by month at Hampden (EL 1165A), Harp (EL 1165B), Mid and Stn 19. 60
 Table 18. Delphinid clicks: Percent days with detections (manual or automated) and number of automated detections by month at Hampden (EL 1165A), Harp (EL 1165B), Mid and Stn 19. 61
 Table 19. Sperm whale: Percent days with detections (manual or automated) and number of automated detections by month at Hampden (EL 1165A), Mid and Stn 19. 63
 Table 20. Harbour porpoises: Percent days with detections (manual or automated) and number of automated detections by month at Harp (EL 1165B) and Mid..... 65
 Table 21. Northern bottlenose whales: Percent days with detections (manual or automated) and number of automated detections by month at Hampden (EL 1165A), Mid and Stn 19..... 67
 Table 22. Sowerby’s beaked whales: Percent days with detections (manual or automated) and number of automated detections by month at Hampden (EL 1165A). 69

Table 23. Geacoustic parameters for the transmission loss modelling at the shallow station (Harp (EL 1165B)). C-5

Table 24. Geacoustic parameters for the transmission loss modelling at the deep stations (Hampden (EL 1165A), Mid and Stn 19). C-5

Table A-1. Deciddecade band frequencies (Hz).A-4

Table A-2. Decade-band frequencies (Hz).A-5

Table B-1. Parameters for the auditory weighting functions recommended by NMFS (2018) and Temporary Threshold Shift (TTS) onset thresholds.B-1

Table C-1. Marine mammal input parameters. The detection threshold refers to the threshold of the relevant detectors. C-2

Table C-2. Detection ranges associated with three ambient noise percentile and three probability of detection (Pd) at Stn 19 in March. C-6

Table C-3. Detection ranges associated with three ambient noise percentile and three probability of detection (Pd) at Stn 19 in September..... C-7

Table C-4. Detection ranges associated with three ambient noise percentile and three probability of detection (Pd) at Hampden (EL 1165A) in March..... C-8

Table C-5. Detection ranges associated with three ambient noise percentile and three probability of detection (Pd) at Hampden (EL 1165A) in September. C-9

Table C-6. Detection ranges associated with three ambient noise percentile and three probability of detection (Pd) at Harp (EL 1165B) in March. ND: not detectable..... C-10

Table C-7. Detection ranges associated with three ambient noise percentile and three probability of detection (Pd) at Harp (EL 1165B) in September. ND: not detectable. C-11

Table C-8. Detection ranges associated with three ambient noise percentile and three probability of detection (Pd) at Mid in March. ND: not detectable. C-12

Table C-9. Detection ranges associated with three ambient noise percentile and three probability of detection (Pd) at Mid in September. ND: not detectable. C-13

Table D-1. Fast Fourier Transform (FFT) and detection window settings for all contour-based detectors used to detect tonal vocalizations of marine mammal species expected in the data. D-4

Table D-2. A sample of vocalization sorter definitions for the tonal vocalizations of cetacean species expected in the area. N/A: Not applicable. D-5

Executive Summary

ExxonMobil Canada Ltd (EMCL) conducted exploratory drilling operations in or near the Flemish Pass to look for oil and gas at the Harp (EL 1165B, formerly EL 1135) and Hampden (EL 1165A, , formerly EL 1134) sites from October 2019 to May 2020. Wood PLC (Wood) contracted JASCO Applied Sciences to perform an acoustic monitoring program as part of the overall environmental effects monitoring program. To satisfy the conditions of the Environmental Assessment Decision Statement, EMCL was required to “verify the accuracy of the Environmental Assessment as it pertains to underwater noise levels” (Section 3.12.3). The main objective of the acoustic monitoring was therefore to characterize the sounds produced by a Mobile Offshore Drilling Unit (MODU) and to provide insight into the effects of its sound emissions on marine life, particularly how the measured distances to sound levels associated with temporary hearing threshold shift compared to the distances in the EA. EMCL also wanted to understand the effectiveness of using bottom-mounted recorders for performing sound source characterizations (SSC) of stationary sound sources. Four acoustic recorders were deployed: two near the Harp (EL 1165B) and Hampden (EL 1165A) sites, one near the midpoint between the two well sites and one on the Sackville Spur at a site where baseline marine mammal occurrence data exist from a previous study.

The presence of the MODU had a significant impact on the surrounding soundscape. The total daily sound exposure levels in 300 m of water at a 2 km distance from the MODU (Harp (EL 1165B)) were 25–30 dB higher when the MODU was present compared to when it was absent. The levels were ~20 dB higher 5 km from the MODU in water 1175 m deep (Hampden (EL 1165A)). The presence of the MODU increased the power spectral density by ~25 dB at 100 Hz, 15–20 dB at 1000 Hz, 10 dB at 10000 Hz, and 20 dB at 27000 Hz. Broadband (10 Hz – 200 kHz) levels measured at 2 km (Harp) and 5 km (Hamden) from the MODU were ~ 20 dB and ~ 17 dB higher, respectively, compared to baseline levels. These increases are generally consistent with previous measurements in the Flemish Pass where the increase in broadband sound levels measured 13 km from a MODU was 13 dB (Maxner et al. 2017). The MODU underwater radiated noise was computed using the Harp (EL 1165B) data. The median broadband source factor was 191.2 dB re 1 $\mu\text{Pa}^2\cdot\text{m}^2$. The maximum decade was the 200 Hz band, which had a median source factor of 183.4 dB re 1 $\mu\text{Pa}^2\cdot\text{m}^2$. Acoustic modelling conducted for the deep (>2000 m) Scotian Basin Exploration Drilling Project conservatively assumed broadband source levels for a drillship and semi-submersible to be approximately 197 dB re 1 μPa @ 1 m RMS SPL (Zykov 2016).

The Environmental Assessment considered the potential of EMCL’s exploratory drilling activities to illicit underwater noise effects on marine mammals based on studies by Zykov (2016) and Quijano et al. (2017). Zykov (2016) modelled sound levels associated with several oil and gas activities, including an operating semi-submersible platform such as that used in this study, in deep water off the Scotian Shelf. Quijano et al. (2017) provided a qualitative assessment on the applicability of the Zykov (2016) modelled ranges to various sound level thresholds based on environmental conditions in the Flemish Pass. They concluded that for shallow sites, such as Harp (EL 1165B), distances to thresholds corresponding to high levels (e.g., sound pressure level (SPL) thresholds of 180–190 dB re 1 μPa) could be longer than those modelled for the Scotian Basin Exploration Drilling Project. The opposite would be expected for lower sound level thresholds (e.g., SPL of 120 dB re 1 μPa), which should yield shorter ranges. Due to similarities in source levels, seabed geoacoustics, and sound speed profiles, Quijano et al. (2017) indicated that the Zykov (2016) results provided a good reference for the expected sound levels at deep sites of the current Project (e.g. Hampden (EL1165A), 1175 m deep). Therefore, distances to thresholds for scenarios involving a drillship/semisubmersible platform with or without a supporting vessel were predicted to be similar to those for the Scotian Basin modelling sites. The 120 dB re 1 μPa SPL threshold was expected to be reached at maximum distances $R_{\text{max}} > 150$ km in winter and $R_{\text{max}} \sim 51.6$ km in summer. The long winter propagation ranges were not observed in this study, and propagation in general may have only, at best, approached the summer ranges in Zykov (2016).

In a more recent modelling study involving sites close to those monitored in this program, Zykov (2018) estimated ranges to sound level thresholds for a drillship whose source level was comparable to that of the MODU used in this drilling program. The ranges to various SPL isopleths were about five times shorter than in the Scotian Shelf study (Zykov 2016). In the study described in this report, sound levels from the MODU measured in 875 m of water about 30 km away (Mid) showed that SPL in the 100-1000

Hz band increased by ~ 9 dB when the MODU was present and reached ~ 112-115 dB re 1 μ Pa. In comparison, Zykov (2018) estimated that SPL would remain above 120 dB within 10.5-34 km from the drill ship, depending on the season. These modeling results are more consistent with the measured levels presented here, particularly considering that near-bottom sound levels presented here are expected to be lower than the maximum-over-depth levels presented in the modeling studies.

Marine mammal occurrence at the Sackville Spur in 2019-2020, where the acoustic signature of the MODU at Harp (EL 1165B) was not detected, was remarkably consistent with the patterns observed at the same location in 2016-2017 for all species. Acoustic detections of blue whale, fin whales, delphinids and harbour porpoises at Harp (EL 1165B) declined noticeably after the arrival of the MODU. A period of increased detections from mid-December to February for all these species but blue whales suggests that their signals were detectable in the presence of the MODU and that the initial drop in detections may have been caused by avoidance of the area, rather than masking. Habituation to the MODU's acoustic signature, which may have initially induced a change in acoustic behavior (i.e. reduced, or cessation of, calling) could also explain this detection period although the synchronized reappearance of several species suggests that environmental factors may rather be at play in this case. At Hampden, acoustic detections generally showed no change in occurrence in response to the presence of the MODU, except for pilot whales whose detections decreased substantially after its arrival and resumed just after its departure. There was no evidence of changes in distribution after the arrival of the MODU at Harp beyond 32 km since no changes in acoustic occurrence were observed at Mid and Hampden.

Smaller-scale displacements may have occurred in species with high hearing sensitivity in the frequency bands where most of the MODU's acoustic emissions are concentrated to mitigate the effects of extended noise exposures on their auditory organs ([NMFS] National Marine Fisheries Service (US) 2018). Indeed, sound levels emitted by the West Aquarius MODU at Harp (EL 1165B) and recorded 2 km away from the MODU exceeded the threshold for the onset of temporary threshold shift for continuous sound sources in low-frequency cetaceans (baleen whales) on 159 days out of 229 days of operations. TTS thresholds for high-frequency cetaceans (e.g. harbour porpoises) were also exceeded on 89 days. Temporary threshold shifts (TTS) represents a temporary loss of hearing sensitivity. These results are consistent with those from Zykov (2018), who showed that the threshold for the onset of temporary threshold shift could be exceeded at a distance of up to 3.25 km from a drillship in baleen whale and 5.9 km in high-frequency cetaceans. Both the measured and modelled results assume that an animal remained at the threshold distance for a full 24 hours. An animal that passes closer than this distance will have a more rapid onset of TTS. An animal that exhibits aversion behavior, as would be expected, and leaves the area when sound exceeds the TTS accumulation threshold will not suffer TTS.

Other effects of noise in the study area included a reduction of the available listening range for all species analyzed. The effects were most prominent for the low-frequency cetaceans where the available listening range estimated 2 km from the MODU was reduced to less than 5% of the best case when the MODU was present. Fin whale choruses also had the ability to significantly reduce their available listening range.

1. Introduction

1.1. Program Overview and Contextual Information

ExxonMobil Canada Ltd (EMCL) conducted exploratory drilling operations in or and near the Flemish Pass to look for oil and gas at the Harp (EL 1165B, formerly EL 1135) and Hampden (EL 1165A, formerly EL 1134) sites from October 2019 to May 2020 (Figure 1). The Harp (EL 1165B) well was drilled from October 2019 to April 2020, and then surface drilling at the Hampden (EL 1165A) well was performed in May 2020. Concerns surrounding the potential effects of sound on marine life were noted in the Environmental Assessment Report published by the Canadian Environmental Assessment Agency on 15 Apr 2019. The study area is known to be used by many marine mammal species including noise-sensitive beaked whales, such as northern bottlenose (Davis Strait-Baffin Bay-Labrador Sea population) and Sowerby's beaked whales, as well as endangered blue (Atlantic population) and sei (Atlantic population) whales (Delarue et al. 2018) (Table 1). High levels of sound have been associated with hearing injury (Southall et al. 2019b), displacement of marine mammals (Richardson et al. 1990, Richardson et al. 1999), and masking of mammal communications (Hatch et al. 2012, Erbe et al. 2016, Pine et al. 2018, Southall et al. 2019a).

Wood PLC (Wood) contracted JASCO Applied Sciences to perform an acoustic monitoring program as part of the overall environmental effects monitoring program. The objective of the acoustic monitoring was to characterize the sounds produced by a Mobile Offshore Drilling Unit (MODU) and to provide insight into the effects of its sound on marine life including auditory injury as well as possible displacement and masking of communications. In order to satisfy the conditions of the Environmental Assessment, EMCL was required to “verify the accuracy of the Environmental Assessment as it pertains to underwater noise levels” (section 3.12.3). EMCL also wanted to understand the effectiveness of using bottom-mounted recorders for performing sound source characterizations (SSC) of stationary sound sources, as they may wish to perform an SSC on subsurface pressurization systems in the future.

The Environmental Assessment considered the potential of EMCL's exploratory drilling activities to illicit underwater noise effects on marine mammals based on studies by Zykov (2016) and Quijano et al. (2017). Zykov (2016) modelled sound levels associated with several oil and gas activities, including an operating semi-submersible platform such as the one used in this study, in deep water off the Scotian Shelf. Quijano et al. (2017) provided a qualitative assessment on the applicability of the Zykov (2016) modelled ranges to various sound level thresholds based on environmental conditions in the Flemish Pass. They concluded that at shallow sites, such as Harp (EL 1165B), the distances to thresholds corresponding to high levels (e.g., sound pressure level (SPL) thresholds of 180–190 dB re 1 μ Pa) could be longer than those modelled for the Scotian Basin Exploration Drilling Project. Shorter ranges than the Scotian Shelf results would be expected for lower sound level thresholds (e.g., SPL of 120 dB re 1 μ Pa). Due to similarities in source levels, seabed geoacoustics, and sound speed profiles, Quijano et al. (2017) indicated that the Zykov (2016) results provided a good reference for the expected sound levels at deep sites of the current Project (e.g. Hampden, 1175 m). Therefore, distances to thresholds for scenarios involving a drillship/semisubmersible platform with or without a supporting vessel should be similar to those for the Scotian Basin modelling sites. The 120 dB re 1 μ Pa SPL threshold was expected to be reached at maximum distances $R_{\max} > 150$ km in winter and $R_{\max} \sim 51.6$ km in summer. We note that while the 120 dB re 1 μ Pa isopleth is based on older research (Malme et al. 1983, Malme et al. 1984, Malme et al. 1986), it remains in use as a regulatory threshold ([NOAA] National Oceanic and Atmospheric Administration (US) 2019) or as an indicative threshold for suitable marine mammal habitat (DFO 2012).

Baseline information on the soundscape along the eastern Grand Banks and Flemish Pass is available from acoustic monitoring programs conducted by JASCO (Figure 1). Equinor (Statoil) previously collected data in the region in 2014 and 2015 during a drilling campaign north of the current project site (CM2 in Figure 1; (Maxner et al. 2017)). JASCO collected data throughout Canada's east coast in 2015–2017 under an Environmental Studies Research Fund (ESRF) collaborative agreement. ESRF stations 17, 7, 18, and 19 provide near-continuous acoustic data in the project area (Figure 1). The project reported on the soundscape and marine mammal acoustic occurrence across the region (Delarue et al. 2018). The

nearest site to the current program is ESRF Stn 19 from 2016–2017 (Figure 1), located 102 km from Harp (EL 1165B) and 156 km from Hampden (EL 1165A) drill sites. Data from this station can be considered representative of the soundscape expected at the drill sites for ambient sound levels as well as marine mammal presence for some species. The current project includes a deployment at ESRF Station 19 (hereafter called Stn 19) for comparison of the soundscape and mammal presence with the drilling program compared to the pre-drilling period (Figure 1).

The drilling period spanned the full range of propagation conditions in the project area: summer through fall, and then winter and into spring. JASCO's ESRF project performed acoustic propagation modelling of the footprint from seismic surveys at the ESRF monitoring sites (Deveau 2018), which were drawn upon to inform the expected sound propagation. During summer, a layer of warmer water near the surface is expected to refract sound toward the seabed, whereas in winter the sound is expected to be trapped near the surface. This could induce a seasonal change in sound levels at the seabed that is the opposite of the change that will occur near the surface.

The drilling program employed the West Aquarius MODU, which was previously measured off Nova Scotia for BP in 2300 m of water (Martin et al. 2019a). The results of the BP program suggested that some marine mammals, particularly odontocetes, may have left the area around the MODU. The design of the present program included acoustic recorders 2 km from each well site and near the mid point between the sites. One of the 2km recorders ended up being located 5 km from the MODU (Hampden). The main implication of this change is that the acoustic emissions of the MODU measured at Harp and Hampden are not directly comparable. The lower sound levels measured at Hampden can be explained by its greater distance to the MODU. The distance differential also highlighted the limitations of shallow-water source characterization, with the monopole source level being lower at Harp than Hampden and that source characterization are best performed using data acquired as close to the source as possible. By comparing the changes in marine mammal presence between sites, as well as at ESRF Stn 19, a goal of the program was to provide insight into whether changes in mammal presence are related to the MODU or simply changes in vocalization detectability. The data were also analyzed to examine the differences in listening range for hearing groups of marine mammals present in the project area at each recorder location.

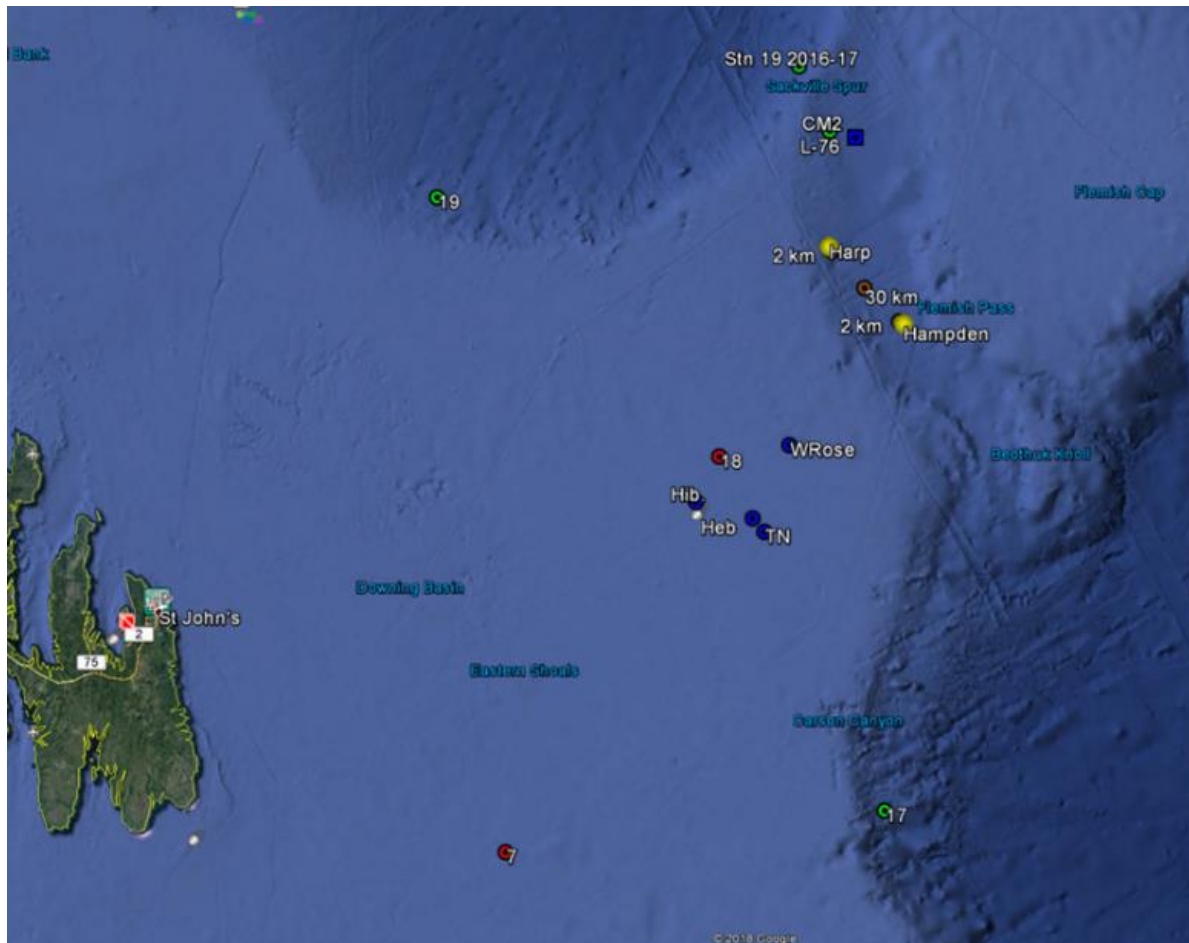


Figure 1. Overview of the project area, existing acoustic data sets and acoustic monitoring locations. White Rose (WRose), Hebron (Heb), Terra Nova (TN) and Hibernia (Hib) are existing production platforms. Baseline acoustic recordings were available from JASCO's ESRF program are 7, 17, 18, and 19 (2016-17), as well as Statoil's existing data collected while West Hercules was drilling in 2015 at well CM2. Harp (EL 1165B) and Hampden (EL 1165A) are the drill sites of this project.

1.2. Marine Mammal Acoustic Monitoring

Passive acoustic monitoring relies on the premise that the monitored species produce detectable sound. While several marine taxa produce sounds (e.g., fish and invertebrates), the biological focus of this study was on marine mammals. Marine mammals can be important contributors to the underwater soundscape. For instance, fin whale songs can raise sound levels in the 18–25 Hz band by 15 dB for extended durations (Simon et al. 2010). Marine mammals, cetaceans in particular, rely almost exclusively on sound for navigating, foraging, breeding, and communicating (Clark 1990, Edds-Walton 1997, Tyack and Clark 2000). Although species differ widely in their vocal behaviour, most can be reasonably expected to produce sounds on a regular basis. Passive acoustic monitoring is therefore increasingly preferred as a cost-effective and efficient survey method. Seasonal and sex- or age-biased differences in sound production, as well as signal frequency, source level, and directionality all influence the applicability of acoustic monitoring, and its effectiveness must be considered separately for each species.

Twenty cetacean and two pinniped species have a reasonable likelihood of being present and acoustically detected in the study area (Table 1). A few other species with very sparse records, if any, in the Flemish Pass area have not been included here (see Environmental Assessment Report for details). Delarue et al. (2018) provided a detailed description of marine mammal species detected acoustically

during a 2-year study in eastern Canadian waters involving 20 stations, including three deployed near the monitoring sites in this study. Delarue et al. (2018) highlighted, among several findings, the importance of the Flemish Pass area for several endangered or threatened baleen whale species as well as the regular presence of several beaked whale species. It also showed that stations deployed at both ends of the Flemish Pass had the highest year-round species diversity among the areas monitored during this study (Delarue et al. 2018). Another study described the acoustic occurrence of marine mammals from late spring to early fall 2014 and 2015 in the northern Flemish Pass (Maxner et al. 2017), finding patterns of acoustic occurrence consistent with those in Delarue et al. (2018).

Knowledge of the acoustic signals of the marine mammals expected in the study area varies across species (Table 2). These sounds can be split into two broad categories: Tonal signals, including baleen whale moans and delphinid (i.e. member of the Delphinidae family; includes all dolphins, killer and pilot whales, etc.) whistles, and echolocation clicks produced by all odontocetes mainly for foraging and navigating (see glossary for definitions of species groups). Although the signals of most species have been described to some extent, these descriptions are not always sufficient for reliable systematic identification, let alone to design automated detectors to process large data sets. For instance, although the whistles of species in the subfamily *Delphininae* (small dolphins) in the area have all been described, the overlap in their spectral characteristics complicates their identification by both analysts and automated detectors (Ding et al. 1995, Gannier et al. 2010). The echolocation clicks of all expected beaked whale species have been described to varying extent making it possible to distinguish these species. In most cases, baleen whale signals can be reliably identified to the species level, although, seasonal variation in the types of vocalizations result in seasonal differences in our ability to detect these species acoustically. For example, the tonal signals produced by blue, fin, and sei whales tend to overlap in late spring and summer but are markedly different from September to April.

Table 1. List of cetacean and pinniped species known to occur (or possibly occurring) in the study area and their Committee on the Status of Endangered Wildlife in Canada (COSEWIC) and Species at Risk Act (SARA) status.

Species	Scientific name	COSEWIC status	SARA status
<i>Baleen whales</i>			
Minke whale	<i>Balaenoptera acutorostrata</i>	Not at risk	Not listed
Sei whale – Atlantic population	<i>Balaenoptera borealis</i>	Endangered	Not Listed
Blue whale – Atlantic population	<i>Balaenoptera musculus</i>	Endangered	Endangered
Fin whale – Atlantic population	<i>Balaenoptera physalus</i>	Special concern	Special concern
Humpback whale – Western North Atlantic population	<i>Megaptera novaeangliae</i>	Not at risk	Not Listed
North Atlantic right whale	<i>Eubalaena glacialis</i>	Endangered	Endangered
<i>Toothed whales</i>			
Short-beaked common dolphin	<i>Delphinus delphis</i>	Not at risk	Not listed
Striped dolphin	<i>Stenella coeruleoalba</i>	Not at risk	Not listed
White-beaked dolphin	<i>Lagenorhynchus albirostris</i>	Not at risk	Not listed
Atlantic white-sided dolphin	<i>Lagenorhynchus acutus</i>	Not at risk	Not listed
Risso’s dolphin	<i>Grampus griseus</i>	Not at risk	Not listed
Killer whale	<i>Orcinus orca</i>	Special concern	Not listed
Long-finned pilot whale	<i>Globicephala melas</i>	Not at risk	Not listed
Harbour porpoise – Northwest Atlantic population	<i>Phocoena phocoena</i>	Special concern	Not listed
Pygmy sperm whale	<i>Kogia breviceps</i>	Not at risk	Not listed
Sperm whale	<i>Physeter macrocephalus</i>	Not at risk	Not listed
Cuvier’s beaked whale	<i>Ziphius cavirostris</i>	Not at risk	Not listed
Sowerby’s beaked whale	<i>Mesoplodon bidens</i>	Special concern	Special concern
Northern bottlenose whale – Scotian shelf population	<i>Hyperoodon ampullatus</i>	Endangered	Endangered
Northern bottlenose whale – Davis Strait-Baffin Bay-Labrador Sea population		Special concern	Special concern
True’s beaked whale	<i>Mesoplodon mirus</i>	Not at risk	Not listed
<i>Pinnipeds</i>			
Hooded seal	<i>Cystophora cristata</i>	Not at risk	Not listed
Harp seal	<i>Phoca groenlandica</i>	Not at risk	Not listed

Table 2. Acoustic signals used for identification and automated detection of the species expected in the study area and supporting references. 'NA' indicates that no automated detector was available for a species.

Species	Identification signal	Automated detection signal	Reference
Minke whale	Pulse train	NA	Risch et al. (2013)
Sei whales	Tonal downsweep	Tonal downsweep	Baumgartner et al. (2008)
Blue whale	A-B vocalization, tonal downsweep	A-B vocalization	Mellinger and Clark (2003), Berchok et al. (2006)
Fin whale	20-Hz pulse, tonal downsweep	20-Hz pulse	Watkins (1981), Watkins et al. (1987)
Humpback whale	Moan, grunt	Moan	Dunlop et al. (2008), Kowarski et al. (2018)
North Atlantic right whale	Tonal upsweep, gunshot	Upsweep	Parks et al. (2005), Parks and Tyack (2005)
Small dolphins ¹	Whistle	Whistle >6 kHz	Steiner (1981), Rendell et al. (1999), Oswald et al. (2003)
Killer whale	Whistle, pulsed vocalization	Tonal signal <6 kHz	Ford (1989), Deecke et al. (2005)
Long-finned pilot whale	Whistle, pulsed vocalization	Tonal signal <6 kHz	Nemiroff and Whitehead (2009)
Harbour porpoise	Click	Click	Au et al. (1999)
Pygmy sperm whale	Click	Click	Marten (2000)
Sperm whale	Click	Click	Møhl et al. (2000), Møhl et al. (2003)
Cuvier's beaked whale	Click	Click	Zimmer et al. (2005)
Sowerby's beaked whale	Click	Click	Cholewiak et al. (2013)
Northern bottlenose whale	Click	Click	Hooker and Whitehead (2002), Wahlberg et al. (2012)
True's beaked whale	Click	NA	DeAngelis et al. (2018)
Hooded seal	Unknown	NA	Risch et al. (2007)
Harp seal	Grunt, yelp, bark	NA	Terhune (1994)

¹ Table 1 lists the dolphin species likely to be detected by the dolphin whistle detector.

1.3. Ambient Ocean Soundscape

The ambient, or background, sound levels that create the ocean soundscape are comprised of many natural and anthropogenic sources (Figure 2). The main environmental sources of sound are wind, precipitation, and sea ice. Wind-generated sound in the ocean is well-described (e.g., Wenz 1962, Ross 1976), and surf sound is known to be an important contributor to near-shore soundscapes (Deane 2000). In polar regions, sea ice can produce loud sounds that are often the main contributor of acoustic energy in the local soundscape, particularly during ice formation and break up. Precipitation is a frequent sound source, with contributions typically concentrated at frequencies above 500 Hz. At low frequencies (<100 Hz), earthquakes and other geological events contribute to the soundscape (Figure 2).

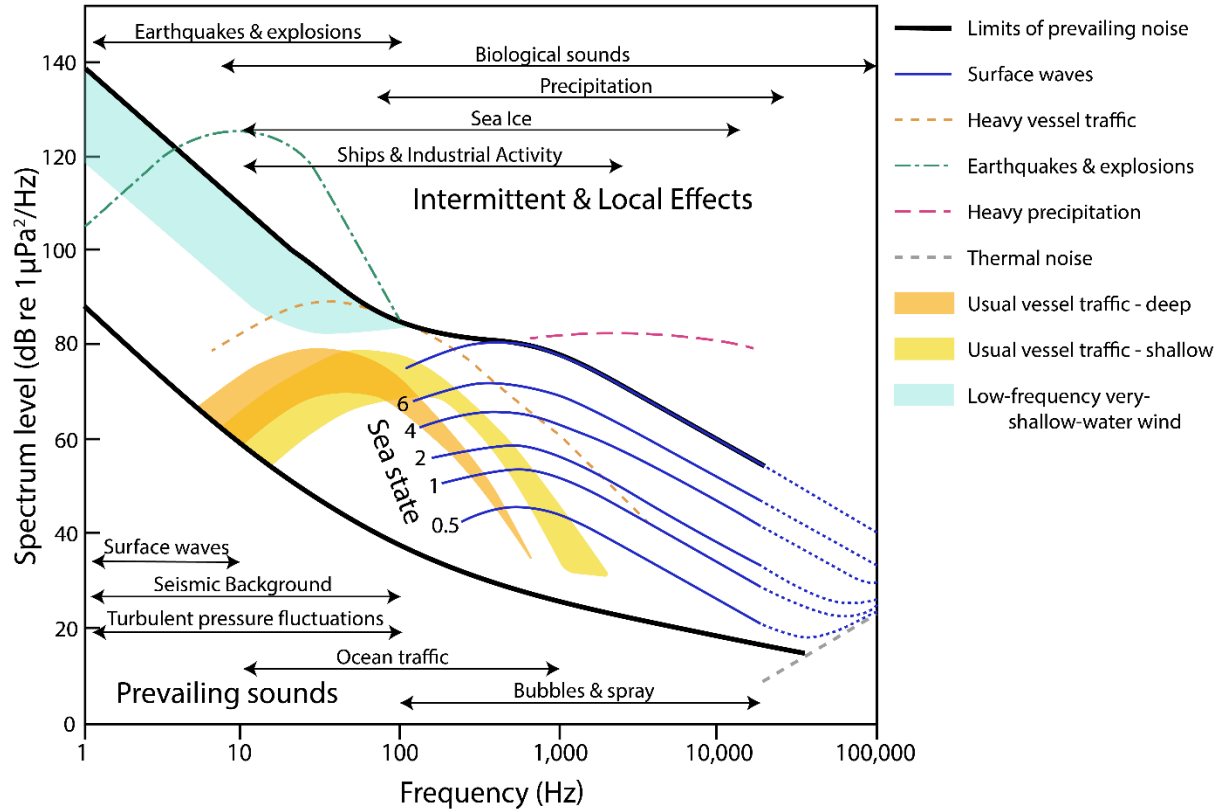


Figure 2. Wenz curves describing pressure spectral density levels of marine ambient sound from weather, wind, geologic activity, and commercial shipping (adapted from NRC 2003, based on Wenz 1962). Thick lines indicate limits of prevailing ambient sound.

1.4. Anthropogenic Contributors to the Soundscape

Anthropogenic (human-generated) sound can be a by-product of vessel operations, such as engine sound radiating through vessel hulls and cavitating propulsion systems, or it can be a product of active acoustic data collection with seismic surveys, military sonar, and depth sounding as the main contributors. Marine construction projects often involve nearshore blasting and pile driving that can produce high levels of impulsive sounds. The contribution of anthropogenic sources to the ocean soundscape has increased from the 1950s to 2010, largely driven by greater maritime shipping traffic (Ross 1976, Andrew et al. 2011). Recent trends suggest that global sound levels are leveling off or potentially decreasing in some areas (Andrew et al. 2011, Miksis-Olds and Nichols 2016). Oil and gas exploration with seismic airguns, marine pile driving and oil and gas production platforms elevate sound levels over radii of 10 to 1000 km when present (Bailey et al. 2010, Miksis-Olds and Nichols 2016, Delarue et al. 2018). The extent of seismic survey sounds has increased substantially following the expansion of oil and gas exploration into deep water, and seismic sounds can now be detected across ocean basins (Nieukirk et al. 2004). How these natural and anthropogenic factors influence the sound levels is dependent on the regional acoustic propagation conditions, which in turn depend on the vertical sound speed profile, bottom contours, and geoacoustic properties.

The main anthropogenic contributors to ambient acoustic environment in the present study were the West Aquarius Mobile Offshore Drilling Unit (MODU) which was active at both the Hampden (EL 1165A) and Harp (EL 1165B) well sites during the study period, and vessel presence. The study area was not in a shipping lane, but was subject to localized denser vessel traffic related to well sites, seismic surveys and fishing effort, as depicted in Figure 3 for 2017. This figure shows vessel traffic outside the exploration drilling timeframe but representative of the level of traffic in a typical year.

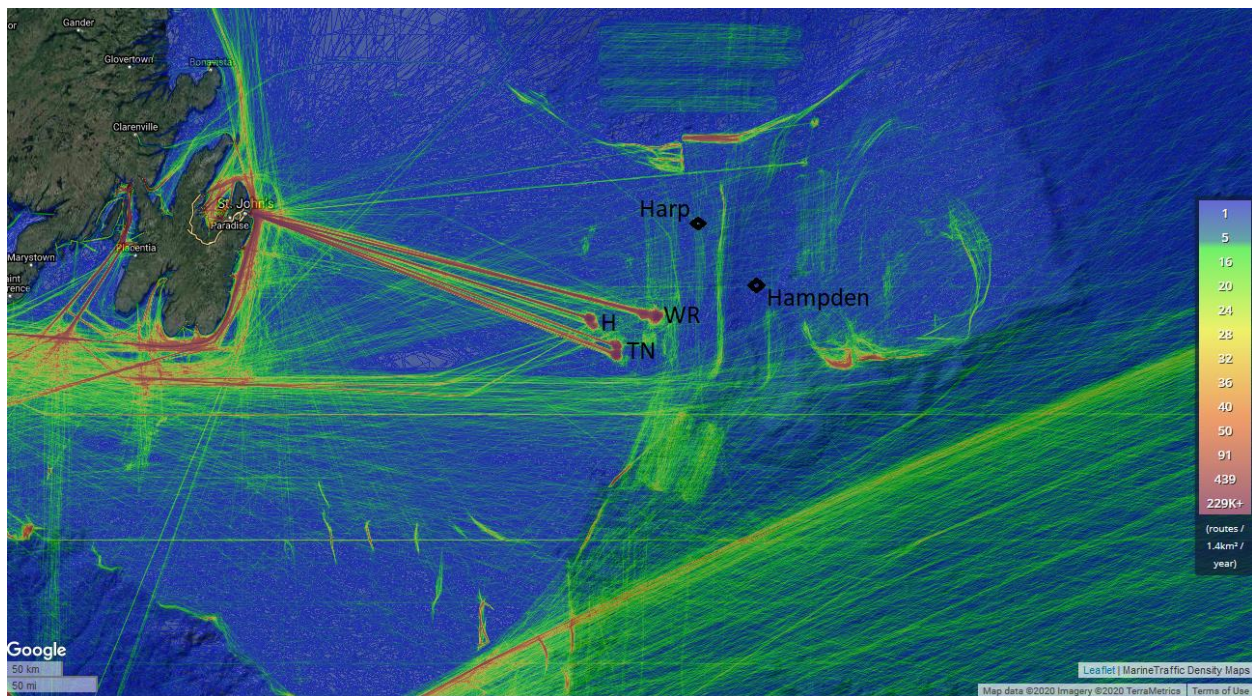


Figure 3. Vessel traffic off the coast of Newfoundland in 2017 WR: White Rose; H: Hibernia-Hebron; TN: Terra Nova (source: marinetraffic.com; accessed 9 Sep 2020).

2. Methods

2.1. Acoustic Data Acquisition

JASCO and Wood deployed four Autonomous Multichannel Acoustic Recorders Generation 4 (AMAR G4s; manufactured by JASCO) long-term passive acoustic recorders equipped with M36-V35-100 hydrophones (manufactured by JASCO GeoSpectrum Technologies Inc) at the locations outlined in Table 3 and shown in Figure 1. All AMARs were calibrated before deployment and again after retrieval to assess any changes in recorder’s sensitivity during the recording period (none observed). Each AMAR recorded for 8 min sampling at 32 kHz, 1 min sampling at 512 kHz, followed by 11 min of sleep. All systems successfully recorded data throughout the deployment. The West Aquarius Mobile Offshore Drilling Unit (MODU) arrived at the Harp (EL 1165B) site 1 Oct 2019 and departed 1 May 2020 for the Hampden (EL 1165A) site where operations were conducted until 14 May 2020. The recorders were returned to JASCO for analysis on 16 Jun 2020. The mooring design used is shown in Figure 4. The Harp (EL 1165B) and Hampden (EL 1165A) Well Sites are 65.4 km apart.

Table 3. Operation period, location, and depth of the Autonomous Multichannel Acoustic Recorders (AMARs)

Station	Latitude	Longitude	Depth (m)	Deployment	Retrieval	Duration (days)	Distance/ bearing from	Bearing	Distance (km)
Stn 19	48.381	-46.523	1600	2019 Aug 29	2020 May 27	272	Harp (EL 1165B) Well Site	33°	114.1
Harp (EL 1165B) Well Site	47.513	-47.357	300	2019 Aug 30	2020 May 17	261	Harp (EL 1165B) Well Site	145°	2.1
Hampden (EL 1165A) Well Site	47.023	-46.878	1175	2019 Aug 31	2020 May 25	268	Hampden (EL 1165A) Well Site	335°	5.3
Mid Flemish Pass	47.268	-47.1183	875	2019 Aug 30	2020 May 26	268	Hampden (EL 1165A) Well Site	326°	38.1

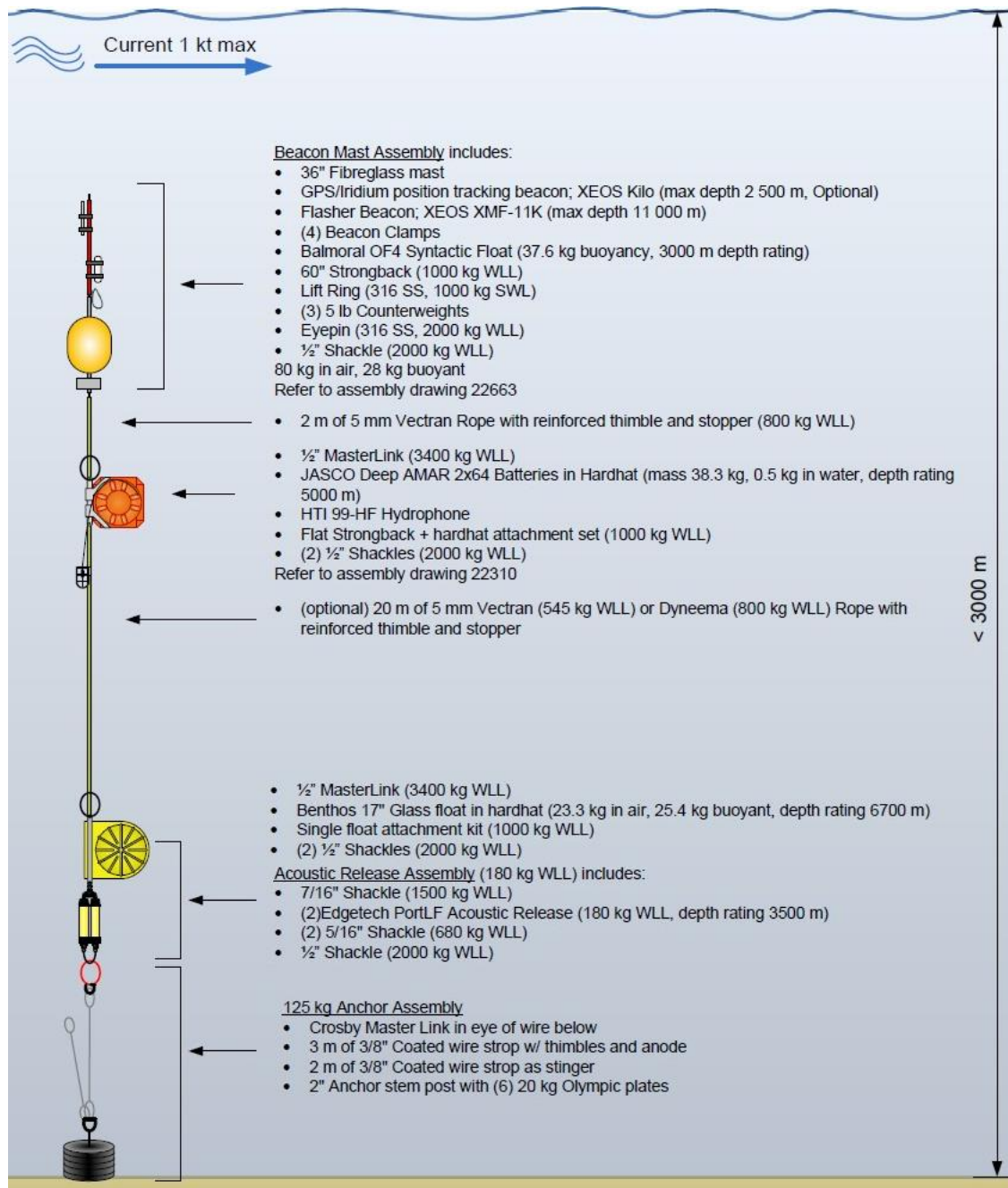


Figure 4. Mooring design used at each of the four stations. The optional 20 m section was not used.

2.2. Automated Data Analysis

The AMARs collected approximately 9.5 TB of acoustic data during this study. We used our specialized computing platform (PAMlab) capable of processing acoustic data hundreds of times faster than real time. The system performed automated analysis of total ocean sound and sounds from vessels, seismic surveys, and marine mammal vocalizations. Appendix D outlines the stages of the automated analysis.

2.2.1. Total Ocean Sound Levels

The data collected near the Flemish Pass spans nine months at four locations, over the frequency band of 10–256000 Hz. The goal of the total ocean sound analysis is to present this expansive data in a manner that documents the baseline underwater sound conditions in Flemish Pass and allows us to compare between stations, over time, and with external factors that change sound levels such as weather and human activities.

The first stage of the total sound level analysis involves computing the peak and rms sound pressure level (SPL) for each minute of data. This reduces the data to a manageable size without compromising the value for characterizing the soundscape (ISO 2017b, Ainslie et al. 2018, Martin et al. 2019b). The SPL analysis is performed by averaging 120 fast-Fourier transforms (FFTs) that each include one second of data with a 50% overlap and that use the Hann window to reduce spectral leakage. The one minute average data were stored as power spectral densities (1 Hz resolution) and summed over frequency to calculate decidecade band SPL levels.

Table A-1 lists the decidecade band frequencies, and Table A-2 lists the decade-band frequencies. The decidecade analysis sums the frequency range from the 180,000 frequencies (representing the frequency range 1 Hz to 180 kHz) in the power spectral density data to a manageable set of 43 bands that approximate the critical bandwidths of mammal hearing. The decade bands further summarize the sound levels into four frequency bands for manageability. Detailed descriptions of the acoustic metrics and decidecade analysis can be found in Appendices A.1 and A.2 .

Weather conditions throughout the recording periods were gathered to inform the discussion on the factors driving sound levels and influencing marine mammal detections. Wind speed and wave height data were provided by Wood (see Figures 5 and 6). The wind speed was taken from the West Aquarius Helideck Monitoring system and the wave height from the Harp (EL 1165B) buoy deployed by Wood.

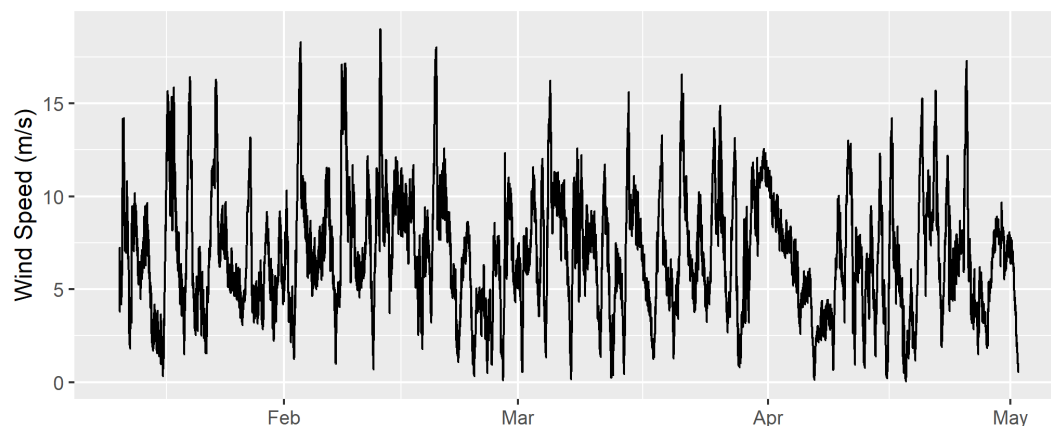


Figure 5. Wind speeds measured at Harp (EL 1165B) well site.

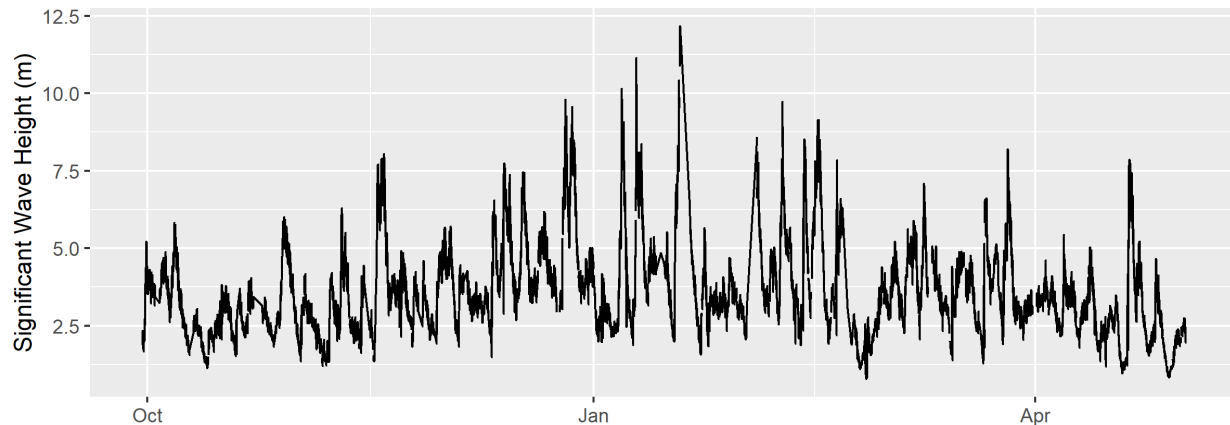


Figure 6. Significant wave height measured at the Harp (EL 1165B) well site.

In Section 3.1, the total sound levels are presented as:

- Band-level plots:** These strip charts show the averaged received sound pressure levels as a function of time within a given frequency band. We show the total sound levels (across the entire recorded bandwidth, specifically from 10 Hz to the top of the last fully captured decade (224404 Hz; see Appendix A.2); this band is labelled 10-200000 Hz for simplicity) and the levels in every whole decade band (10–100, 100–1000, 1000–10,000, and 10,000–100,000 Hz). The 10–100 Hz band is associated with fin, sei, and blue whales, large shipping vessels, pseudo-noise from flow and mooring movement, as well as seismic survey pulses. Sounds within the 100–1000 Hz band are generally associated with the physical environment such as wind and wave conditions but can also include both biological and anthropogenic sources such as minke, right, and humpback whales, fish, nearby vessels, and pile driving. Sounds above 1000 Hz include high-frequency components of humpback whale sounds, odontocete whistles and echolocation signals, wind- and wave-generated sounds, and sounds from human sources at close range including pile driving, vessels, seismic surveys, and sonars.
- Long-term Spectral Averages (LTSAs):** These colour plots show power spectral density levels as a function of time (x -axis) and frequency (y -axis). The frequency axis uses a logarithmic scale, which provides equal vertical space for each decade increase in frequency and allows the reader to equally see the contributions of low and high-frequency sound sources. The LTSAs are excellent summaries of the temporal and frequency variability in the data.
- Decidecade box-and-whisker plots:** In these figures, the ‘boxes’ represent the middle 50% of the range of sound pressure levels measured, so that the bottom of the box is the sound level 25th percentile (L_{25}) of the recorded levels, the bar in the middle of the box is the median (L_{50}), and the top of the box is the level that exceeded 75% of the data (L_{75}). The whiskers indicate the maximum and minimum range of the data.
- Spectral density level percentiles:** The decidecade box-and-whisker plots are representations of the histogram of each band’s sound pressure levels. The power spectral density data has too many frequency bins for a similar presentation. Instead coloured lines are drawn to represent the L_{eq} , L_5 , L_{25} , L_{50} , L_{75} , and L_{95} percentiles of the histograms. Shading is provided underneath these lines to provide an indication of the relative probability distribution. It is common to compare the power spectral densities to the results from Wenz (1962), which documented the variability of ambient spectral levels off the US Pacific coast as a function of frequency of measurements for a range of weather, vessel traffic, and geologic conditions. The Wenz levels are appropriate for approximate comparisons only since the data were collected in deep water, largely before an increase in low-frequency sound levels (Andrew et al. 2011).
- Daily sound exposure levels (SEL; $L_{E,24h}$):** The SEL represents the total sound energy received over a 24-hour period, computed as the linear sum of all 1-min values for each day. It has become

the standard metric for evaluating the probability of temporary or permanent hearing threshold shift. Long-term exposure to sound impacts an animal more severely if the sounds are within its most sensitive hearing frequency range. Therefore, during SEL analysis recorded sounds are typically filtered by the animal's auditory frequency weighting function before integrating to obtain SEL. For this analysis the 10 Hz and above SEL were computed as well as the SEL weighted by the marine mammal auditory filters (Appendix B) (NMFS 2018). The SEL thresholds for the onset of hearing impacts (temporary threshold shifts, TTS) from sound on marine mammals are provided in Table B-1 and further described in NMFS (2018). Weighted daily SEL were estimated from the 512 kHz data sampled 1 min out of every 20 min using the interpolation method of Martin et al. (2019b).

2.2.2. Vessel Noise Detection

Vessels are detected in two steps (Martin 2013):

1. Detect constant, narrowband tones produced by a vessel's propulsion system and other rotating machinery (Arveson and Vendittis 2000). These sounds are also referred to as tonals. We detect the tonals as lines in a 0.125 Hz resolution spectrogram of the data (8 s of data, Hann window, 2 s advance).
2. Assess the SPL for each minute in the 40–315 Hz shipping frequency band, which commonly contains most sound energy produced by mid-sized to large vessels. Background estimates of the shipping band SPL and system-weighted SPL are then compared to their mean values over a 12 h window, centred on the current time.

Vessel detections are defined by the following criterion (Figure 7):

1. SPL in the shipping band (40–315 Hz) is at least 3 dB above the 12 h mean for the shipping band for at least 5 min.
2. A least three shipping tonals (0.125 Hz bandwidth) are present for at least 1 min per 5 min window. Tonals are difficult to detect during turns and near the closest points of approach (CPA) due to Lloyds' mirror and Doppler effects.
3. SPL in the shipping band is within 12 dB of the system weighted SPL.

The duration where these constraints are valid is identified as a period with shipping present. A 10 min shoulder period before and after the detection period is also included in the shipping period. The shipping period is searched for the highest 1 min SPL in the vessel detection band, which is then identified as the closest point of approach (CPA) time. This algorithm is designed to find detectable shipping, meaning situations where the vessel sound can be distinguished from the background. It does not identify cases of two vessels moving together or cases of continuous sound from stationary platforms, such as oil and gas drilling and dynamic positioning operations. Those situations are easily identified from tools such as the daily SEL and long-term spectral average figures.

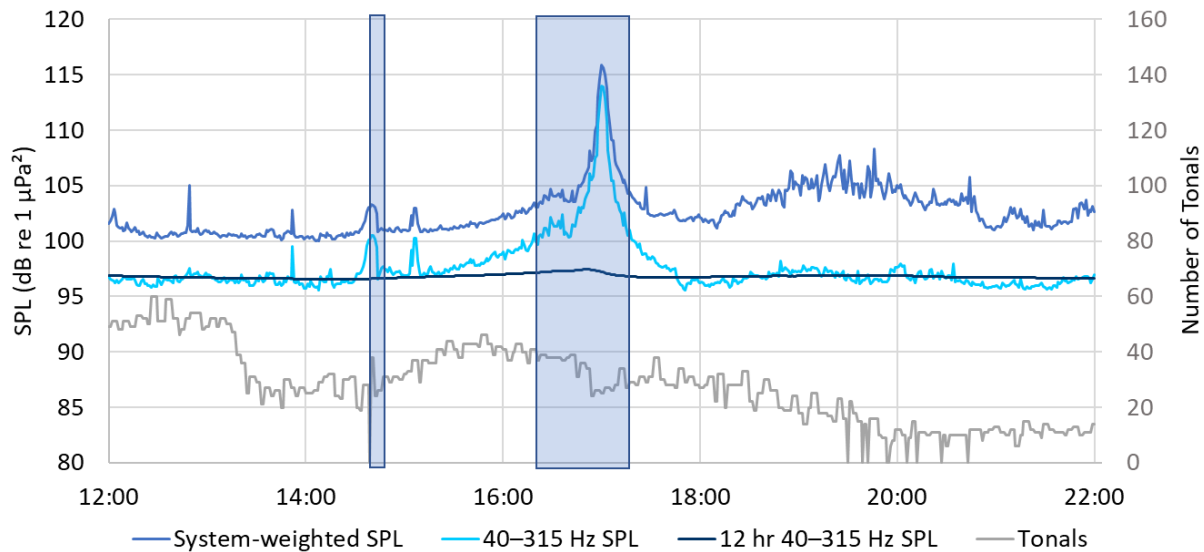


Figure 7. Example of broadband and 40–315 Hz band sound pressure level (SPL), as well as the number of tonals detected per minute as a vessel approached a recorder, stopped, and then departed. The shaded area is the period of shipping detection. Fewer tonals are detected at the vessel’s closest point of approach (CPA) at 17:00 because of masking by broadband cavitation noise and due to Doppler shift that affects the tone frequencies.

2.2.3. Seismic Survey Event Detection

Seismic pulse sequences were detected using correlated spectrogram contours. We calculated spectrograms using a 300 s long window with 4 Hz frequency resolution and a 0.05 s time resolution (Reisz window). All frequency bins were normalized by their medians over window the 300 s window. The detection threshold is three times the median value at each frequency. Contours were created by joining the time-frequency bins above threshold in the 7–1000 Hz band using a 5 × 5 bin kernel. Contours 0.2–6 s in duration with a bandwidth of at least 60 Hz were further analyzed.

An “event” time series was created by summing the normalized value of the frequency bins in each time step that contained detected contours. The event time series was auto-correlated to look for repeated events. The correlated data space was normalized by its median, and a detection threshold of 3 was applied. Peaks larger than their two nearest neighbours were identified, and the list of peaks was searched for entries with a set repetition interval. The allowed spacing between the minimum and maximum time peaks was 4.8 to 65 s, which captures the normal range of seismic pulse periods. Where at least six regularly spaced peaks occurred, the original event time series was searched for all peaks that match the repetition period within a tolerance of 0.25 s. The duration of the 90% SPL window of each peak was determined from the originally sampled time series, and pulses more than three second long were rejected.

2.3. Detection Range Modelling

Detection Range Modelling (DRM) was conducted to estimate the detectability of marine mammal vocalizations for the species detected in the study area. DRM considered the following data inputs to estimate species-specific detection distances:

- Published marine mammal vocalization source level and bandwidth characteristics, as well as vocalization depth (see Appendix C.2),
- Ambient decidecade SPL percentiles measured in the study area, and
- Local bathymetry, geology, and sound speed profile (see Appendix C.3).

The detection range is defined as the range where the expected sound level of a mammal vocalization is X dB (where X is the detection threshold of the relevant detector for a given species) above the expected background level. Modelled signal-to-noise ratios (SNR) were calculated at locations within a three-dimensional (3-D) volume (easting, northing, and depth) to predict a detection range. The detection range, therefore, represents the maximum range at which a signal of a given source level can be identified by a detector in given background noise conditions. This underestimates the range to which vocalizations could be detected by experienced human analysts conducting a fine scale analysis.

To compute the detection range, an estimate of the sound's propagation loss between the vocalizing animal and our seafloor recorders was required. To perform the propagation loss calculations in a computationally efficient manner, we applied the reciprocity principle which states that an identical signal will be received between a source and receiver pair if their coordinates are inter-changed (Jensen et al. 2011). Rather than performing individual propagation loss calculations for a source at many locations (e.g., an animal) to the receiver (seafloor recorder) to estimate SNR and detectability, the loss between source and receiver is computed by setting the source location for the propagation model to be the location of the seafloor recorder. The propagation loss from this position was then calculated to locations within the ocean interior in a single calculation, thereby reducing the number of individual propagation loss computations that would be required otherwise.

Depending on the frequency characteristics of the marine mammal source level inputs, two potential sound propagation models were used to predict the loss between animal and recorder:

- JASCO's Marine Operations Noise Model (MOMN) a range-dependent parabolic equation model for frequencies up to 2 kHz and/or,
- The BELLHOP Gaussian beam acoustic ray-trace model for frequencies from 2 to 100 kHz.

The MONM and BELLHOP results were combined as required to produce results for the full frequency range for the species of interest. Appendix C.1 contains additional information on the propagation models used for detection range estimation.

Propagation loss was calculated up to a distance of 100 km for frequencies up to 2 kHz and 50 km for frequencies above 2 kHz from each recorder location. A horizontal separation of 20 m between receiver points along the modelled radials was used. The sound fields were modelled with a horizontal angular resolution of 10° for a total of 36 radial planes. Receiver depths were chosen to span the entire water column over the modelled areas, from 2 m to a maximum of 3000 m, with step sizes that increased with depth.

Ambient decidecade SPL percentile information were derived from the measurements performed on the data recorded at each station. Detection ranges were modelled for March and September. These months were chosen because they had sound speed profiles at the opposite ends of the observed range. In addition, the MODU was not anchored near Harp (EL 1165B) in September, providing a relatively pristine soundscape in comparisons with other months with the MODU was operating. These two months were thereby expected to provide representative upper and lower bounds for detection ranges (see Appendix C.3.2). The modelling was aimed at the most common signals identified by analysts and detectors during the study (i.e., acoustic signals from blue, fin, sei, humpback, minke, killer, sperm, northern bottlenose, and Sowerby's beaked whales as well as delphinids and harbour porpoises).

We defined two geoacoustic profiles based on previous modelling projects in the same area. One profile was used for the only on-shelf station (Harp (EL 1165B)) and the other was applied to the three other deep stations (see Appendix C.3.3).

To evaluate the detection ranges, the following model of the received level, $RL(r)$, measured at the distance r from the source, was used:

$$RL(r) = SL - TL(r), \quad (1)$$

where SL is the source level; and $TL(r)$ is the transmission loss. The detection of sound is the event that satisfies the condition:

$$RL(r) \geq NL + c, \quad (2)$$

where NL is the background noise level; and c is a constant specifying the detection threshold. $TL(r)$ is a non-random parameter computed by the MONM or BellHop (Porter and Liu 1994) algorithms, such that Equations 1 and 2 include two independent random variables, NL and RL .

The joint probability of the events that NL takes some value $NL = NL_i$, and RL takes a value of $RL = RL_j$ is $P(NL_i, RL_j)$. Using Bayes theorem, the joint probability can be represented as a product:

$$P(NL_i, RL_j) = P(NL_i|RL_j)P_R(RL_j) = P(RL_j|NL_i)P_N(NL_i) \quad (3)$$

where $P(RL_j|NL_i)$ is a conditional probability, i.e., the likelihood of event $RL = RL_j$ occurring given that $NL = NL_i$; $P_R(RL_j)$ are the probabilities of observing RL_j and NL_i respectively.

Taking Equation 3 into account, we may introduce two types of detection probabilities. The conditional probability of detection of a sound at the distance r from the source computed under a certain value of NL is:

$$P_{DC}(r|NL) = \sum_{RL < NL+c} P_R(RL(r)) = CDF_R(NL + c), \quad (4)$$

where $CDF_R(x)$ is the cumulative distribution function of the received level. The unconditional probability of detection is:

$$P_{DU}(r) = 1 - \sum_{NL} P_N(NL) \sum_{RL < NL+c} P_R(RL(r)) = 1 - \sum_{NL} P_N(NL) CDF_R(NL + c). \quad (5)$$

The unconditional probability of detection is used to display the detection ranges.

2.4. Available Listening Range

The available listening range (ALR) estimates how the percentage of the maximum possible listening range for marine life changes as a function of time. ALR is computed using the sound levels in specific critical hearing bands (see Equation 6). In Equation 6, NL_2 is the sound pressure level at the time analyzed, NL_1 is the lowest typical sound pressure level, and N is the geometric spreading coefficient for the acoustic propagation environment. If an animal's threshold of hearing is higher than NL_1 , NL_1 is replaced with the hearing threshold. The sound pressure levels are computed for decidecade bands that are representative of the important listening frequencies for animals of interest.

$$ALR = 100 * \left(10^{\frac{NL_2 - NL_1}{N}}\right) \quad (6)$$

ALR was computed for each recorder throughout the deployments. The value of NL_1 was chosen to be the 10th percentile of sound pressure level in each decidecade band at the reference recorder, Stn 19 (i.e., the SPL that exceeded the lowest 10% of the 1-min samples). The analysis was performed for low- and mid-frequency cetaceans. The specifics for which decidecades were analyzed and the rationale for selections those bands are given in Table 4. ALR was not computed for high-frequency cetaceans because the data were system noise-limited at the key frequency band of 125 kHz and thus the results would not be valid.

ALR is equal to $100 - LRR$, where LRR is the listening range reduction. LRR is similar to the concept of listening space reduction (Pine et al. 2020) that estimates how much of an animal's listening range is lost due to a masking noise source. ALR was employed for this analysis after discussions within JASCO

indicated it was a more intuitive metric than LRR. To simplify presentation of the ALR, it was computed for each minute of recorded data, and then the median value for each day (UTC) was presented.

Table 4. Decidecade bands analyzed for the Available Listening Range. If the audiogram level is above the 10th percentile of the decidecade SPL measured at Stn 19, then the species was *hearing* limited rather than *noise* limited. Audiograms sensitivity is based on Finneran (2016).

Species or group	Decidecade band centre frequency (Hz)	Rational for selecting band	10th percentile of measured decidecade SPL at Stn 19 (dB re 1 μ Pa ²)	Audiogram level (hearing sensitivity, dB re 1 μ Pa ²)
Low-frequency cetaceans	20	Centre frequency for fin whale downsweeps and similar to blue whale A-B calls	87.3	78.9
	80	Frequency used by fin, blue, sei, minke, and humpback whales	90.3	68.1
	200	Common frequency for humpback song; overlaps with peak energy from MODU	90.1	62.2
	1000	High end of humpback song notes	88.7	55.9
Mid-frequency cetaceans	1000	Low end of killer and pilot whale whistles	88.7	78.9
	6300	High end of killer and pilot whale whistles; low end of small delphinid whistles	81.7	69.8
	12500	High end of small delphinid whistles	78.6	62.2
	25000, 31500, and 40000	Frequency range for most odontocete echolocation	78.6	55.1

2.5. Computing MODU Underwater Radiated Noise

To compute underwater radiated noise (URN) of the MODU, the propagation loss from the MODU to the receiver is added to the sound pressure level measured at the receiver, which is the inverse of Equation 6. The propagation loss was estimated in the same manner as for the Detection Range Modelling (Section 2.3 and Appendix C), and added to the measured SPL in each decidecade band from 10–10000 Hz. For computing the MODU source level, the monthly propagation losses were estimated using the GDEM sound speed profiles (Carnes 2009). The URN was computed for each minute of data where the MODU was present, and then the distribution of these levels was presented using box-and-whisker plots for each decidecade. This allows us to visualize the range of URN that corresponds to different Dynamic Positioning system thrust levels and operational states of the MODU. The analysis was repeated for the MODU at Harp (EL 1165B) and for its 10 days at Hampden (EL 1165A).

When the fully modelled acoustic propagation loss is used to compute URN, the result is the monopole source level (MSL) which accounts for surface and seabed reflections and depends on the source depth being accurately known. Here we assumed the source depth to be 10 m. An alternate approach is to use

the spherical spreading loss ($20 \cdot \log_{10}(\text{distance})$) as the propagation loss. This approach provides a value known as the radiated noise level (RNL). In deep water, it is expected that the MSL will be higher than the RNL at low frequencies (below ~ 100 Hz) and the RNL will be ~ 3 dB higher than MSL at higher frequencies (above ~ 1000 Hz). In geometries where the measurement range is greater than several water depths, the propagation loss is generally less than spherical spreading, in which case the RNL is unreliable. The MSL is required to model the effects of a source on the soundscape. RNL is easier to compute and useful for comparing vessels to a benchmark or to each other.

To assess the effectiveness of using the bottom mounted recorders to assess the URN from the MODU the RNL and MSL from both Harp (EL 1165B) and Hampden (EL 1165A) were compared.

2.6. Marine Mammal Detection Overview

We used a combination of automated detectors and manual review by human analysts to determine the presence of sounds produced by marine mammals. First, automated detectors identified acoustic signals potentially produced by odontocetes and mysticetes (Appendices D.1 and D.2). We then manually reviewed (validated) automated detections within a sample of sound files for each data set (Appendix D.3). A data set consists of data recorded at a given sampling rate and station. The level of validation effort was set at 2% of the data based on the evaluation of divergence curves, which represent the minimum validation effort required to ensure that the sample is representative of the distribution of automated detections throughout each data set (Appendix D.4). This level of review is above the typical 1% validation effort routinely applied to long-term datasets (e.g. Delarue et al. 2018). Finally, we critically reviewed the results of each automated detector and restricted their output, where necessary, to maximize their performance metrics (Appendix D.5). Automated detector performance metrics are only presented for those species and/or vocalization types exceeding a pre-set precision (P) level ($P = 75\%$), which ensures a level of reliability in the description of marine mammal acoustic occurrence. When the precision was below that threshold, manual detections are presented.

In this report, the term “detector” is used to describe automated algorithms that combine detection and classification steps. A “detection” refers to an acoustic signal that has been automatically flagged as a sound of interest based on spectral features and subsequently classified based on similarities to several templates in a library of marine mammal signals. Detections are reviewed by analysts as part of a process called validation. Manual detections refer to signals detected by an analyst but not the detector during the validation process.

2.6.1. Odontocete Click Detection

Odontocete clicks are high-frequency impulses with energy ranging from ~ 1 to over 150 kHz (Au et al. 1999, Møhl et al. 2000). JASCO’s click detectors are based on zero-crossings in the acoustic time series. Zero-crossings are the rapid oscillations of a click’s pressure waveform above and below the signal’s normal level. Zero-crossing-based features of detected events are then compared to templates of known clicks for classification (see Appendix D.1 for details). Clicks were classified individually and as trains. Detected clicks that cannot be classified as one of the targeted species are pooled in an “Unidentified Click” category. The suite of click detectors is presented in Table 5.

Table 5. List of automated detectors used to identify clicks produced by odontocetes.

Species targeted	Comments
Sowerby's beaked whale	
Northern bottlenose whale	
Cuvier's beaked whale	
True's beaked whale	
Unidentified beaked whale	Targeting long, frequency-modulated clicks
Unidentified beaked whale @ 51 kHz	Could be produced by True's beaked whales
Sperm whale	
Killer whale	
Pilot whale	
Atlantic white-sided dolphin	
Risso's dolphin	The detector includes two click types (short and long)
Dolphins	Generic dolphin click, will capture clicks from a range of dolphin species (e.g., short-beaked common and white-sided dolphins)
NBHF species	Targets clicks produced by harbour porpoises or pygmy sperm whales (in this area)

2.6.2. Tonal Signal Detection

Tonal signals are narrowband, often frequency-modulated, signals produced by many species across a range of taxa (e.g., baleen whale moans and delphinids whistles). The signals of some pinniped species, such as bearded seal trills, also have tonal components. The frequency range of baleen whale moans vary among species but is generally below 1 kHz and as low as 17 Hz in blue whales (see e.g., Parks and Tyack 2005, Berchok et al. 2006, Dunlop et al. 2007). Delphinid tonal signals are generally much more broadband and range from ~700 Hz up to 18 kHz (see e.g., Steiner 1981, Ford 1989, Rendell et al. 1999, Oswald et al. 2003) but can be as high as 68 kHz in some species (Samarra et al. 2010). The tonal signal detector identified continuous contours of elevated energy and classified them against a library of marine mammal signals (see Appendix D.2 for details). The suite of tonal detectors applied to the data is presented in Table 6.

Table 6. List of automated detectors used to identify tonal signals produced by baleen whales and delphinids. FW: fin whale; SW: sei whale; BW: blue whale; RW: right whale; MW: minke whale.

Detector name	Species targeted	Signal targeted
Atl_BlueWhale_GL_IM	Blue whales	A-B call, tonal song note @ 17 Hz
Atl_BlueWhale_IM	Blue whales	A-B call, tonal song note @ 17 Hz
Atl_BlueWhale_IM2	Blue whales	A-B call, tonal song note @ 17 Hz
Atl_FinWhale_130	Fin whales	130-Hz song note
Atl_FinWhale_21.2	Fin whales	20-Hz pulse
Atl_FinWhale_21	Fin whales	20-Hz pulse
minkeWhalePulses	Minke whales	Pulse train
N_RightWhale_Up1	North Atlantic right whales	Upcall
N_RightWhale_Up2	North Atlantic right whales	Upcall
N_RightWhale_Up3	North Atlantic right whales	Upcall
SW	Sei whales	Broadband downsweep
WhistleLow	Pilot whale/Killer whales	Whistle with energy between 1–10 kHz
WhistleHigh	Other delphinids	Whistle with energy between 4–20 kHz
VLFMoan	Baleen whales, FW/SW/BW	Downsweeps/upsweeps
LFMoan	Baleen whales, SW/BW/RW	Downsweeps/upsweeps
ShortLow	Baleen whales, possibly MW	Moans, pulses
MFMoanLow	Humpbacks	Moans
MFMoanHigh	Humpbacks	Moans

2.6.3. Automated Detector Validation

We develop and test automated detectors with example data files that contain a range of vocalization types and background noise conditions. However, test files cannot cover the full range of possible vocalization types and noise conditions. Therefore, a selection of files representing 2% of each data set was manually validated to check each detector's performance for a specific location and timeframe to determine how best to refine the detector results, or when to entirely rely on manually validated results, to accurately represent marine mammal occurrence (see details in Appendix D.3).

To determine the per-file performance of each detector and any necessary thresholds, the automated and validated results (excluding files where an analyst indicated uncertainty regarding species identity) were fed to a maximum likelihood estimation algorithm that maximizes the probability of detection and minimizes the number of false alarms using the 'MCC-score' (see Appendix D.5 for details). The algorithm also estimates the precision (P) and recall (R) of the detector. P represents the proportion of files with detections that are true positives. A P value of 0.9 means that 90% of the files with detections truly contain the targeted signal, but it does not indicate whether all files containing acoustic signals from the species were identified. R represents the proportion of files containing the signal of interest that were identified by the detector. An R value of 0.9 means that 90% of files known to contain a target signal had automated detections, but it says nothing about how many files with detections were incorrect. An MCC-score is a combined measure of P and R , where an MCC-score of 1 indicates perfect performance—all events were detected with no false alarms.

The algorithm determines a threshold for each detector based on detection count per file that maximizes the MCC-score (see Appendix D.5). The resulting thresholds, P s, and R s are presented in Section 3.4.1.

3. Results

3.1. Soundscape Characterization

Long-term spectra averages, power spectral density, decade band box plots, cumulative sound exposure levels, and decade band box plots for each are shown in Figures 8-10. Baseline sound levels (MODU not present, e.g. September 2019) were consistent with previous soundscape characterizations in the Flemish Pass (Maxner et al. 2017). The differences in the sound levels due to the MODU are easily detected in these figures, for example by the bright yellow-red section of the LTSA at Harp (EL 1165B) (Figure 8). The total daily sound exposure in 300 m of water at a 2 km distance from the MODU (Harp (EL 1165B)) were 25–30 dB higher when the MODU was present compared to when it was absent (Figure 10). The levels were ~20 dB higher 5 km from the MODU in water 1175 m deep (Hampden (EL 1165A); Figure 10). The presence of the MODU increased the power spectral density by ~25 dB at 100 Hz, 15–20 dB at 1000 Hz, 10 dB at 10000 Hz, and 20 dB at 27000 Hz due to the USBL source (Figure 9). Broadband (10 Hz – 200 kHz) sound levels measured at 2 km (Harp) and 5 km (Hamden) from the MODU were ~ 20 dB and ~ 17 dB higher, respectively, compared to baseline levels. These increases are generally consistent with previous measurements in the Flemish Pass where the increase in broadband sound levels measured 13 km from a MODU was 13 dB (Maxner et al. 2017).

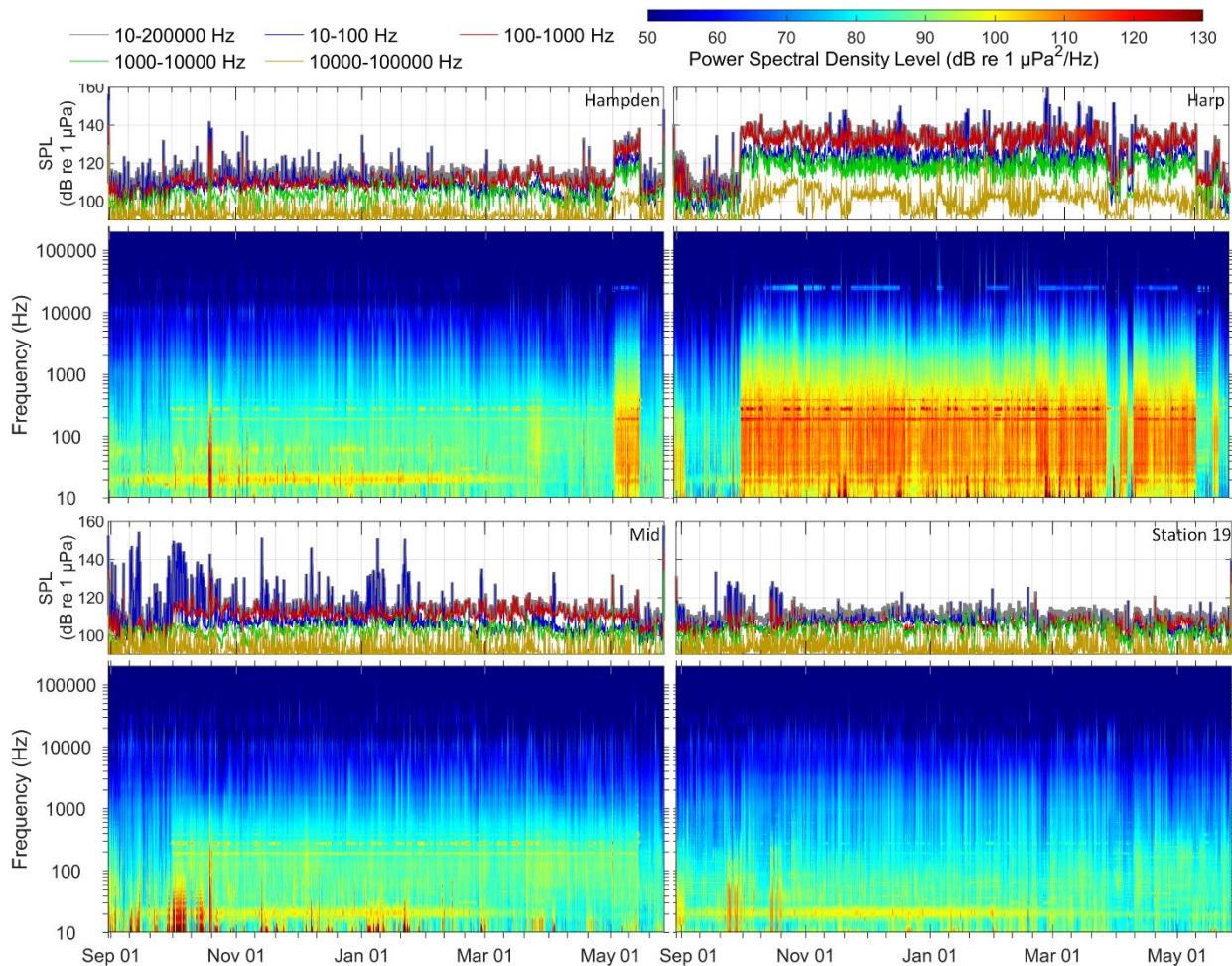


Figure 8. (Top) In-band sound pressure level (SPL) and (bottom) spectrogram (or long-term spectral average; LTSA) of underwater sound for each station.

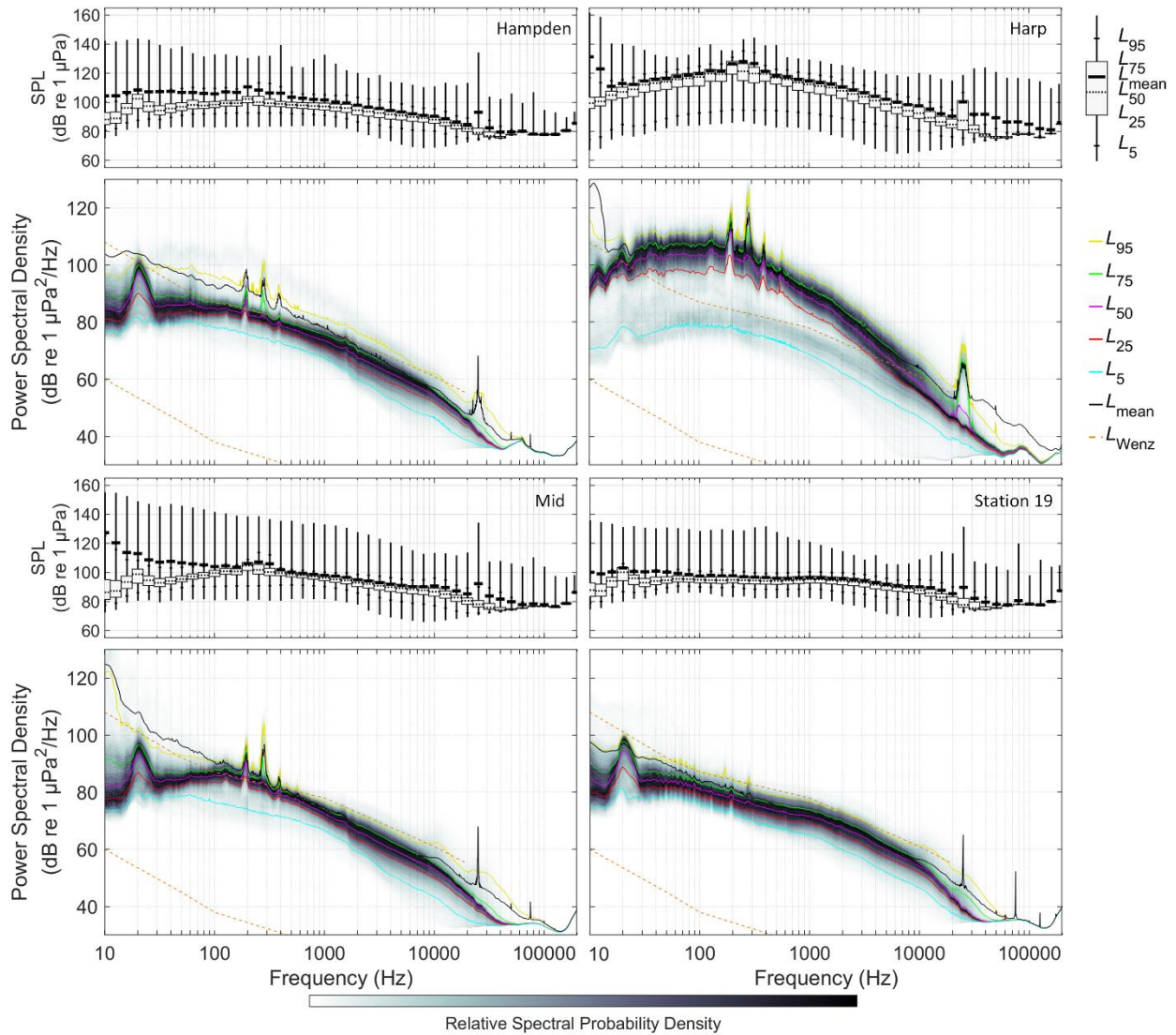


Figure 9. Percentiles and mean of decidecade sound pressure level (SPL) and exceedance percentiles and probability density (grayscale) of 1-min power spectral density levels compared to the Wenz curve limits of prevailing noise (Wenz 1962) for each and station.

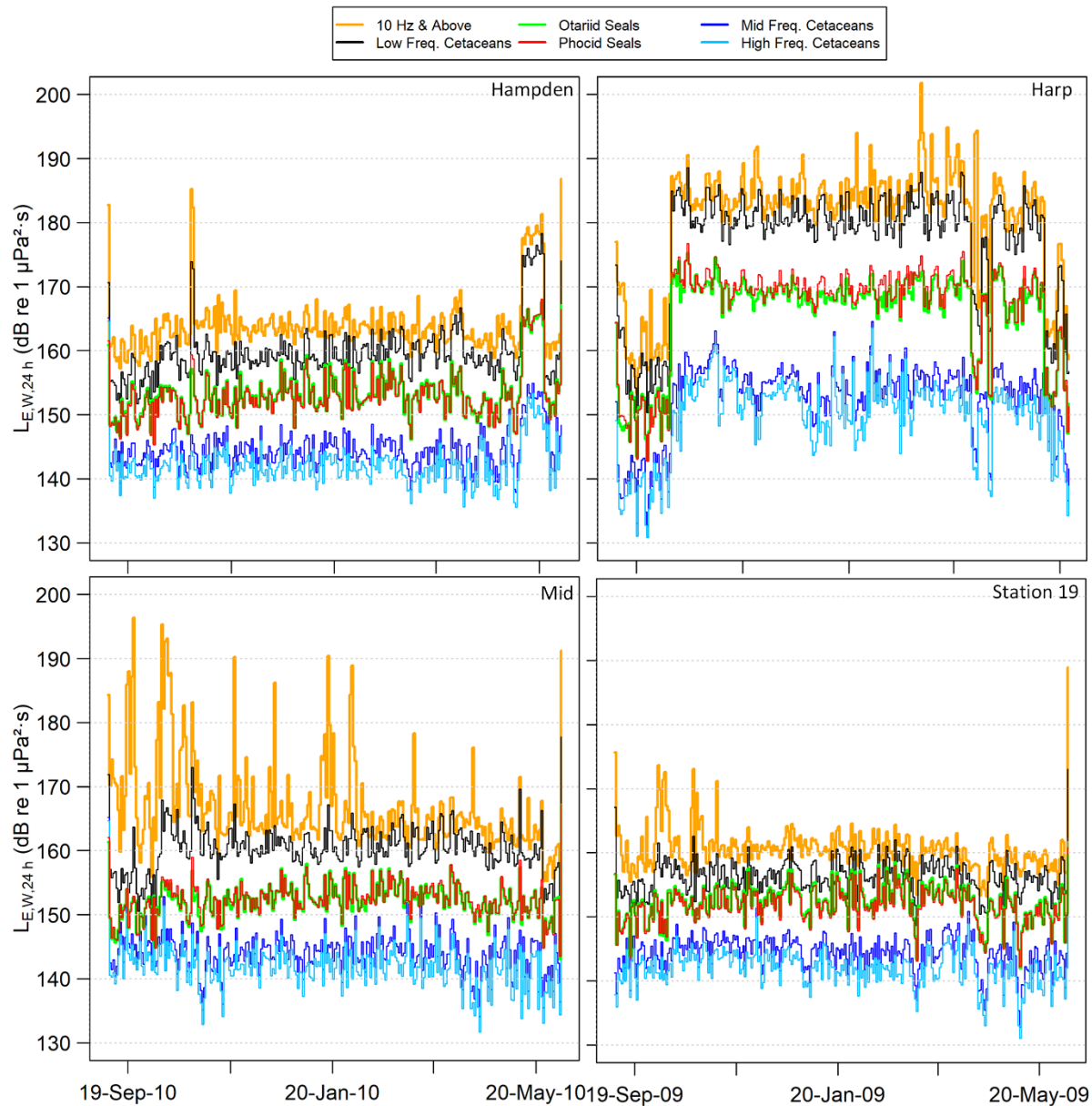


Figure 10. Auditory Frequency Weighted as well as 10 Hz and above daily sound exposure levels (SEL) for each station (NMFS 2018). High daily SEL for the 10 Hz and above frequency band that are not also associated with an increased daily SEL for the low-frequency cetacean auditory frequency weighting are an indication of pseudo-sound from water flowing over the hydrophones affecting the measured levels. This is also manifested as dark red patches below 30 Hz in Figure 8.

Three sound sources stand out in the measured soundscapes: fin whales, the MODU, and seismic surveying (Figure 11):

- Fin whales are well known to produce a mating song centred at 20 Hz in fall and winter in the North Atlantic (Delarue et al. 2018). The sound from the fin whales is evident as the bright band at 20 Hz in Figure 8 and the peak in the percentile plots of Figure 9. The presence of fin whales is evident at all stations, although the bright band and peak are not as clear for Harp (EL 1165B), because the broadband MODU' dynamic positioning system sound is present at levels higher than the fin whale vocalizations.

- The MODU had three sound components that were detectable—its overall broadband sound; three distinct tones at 195, 293, and 397 Hz; and sounds from ultra-short-baseline (USBL) transponders deployed around the platform (Figure 12). The MODU was on dynamic position assist (DP) throughout the operations at HARP (EL 1165B), which contributed to the broadband sound. Figures 8–10 start at 10 Hz, which is generally considered the lowest frequency that is well calibrated and often free from flow and movement noise contamination. The MODU generated a 5 Hz tone (300 rpm) that was below the 10 Hz cut-off. The energy in this tone was lower than that in the broad tones at 195, 293, and 397 Hz (Figure 13); excluding this energy from the 10 Hz and above daily SEL would not affect the total.
- Seismic surveys occurred between 1–8 Oct and 18–20 Oct 2019. These surveys increased sound levels from ~10–300 Hz at Hampden (EL 1165A), Mid, and Stn 19 to varying degrees, which was reflected in the LTSA (Figure 8) and SEL (Figure 10). Because the surveying duration was only a few days out of a nine-month deployment, the elevated levels did not influence the percentiles in Figure 9. Figure 14 shows an example of the time-series and spectrogram when seismic surveying was present.

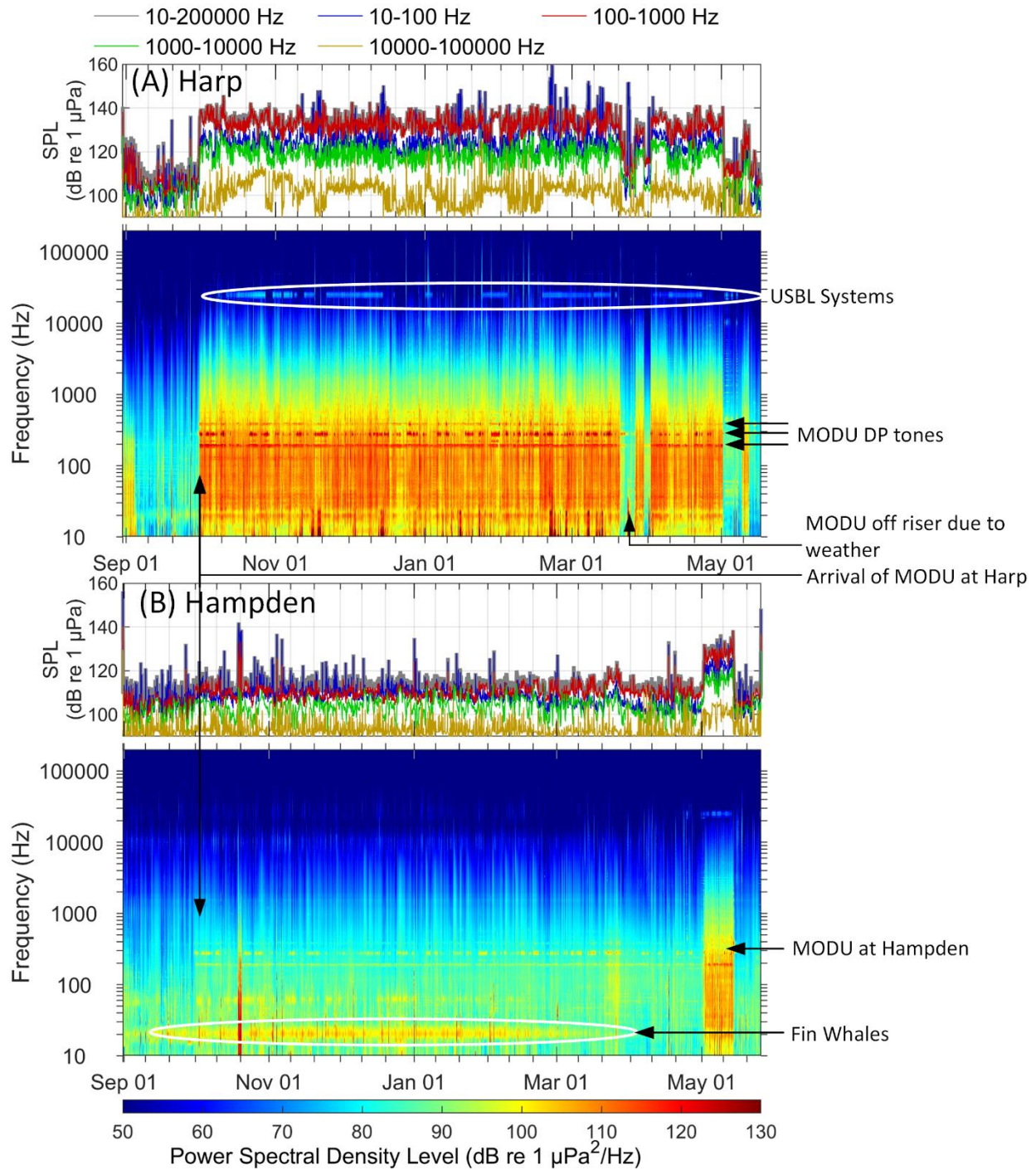


Figure 11. Annotated summary of the sound levels measured at (A) Harp (EL 1165B) and (B) Hampden (EL 1165A) from September 2019 to May 2020. In each figure, the top panel shows the mean hourly in-band sound pressure level for five bands: the complete recording band of 10–200000 Hz as well as the decade bands of 10–100, 100–1000, 1000–10000, and 10000–100000 Hz. The bottom panels show the long-term spectral averages using a logarithmic frequency scale for the vertical axes. Notable elements of the soundscape are identified.

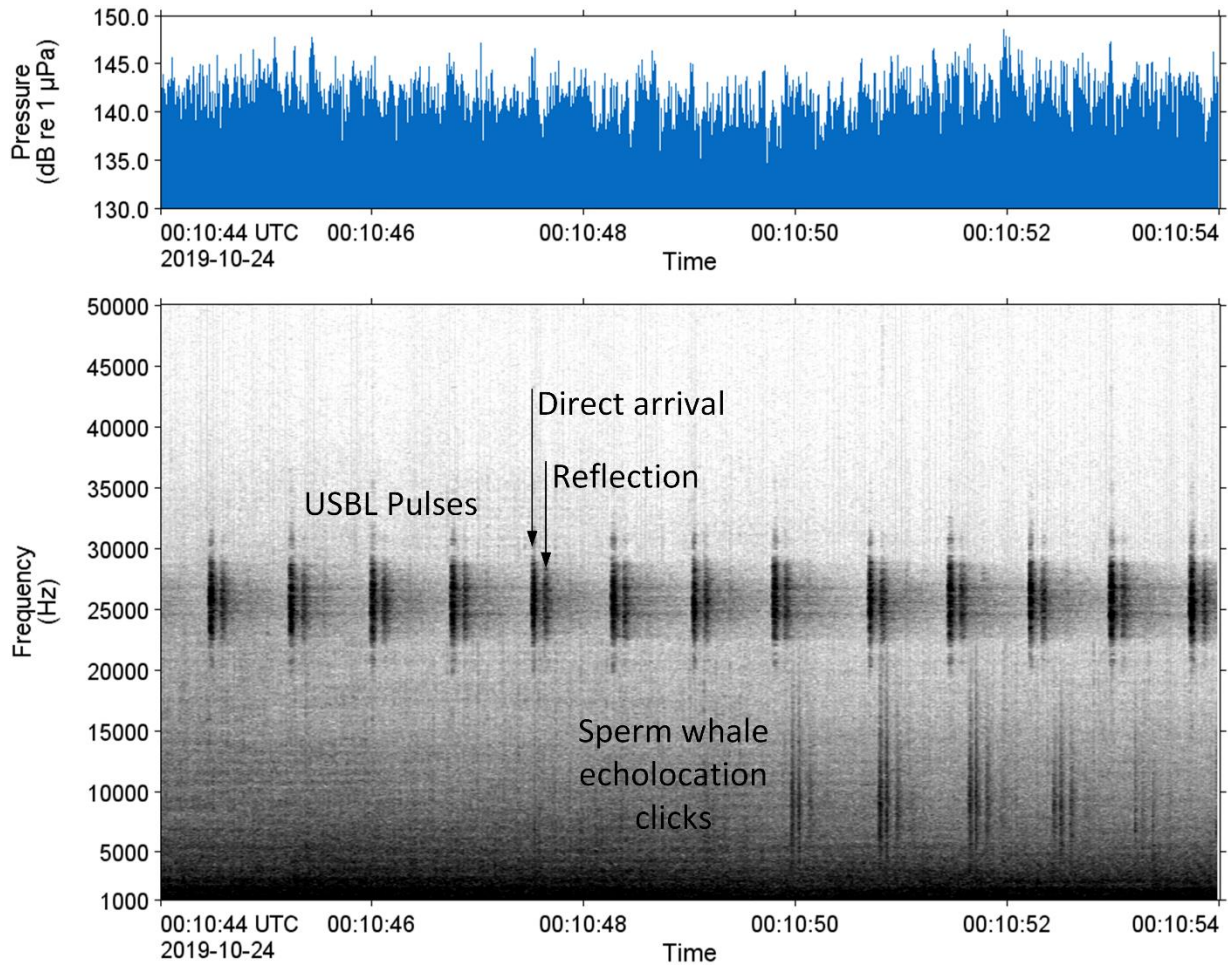


Figure 12. Ten seconds of data from 24 Oct 2019 at Harp (EL 1165B) showing the presumed pulses from the ultra-short-baseline (USBL) system as well as a series of echolocation clicks from a sperm whale. Both the USBL and sperm whale clicks show an arrival directly from the source as well as one or two reflections from the seabed.

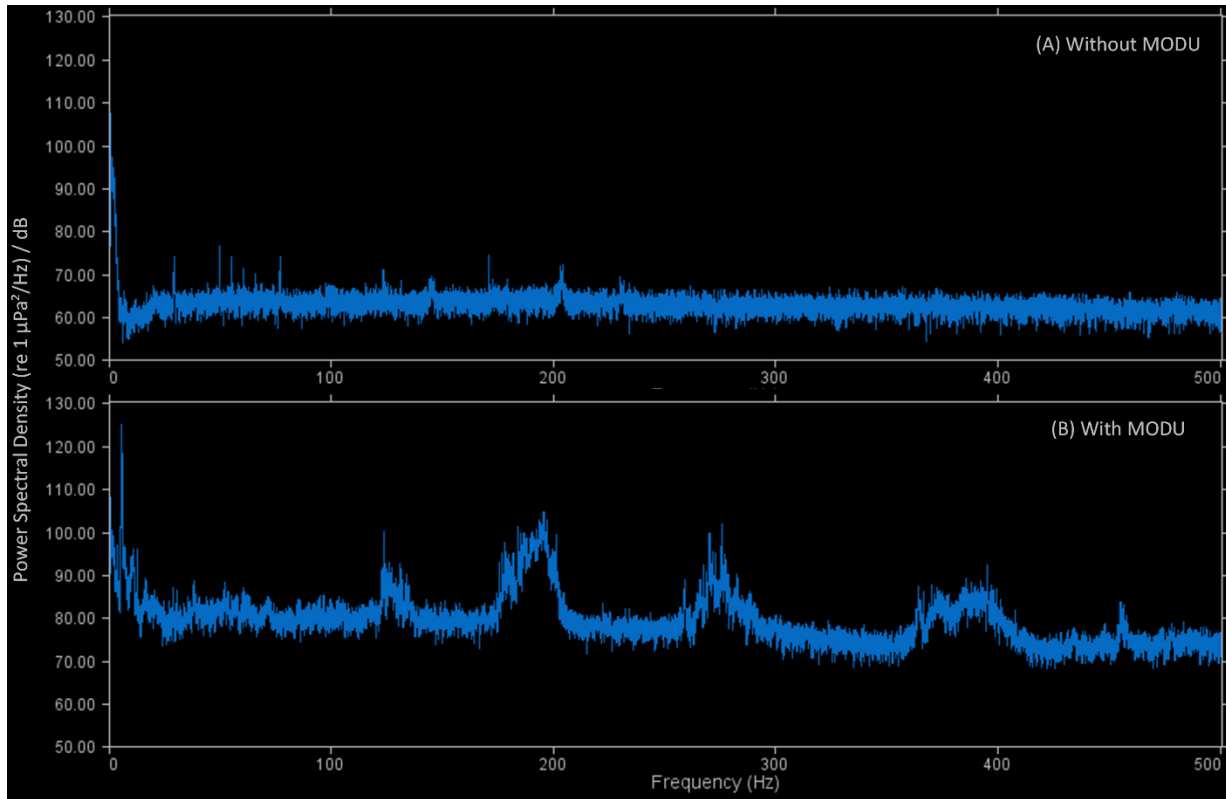


Figure 13. Comparison of the spectra measured at Harp (EL 1165B) (A) without and (B) with the MODU present. (32,000 Hz sampling rate, Fast Fourier Transform parameters: 1,024,000 pts, 512,000 pt overlap, Hann window, 10 averages).

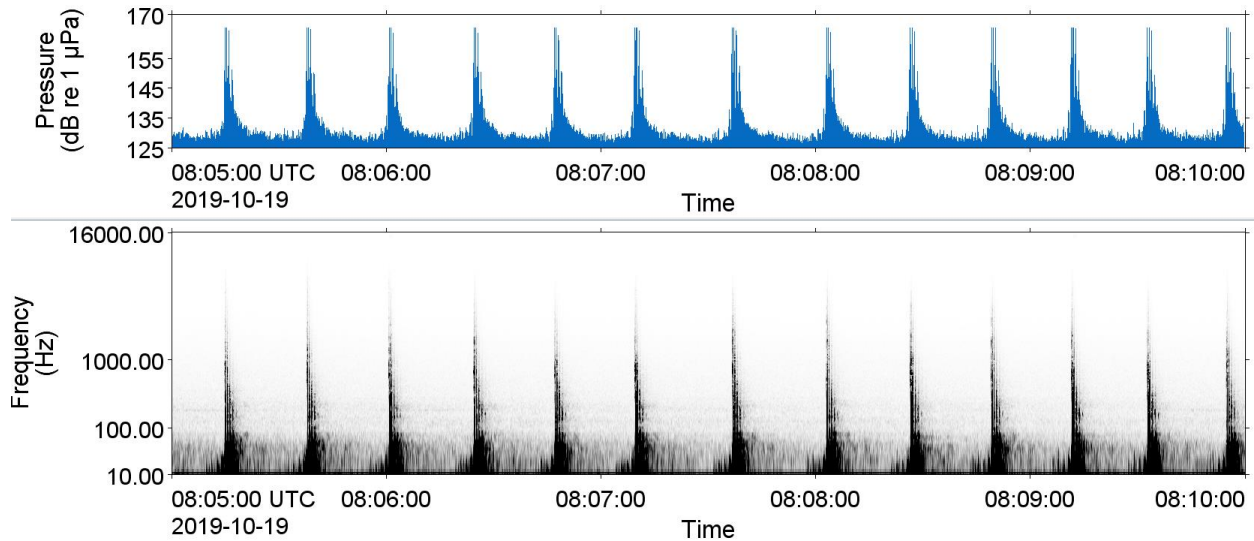


Figure 14. Five seconds of data from the Hampden (EL 1165A) site during seismic surveying.

3.2. Detection Range Modelling

Detection Range Modelling (DRM) was performed for the most common signal of each species detected during the study. We modelled transmission losses for the two months with the most different sound speed profile (September and March) (Table 7). The resulting detection ranges were generally comparable, with the exception of Harp where they were substantially lower in March. The MODU was not present at Harp in September. Here we present spatial detection range plots for March (Figure 15 to 25; see also Appendix C.5 for ranges modeled for September).

Delphinid and beaked whale echolocation clicks appeared to be detectable at similar ranges regardless of station. Sperm whale clicks had generally longer detection ranges, particularly at Harp in September, but the presence of the MODU led to significant decrease in detection ranges. Sperm whale clicks are lower in frequency than those of other detected odontocetes and, therefore, are more affected by MODU masking noise, which is highest below 5 kHz where sperm whale clicks can contain significant energy. There is additional attenuation of higher frequencies in shallow water as well that also affected detection range. In the case of sperm whales, it should be noted that the maximum recorded source factor of a click (236 dB re $1\mu\text{Pa}^2\cdot\text{m}^2$, recorded on-axis; Møhl et al. (2003)) is substantially higher than that used in the modelling and would yield significantly higher detection ranges. However, it would apply to a minority of cases, and we believe that the ranges presented here, as for the other odontocete clicks, are more representative of the majority of detection events where the clicks would be received off-axis. Harbour porpoise clicks can be detected, in optimal conditions (i.e. signal at the upper end of the source level range in low noise conditions), up to about 1.5 km; beaked whale and delphinid clicks up to 9.7 km; and sperm whale clicks up to 50 km. (Appendix C.5).

Killer whale tonal calls and delphinid whistles had the longest detection ranges at Harp, where they were detectable up to 6.5 to 15.7 km, respectively, in the best scenarios (Appendix C.5). At the other stations, a 50% probability of detection in median ambient noise conditions was achievable at a range of ~100 m at Stn 19 and Hampden, and up to 600 m at Mid (Table 7; Figures 19 and 20).

Among baleen whales, blue whales had the longest median detection ranges, followed by fin whales (Figures 15 and 16). Calls were detectable up to a maximum of 76–100 km at all stations for both species (Appendix C.5). However, median detection ranges (Table 7) showed much more variability.

Vocalizations in median noise conditions were generally detectable with a 50% probability at long and similar ranges at Hampden (EL 1165A) and Mid but had shorter detection ranges at Stn 19. Seasonal variations in detection ranges were limited except at Harp where a large decrease in the detection ranges of blue and fin whale calls was observed between September and March.

A similar pattern was observed for sei whale vocalizations, albeit with generally shorter ranges than for blue and fin whale calls. Seasonal variations in detection range were most pronounced at Harp. Detection ranges were shortest at Stn 19 and generally highest at Mid and Hampden. For all three baleen whale species, the low ranges at Stn 19 were not intuitive. Propagation was restricted to the south of Stn 19 by of the steep slope of the Sackville Spur in that area, which created a shadow zone to the south. The short ranges for vocalizations produced in the deep waters generally north of Stn 19 likely relate to upward refracting propagation conditions that prevented vocalizations from reaching the recorder (at 1600 m depth). It is also possible that the geoacoustic properties of the seafloor used in the modelling may not accurately represent the composition and thickness of the sediment layers of the Sackville Spur, which could affect the validity of the ranges presented here, particularly for sei whale downsweeps (Figure 17).

Humpback whale vocalizations had low detection ranges compared to other baleen whale species (Figure 18), which is primarily due to lower source levels. They were barely detectable under median noise conditions at all stations except at Mid and Harp in September (Table 7). The maximum potential detection range occurred at Mid in September (~59 km; Appendix C.5).

An advantage of restricted detection ranges for marine mammal vocalizations is knowing that the detected sounds are proximal to the recorder and can be used to describe the occurrence of marine mammals in its vicinity.

Table 7. Detection ranges (kilometers) for species and signals most likely to be encountered near the four monitored stations and for background noise conditions recorded in March and September at each station. The range of distances represent minimum and maximum detection ranges across all modelled azimuths for a 50% probability of detection under median noise conditions for average source levels. They represent the most likely detection ranges. NBW: Northern bottlenose whale; SBW: Sowerby's beaked whale. ND: not detectable. N/A: Not applicable.

Species	Hampden (EL 1165A)		Harp (EL 1165B)		Mid		Stn 19	
	March	September	March	September	March	September	March	September
Blue whale A-B calls	34.0 - 83.9	33.4 - 85.3	9.0 - 16.8	43.6 - 100.0	36.1-98.2	23.6 - 59.5	4.4 - 20.0	4.6-20.9
Fin whale 20-Hz calls	35.4 - 86.7	27.9 - 61.7	9.6 - 18.5	39.1 - 100.0	40.2 - 100.0	31.1 - 74.3	4.1 - 17.2	3.7-8.6
Sei whale downsweeps	12.1 - 22.1	14.4 - 32.1	1.8 - 2.2	13.5 - 73.2	39.1 - 100.0	20.7 - 31.6	2.2-3.3	2.2-3.2
Humpback whale moans	0.0-0.1	0.0-0.1	ND	3.1 - 5.6	ND	3.0 - 4.7	0.0-0.1	0.0-0.1
Killer whale tonal signals	0.0-0.1	0.0-0.1	ND	0.5 - 0.6	ND	ND	0.0-0.1	0.0-0.1
Delphinid whistles	0.0-0.1	0.0-0.1	0.0-0.1	2.3 - 2.4	0.0 - 0.3	0.6 - 0.6	0.0-0.1	0.0-0.1
Delphinid clicks	3.1-3.2	3.2-3.5	2.1 - 2.4	5.1 - 5.6	3.3 - 3.7	3.5 - 5.1	3.1-3.3	3.2-3.4
Sperm whale click	3.9 - 4.4	7.5 - 8.1	1.1 - 1.4	11.4 - 16.4	4.4 - 5.4	6.5 - 7.5	3.0 - 3.9	3.6-4.4
Harbour porpoise clicks	N/A	N/A	0.6 - 1.1	0.9-1.2	0.1-0.7	0.3-1.0	N/A	N/A
NBW, clicks	3.6-3.7	3.5-3.7	2.4 - 2.6	4.4 - 4.7	3.7 - 4.1	3.6 - 3.9	3.4-3.7	3.3 - 3.7
SBW, clicks	1.9-2.1	1.8-2.0	1.9 - 2.3	2.1-2.2	1.9-2.3	2.0-2.2	1.8-2.0	1.9-2.0

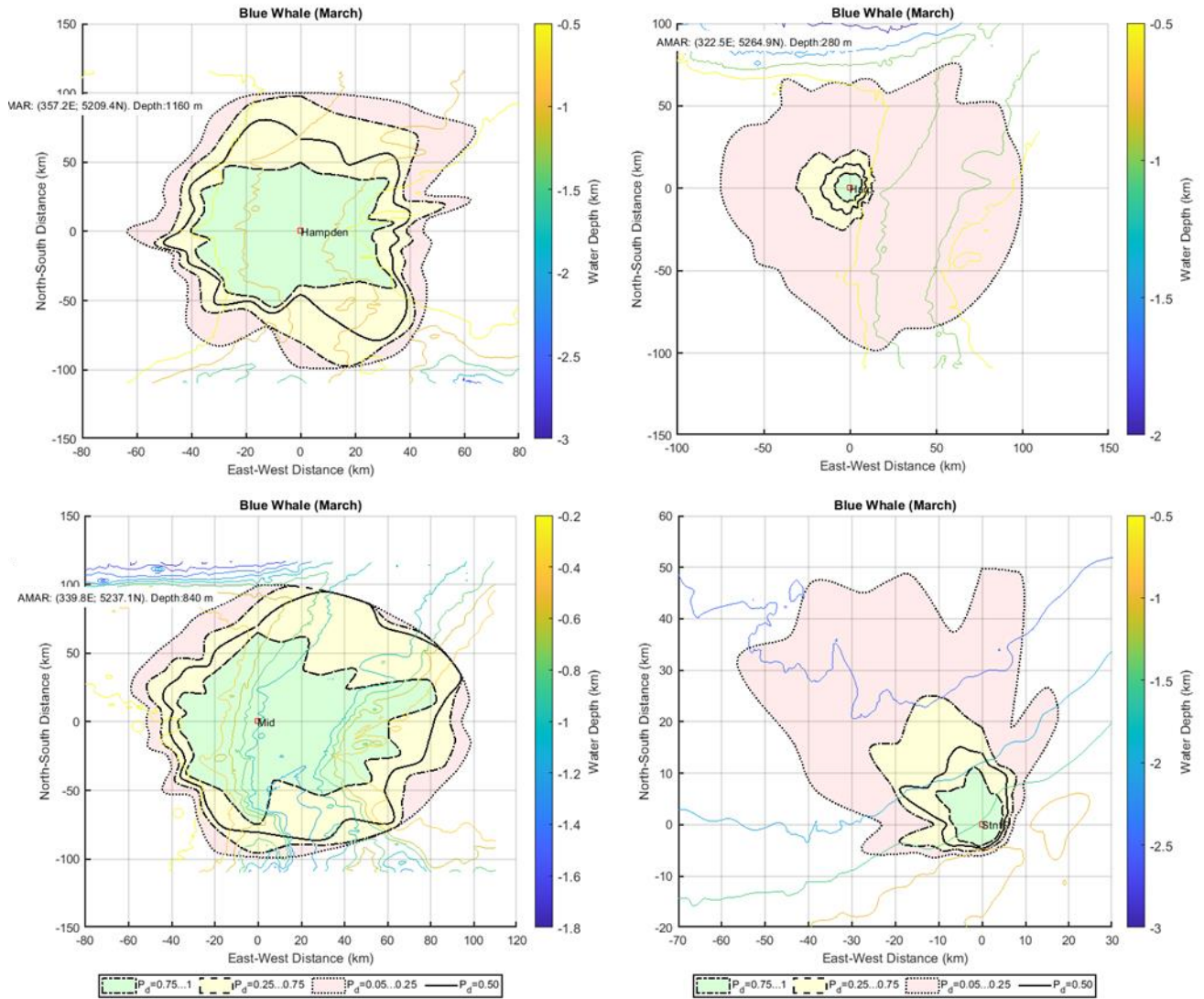


Figure 15. Blue whale infrasonic A-B calls: Detection ranges associated with various probability of detection under noise conditions recorded in March at Hampden (EL 1165A) (top left), Harp (EL 1165B) (top right), Mid (bottom left) and Stn 19 (bottom right), shown at the centre of each figure. The solid black line shows the range for a 50% probability of detection.

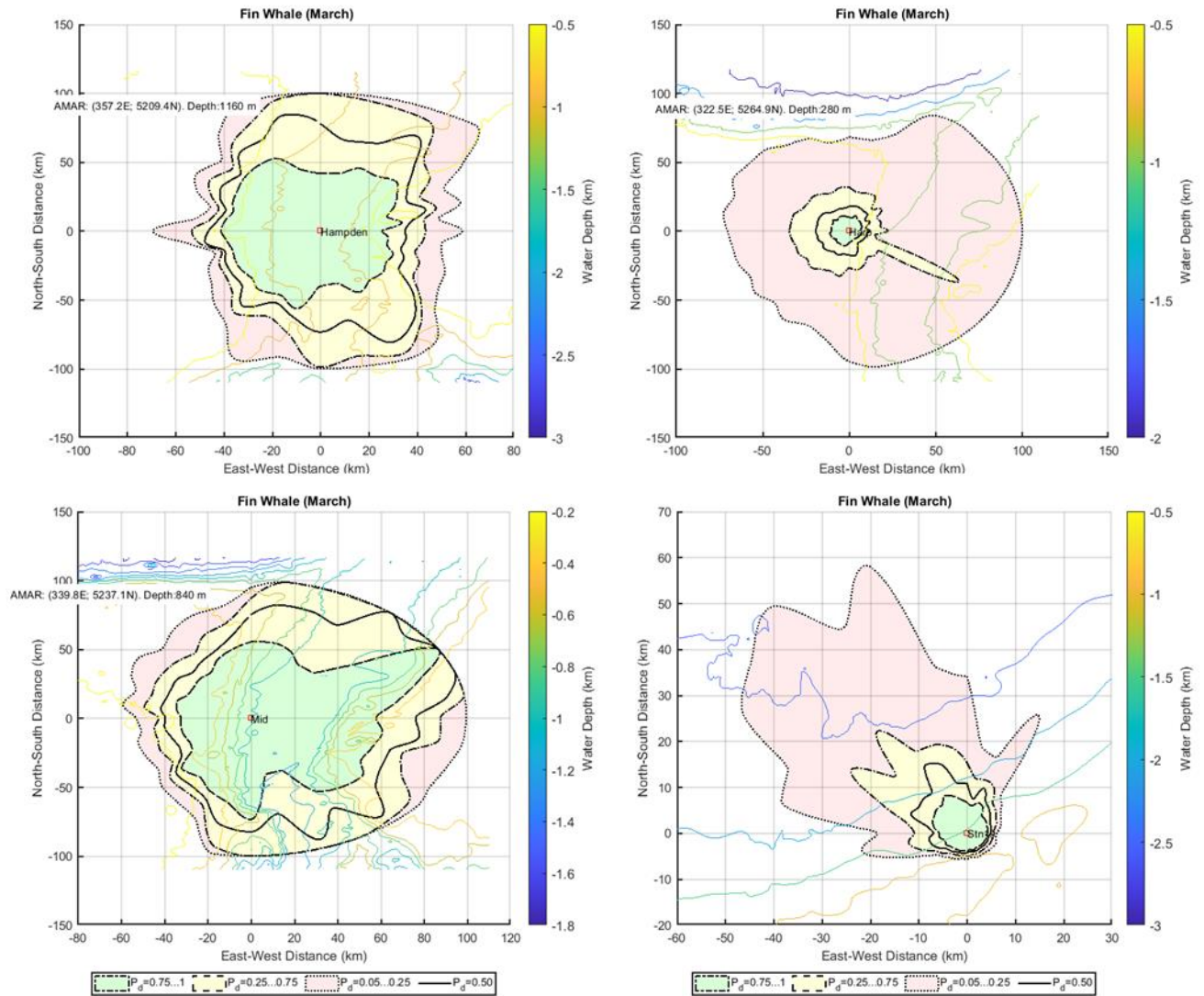


Figure 16. Fin whale 20-Hz calls: Detection ranges associated with various probability of detection under noise conditions recorded in March at Hampden (EL 1165A) (top left), Harp (EL 1165B) (top right), Mid (bottom left) and Stn 19 (bottom right), shown at the centre of each figure. The solid black line shows the range for a 50% probability of detection.

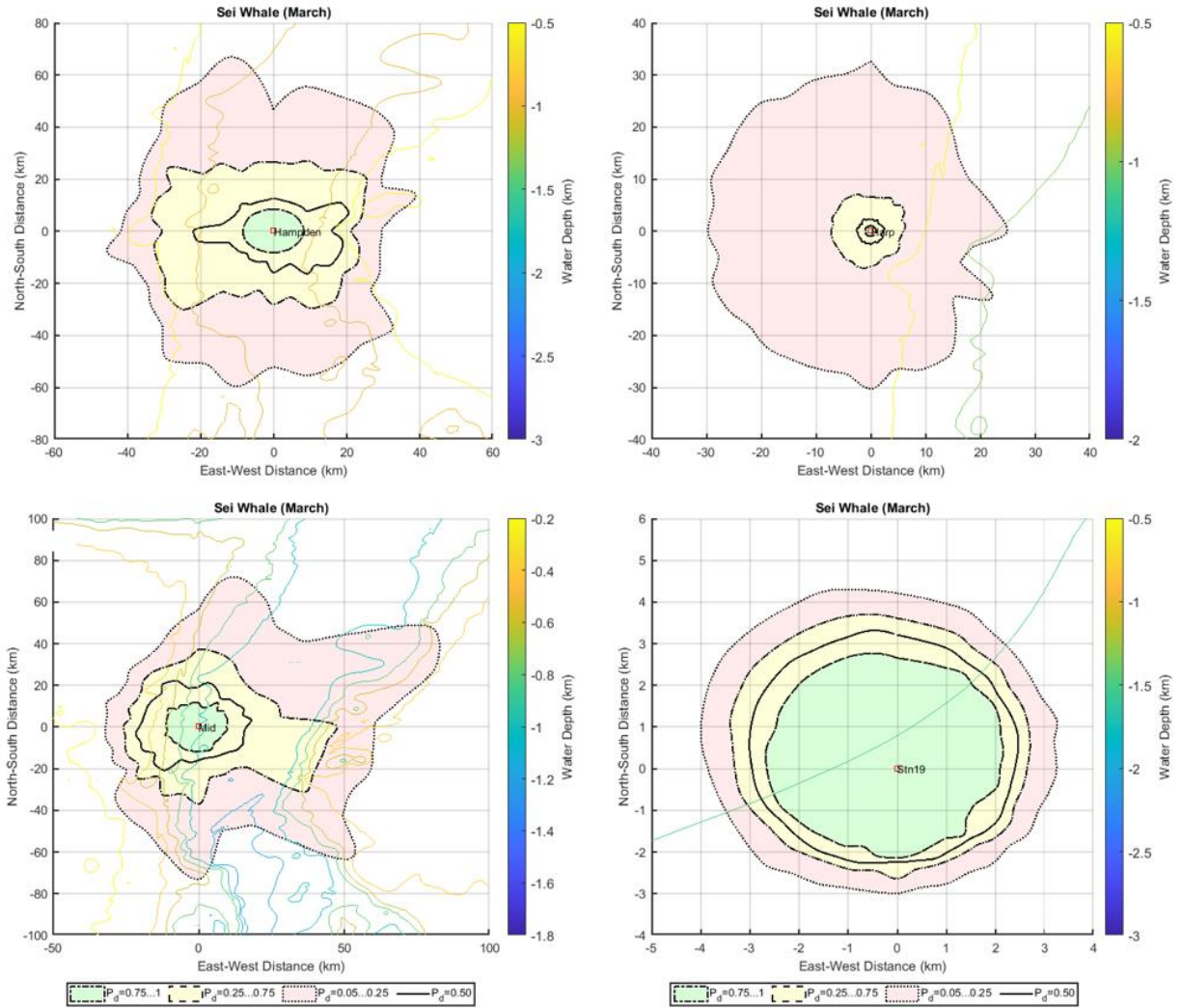


Figure 17. Sei whale downsweeps: Detection ranges associated with various probability of detection under noise conditions recorded in March at Hampden (EL 1165A) (top left), Harp (EL 1165B) (top right), Mid (bottom left) and Stn 19 (bottom right), shown at the centre of each figure. The solid black line shows the range for a 50% probability of detection.

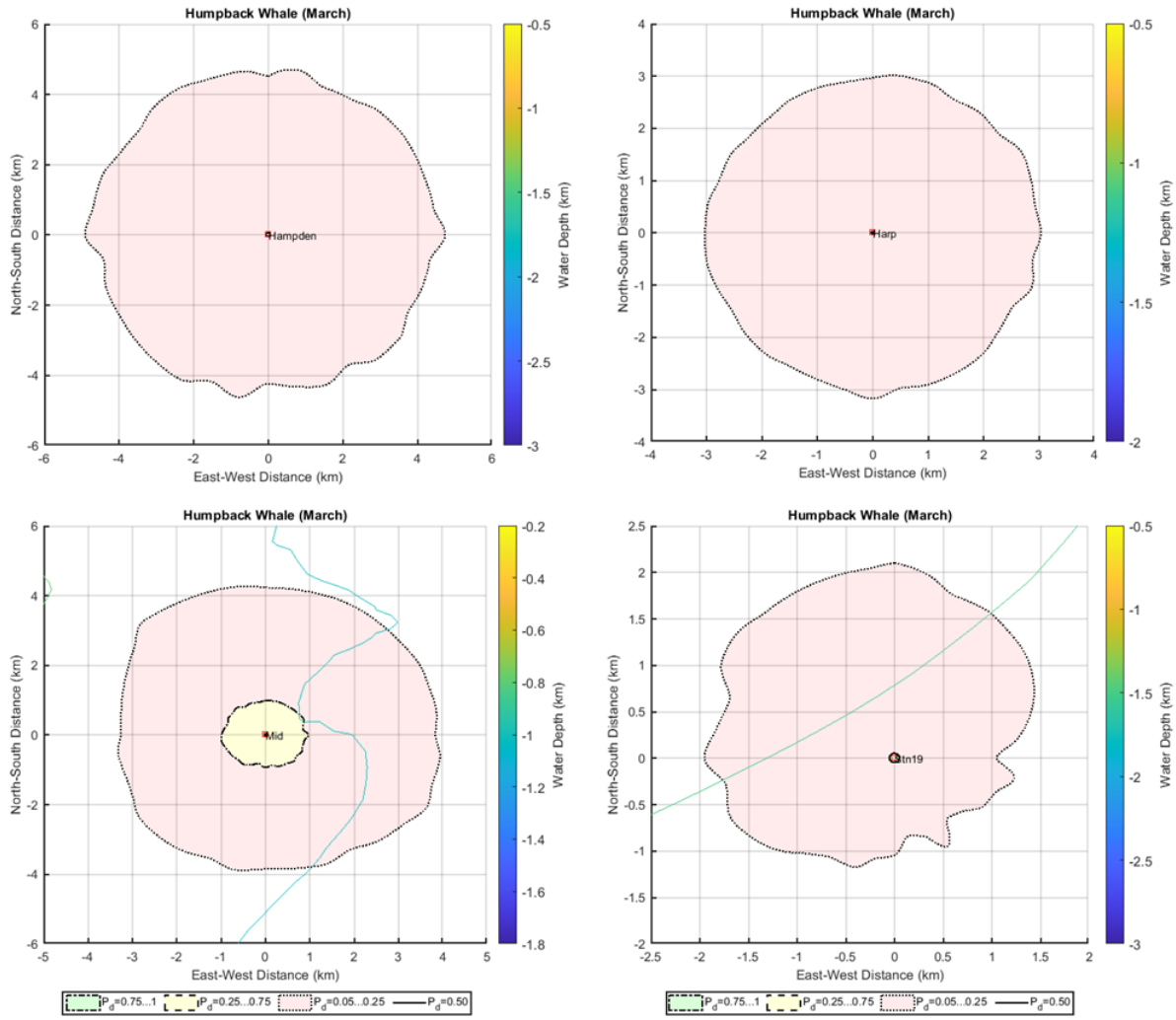


Figure 18. Humpback whale song unit: Detection ranges associated with various probability of detection under noise conditions recorded in March at Hampden (EL 1165A) (top left), Harp (EL 1165B) (top right), Mid (bottom left) and Stn 19 (bottom right), shown at the centre of each figure. The solid black line shows the range for a 50% probability of detection.

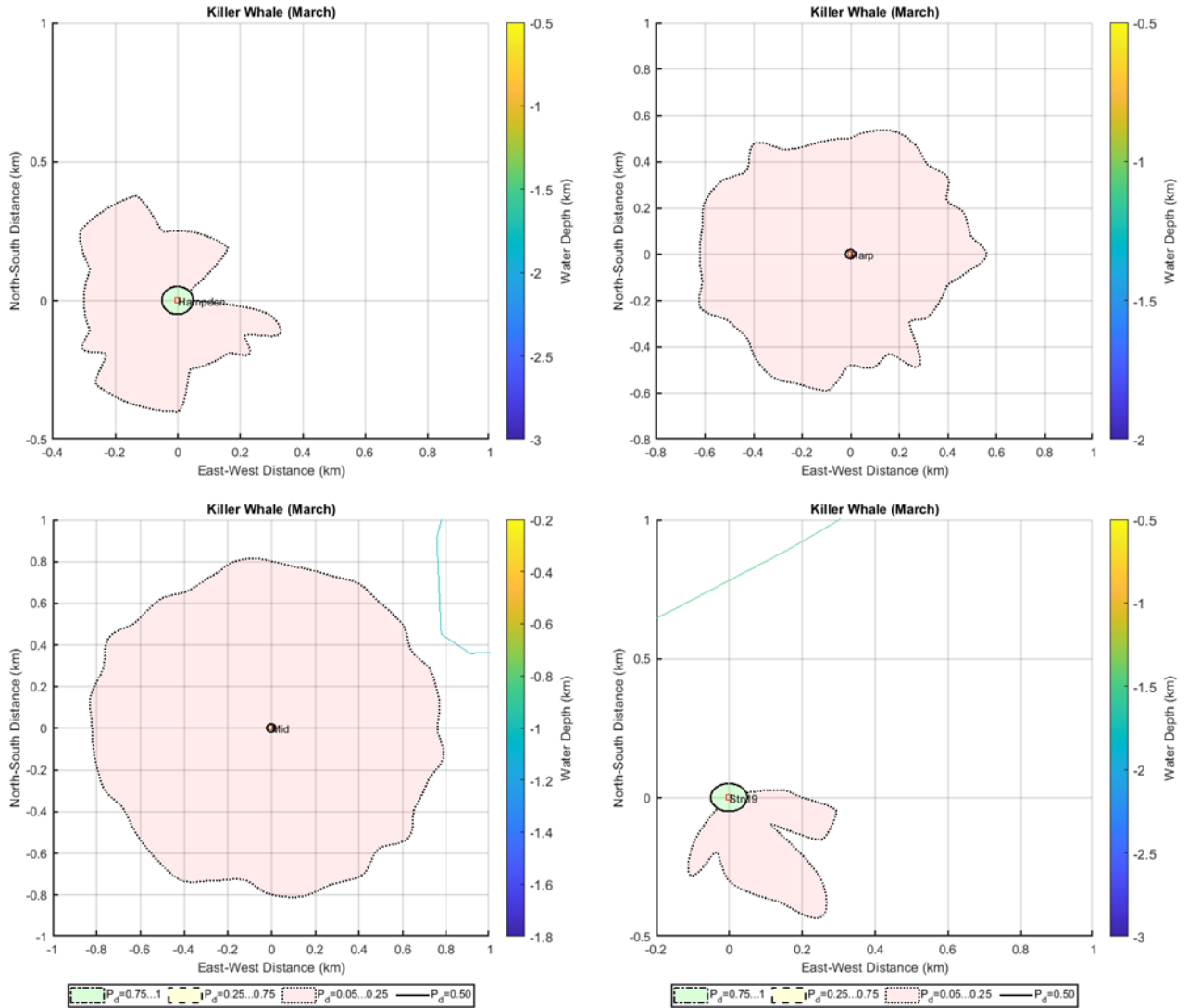


Figure 19. Killer whale tonal calls: Detection ranges associated with various probability of detection under noise conditions recorded in March at Hampden (EL 1165A) (top left), Harp (EL 1165B) (top right), Mid (bottom left) and Stn 19 (bottom right), shown at the centre of each figure. The solid black line shows the range for a 50% probability of detection.

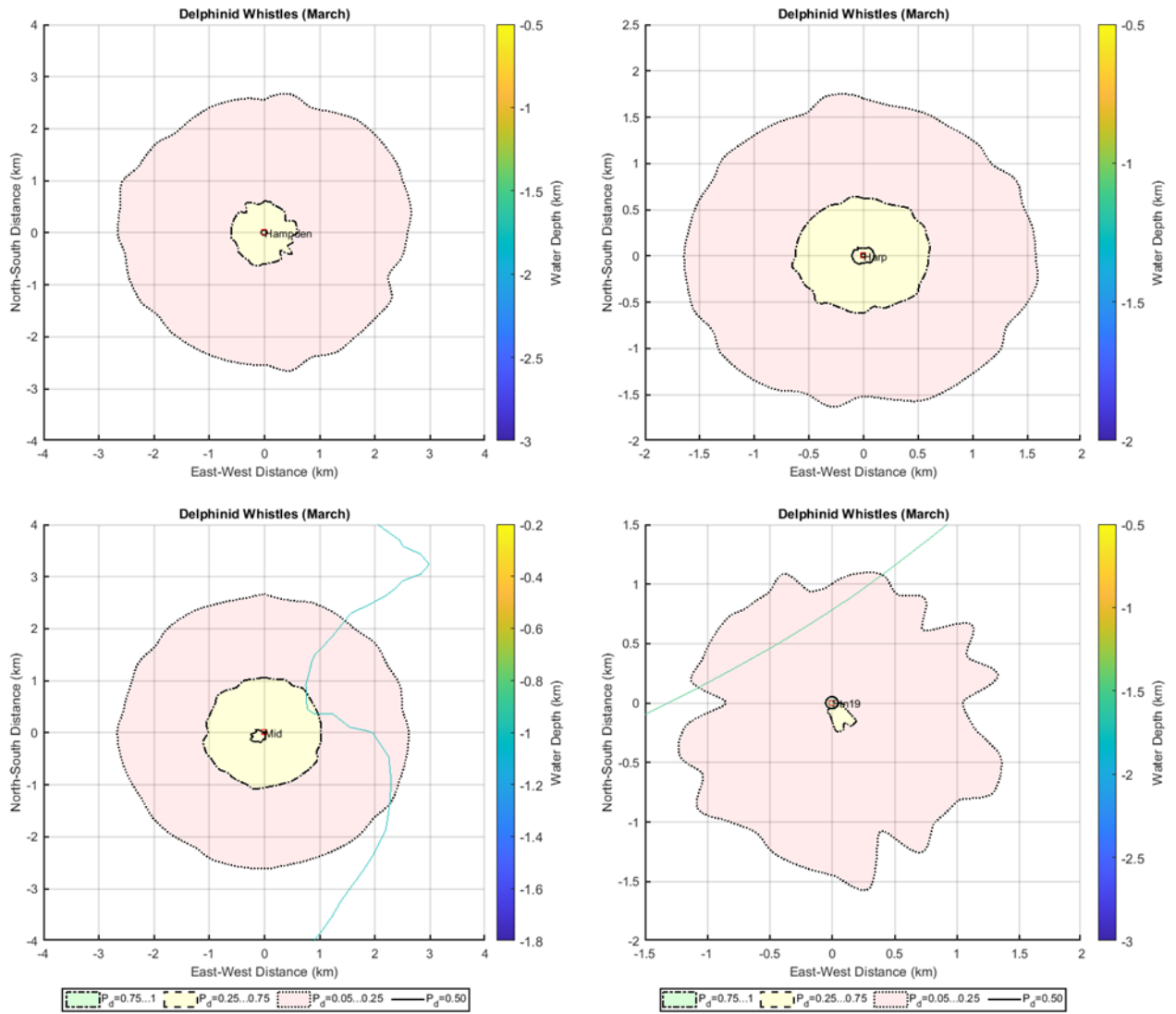


Figure 20. Dolphin whistles: Detection ranges associated with various probability of detection under noise conditions recorded in March at Hampden (EL 1165A) (top left), Harp (EL 1165B) (top right), Mid (bottom left) and Stn 19 (bottom right), shown at the centre of each figure. The solid black line shows the range for a 50% probability of detection.

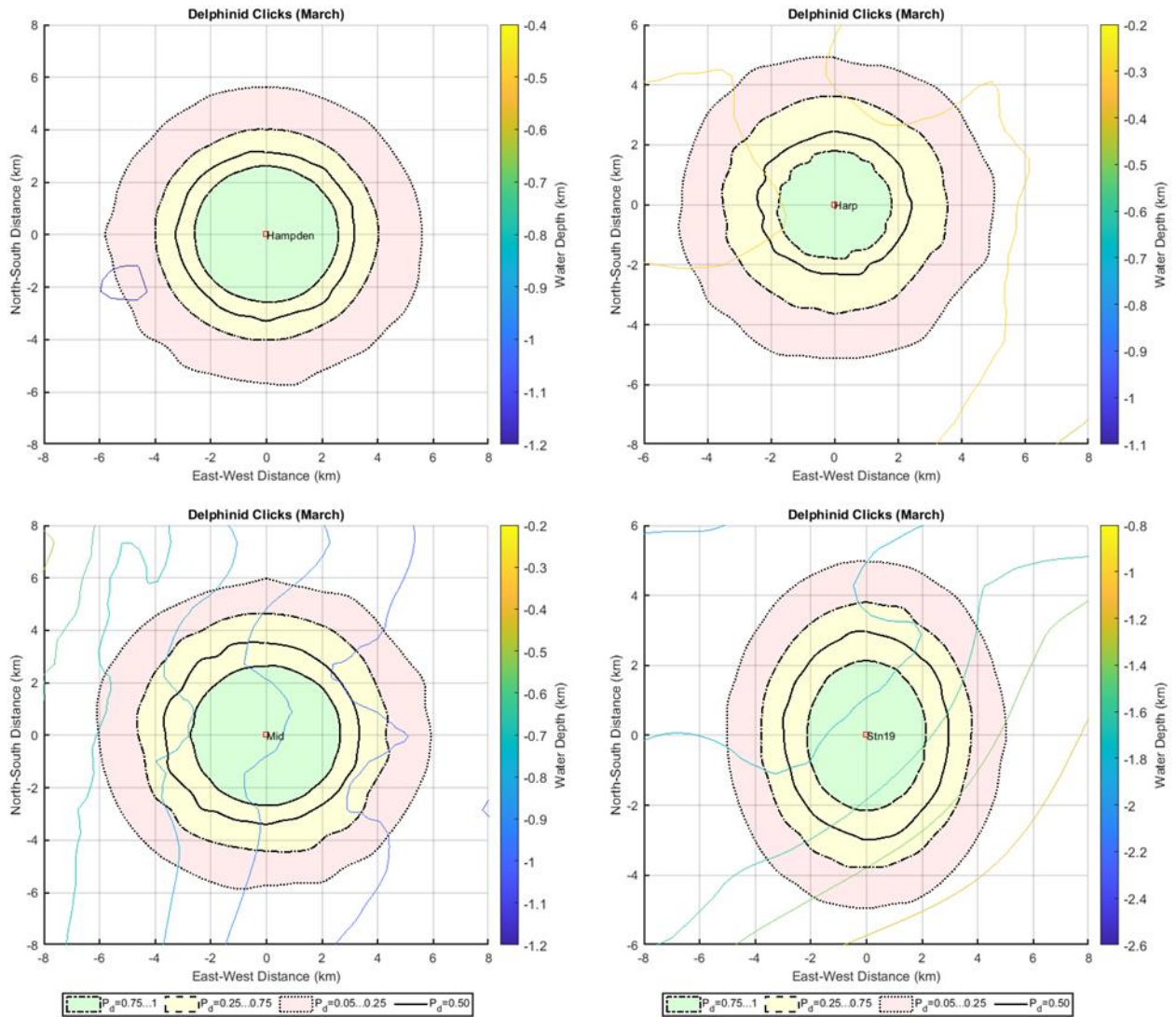


Figure 21. Delphinid clicks: Detection ranges associated with various probability of detection under noise conditions recorded in March at Hampden (EL 1165A) (top left), Harp (EL 1165B) (top right), Mid (bottom left) and Stn 19 (bottom right), shown at the centre of each figure. The solid black line shows the range for a 50% probability of detection.

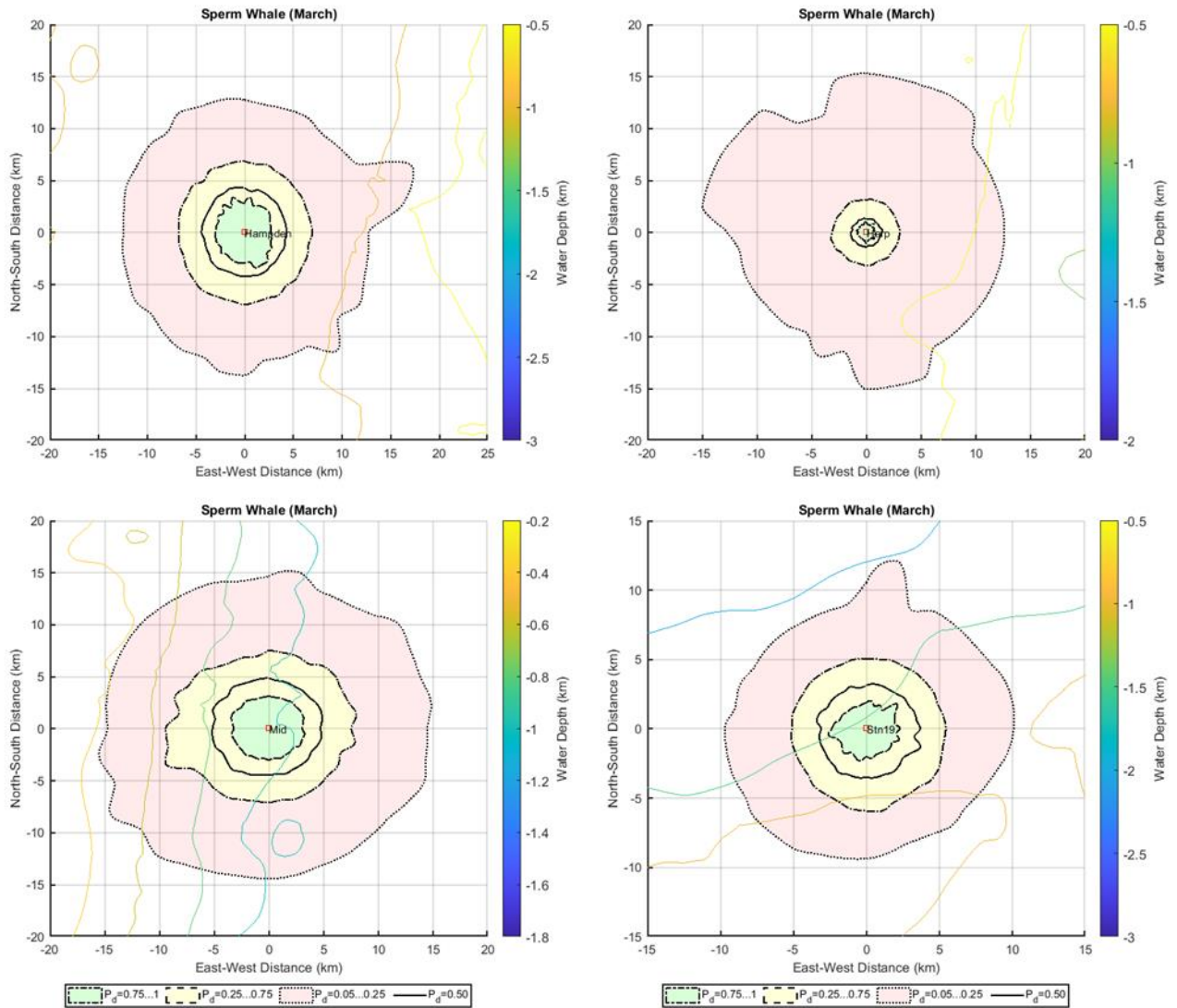


Figure 22. Sperm whale clicks: Detection ranges associated with various probability of detection under noise conditions recorded in March at Hampden (EL 1165A) (top left), Harp (EL 1165B) (top right), Mid (bottom left) and Stn 19 (bottom right), shown at the centre of each figure. The solid black line shows the range for a 50% probability of detection.

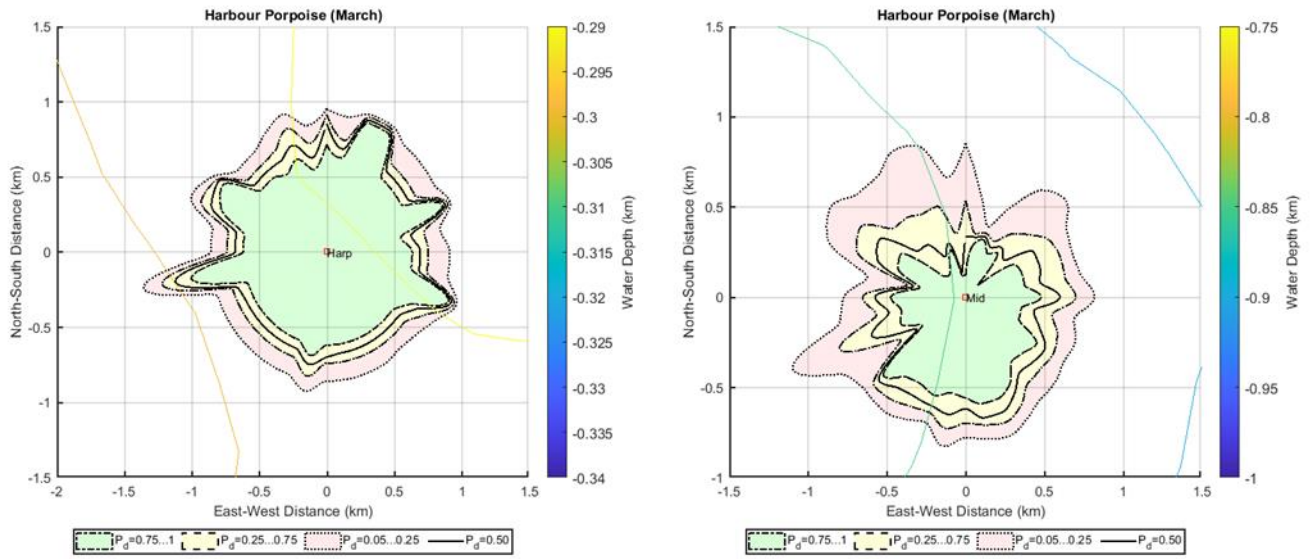


Figure 23. Harbour porpoise clicks: Detection ranges associated with various probability of detection under noise conditions recorded in March at Harp (EL 1165B) (left) and Mid (right). The solid black line shows the range for a 50% probability of detection.

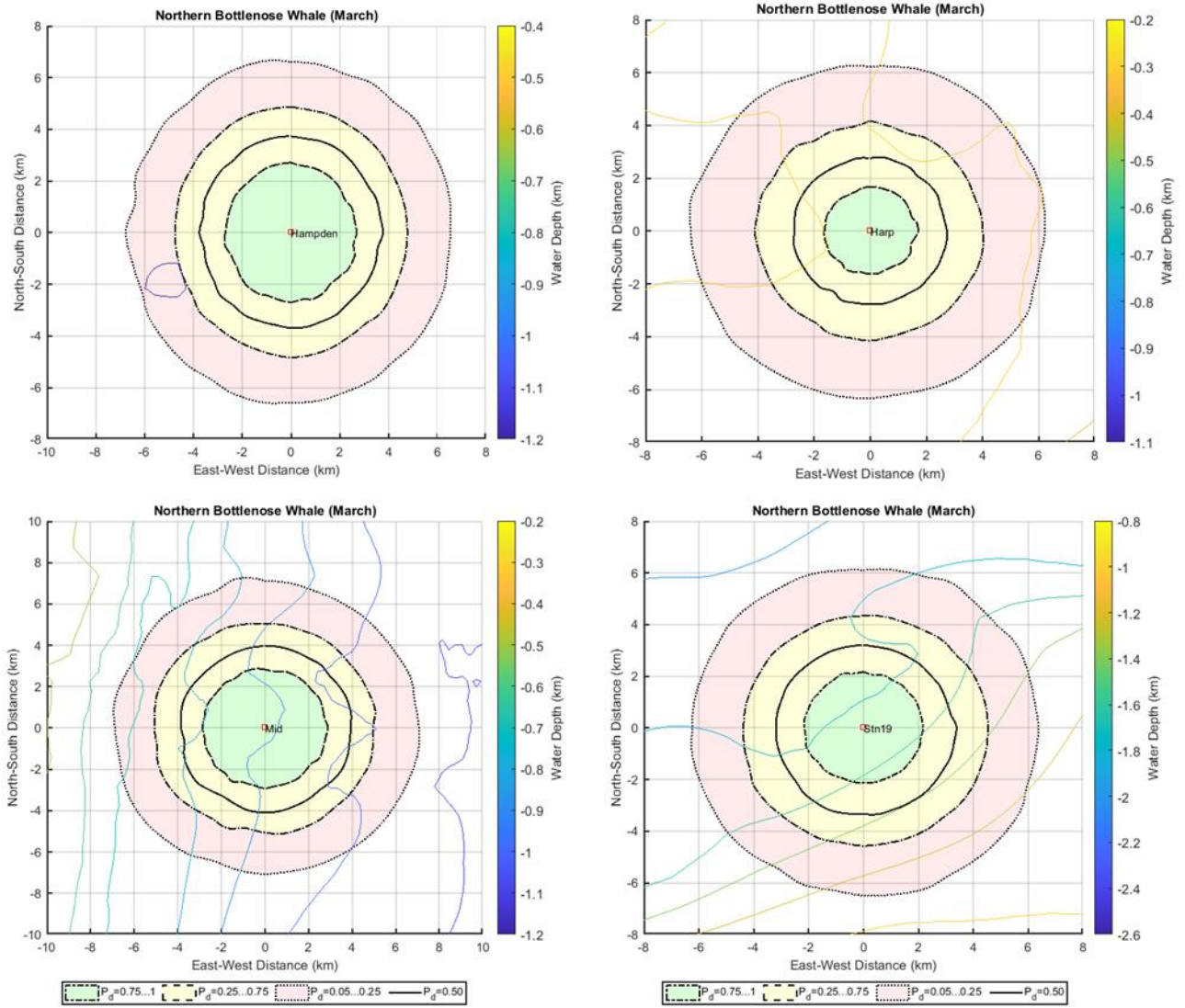


Figure 24. Northern bottlenose whale clicks: Detection ranges associated with various probability of detection under noise conditions recorded in March at Hampden (EL 1165A) (top left), Harp (EL 1165B) (top right), Mid (bottom left) and Stn 19 (bottom right), shown at the centre of each figure. The solid black line shows the range for a 50% probability of detection.

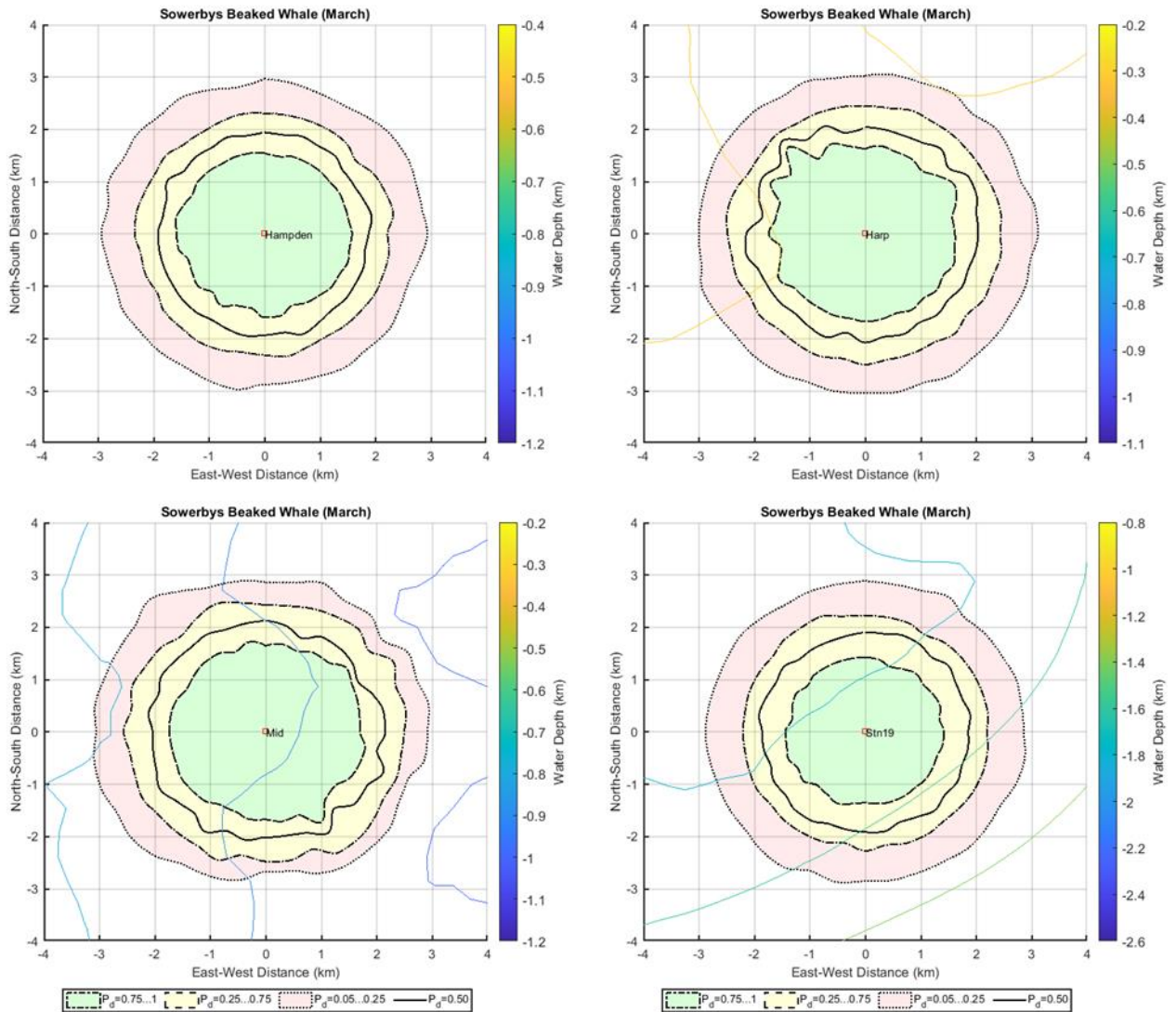


Figure 25. Sowerby's beaked whale clicks: Detection ranges associated with various probability of detection under noise conditions recorded in March at Hampden (EL 1165A) (top left), Harp (EL 1165B) (top right), Mid (bottom left) and Stn 19 (bottom right), shown at the centre of each figure. The solid black line shows the range for a 50% probability of detection.

3.3. MODU Underwater Radiated Noise

The MODU URN was computed by adding the distribution of received sound pressure levels at Harp (EL 1165B) to the modelled propagation loss (Figure 26). The Harp (EL 1165B) data were used because the range to Harp (EL 1165B) was only 2100 m, which was expected to produce better results than could be obtained at Hampden (EL 1165A) where only 10 days of data were collected and at a range of 5300 m. Since there were large amounts of data to work with at Harp (EL 1165B), the months with uninterrupted data (Oct 19 – Feb 20, inclusive) were chosen for analysis. The median broadband source factor was 191.2 dB re 1 $\mu\text{Pa}^2\cdot\text{m}^2$. The maximum decade was the 200 Hz band, which had a median source factor of 183.4 dB re 1 $\mu\text{Pa}^2\cdot\text{m}^2$.

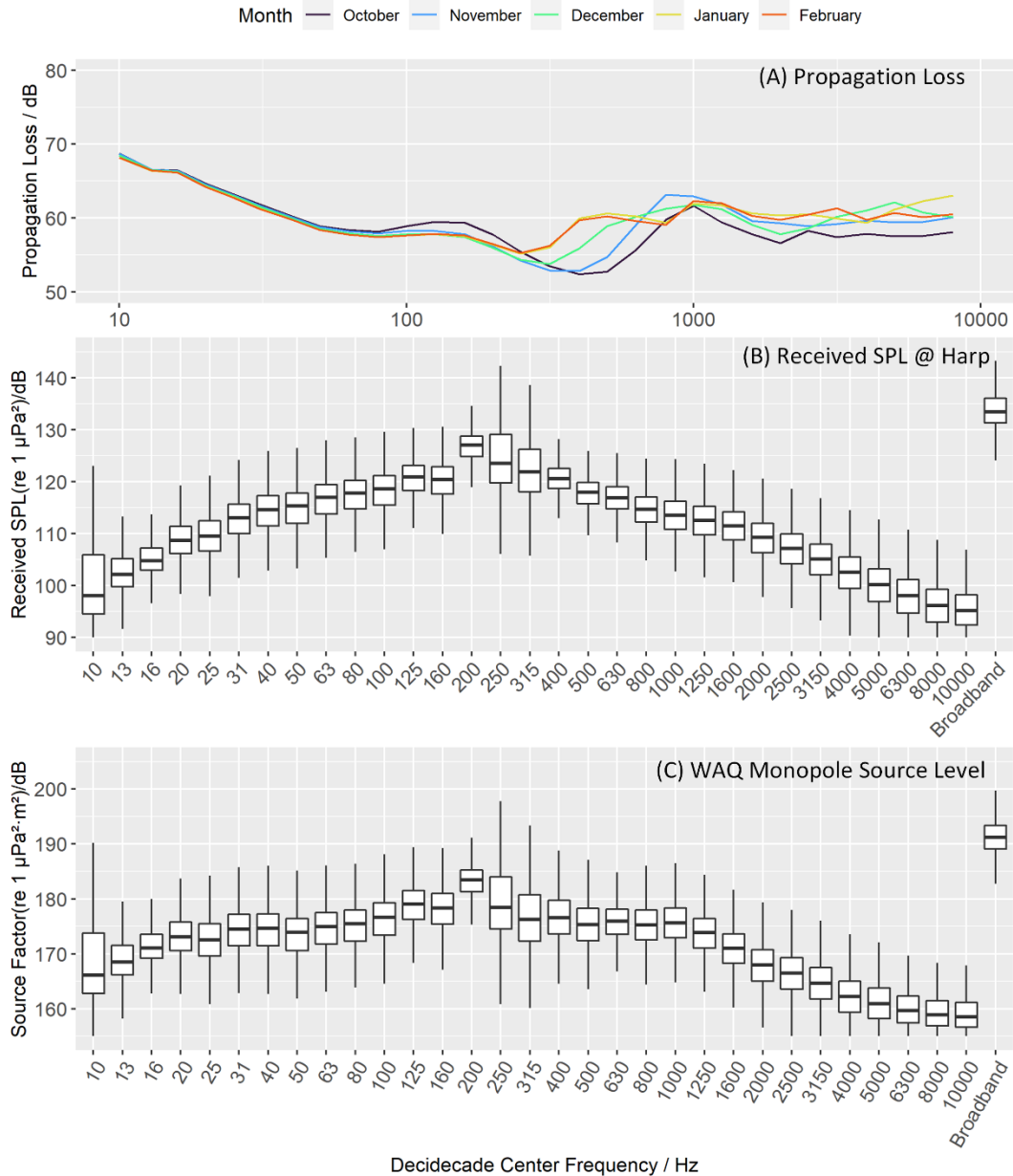


Figure 26. Computing the West Aquarius (WAQ) Source Factor: (A) modeled sound propagation loss for October 2019 to February 2020; (B) distribution of received SPL at Harp (EL 1165B); and (C) sum of (A) and (B) to obtain the distribution of the source factor.

3.4. Marine Mammal Detections

3.4.1. Detector Performance

Detector performance varied across species and stations. Hampden (EL 1165A) and Stn 19 had nine detectors whose precision was higher than 0.75. Mid and Harp (EL 1165B) had seven and five detectors with precision above 0.75, respectively (Tables 8 to 11). The blue and fin whale song note detectors performed consistently well. The humpback and sei whale vocalization detectors performed best at stations least affected by ambient noise, once restricted around the short period of acoustic occurrence highlighted by manual detections. The same observation can be made for the pilot whale tonal vocalization detector although in that case, low number of detections at Harp (EL 1165B) and Mid may reflect habitat preference rather than poor detector performance. Dolphin whistles were detected automatically with high performance scores at all stations.

Where the clicks of a given species were manually detected, the relevant detector usually performed well. The exceptions included sperm whale clicks at Harp (EL 1165B), northern bottlenose whale at Mid and Hampden (EL 1165A), and Sowerby’s beaked whale click at Stn 19. At these cases, the number of manual detections was too low for the performance of the detector to be evaluated.

In the case of delphinid and harbour porpoise clicks, different detectors yielded the highest performance scores for different stations, presumably as a result of different background noise conditions and distance between the source and recorders. It highlights the advantages of running a suite of detectors in cases like this study, whose data are characterized by a broad range of ambient noise and environmental conditions.

Table 8. Hampden (EL 1165A): Detector performance metrics for all detectors with Precision >0.75. SBW: Sowerby’s beaked whale; P: precision; R: Recall; MCC: Matthew’s correlation coefficient. N/A: Not applicable.

Species, Signal	P _{original}	R _{original}	MCC _{original}	Threshold	P _{threshold}	R _{threshold}	MCC _{threshold}	N _{files}	N _{fileswAnn}	N _{fileswdetec}	Exclusion period (inclusive)
Fin whale, 20-Hz note	0.85	0.94	0.74	1	0.85	0.94	0.74	387	221	243	N/A
Blue whale, Infrasonic	0.99	0.75	0.80	1	0.99	0.75	0.80	387	147	111	N/A
Humpback whale, moan	1.00	0.72	0.84	1	1.00	0.72	0.84	387	29	21	18 Dec to 19 Feb
Sei whale, downsweeps	0.75	0.79	0.73	2	0.86	0.71	0.75	387	62	65	7 Dec to 11 Apr
Dolphin whistle	0.97	0.74	0.66	1	0.97	0.74	0.66	387	258	198	N/A
Pilot whale, whistle	0.67	0.51	0.54	2	0.76	0.44	0.54	387	43	33	28 Jan to 31 Mar
Sperm whale, click	0.91	0.65	0.64	1	0.91	0.65	0.64	386	173	124	N/A
SBW, click	0.16	1.00	0.35	35	0.75	0.94	0.83	386	16	102	N/A
Delphinid, click	0.82	0.97	0.75	52	0.95	0.90	0.82	386	209	245	N/A

Table 9. Harp (EL 1165B): Detector performance metrics for all detectors with Precision >0.75. *P*: precision; *R*: Recall; *MCC*: Matthew’s correlation coefficient. N/A: Not applicable.

Species, Signal	<i>P</i> _{original}	<i>R</i> _{original}	<i>MCC</i> _{original}	Threshold	<i>P</i> _{threshold}	<i>R</i> _{threshold}	<i>MCC</i> _{threshold}	Nfiles	NfileswAnn	Nfileswdelec	Exclusion period (inclusive)
Fin whale, 20-Hz note	0.87	0.81	0.76	2	0.95	0.74	0.77	377	129	121	N/A
Blue whale, Infrasonic	0.91	0.74	0.79	1	0.91	0.74	0.79	377	57	46	N/A
Dolphin whistle	0.86	0.56	0.61	2	0.94	0.51	0.62	377	99	64	N/A
Delphinid, click	0.81	0.80	0.76	1	0.81	0.80	0.76	375	82	81	N/A
Harbour porpoise, click	0.72	0.81	0.67	3	0.95	0.69	0.75	281	78	87	26 Feb to 28 Apr

Table 10. Mid: Detector performance metrics for all detectors with Precision >0.75. *P*: precision; *R*: Recall; *MCC*: Matthew’s correlation coefficient. N/A: Not applicable.

Species, Signal	<i>P</i> _{original}	<i>R</i> _{original}	<i>MCC</i> _{original}	Threshold	<i>P</i> _{threshold}	<i>R</i> _{threshold}	<i>MCC</i> _{threshold}	Nfiles	NfileswAnn	Nfileswdelec	Exclusion period (inclusive)
Fin whale, 20-Hz note	0.81	0.90	0.69	1	0.81	0.90	0.69	391	202	224	N/A
Blue whale, Infrasonic	0.96	0.66	0.73	1	0.96	0.66	0.73	391	124	85	N/A
Humpback whale, moan	1.00	0.33	0.57	1	1.00	0.33	0.57	391	24	8	Start to 26 Dec; 19 Feb to end
Dolphin whistle	0.95	0.71	0.65	1	0.95	0.71	0.65	391	231	172	N/A
Sperm whale, click	0.95	0.70	0.63	1	0.95	0.70	0.63	389	230	169	N/A
Dolphin, click	0.92	0.86	0.75	1	0.92	0.86	0.75	389	226	210	N/A
Harbour porpoise, click	0.56	0.73	0.59	7	0.85	0.70	0.75	389	40	52	N/A

Table 11. Stn 19: Detector performance metrics for all detectors with Precision >0.75. NBW: Northern bottlenose whale; *P*: precision; *R*: Recall; MCC: Matthew's correlation coefficient. N/A: Not applicable.

Species, Signal	$P_{original}$	$R_{original}$	$MCC_{original}$	Threshold	$P_{threshold}$	$R_{threshold}$	$MCC_{threshold}$	Nfiles	NfileswAnn	Nfileswdetec	Exclusion period (inclusive)
Fin whale, 20-Hz note	0.63	0.95	0.54	4	0.89	0.76	0.63	392	174	262	N/A
Blue whale, Infrasonic	1.00	0.54	0.65	1	1.00	0.54	0.65	392	141	76	26 Feb to 15 May
Humpback whale, moan	0.96	0.47	0.64	1	0.96	0.47	0.64	392	49	24	Start to 23 Dec; 27 Feb to end
Sei whale, downsweeps	0.79	0.59	0.65	3	0.96	0.57	0.72	392	44	33	Sep; 8 Dec to 31 Mar
Dolphin whistle	0.98	0.58	0.45	1	0.98	0.58	0.45	392	308	183	N/A
Pilot whale, whistle	0.89	0.37	0.45	1	0.89	0.37	0.45	392	147	61	N/A
Sperm Whale, click	0.92	0.78	0.60	4	0.98	0.73	0.63	391	268	225	N/A
NBW, click	0.33	0.95	0.42	52	0.89	0.74	0.76	391	65	189	1 Mar to 18 May
Delphinid, click	0.92	0.78	0.69	5	0.98	0.74	0.72	391	215	183	N/A

3.4.2. Blue Whales

Blue whale calls (Figure 27 and Figure 28) were detected at all stations. Harp (EL 1165B) had 20 detection days, primarily in September. Detections at Mid, Hampden (EL 1165A), and Stn 19 occurred regularly from September to February, and declined or stopped after that, with the exception of two waves of detections in late February and early March at Hampden (EL 1165A) and Mid. Hampden (EL 1165A) and Mid had similar number of detection days (113–115), but Hampden (EL 1165A) had nearly twice as many detections (Figure 29; Table 12), despite having shorter median detection ranges (see Section 3.2 and Appendix C.5). The near disappearance of detections at Harp (EL 1165B) after September is presumably the result of the arrival of the MODU at this station, which also led to the shorter detection ranges there. The lower number of detections and detection days at Stn 19 may be the result of the shorter detection ranges modelled at that station, considering that the period of acoustic occurrence is otherwise similar to those observed at Hampden (EL 1165A) and Mid.

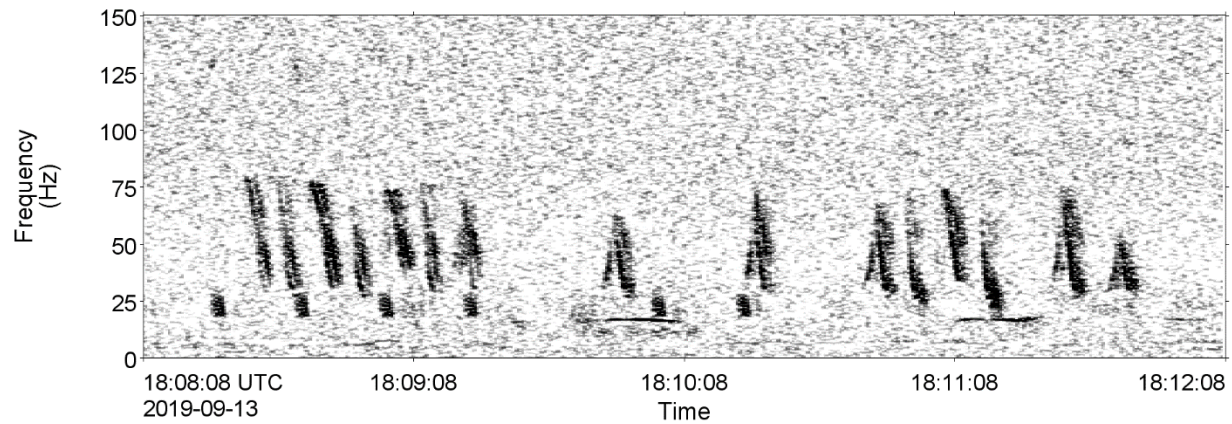


Figure 27. Spectrogram of blue whale arch calls recorded at Hampden (EL 1165A) on 13 Sep 2019 (0.4 Hz frequency resolution, 2 s time window, 0.5 s time step, Hamming window). The window length is 240 s.

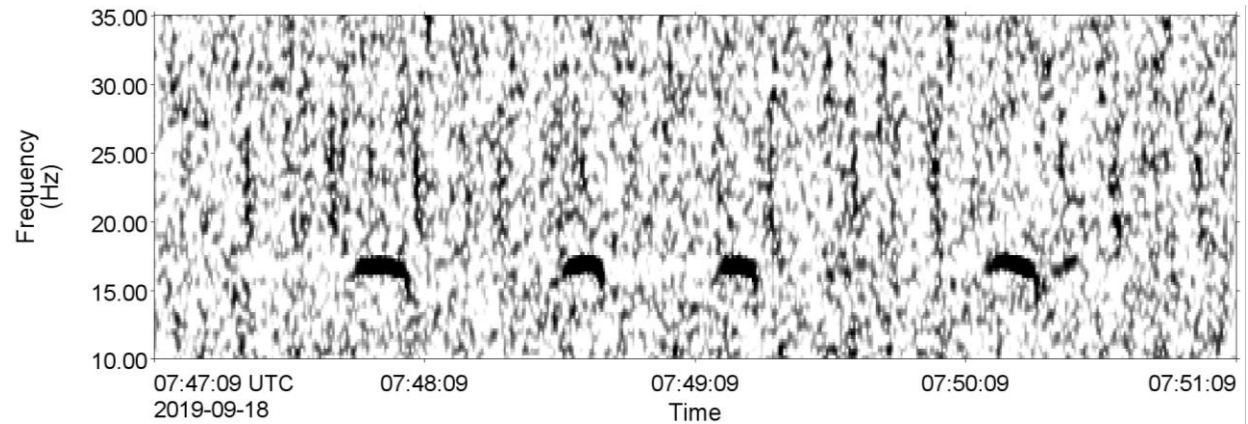


Figure 28. Spectrogram of blue whale infrasonic A-B vocalizations recorded at Stn 19 on 18 Sep 2019 (0.4 Hz frequency resolution, 2 s time window, 0.5 s time step, Hamming window). The window length is 240 s.

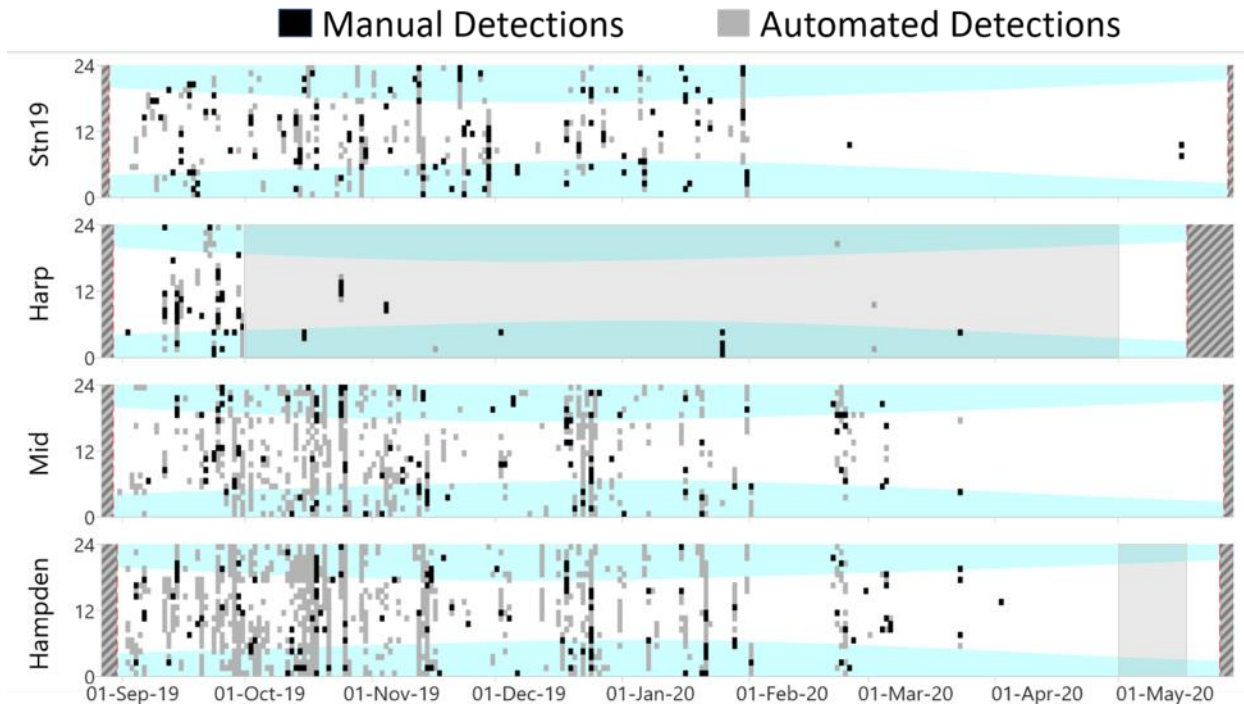


Figure 29. Daily and hourly occurrence of automatically and manually detected blue whale song notes. Red dashed lines indicate recorder deployment and retrieval dates or recording end. Hashed lines indicate no recordings. Blue shaded areas indicate hours of darkness. Grey shaded areas indicate the presence of the MODU near the recorder.

Table 12. Blue whales: Percent days with detections (manual or automated) and number of automated detections by month at Hampden (EL 1165A), Harp (EL 1165B), Mid and Stn 19. D: detections.

Month	Hampden (EL 1165A) ¹		Harp (EL 1165B) ²		Mid		Stn 19	
	% days with D	Detections	% days with D	Detections	% days with D	Detections	% days with D	Detections
Sep	80.0	829	40.0	330	73.3	225	70.0	100
Oct	90.3	1628	6.5	53	96.8	844	58.1	300
Nov	53.3	352	6.7	9	56.7	267	50.0	427
Dec	61.3	480	0.0	0	64.5	401	38.7	93
Jan	41.9	306	3.2	10	48.4	107	29.0	148
Feb	28.6	140	3.6	1	25.0	97	3.6	0
Mar	16.1	24	6.5	3	9.7	7	0.0	0
Apr	0.0	0	0.0	0	0.0	0	0.0	0
May	0.0	0	0.0	0	0.0	0	3.2	2
Total	113	3759	20	406	115	1949	76	1070

¹MODU present from 2-14 May 2020

²MODU present from 1 Oct 2019-1 May 2020

3.4.3. Fin Whales

Fin whales were detected at all stations. Vocalizations (Figure 30) were detected nearly daily from September to February at Hampden (EL 1165A), Mid, and Stn 19. Detections decreased rapidly by early March at Stn 19 and mid-March at Hampden (EL 1165A) and Mid and were rare area-wide from early April. Detections occurred regularly at Harp (EL 1165B) in September but decreased abruptly in early October, coinciding with the arrival of the MODU. Hampden (EL 1165A) and Mid had nearly the same number of detection days but Hampden’s detection count was 44% higher than at Mid (Figure 31; Table 13). Stn 19 had more detections than Mid despite having 37 fewer detection days and substantially lower median detection ranges (see Section 3.2 and Appendix C.5). The difference in detection counts is largely the result of a large offset in September in favour of Stn 19, while from January onward detection counts were higher at Mid and Hampden (EL 1165A). This may indicate that fin whales gradually moved south along the Flemish Pass in winter (Table 13).

The rare occurrence of fin whale 20-Hz calls from April onward is a phenomenon observed across their range and coincides with the end of song production period (Davis 2020). It shall not be interpreted as a departure from the area as there is ample evidence for fin whale presence off Newfoundland in the spring and summer months (Lawson and Gosselin 2009, 2018).

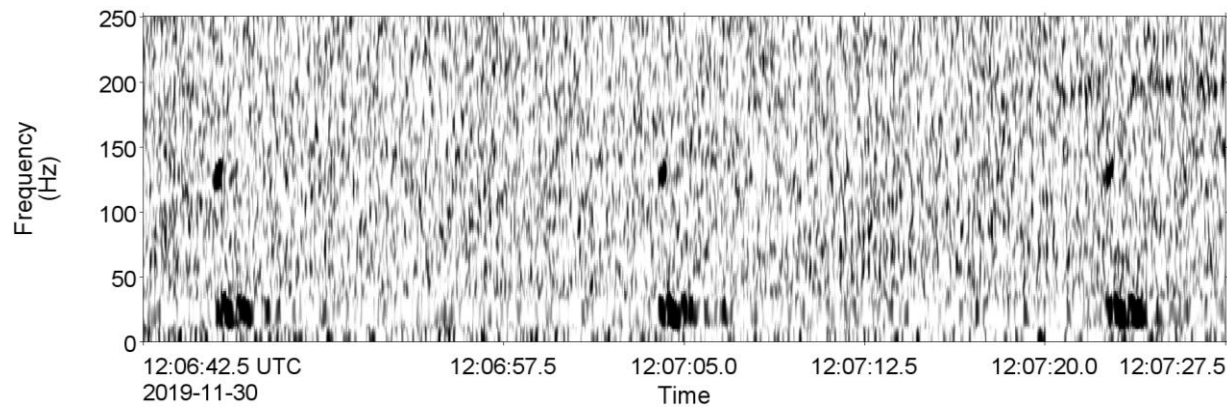


Figure 30. Spectrogram showing fin whale 20-Hz and the 130-Hz song notes recorded at Hampden (EL 1165A) on 30 Nov 2019 (2 Hz frequency resolution, 0.128 s time window, 0.032 s time step, Hamming window). The window length is 45 s.

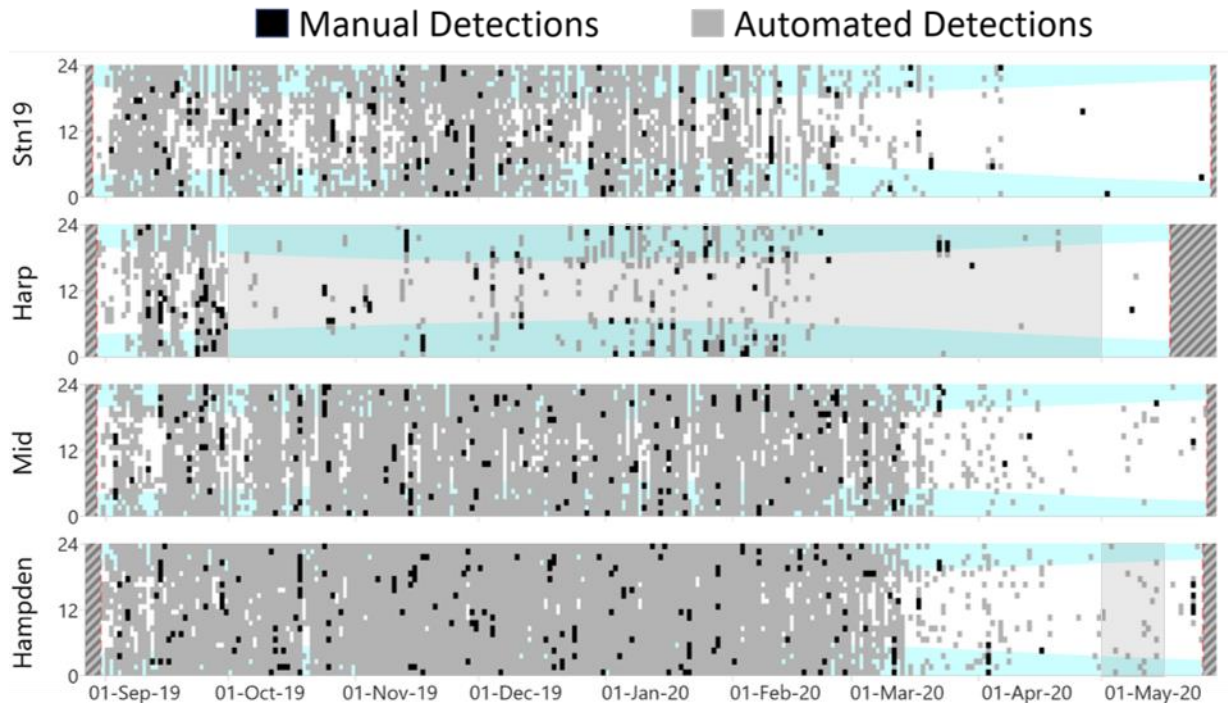


Figure 31. Daily and hourly occurrence of automatically and manually detected fin whale 20-Hz calls. Red dashed lines indicate recorder deployment and retrieval dates or recording end. Hashed lines indicate no recordings. Blue shaded areas indicate hours of darkness. Grey shaded areas indicate the presence of the MODU near the recorder.

Table 13. Fin whales: Percent days with detections (manual or automated) and number of automated detections by month at Hampden (EL 1165A), Harp (EL 1165B), Mid and Stn 19. D: Detections

Month	Hampden (EL 1165A) ¹		Harp (EL 1165B) ²		Mid		Stn 19	
	% days with D	Detections	% days with D	Detections	% days with D	Detections	% days with D	Detections
Sep	100.0	6182	96.7	6104	100.0	3998	100.0	9218
Oct	100.0	7296	35.5	182	100.0	4128	100.0	5618
Nov	100.0	10271	33.3	326	100.0	6587	100.0	9012
Dec	100.0	8184	67.7	413	100.0	6600	100.0	6379
Jan	100.0	9891	87.1	1364	100.0	6826	93.5	5789
Feb	93.5	5845	67.7	589	93.5	4519	87.1	2460
Mar	96.8	1514	9.7	36	93.5	1481	54.8	437
Apr	61.3	119	12.9	10	58.1	55	19.4	113
May	48	40	5.9	2	42.3	25	3.7	7
Total	244	49342	129	9026	241	34219	204	39033

¹MODU present from 2-14 May 2020

²MODU present from 1 Oct 2019-1 May 2020

3.4.4. Sei Whales

Sei whales were detected at all stations although the automated detector only yielded results with precision greater than 0.75 at Hampden (EL 1165A) and Stn 19. Detections were concentrated in October and November at Stn 19. A similar pattern was observed at Hampden (EL 1165A) although vocalizations (Figure 32) were detected in September and sporadically from December to May, February being the only month with no detections. Detection counts at Stn 19 and Hampden (EL 1165A) were comparable in October, but more than double at Hampden (EL 1165A) in November (Figure 33; Table 14). The near-absence of detections at Harp (EL 1165B) and lower occurrence at Mid is likely related to higher background noise levels causing masking. Detection ranges were markedly lower at Stn 19, possibly biasing detection counts downward compared to the other stations (see Section 3.2 and Appendix C.5).

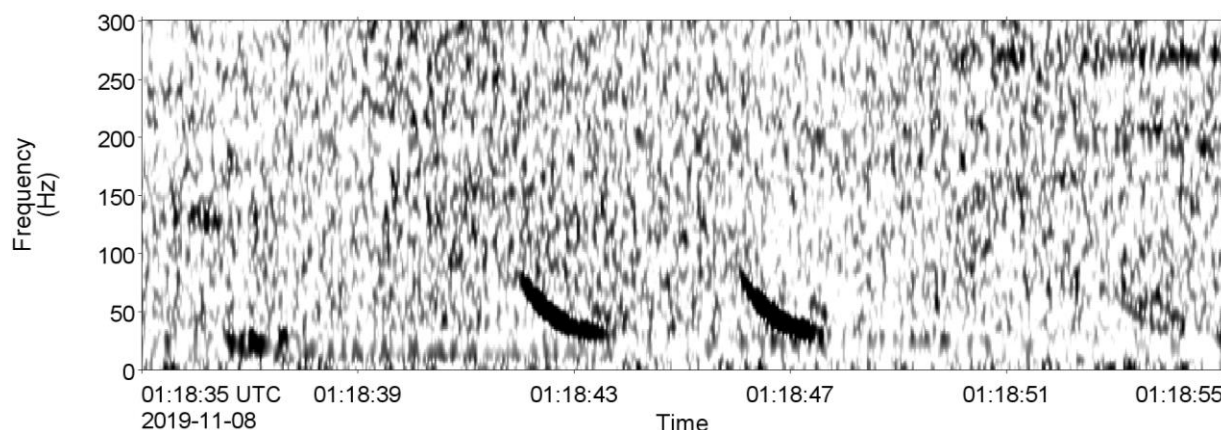


Figure 32. Spectrogram of a sei whale paired downsweep recorded at Mid on 8 Nov 2019 (2 Hz frequency resolution, 0.128 s time window, 0.032 s time step, Hamming window). The window length is 20 s.

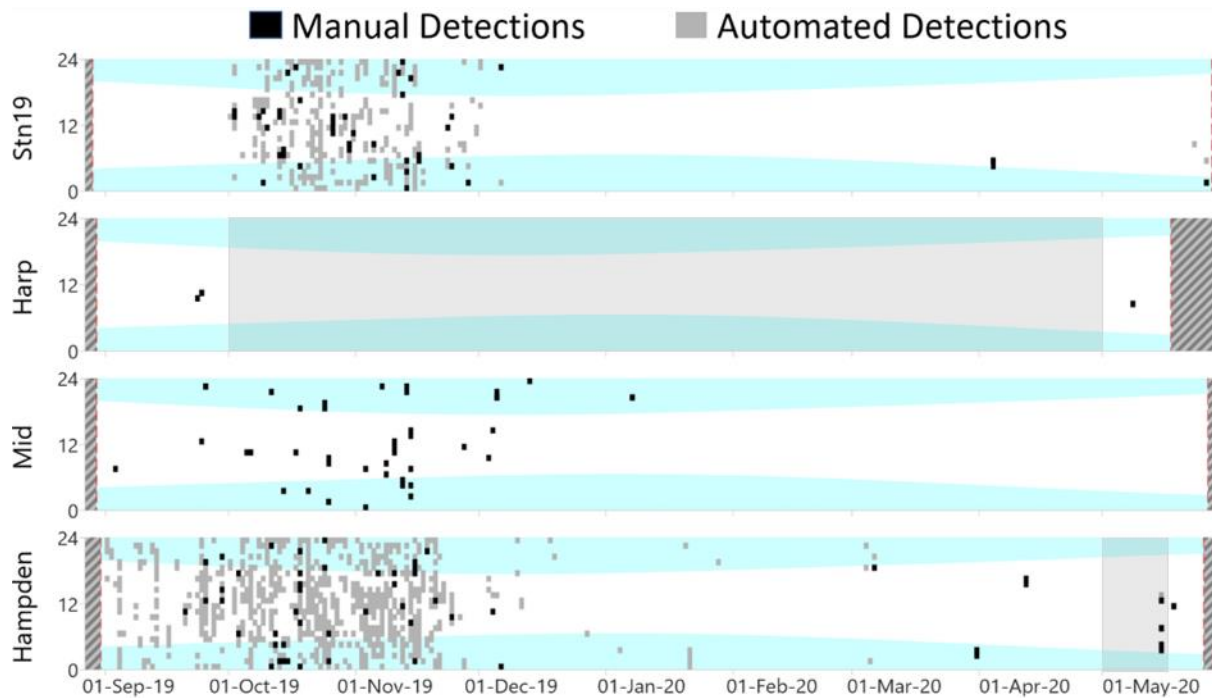


Figure 33. Daily and hourly occurrence of automatically and manually detected sei whale downsweeps. Red dashed lines indicate recorder deployment and retrieval dates or recording end. Hashed lines indicate no recordings. Blue shaded areas indicate hours of darkness. Grey shaded areas indicate the presence of the MODU near the recorder.

Table 14. Sei whales: Percent days with detections (manual or automated) and number of automated detections by month at Hampden (EL 1165A), Harp (EL 1165B), Mid and Stn 19. D: detections. N/A: Not applicable.

Month	Hampden (EL 1165A) ¹		Harp (EL 1165B) ²³		Mid ³		Stn 19	
	% days with D	Detections	% days with D	Detections	% days with D	Detections	% days with D	Detections
Sep	76.7	700	6.7	N/A	13.3	N/A	0.0	0
Oct	100.0	2087	0.0	N/A	29.0	N/A	93.5	1717
Nov	83.3	2037	0.0	N/A	20.0	N/A	76.7	837
Dec	29.0	50	0.0	N/A	16.1	N/A	12.9	40
Jan	9.7	26	0.0	N/A	3.2	N/A	0.0	0
Feb	0.0	0	0.0	N/A	0.0	N/A	0.0	0
Mar	12.9	20	0.0	N/A	0.0	N/A	0.0	0
Apr	3.2	2	0.0	N/A	0.0	N/A	3.2	12
May	8	26	5.9	N/A	0.0	N/A	7.4	9
Total	98	4948	3	N/A	24	N/A	59	2615

¹ MODU present from 2-14 May 2020

² MODU present from 1 Oct 2019-1 May 2020

³ Results based on manual detections only

3.4.5. Humpback Whales

Humpback whale vocalizations (Figure 34) were detected at all stations except Harp (EL 1165B), which was likely the result of higher background noise levels connected to the presence of the MODU during the detection period. All vocalizations were detected between late December and late February, which can be attributed to animals migrating south on their way towards the breeding grounds. The timing of these detections is consistent with that observed at nearby locations between 2015 and 2017 (Delarue et al. 2018). Stn 19 had the highest number of detection days and detections, followed by Hampden (EL 1165A) and Mid (Figure 35; Table 15). All detections consisted of songs or song fragments. For all stations, the modelled detection ranges were negligible in average background noise conditions and up to 3–7 km depending on the station in the best conditions (see Section 3.2 and Appendix C.5).

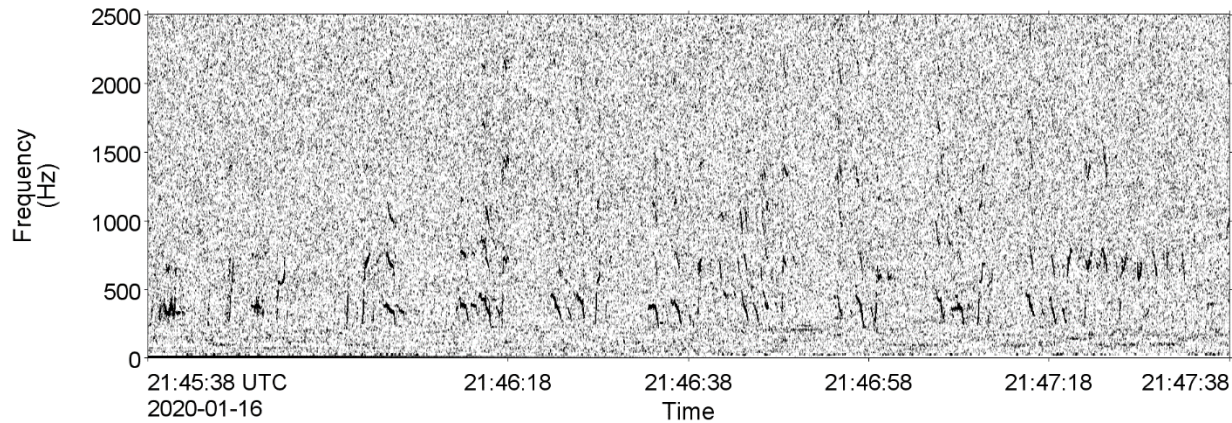


Figure 34. Spectrogram of humpback whale vocalizations (song) recorded at Stn 19 on 16 Jan 2020 (2 Hz frequency resolution, 0.128 s time window, 0.032 s time step, Hamming window). The window length is 120 s.

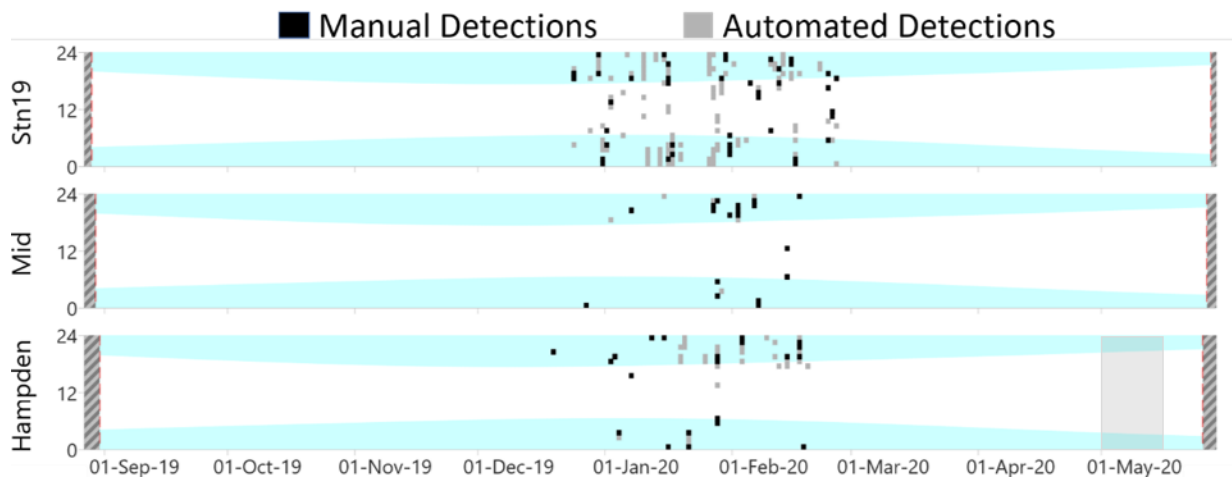


Figure 35. Daily and hourly occurrence of automatically and manually detected humpback whale song notes. Red dashed lines indicate recorder deployment and retrieval dates or recording end. Hashed lines indicate no recordings. Blue shaded areas indicate hours of darkness. Grey shaded areas indicate the presence of the MODU near the recorder.

Table 15. Humpback whales: Percent days with detections (manual or automated) and number of automated detections by month at Hampden (EL 1165A), Mid and Stn 19. D: detections.

Month	Hampden (EL 1165A) ¹		Mid		Stn 19	
	% days with D	Detections	% days with D	Detections	% days with D	Detections
Sep	0.0	0	0.0	0	0.0	0
Oct	0.0	0	0.0	0	0.0	0
Nov	0.0	0	0.0	0	0.0	0
Dec	6.5	7	3.2	0	12.9	80
Jan	33.3	175	13.3	11	53.3	572
Feb	29.0	124	16.1	115	48.4	75
Mar	0.0	0	0.0	0	0.0	0
Apr	0.0	0	0.0	0	0.0	0
May	0.0	0	0.0	0	0.0	0
Total	21	306	11	126	35	727

¹MODU present from 2-14 May 2020

3.4.6. Killer Whales

Killer whale tonal calls (Figure 36) were manually detected at Mid on 7 Sep 2019 and on 4 and 24 Mar 2020. They were detected once at Harp (EL 1165B) on 30 Mar 2020.

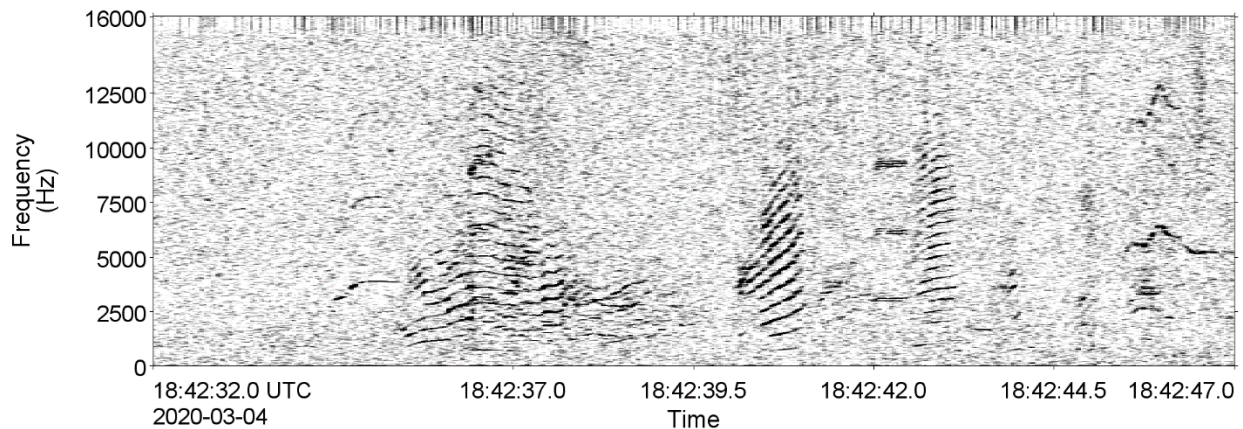


Figure 36. Spectrogram showing killer whale vocalizations recorded at Mid on 4 Mar 2020 (2 Hz frequency resolution, 0.128 s time window, 0.032 s time step, Hamming window). The window length is 15 s.

3.4.7. Pilot Whales

Pilot whale tonal calls (Figure 37) were detected at all stations, although the automated detector only yielded results with precision greater than 0.75 at Hampden (EL 1165A) and Stn 19. Pilot whale detections were approximately three times more common at Stn 19 than Hampden (EL 1165A). Detections at both stations showed a seasonal pattern with less detections between December and March. This seasonal trend was more pronounced at Hampden (EL 1165A). There was only one detection in February and March at Hampden, while detections still occurred on about 30% of days between December and March at Stn 19 (Figure 38; Table 16). At Hampden, pilot acoustic detections resumed in April but decreased substantially in early May after the MODU's arrival. They resumed just after its departure. The lack of manual detections in March and April at Harp (EL 1165B) and Mid may be an artifact of the algorithm used to select files to validate automated detections, although the results overall confirm the preference of pilot whales for deeper areas along the continental slope. Detection ranges were low for delphinid whistles, indicating that the results characterize the acoustic occurrence of pilot whales within ~5 km of the recorders (see Section 3.2 and Appendix C.5).

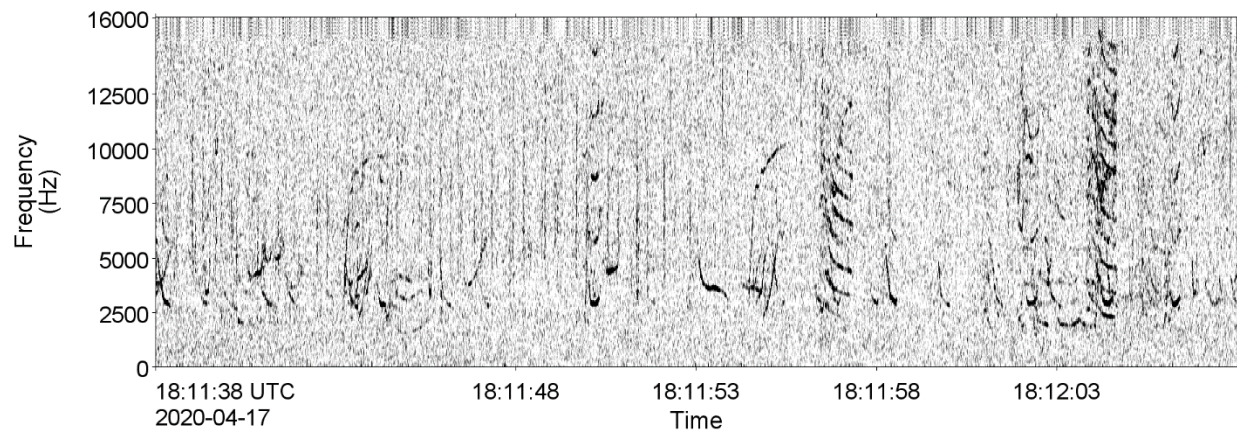


Figure 37. Spectrogram showing pilot whale vocalizations recorded at Hampden (EL 1165A) on 17 Apr 2020 (64 Hz frequency resolution, 0.01 s time window, 0.005 s time step, Hamming window). The window length is 30 s.



Figure 38. Daily and hourly occurrence of automatically and manually detected pilot whale tonal calls. Red dashed lines indicate recorder deployment and retrieval dates or recording end. Hashed lines indicate no recordings. Blue shaded areas indicate hours of darkness. Grey shaded areas indicate the presence of the MODU near the recorder.

Table 16. Pilot whale: Percent days with detections (manual or automated) and number of automated detections by month at Hampden (EL 1165A), Harp (EL 1165B), Mid and Stn 19. D: detections. N/A: Not applicable.

Month	Hampden (EL 1165A) ¹		Harp (EL 1165B) ^{2,3}		Mid ³		Stn 19	
	% days with D	Detections	% days with D	Detections	% days with D	Detections	% days with D	Detections
Sep	30.0	77	16.7	N/A	23.3	N/A	93.3	1275
Oct	25.8	604	3.2	N/A	0.0	N/A	87.1	374
Nov	13.3	103	3.3	N/A	3.3	N/A	70.0	348
Dec	12.9	14	6.5	N/A	6.5	N/A	38.7	62
Jan	16.1	33	3.4	N/A	3.4	N/A	35.5	57
Feb	0.0	0	3.2	N/A	3.2	N/A	25.8	130
Mar	3.2	0	0.0	N/A	0.0	N/A	29.0	51
Apr	54.8	236	0.0	N/A	0.0	N/A	90.3	667
May	20.0	40	6.7	N/A	19.2	n/a	92.6	507
Total	52	1107	13	N/A	17	N/A	172	3471

¹ MODU present from 2-14 May 2020

² MODU present from 1 Oct 2019-1 May 2020

³ Results based on manual detections only

3.4.8. Delphinids

Vocalizations from smaller delphinids were detected daily from September to February at Hampden (EL 1165A), Mid, and Stn 19. Detections of dolphin whistles (Figure 39) declined progressively from March to May at Mid and Hampden (EL 1165A) but continued to occur on at least 83% of days at Stn 19. However, despite a sustained acoustic occurrence, detection counts decreased substantially in April and May at Stn 19. Dolphin whistle detections were lower by all metrics at Harp (EL 1165B) throughout the recording period (Table 17; Figure 42), including before the arrival of the MODU.

Similar spatio-temporal detection patterns were observed for delphinid clicks (Figure 40; Figure 41). These detections include clicks from dolphins as well as pilot whales and killer whales (though the latter are not expected to have contributed many detections given their rare occurrence). In terms of detection days, the decline from March to May was less pronounced at Mid and Hampden (EL 1165A) than for whistles, but the detection counts were much lower for these months. Clicks were detected nearly daily throughout the recording period at Stn 19, but detection counts declined by more than 90% at the end of the study compared to the peak detection months in the fall (Table 18; Figure 43).

Because both click and whistle detections were lower at Harp than any of the other stations even in September, before the arrival of the MODU, it is likely that the low acoustic occurrence of delphinid signals at Harp reflects habitat preference and not avoidance of the area due to the MODU's presence.

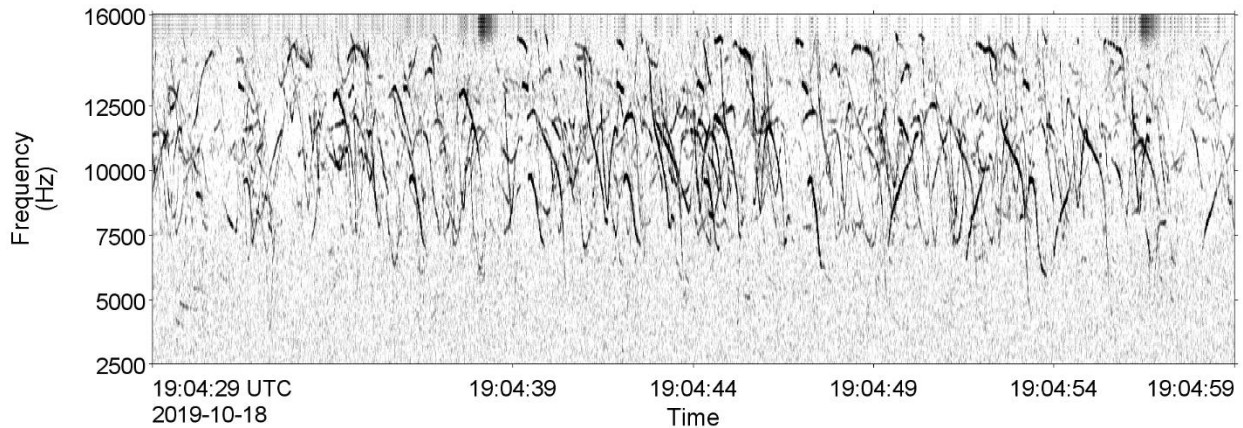


Figure 39. Spectrogram showing unidentified dolphin whistles recorded at Hampden (EL 1165A) on 18 Oct 2019 (64 Hz frequency resolution, 0.01 s time window, 0.005 s time step, Hamming window). The window length is 30 s.

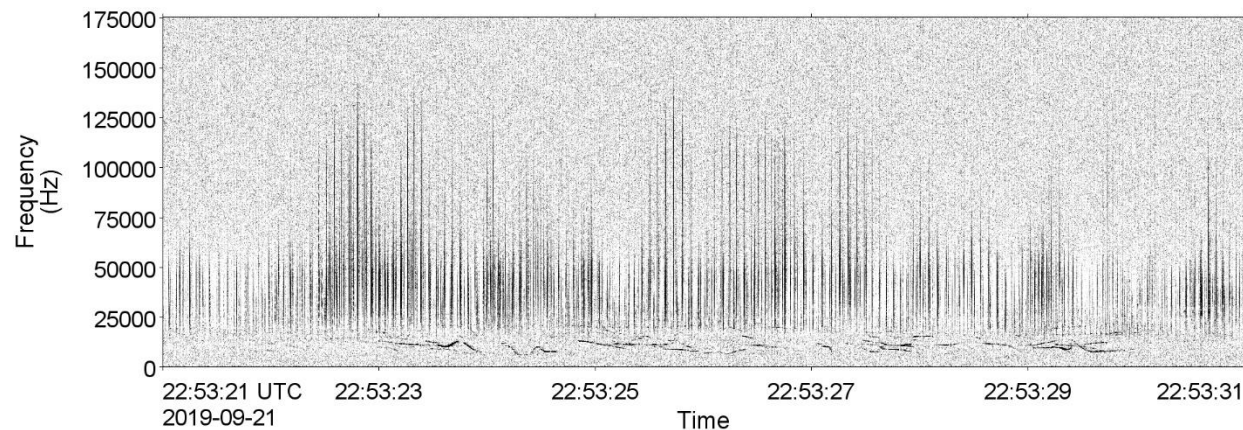


Figure 40. Spectrogram of unidentified delphinid click trains recorded at Hampden (EL 1165A) on 21 Sep 2019 (64 Hz frequency resolution, 0.01 s time window, 0.005 s time step, Hamming window). The window length is 10 s.

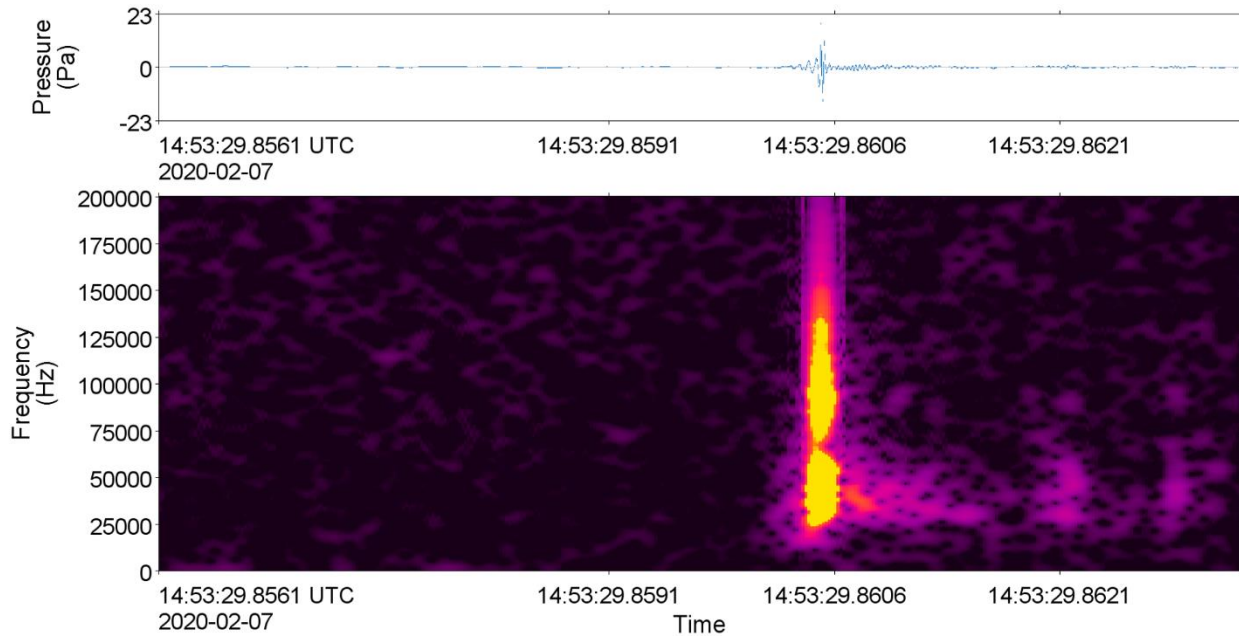


Figure 41. Spectrogram of unidentified dolphin click recorded at Stn 19 on 7 Feb 2020 (512 Hz frequency resolution, 0.266 ms time window, 0.02 ms time step).

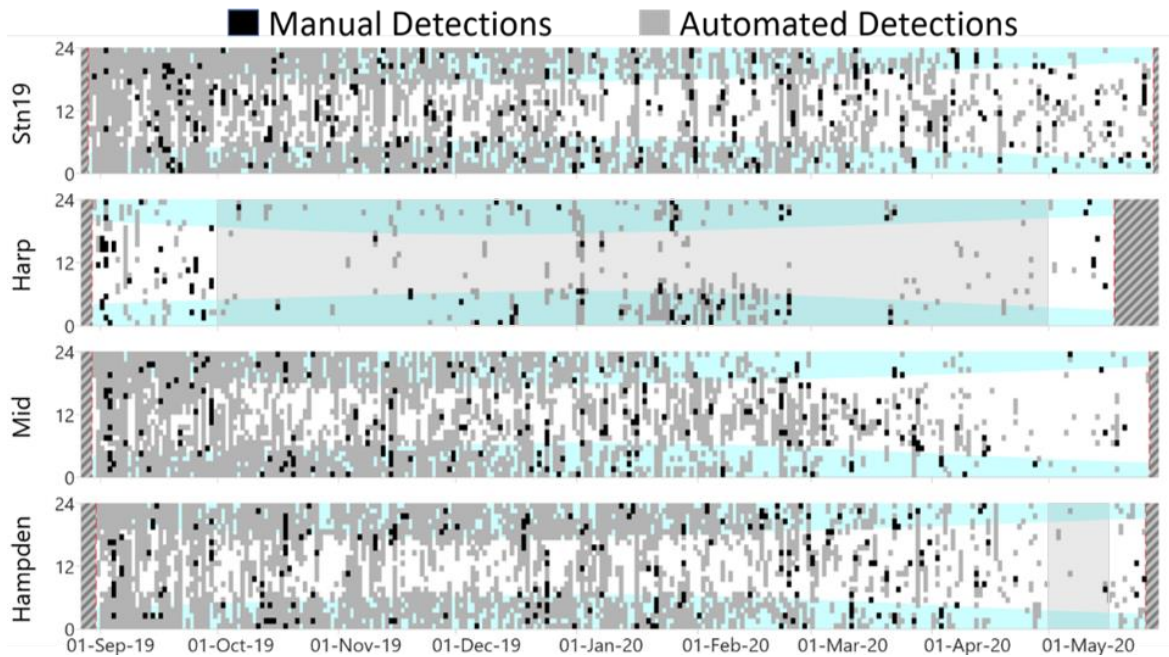


Figure 42. Daily and hourly occurrence of automatically and manually detected dolphin whistles. Red dashed lines indicate recorder deployment and retrieval dates or recording end. Hashed lines indicate no recordings. Blue shaded areas indicate hours of darkness. Grey shaded areas indicate the presence of the MODU near the recorder.

Table 17. Dolphin whistles: Percent days with detections (manual or automated) and number of automated detections by month at Hampden (EL 1165A), Harp (EL 1165B), Mid and Stn 19. D: detections.

Month	Hampden (EL 1165A) ¹		Harp (EL 1165B) ²		Mid		Stn 19	
	% days with D	Detections	% days with D	Detections	% days with D	Detections	% days with D	Detections
Sep	100.0	76156	83.3	4228	100.0	90202	100.0	58743
Oct	100.0	40821	38.7	807	100.0	31579	100.0	24463
Nov	100.0	43309	46.7	1234	100.0	33260	100.0	27862
Dec	100.0	28283	54.8	2806	100.0	22715	100.0	21297
Jan	100.0	42533	71.0	7767	100.0	29241	100.0	17011
Feb	100.0	20636	65.5	7732	100.0	22305	100.0	17680
Mar	96.8	8748	25.8	157	87.1	4390	96.8	13130
Apr	86.7	806	36.7	131	66.7	281	83.3	1908
May	52.0	130	17.6	31	34.6	347	85.2	371
Total	251	261422	131	24893	238	234320	260	182465

¹ MODU present from 2-14 May 2020

² MODU present from 1 Oct 2019-1 May 2020

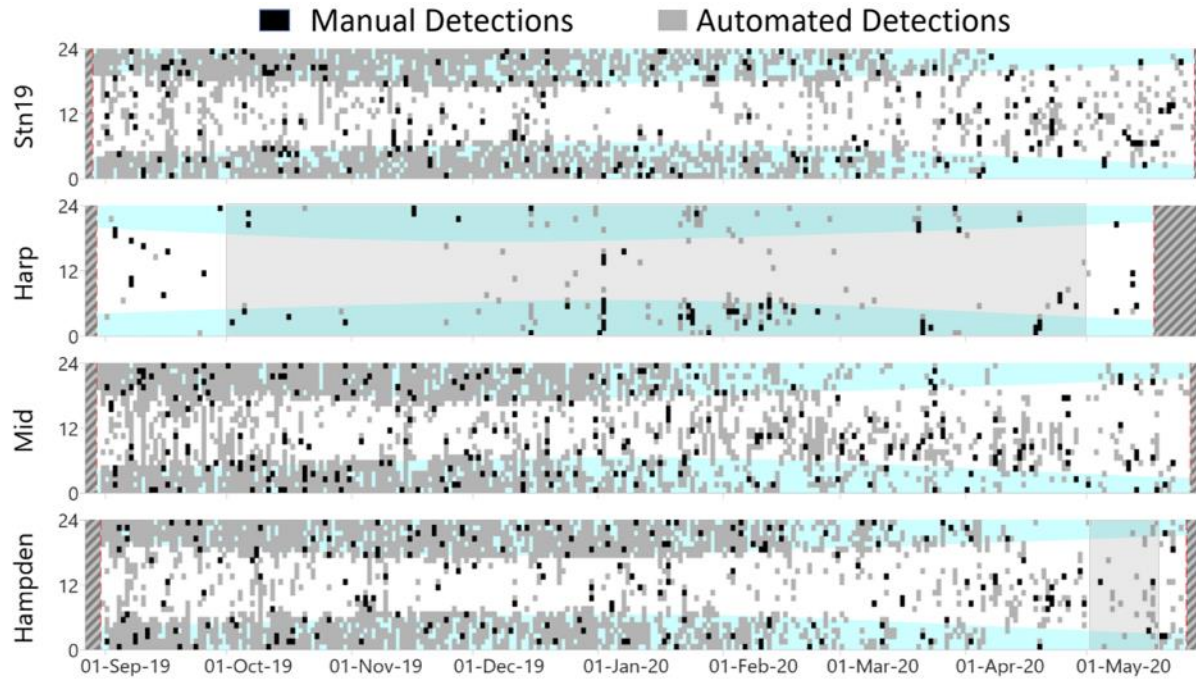


Figure 43. Daily and hourly occurrence of automatically and manually detected delphinid clicks. Red dashed lines indicate recorder deployment and retrieval dates or recording end. Hashed lines indicate no recordings. Blue shaded areas indicate hours of darkness. Grey shaded areas indicate the presence of the MODU near the recorder.

Table 18. Delphinid clicks: Percent days with detections (manual or automated) and number of automated detections by month at Hampden (EL 1165A), Harp (EL 1165B), Mid and Stn 19. D: detections.

Month	Hampden (EL 1165A) ¹		Harp (EL 1165B) ²		Mid		Stn 19	
	% days with D	Detections	% days with D	Detections	% days with D	Detections	% days with D	Detections
Sep	100.0	35164	30.0	29	100.0	69764	100.0	24811
Oct	100.0	34000	16.1	30	100.0	61354	100.0	24701
Nov	100.0	33429	10.0	208	100.0	42756	100.0	25675
Dec	100.0	27672	41.9	142	100.0	31725	100.0	21088
Jan	100.0	24017	41.9	2198	96.8	16766	100.0	13015
Feb	100.0	13082	65.5	2021	100.0	10391	100.0	10225
Mar	96.8	4008	29.0	453	96.8	1510	100.0	7566
Apr	90.0	1795	30.0	84	83.3	648	90.0	2022
May	72.0	621	17.6	46	84.6	663	100.0	1490
Total	257	173824	83	5211	258	235577	267	130593

¹MODU present from 2-14 May 2020

²MODU present from 1 Oct 2019-1 May 2020

3.4.9. Sperm Whales

Sperm whale clicks (Figure 44) were detected nearly daily at Stn 19 and Mid. However, detection counts were systematically higher at Stn 19 in each month and more than three times greater over the whole recording period. The proportion of days with detection was also high at Hampden (EL 1165A), although the acoustic occurrence of clicks declined between December and March, with a minimum in February. Hampden (EL 1165A) had the lowest monthly detection counts in all months but May, when counts were higher than at Mid. All stations recorded vocalization count minima in the late fall-early winter. Mid and Stn 19 both recorded their highest detection counts in March. In April, detection counts at Mid and Hampden (EL 1165A) were similar, suggesting a more even occurrence of sperm whales around these stations at the end of the study (Table 19; Figure 45). The scarcity of detections at Harp (EL 1165B) is likely due to the preference of sperm whales for deep water, as well as the lower detection ranges modelled at that station.

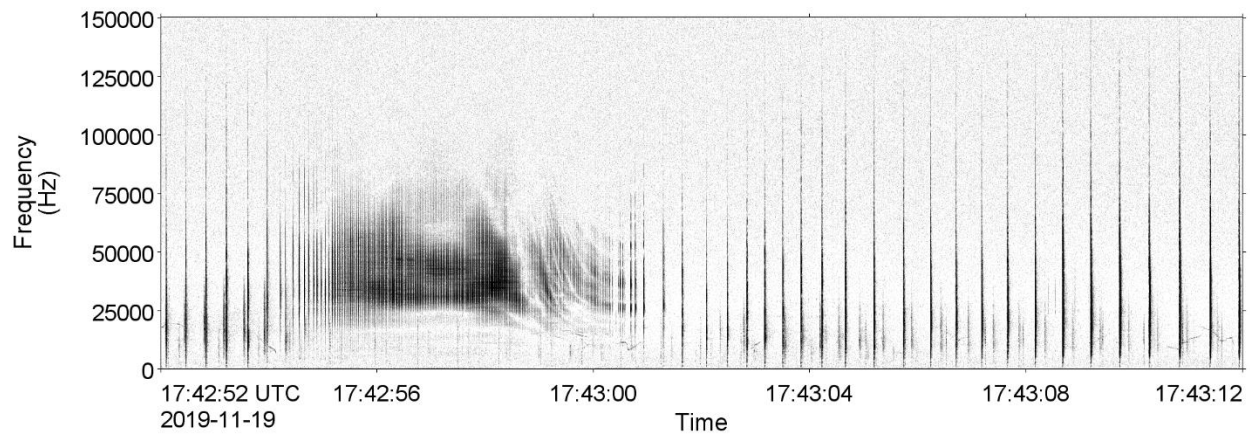


Figure 44. Spectrogram showing sperm whale clicks recorded at Mid on 19 Nov 2019 (64 Hz frequency resolution, 0.01 s time window, 0.005 s time step, Hamming window). The window length is 20 s.

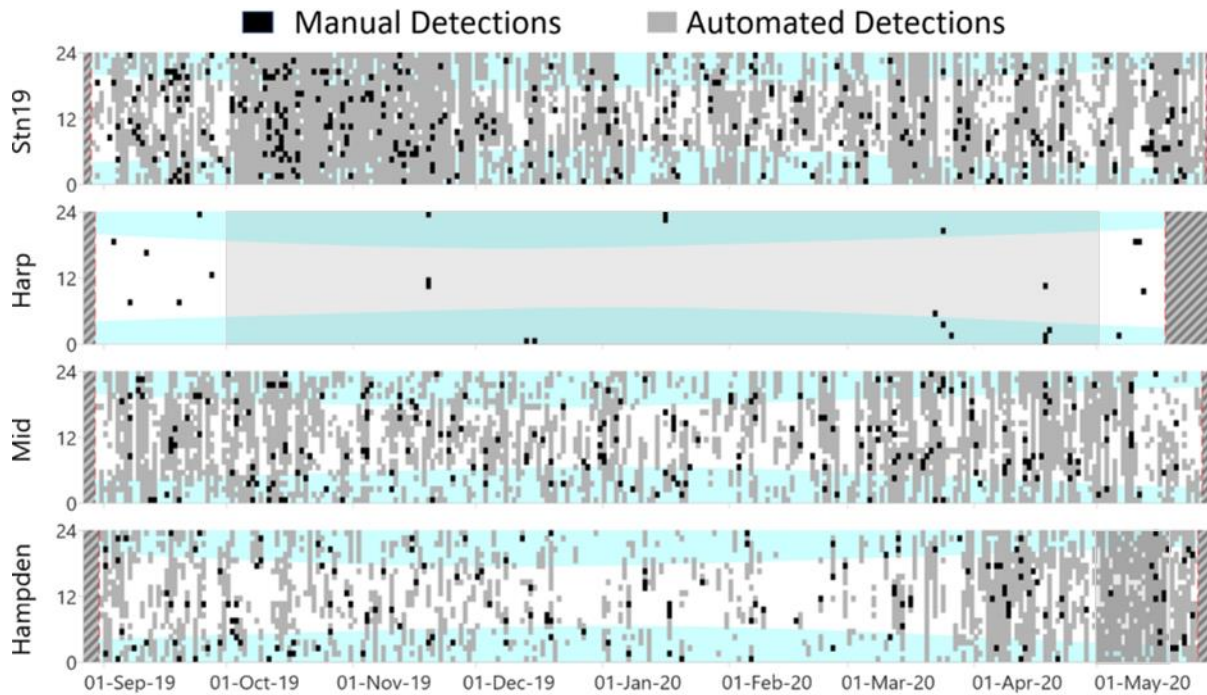


Figure 45. Daily and hourly occurrence of automatically and manually detected sperm whale. Red dashed lines indicate recorder deployment and retrieval dates or recording end. Hashed lines indicate no recordings. Blue shaded areas indicate hours of darkness. Grey shaded areas indicate the presence of the MODU near the recorder.

Table 19. Sperm whale: Percent days with detections (manual or automated) and number of automated detections by month at Hampden (EL 1165A), Mid and Stn 19. D: Detections.

Month	Hampden (EL 1165A) ¹		Harp (EL 1165B) ^{2,3}		Mid		Stn 19	
	% days with D	Detections	% days with D	Detections	% days with D	Detections	% days with D	Detections
Sep	90.0	5550	20.0	N/A	96.7	12676	96.7	20694
Oct	96.8	3491	0.0	N/A	100.0	12830	100.0	56446
Nov	100.0	3092	3.3	N/A	100.0	7578	100.0	54944
Dec	80.6	2141	6.4	N/A	100.0	7936	96.8	26127
Jan	71.0	2349	3.2	N/A	87.1	7536	96.8	27935
Feb	58.6	1495	0.0	N/A	93.1	13784	100.0	18726
Mar	83.9	5394	12.9	N/A	100.0	20006	96.8	63774
Apr	96.7	14247	6.4	N/A	96.7	16361	100.0	23265
May	100.0	11600	12.4	N/A	100.0	8235	100.0	32420
Total	231	49359	19	N/A	261	106942	266	324919

¹ MODU present from 2-14 May 2020

² MODU present from 1 Oct 2019-1 May 2020

³ Results based on manual detections only

3.4.10. Harbour Porpoises

Harbour porpoise clicks (Figure 46; Figure 47) were detected at the two shallowest stations, Harp (EL 1165B) and Mid. Detections occurred twice as often and detection counts were four times higher at Harp (EL 1165B) than Mid. At Harp (EL 1165B), detections were distributed across three main peaks in September, from mid-Dec to late February and in May. Most detections were associated with the first two peaks, but the peak in May may represent the onset of a wave of detections in summer (Table 20; Figure 48).

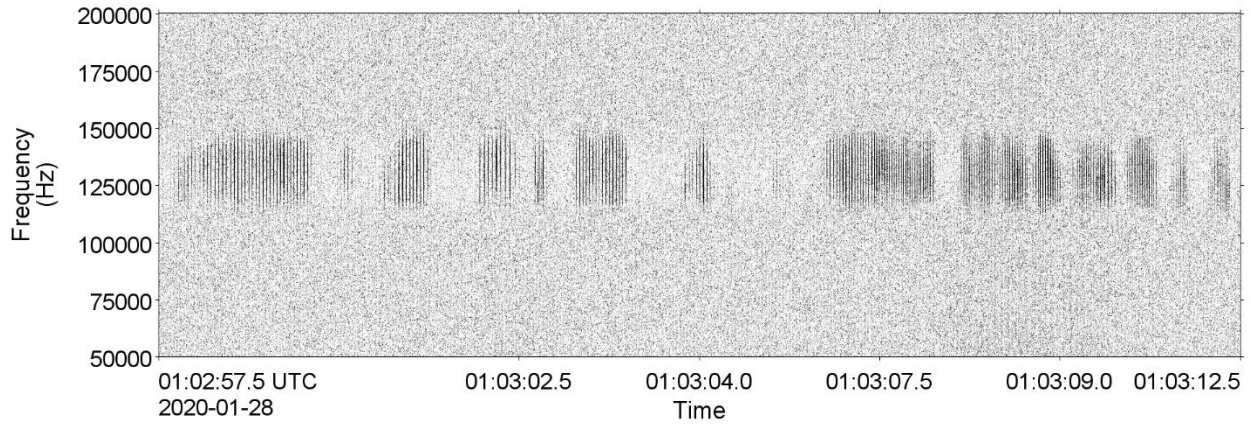


Figure 46. Spectrogram of harbour porpoise clicks recorded at Mid on 28 Jan 2020 (64 Hz frequency resolution, 0.01 s time window, 0.005 s time step, Hamming window). The window length is 15 s.

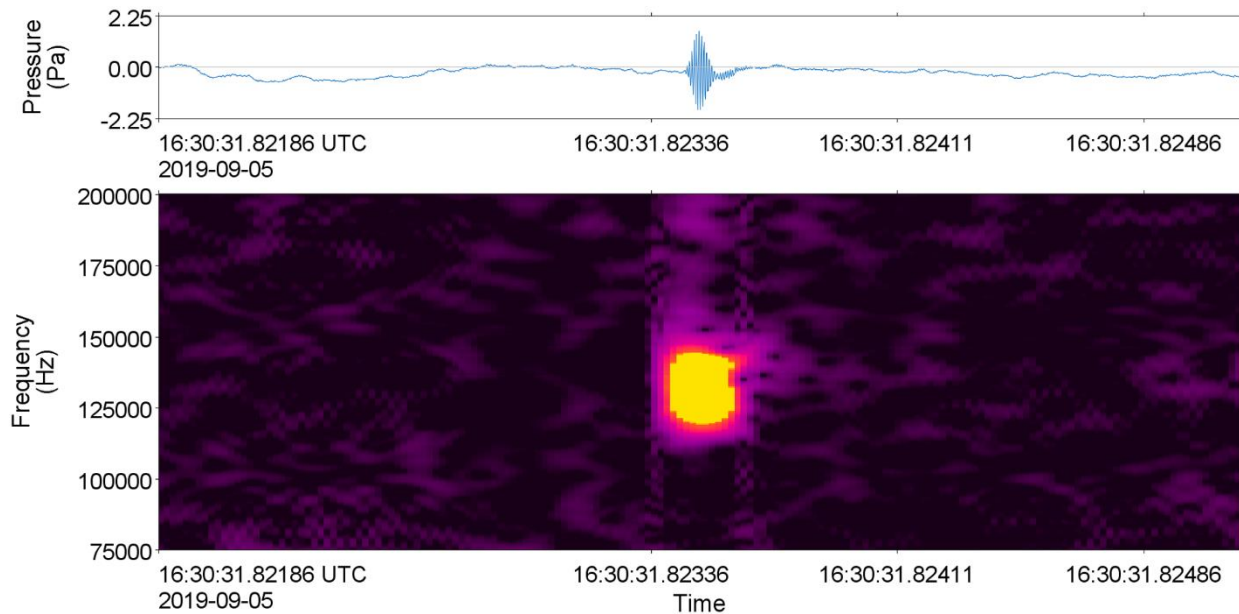


Figure 47. Spectrogram of a harbour porpoise click recorded at Harp (EL 1165B) on 5 Sep 2019 (512 Hz frequency resolution, 0.266 ms time window, 0.02 ms time step).

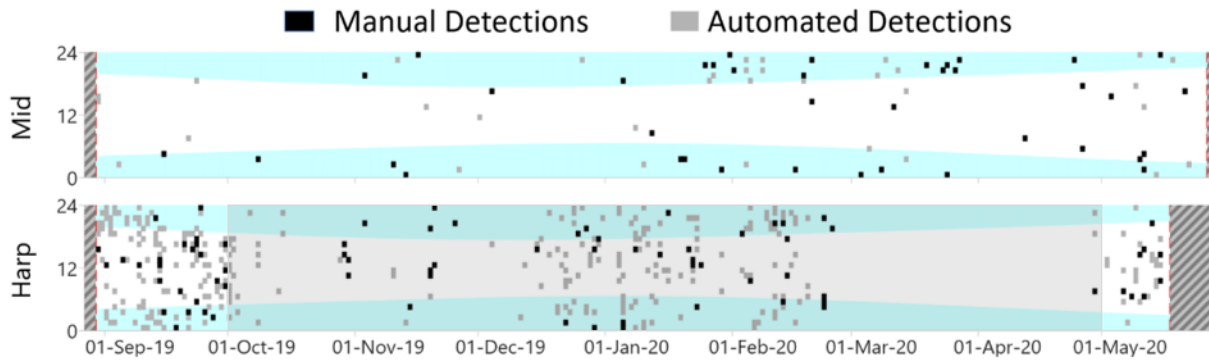


Figure 48. Daily and hourly occurrence of automatically and manually detected harbour porpoise clicks. Red dashed lines indicate recorder deployment and retrieval dates or recording end. Hashed lines indicate no recordings. Blue shaded areas indicate hours of darkness. Grey shaded areas indicate the presence of the MODU near the recorder.

Table 20. Harbour porpoises: Percent days with detections (manual or automated) and number of automated detections by month at Harp (EL 1165B) and Mid. D: detections.

Month	Harp (EL 1165B) ¹		Mid	
	% days with D	Detections	% days with D	Detections
Sep	90.0	1451	13.3	60
Oct	35.5	248	3.2	7
Nov	16.7	250	16.7	84
Dec	60.0	411	10.0	80
Jan	61.3	1444	29.0	274
Feb	60.7	797	25.0	219
Mar	0.0	0	38.7	287
Apr	6.7	11	10.0	39
May	64.7	251	26.9	220
Total	110	4863	51	1270

¹MODU present from 1 Oct 2019-1 May 2020

3.4.11. Northern Bottlenose Whales

Northern bottlenose whale clicks (Figures 49 and 50) were detected at Hampden (EL 1165A), Mid and Stn 19 but only in sufficient numbers to assess the performance of the click detector and use its output at Stn 19. At this station, click detections occurred regularly from September to February but were absent in March and April, before resuming in May. Detection counts were highest in September, reached a minimum in November followed by another peak in January (Table 21; Figure 51). The sparse manual detections at Mid and Hampden (EL 1165A) likely underrepresent the true acoustic occurrence of the species near these stations but suggest nonetheless that they are not common there.

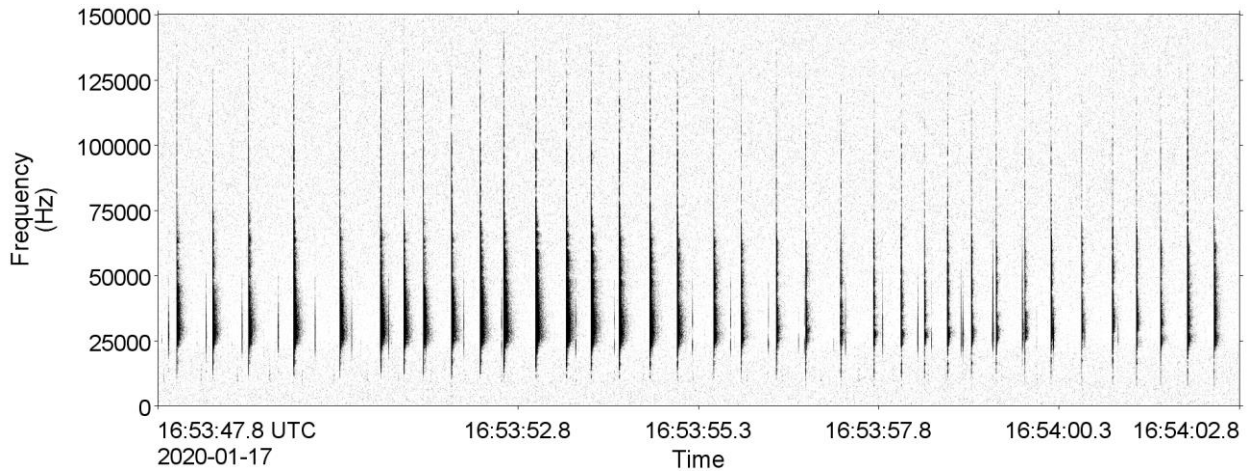


Figure 49. Spectrogram of northern bottlenose whale clicks recorded at Stn 19 on 17 Jan 2020 (64 Hz frequency resolution, 0.01 s time window, 0.005 s time step, Hamming window). The window length is 15 s.

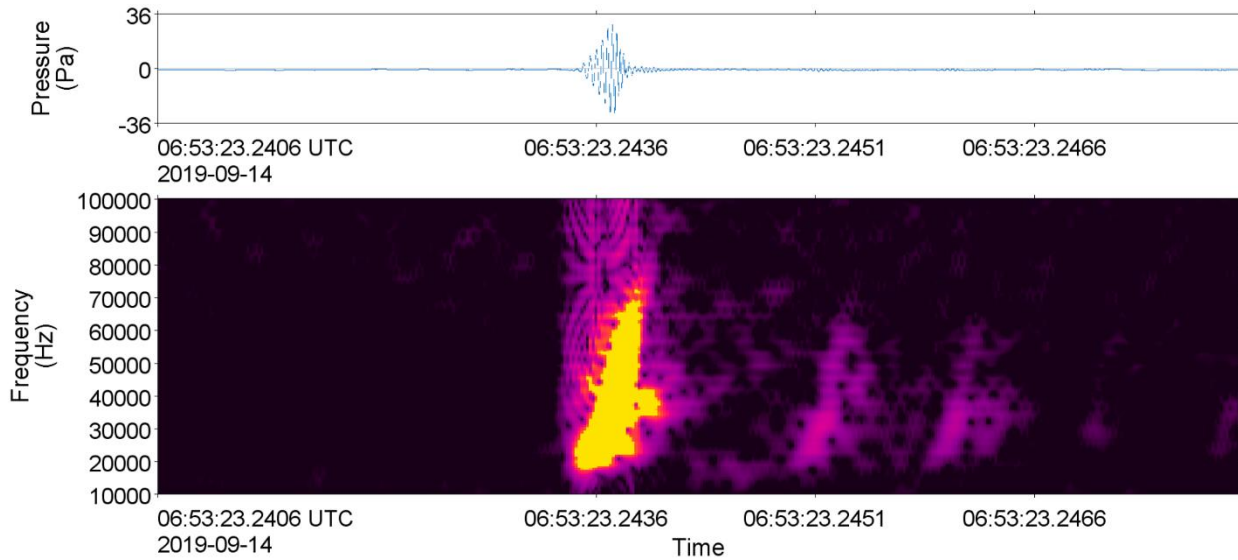


Figure 50. Spectrogram of a northern bottlenose whale click recorded at Stn 19 on 14 Sep 2019 (512 Hz frequency resolution, 0.266 ms time window, 0.02 ms time step).

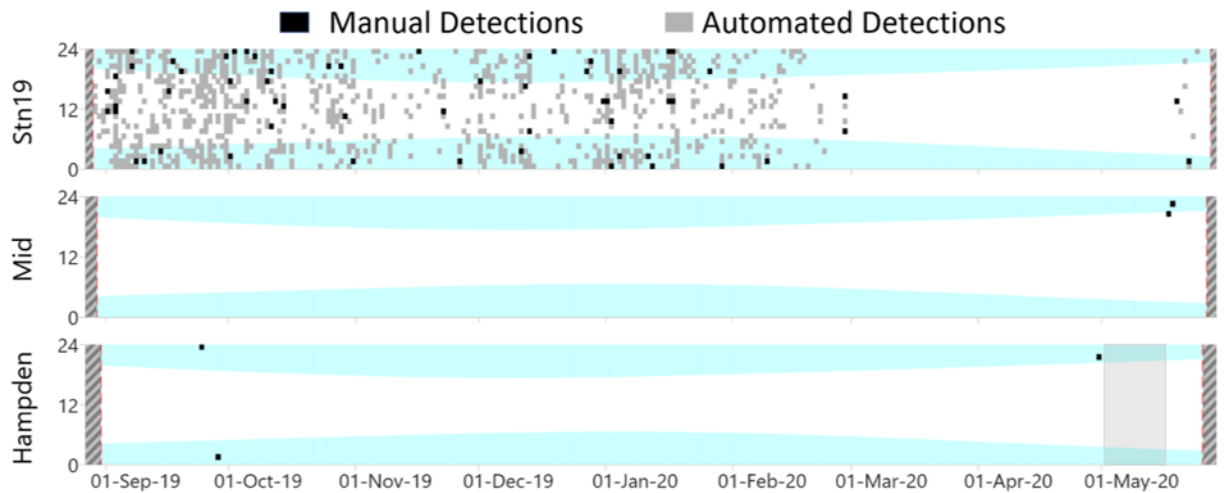


Figure 51. Daily and hourly occurrence of automatically and manually detected northern bottlenose whale clicks. Red dashed lines indicate recorder deployment and retrieval dates or recording end. Hashed lines indicate no recordings. Blue shaded areas indicate hours of darkness. Grey shaded areas indicate the presence of the MODU near the recorder.

Table 21. Northern bottlenose whales: Percent days with detections (manual or automated) and number of automated detections by month at Hampden (EL 1165A), Mid and Stn 19. D: detections.

Month	Stn 19		Mid		Hampden (EL 1165A) ¹	
	% days with D	% days with D	% days with D	% days with D	% days with D	Detections
Sep	100.0	41201	0.0	N/A	6.4	N/A
Oct	93.5	25187	0.0	N/A	0.0	N/A
Nov	76.7	7156	0.0	N/A	0.0	N/A
Dec	90.3	14923	0.0	N/A	0.0	N/A
Jan	96.8	24869	0.0	N/A	0.0	N/A
Feb	82.1	7310	0.0	N/A	0.0	N/A
Mar	0.0	0	0.0	N/A	0.0	N/A
Apr	0.0	0	0.0	N/A	3.2	N/A
May	22.2	792	7.7	N/A	0.0	N/A
Total	172	122769	2	N/A	3	N/A

¹MODU present from 2-14 May 2020

3.4.12. Sowerby’s Beaked Whales

Sowerby’s beaked whale clicks (Figures 52 and 53) were detected sporadically but consistently throughout the recording period at Hampden (EL 1165A). Manual detections at Stn 19 similarly indicate that this species was present at this station, but presumably at low levels. Detection counts showed more monthly variations than the detection time series, possibly reflecting differences in the number of vocalizing animals or their distance and orientation with respect to the recorder (Table 22; Figure 54).

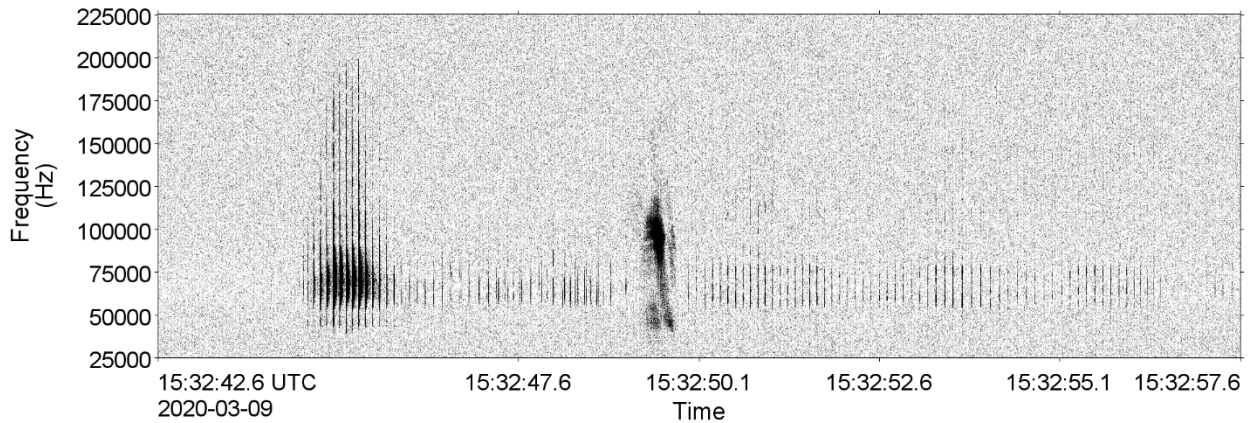


Figure 52. Spectrogram of Sowerby's beaked whale clicks recorded at Hampden (EL 1165A) on 9 Mar 2020 (64 Hz frequency resolution, 0.01 s time window, 0.005 s time step, Hamming window). The window length is 15 s.

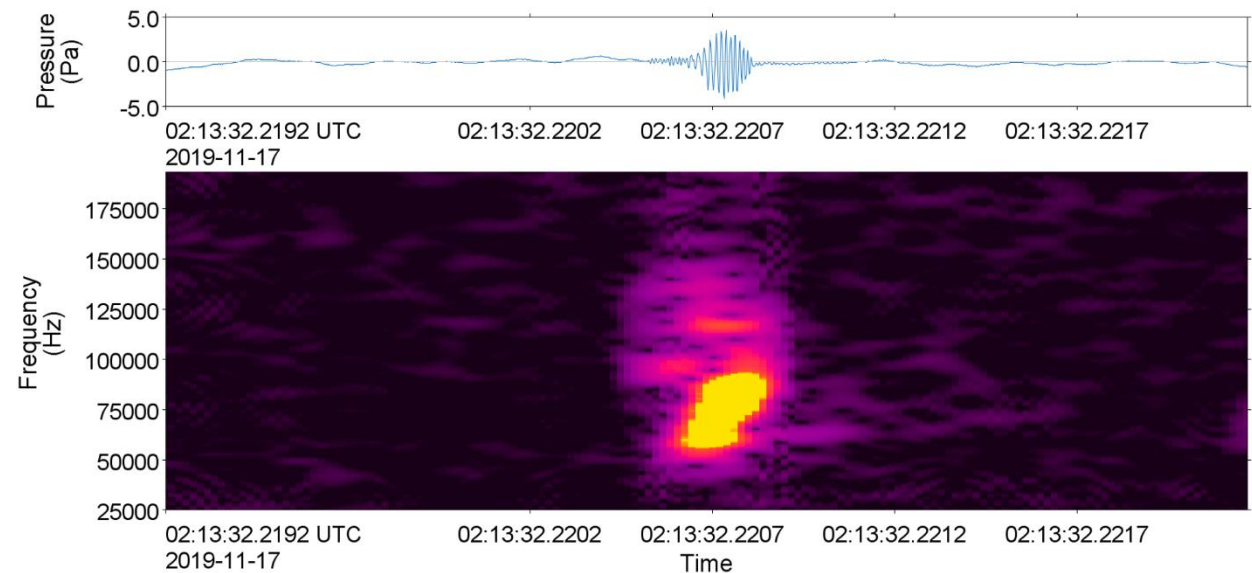


Figure 53. Spectrogram of a Sowerby's beaked whale click recorded at Mid on 19 Nov 2019 (512 Hz frequency resolution, 0.266 ms time window, 0.02 ms time step).

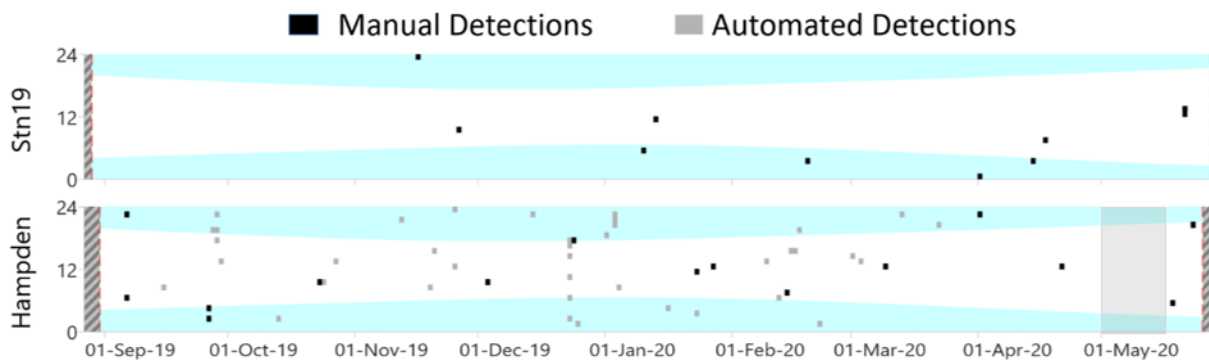


Figure 54. Daily and hourly occurrence of automatically and manually detected Sowerby's beaked whale clicks. Red dashed lines indicate recorder deployment and retrieval dates or recording end. Hashed lines indicate no recordings. Blue shaded areas indicate hours of darkness. Grey shaded areas indicate the presence of the MODU near the recorder.

Table 22. Sowerby’s beaked whales: Percent days with detections (manual or automated) and number of automated detections by month at Hampden (EL 1165A). D: Detections.

Month	Stn19		Hampden (EL 1165A) ¹	
	% days with D	Detections	% days with D	Detections
Sep	0.0	N/A	23.3	837
Oct	0.0	N/A	9.7	219
Nov	6.4	N/A	16.7	298
Dec	0.0	N/A	16.1	943
Jan	6.2	N/A	19.4	710
Feb	3.6	N/A	25.0	851
Mar	0.0	N/A	16.1	292
Apr	10.0	N/A	6.7	160
May	3.7	N/A	8.0	108
Total	9	N/A	42	4418

¹MODU present from 2-14 May 2020

3.4.13. Cuvier’s Beaked Whales

Cuvier’s beaked whales (Figure 55; Figure 56) were detected at Stn 19 on 25 Dec 2019, 6 Feb 2020, and 5 Apr 2020.

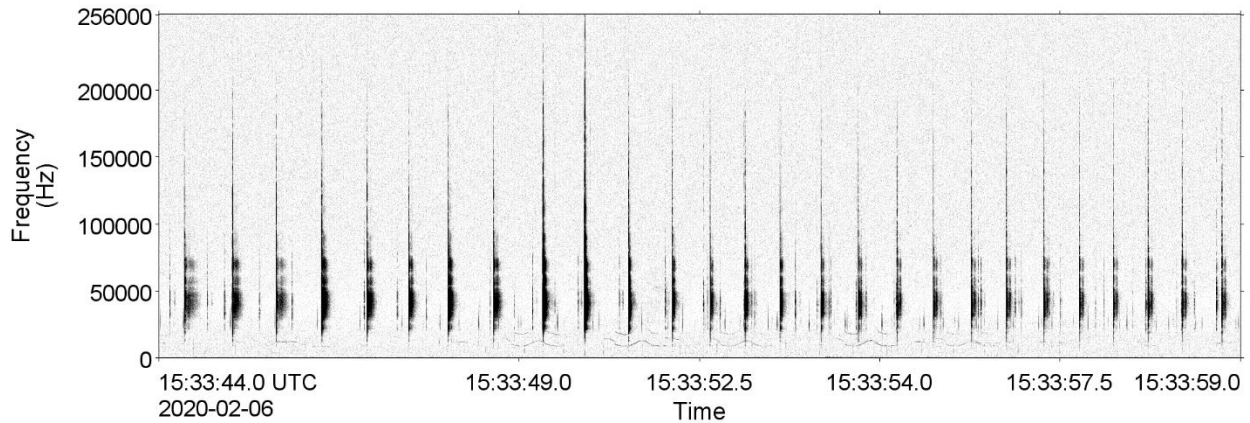


Figure 55. Spectrogram of Cuvier’s beaked whale clicks recorded at Stn 19 on 6 Feb 2020 (64 Hz frequency resolution, 0.01 s time window, 0.005 s time step, Hamming window). The window length is 15 seconds.

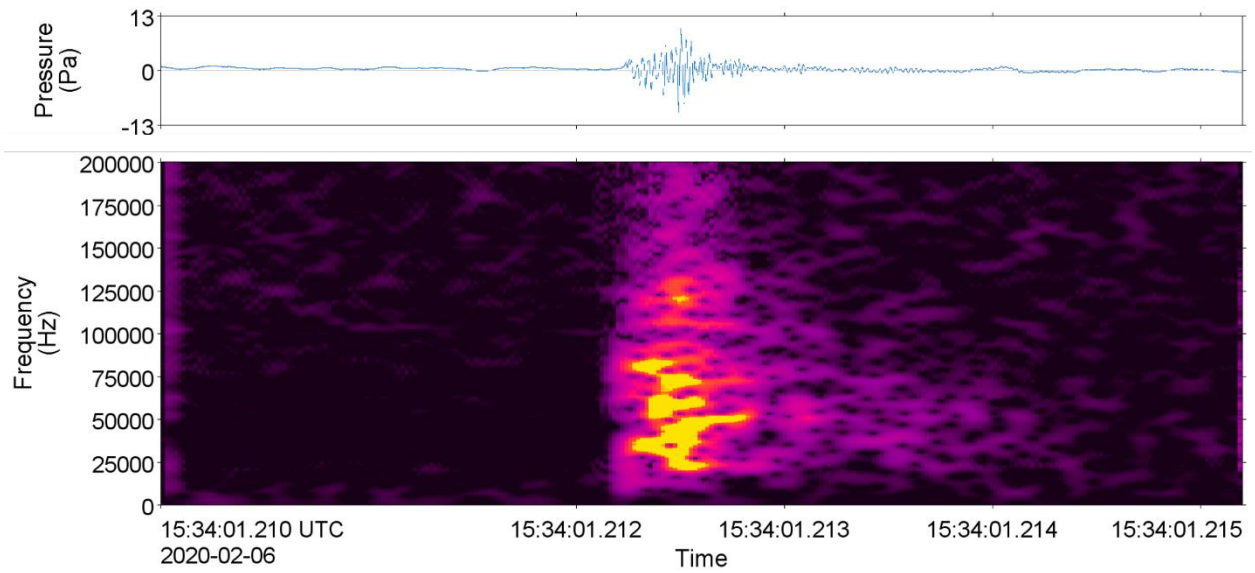


Figure 56. Spectrogram of a Cuvier's beaked whale click recorded at Stn 19 on 6 eb 2020 (512 Hz frequency resolution, 0.266 ms time window, 0.02 ms time step).

4. Discussion and Conclusion

4.1. Dependence of measured sound levels on wind conditions

The influence of weather and sea state on the underwater soundscape was assessed by correlating the decidecade SPL at 20, 80, 630, and 3150 Hz with the wind speed (Figures 5 and 57). The decidecade bands were selected as representative for the following reasons: fin whales (20 Hz), vessel traffic (80 Hz), peak wind (630 Hz), and the upper limit of wind (3150 Hz). The correlations used data with 30 min spacing, and calculated values over seven days to allow for development of variation in wind speed. Each station was compared to wind speeds at Harp (EL 1165B) well site that were available between January and May. There were notable storms with significant wave heights of over 6 m measured at Harp (EL 1165B) station on the following dates: 10–11 Dec, 13–15 Dec, 17–18 Dec, 20–22 Dec, 25–30 Dec, 6–7 Jan, 9–11 Jan, 18–19 Jan, 3 Feb, 8 Feb, 13 Feb, 8 Mar, 19 Apr (dates given by Wood). Most of the storms resulted in the rig being disconnected.

Figure 57 shows the calculated correlation coefficients between wind speeds and the sound levels measured in the four decidecade bands. Correlations are highest in the 630 and 3150 Hz bands, as expected (Wenz 1962, Carey and Evans 2011). Harp (EL 1165B) had the lowest correlation with wind speeds in all decidecade bands, which is the result of the ongoing MODU and DP usage dominating the measured sounds. This indicates that the DP sounds were not proportional to wind speed. This site is the shallowest (300 m), so we expected the highest correlations to wind and wave noise if the DP not been in use. The correlation with the 20 Hz fin whale band and the 80 Hz vessel band are also low, again likely due to the MODU broadband noise.

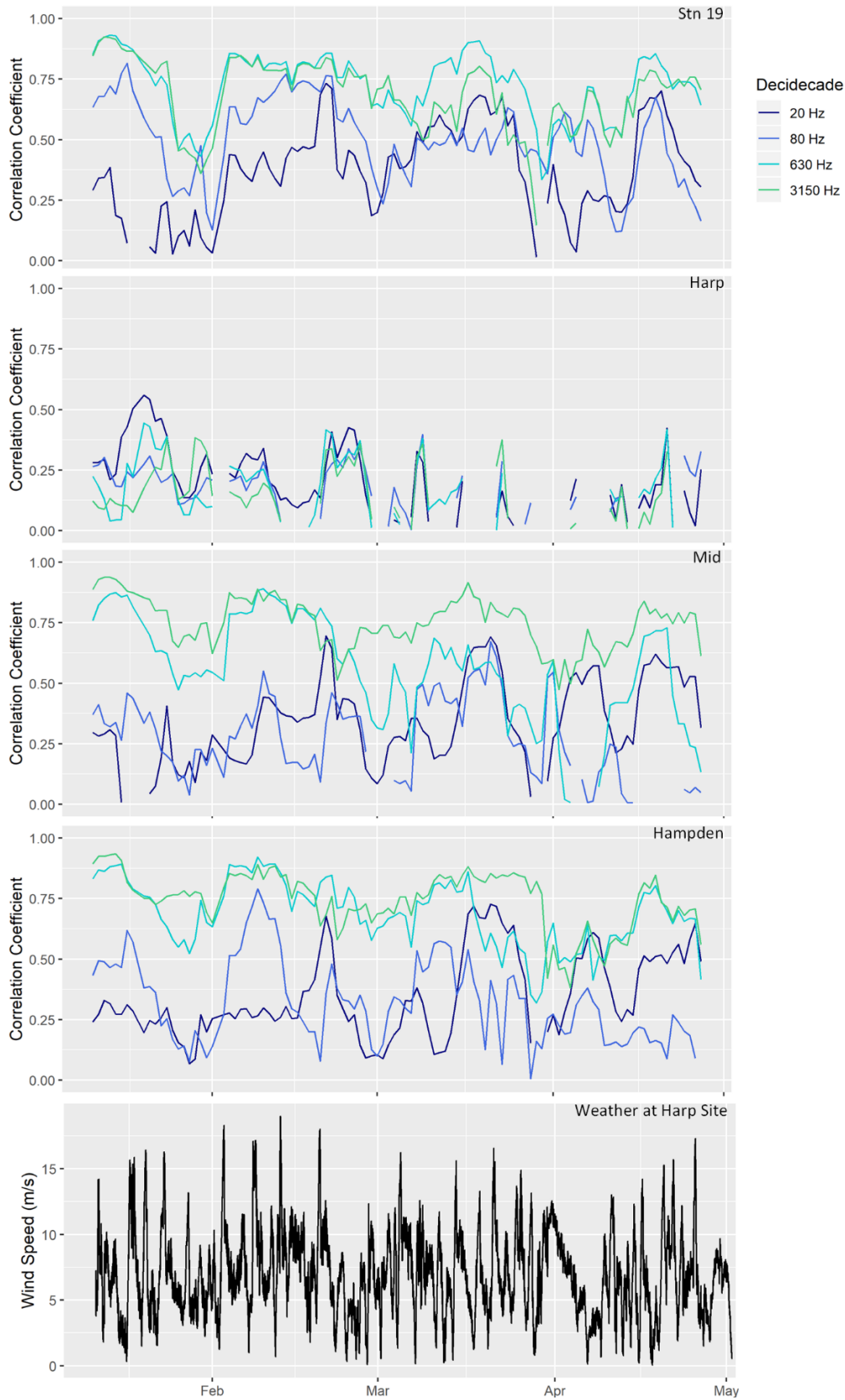


Figure 57. Weekly correlation coefficient between decade bands at 20, 80, 630, and 3150 Hz and wind speeds measured at Harp (EL 1165B) well site.

4.2. Comparison of Median Power Spectral Densities

The data in Figure 9 may be summarized by plotting each recorder’s median power spectral density (PSD) on a single axes (the median PSD is the sound spectrum that occurred for at least half of the deployment (Figure 58)). In the case of Harp (EL 1165B) and Hampden (EL 1165A), the deployment was divided into periods with and without the MODU nearby. The median power spectral densities show that all four locations had similar spectral without the MODU, and that MODU changed the spectra in the same way at both sites for both broadband levels and tones. The water depth had an interesting effect on the received power spectral density—above 5000 Hz the power spectral density levels 5 km from the MODU (at Hampden (EL 1165A), 1175 m deep) were higher than those received 2 km from Harp (EL 1165B) in 300 m of water. This was likely due to additional interactions with the seabed in the shallower water near Harp (EL 1165B) that increased the scattering of high-frequency sound.

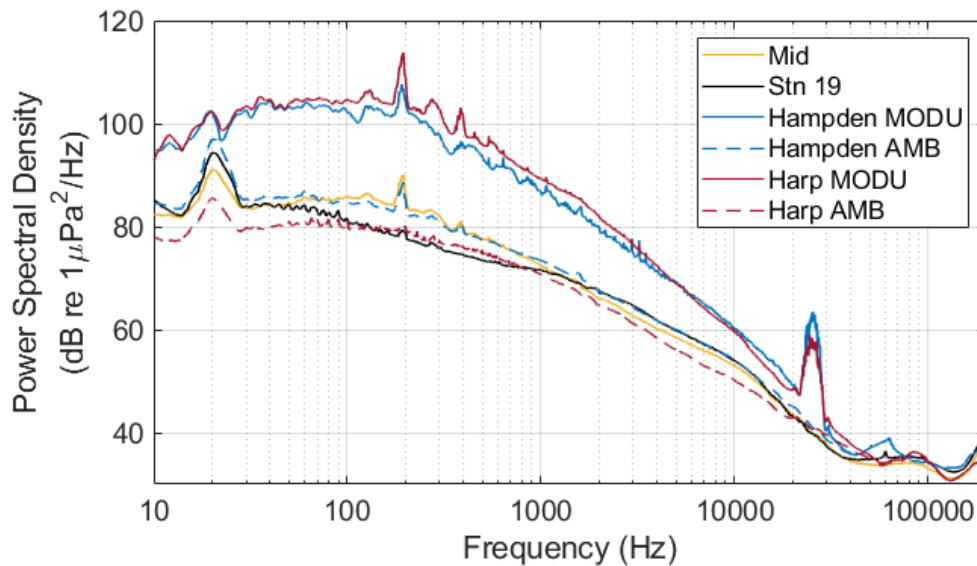


Figure 58. Comparison of the median power spectral densities in six conditions: the full duration at the Mid and Stn 19 recorders as well as the Harp (EL 1165B) and Hampden (EL 1165A) sites with the MODU nearby and for time without the MODU (marked as AMBient). The peak at 20 Hz is from fin whales, at 195 Hz from the West Aquarius, and at 25 kHz from the USBL transponders associated with the West Aquarius operations.

4.3. Measuring MODU Underwater Radiated Noise with Fixed Recorders

One of EMCL's objectives was to assess the utility of fixed recorders at some distance from the rig for measuring the URN. The recommended recorder configuration for measuring a vessel's URN is to have three hydrophones in a vertical array that make angles of approximately 15, 30, and 45 degree with the horizontal in deep water ([ISO] International Organization for Standardization 2016) (Figure 59). For this project, the single hydrophone recorders were placed on the seabed 2100 m from Harp (EL 1165B) and 5300 m from Hampden (EL 1165A). The water depth at Harp (EL 1165B) was ~300 m and ~1150 m at Hampden (EL 1165A), which means the deep-water constraint was not satisfied. However, by employing acoustic propagation modeling, it was expected we could compensate for this deficiency. A similar geometry is employed by many other groups as single hydrophone systems greatly simplify equipment handling and costs (e.g., McKenna et al. 2012, Simard et al. 2016, MacGillivray et al. 2019).

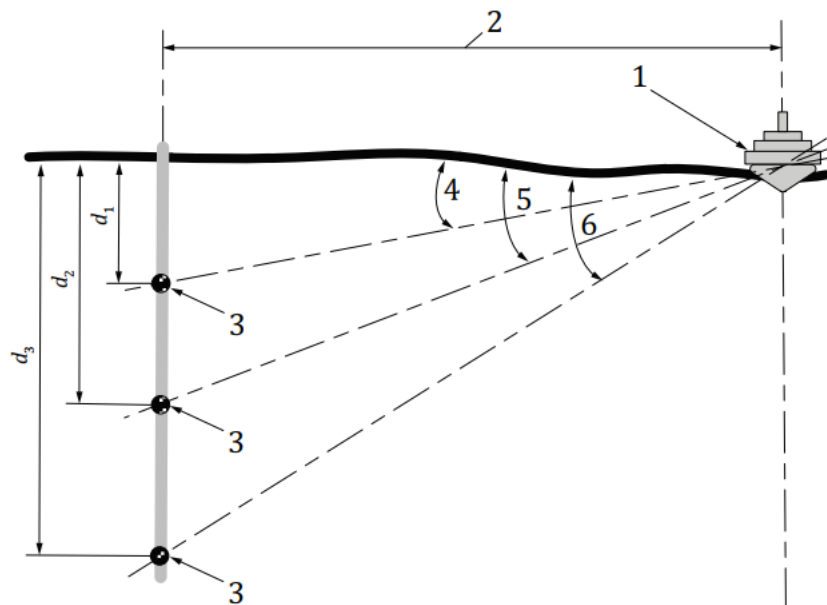


Figure 59. Recommended geometry for making underwater radiated noise measurements. (1) the vessel. (2) the closest point of approach (CPA) distance, which should be longer of 100 m or the vessel length. (3) hydrophones. (4, 5, 6) angles to the hydrophones with target angles of 15, 30, and 45 degrees. The water depth must be greater than the CPA distance for this geometry. From ISO Standard 17208-1 (2016).

A full comparison of the URN computed at Harp (EL 1165B) and Hampden stations is shown in

Figure 60. A summary of the median levels are shown in Figure 61. Because the measurement ranges were 5–7 times the water depths, the RNL were not expected to be reliable; however the two RNL results were very similar for the 200 Hz decade where the MODU signature was strongest. The MSL result at Harp (EL 1165B) was much lower than the Hampden (EL 1165A) RNL, as expected, but also much lower than the MSL at Hampden (EL 1165A). The analysis was repeated using at 20 m source depth for computing the MSL values, which yielded poorer results. This suggests that the seabed geoacoustics used in the propagation modeling were incorrect.

The difficulties with knowing the seabed composition are one of the reasons the ISO 17208-1 and -2 standards recommend making the measurements in deep water. For deep-water seabed measurements, it is preferable to place the recorder within one water depth of the platform to ensure that the dominant propagation path is spherical spreading; however, the propagation conditions still need to be considered. Even the MSL result measured at Harp (EL 1165B) were 6–8 dB higher than the RNL measured for the West Aquarius in 2300 m water depth off Nova Scotia (Martin et al. 2019a). The recorder was on the

seabed 2000 m from the well head, which satisfies the 45-degree criteria for measuring URN in deep water. Given the strongly upward refracting propagation conditions off Nova Scotia, the sound levels reaching the recorder may have been decreased by refraction. Methods to make accurate shallow water measurements of vessel source levels are currently being investigated by JASCO and DW Ship Consult for Transport Canada.

The results of this analysis indicate that accurate estimates the source level of an operational MODU are challenging to perform. The use of seabed instruments simplified data collection and minimized flow noise contamination of the data. However, because of the relatively long distance between the source and receiver (~6 water depths), the source level results were sensitive to our parameterization of the seabed geoacoustic properties. Future measurements should be made closer to the drill rigs, and perhaps using a vertical array of hydrophones.

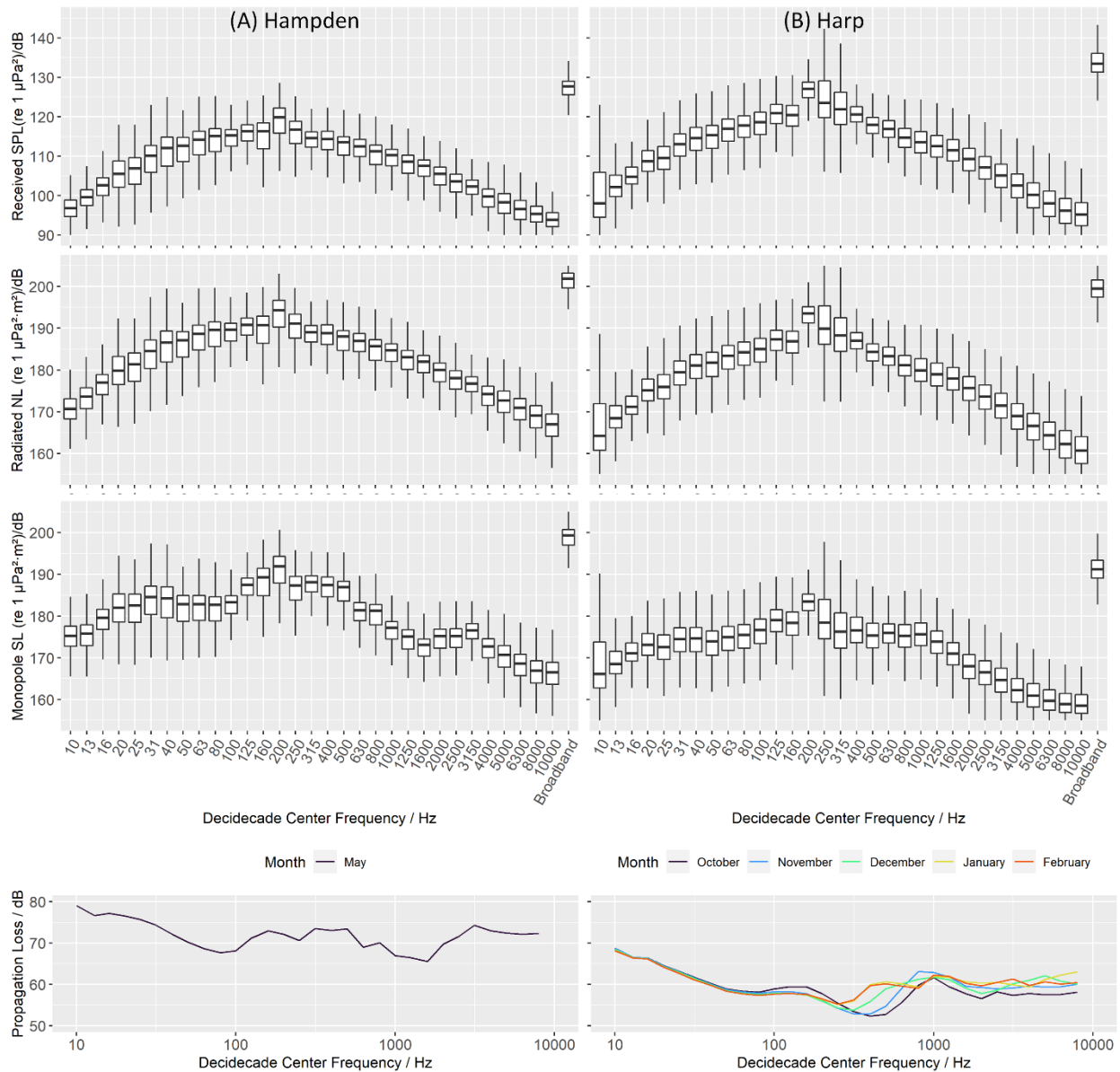


Figure 60. Summary of the underwater radiated noise (URN) of the West Aquarius Mobile Offshore Drilling Unit (MODU) measured at (A) Hampden (EL 1165A) and (B) Harp (EL 1165B). The top row show the decidecade received sound pressure level (SPL), the second row is the computed radiated noise level (RNL), the third row is the computed monopole source level (MSL), and the bottom row shows propagation losses predicted by acoustic propagation modeling for computing the MSL.

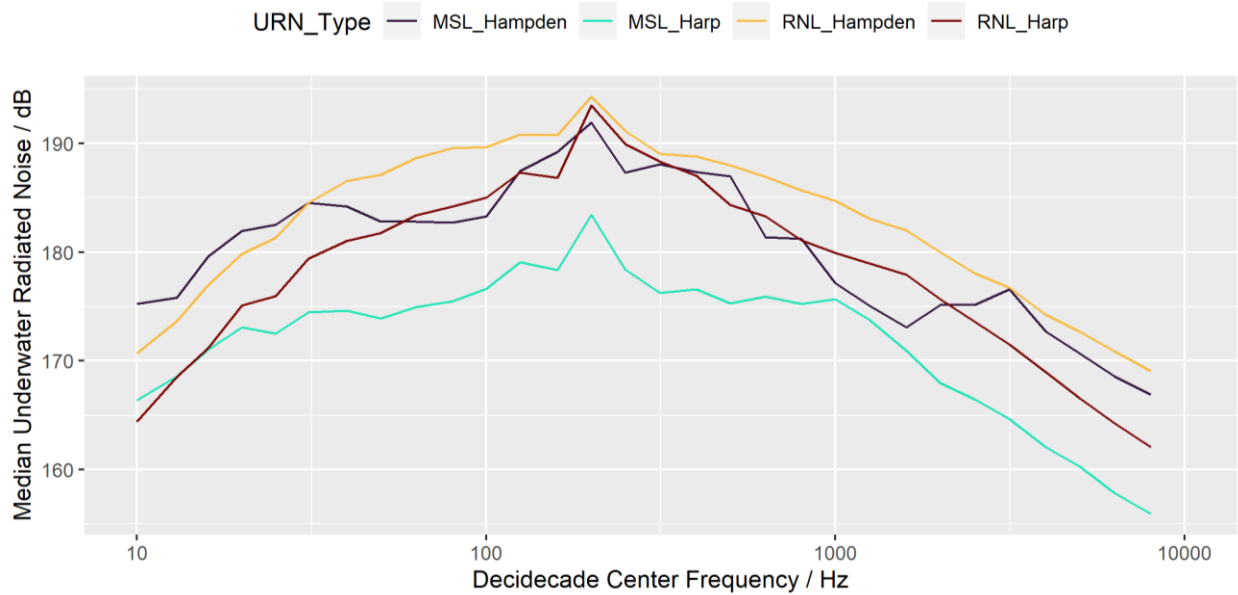


Figure 61. Comparison of the median underwater radiated noise (URN) computed from 10 days of data at Hampden (EL 1165A) and 5 months of data at Harp (EL 1165B). Since there were large amounts of data to work with at Harp (EL 1165B), the months with uninterrupted data (Oct 19 – Feb 20, inclusive) were chosen for this analysis.

4.4. Marine Mammal Occurrence

This study included a recorder (Stn 19) deployed at the same location as one of the stations of an ESRF-funded long-term acoustic monitoring program conducted from Aug 2015 to July 2017 (Delarue et al. 2018), which provided a baseline against which to assess the acoustic detections during this study. Ambient noise at Stn 19 was unaffected by drilling operations at Harp (EL 1165B). Marine mammal occurrence at this station in 2019-2020 was remarkably consistent with the patterns observed at the same location in 2016-2017 as well as other locations in the northern Flemish Pass (Maxner et al. 2017). Species exhibiting seasonal patterns of detections generally occurred during the same periods. For instance, humpback whale detections were restricted to December-February in both studies; delphinid detections occurred nearly daily but decreased in late winter and spring; fin, sei and blue whale detections coincided with their song production period. Except for sei whales, which presumably leave the area in December, the marked decline in detections of fin and blue whales past the end of winter is more likely to reflect changes in acoustic behavior rather than a departure from the areas surrounding the recorders, particularly considering the long detection ranges of their signals. In both studies, pilot whale detections declined significantly in late fall-early winter but resumed in spring, ahead of the increase in dolphin detections after the spring minimum. One minor difference between both studies is that northern bottlenose whale click detections declined in spring in 2016-17 whereas they were absent in March and April 2020 at Stn 19. Because the MODU was not detected at Stn 19, this is not likely to be connected to its presence at Harp (EL 1165B).

Potential displacement of blue and fin whales by the MODU at Harp (EL 1165B) was assessed by comparing detection counts at stations where the MODU’s acoustic signature was detectable (Harp (EL 1165B), Mid and Hampden (EL 1165A)). Displacement was assessed by dividing the detections per month (Table 12, Table 13) by the minimum detection range of their calls (Table 7) and comparing the

detections per km² as a function of distance from the MODU and month. Blue whales had increasing detection counts per km² with increasing distance from Harp (EL 1165B) (Figure 62, left). Because this gradient was observed in September, before the arrival of the MODU, and persisted throughout the fall and winter, it likely represents habitat preference by blue whales more than avoidance behaviour. This is also consistent with results from Delarue et al. (2018) that showed blue whale detections to be more common on the continental slope than on the shelf. The increase in call density in October may represent an increase in song production as whales progress into their breeding season, or an acoustic response to increased noise as previously observed in this species during exposures to different types of signals (Di Iorio and Clark 2009, Melcon et al. 2012). The decline in call density after October may reflect a decreasing number of individuals in the study area.

Fin whale detection counts per unit area also generally increased with range from the MODU, but the increase was more pronounced between Mid and Hampden than between Harp and Mid (Figure 62, right). Delarue et al. (2018) showed that fin whales off Newfoundland were more commonly detected on the continental shelf than off the continental slope, which suggests that call density should be higher at Harp than Mid or Hampden. This was only observed in January and February between Harp and Mid (Figure 62), driven by the increase in detections at Harp in these months. Call densities declined at all stations in October but returned to their baseline (September) levels after October. It is unclear whether the October decline, at a point in time when call densities should still be increasing, could represent an acoustic reaction to the MODU's exposure, as this species is known to alter its acoustic behavior in the presence of shipping and airgun sounds (Castellote et al. 2012).

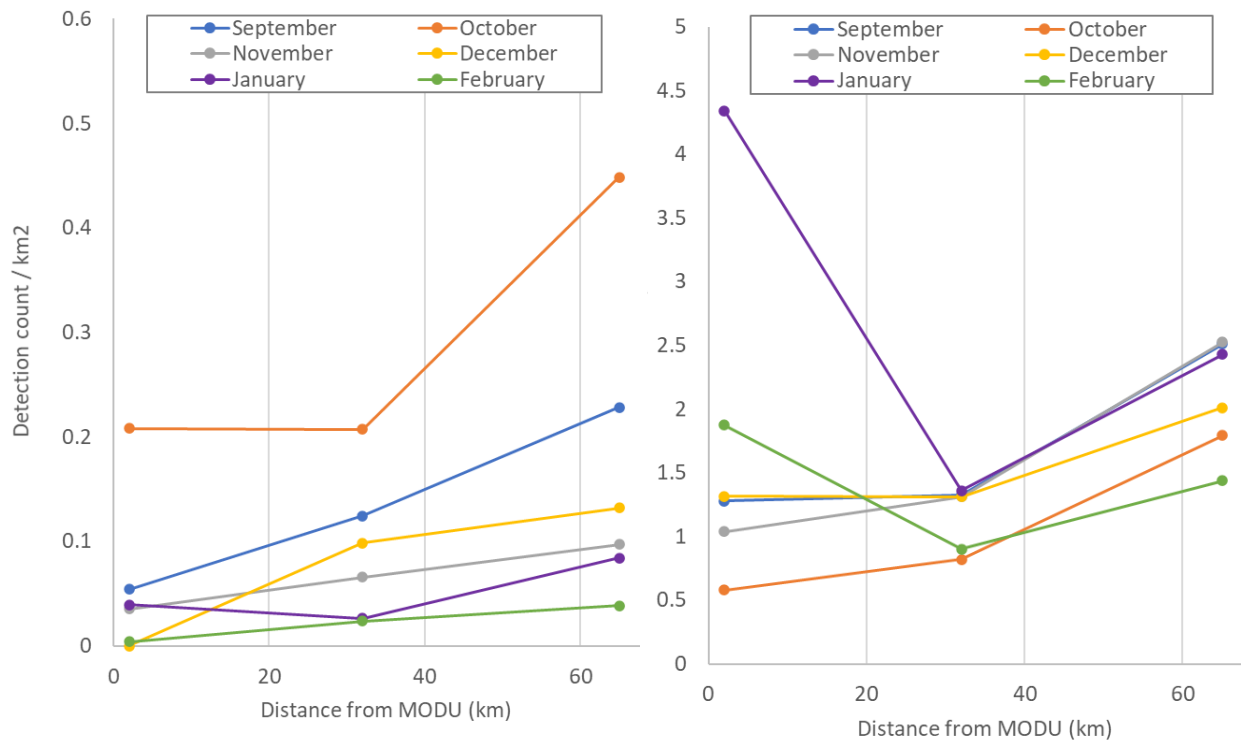


Figure 62. Detection count per km² by month as a function of distance from the MODU for blue (left) and fin (right) whales. The detection area was calculated as a circular area around each recorder with a radius equal to the minimum detection ranges across all modelled azimuths for a 50% probability of detection under median noise conditions for average source levels (see Table 7). The September detection ranges were used for September. The March detection ranges were used for all other months. There were not enough detections after February to include in this figure. The dots represents measurements at (from left to right) Harp, Mid and Hampden.

Delphinids and sperm whales produce signals that were less likely to be masked by the acoustic emissions of the MODU and had comparable detection ranges across stations (see Section 3.2).

Delphinid click and whistle detections were lower at Harp than any of the other stations before the arrival of the MODU. Despite a slight increase in detections in January and February, which was also noted in fin whales and harbour porpoises, delphinid detection counts at Harp were a fraction of those at the other stations. These two observations suggest a preference of the vocalizing species for the deeper water and slope habitat found at Mid, Hampden and Stn 19. The decline in click and whistle detections at Harp following the arrival of the MODU may be due to masking or avoidance. Whistle detections were higher at Hampden than Mid, but the opposite was true for clicks, confusing any assessment of potential long-range effects of the MODU.

There were no detectable effects of the MODU on sperm whale click detections. Their occurrence at Harp was only assessed using manual detections (due to sub-threshold precision of automated detector), which may underestimate their true occurrence, but these results are consistent with the known preference of sperm whales for deep water.

4.5. Effects of underwater noise on Marine Mammals

4.5.1. Comparisons to Regulatory Thresholds and Environmental Assessment Assumptions

The current best available scientific guidance for determining the effects of human-generated sound on marine mammals recommends assessing the distance at which the auditory frequency weighted daily SEL could cause hearing threshold shifts (NMFS 2018, Southall et al. 2019b). Temporary threshold shifts represent a temporary loss of hearing sensitivity. Exposure to a sound with sufficient duration and sound pressure level may result in an elevated hearing threshold, i.e., a loss of hearing sensitivity. If the threshold eventually returns to its baseline level, it is called a temporary threshold shift. If the threshold does not return to its baseline after some time, the offset is called a permanent threshold shift. Sound levels emitted by the West Aquarius at Harp (EL 1165B) and recorded 2 km away from the MODU exceeded the threshold for the onset of temporary threshold shift for continuous sound sources on 159 days in low-frequency cetaceans (baleen whales) and 86 days in high-frequency cetaceans (here, harbour porpoise) out of 229 days of operations (Figures 10 and 63). Sound levels never exceeded the threshold for the onset of permanent threshold shift for continuous sound sources in any species group. Results from the Scotian Basin's modelled operating drilling installations predicted that cumulative SELs (over 24 hours) would decrease to below threshold values for PTS at distances between 120 and 470 m from the source (depending on the species group and environmental conditions) (Zykov 2016). However, these predictions relied on NOAA 2015, whose onset thresholds are different from those used here. The most comparable results are those from Zykov (2018). PTS onset was found to occur up to 250 m, while TTS-onset could occur up to 3.2 (LFC)-5.9 (HFC) km in winter and 1.3 (LFC)-4.8 (HFC) km in summer. The winter ranges are generally consistent with those observed here.

Behavioural reactions are expected to occur well before the onset of TTS. In other words, cetaceans in the vicinity of the MODU may likely have taken evasive actions to avoid hearing damage. There are currently no accepted thresholds for the onset of behavioural reactions, which reflects the variability in intra- and inter-specific responses observed in marine mammal field studies as well as the influence of the context of exposure and the experience, motivation, and conditioning of exposed animals, which will vary greatly between areas and activities (Southall et al. 2007, Southall et al. 2019a).

A less sophisticated, though still widely used, metric for assessing possible behavioural disturbance to marine mammals (NMFS 1995, NOAA 2019) or habitat suitability (DFO 2012) is the distance at which the sound pressure levels exceed 120 dB re 1 μ Pa. Figure 64 is a comparison of the measured sound pressure levels as a function of range for Oct 2019 – Feb 2020 using our measurements made at the seabed. The range to the 120 dB re 1 μ Pa isopleth is 15-30 km. The Environmental Assessment considered the potential of EMCL's exploratory drilling activities for underwater noise effects on marine mammals based on studies by Zykov (2016) and Quijano et al. (2017). Zykov (2016) estimated the 95% percentile ($R_{95\%}$) of the horizontal range to the 120 dB re 1 μ Pa isopleth for drilling activities and sources similar to those monitored in this study (i.e. semi-submersible drilling unit with support vessel) to be

>150 km in winter and 27.8 km in summer in deep water off the Scotian Shelf. Quijano et al (2017) concluded that for high sound levels such as those emitted by the MODU, ranges would be longer at shallow sites (e.g. Harp (EL 1165B)) and similar at the deep sites (e.g. Hampden (EL 1165A)). The results presented here show the ranges to various thresholds to be shorter than those of Zykov (2016), particularly in winter, and much more comparable to those estimated by Zykov (2018) in a modeling study involving a deep (~ 1500 m) site near the study area, in the northern Flemish Pass (Figure 64). For a drillship, $R_{95\%}$ to the 120 dB isopleth was estimated at 25.1 km in winter and 5.8 km in summer (Zykov 2018).

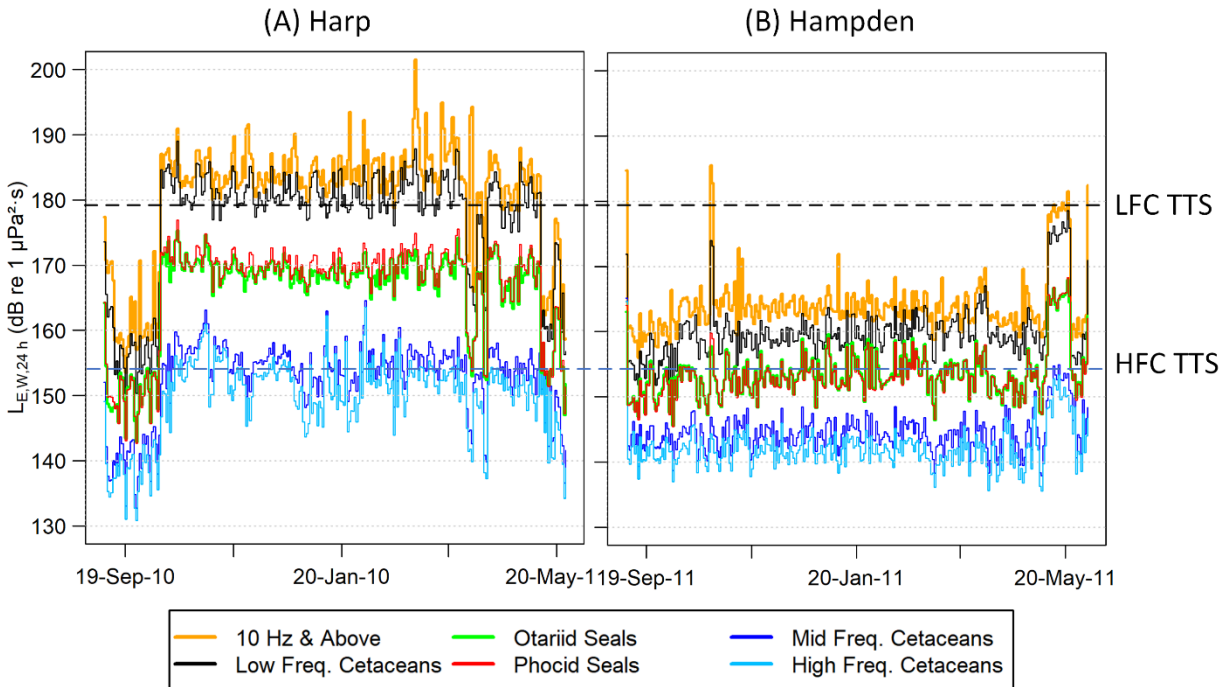


Figure 63. Comparison of the estimated daily sound exposure levels for the full spectrum (10 Hz and above) as well as weighted for each of the NMFS (2018) marine mammal hearing groups. The temporary threshold shift (TTS) thresholds from NFMS (2018) are shown for the low-frequency cetacean group (baleen whales) and the high-frequency cetacean group (porpoise and *Kogia* species (dwarf and pygmy sperm whales)).

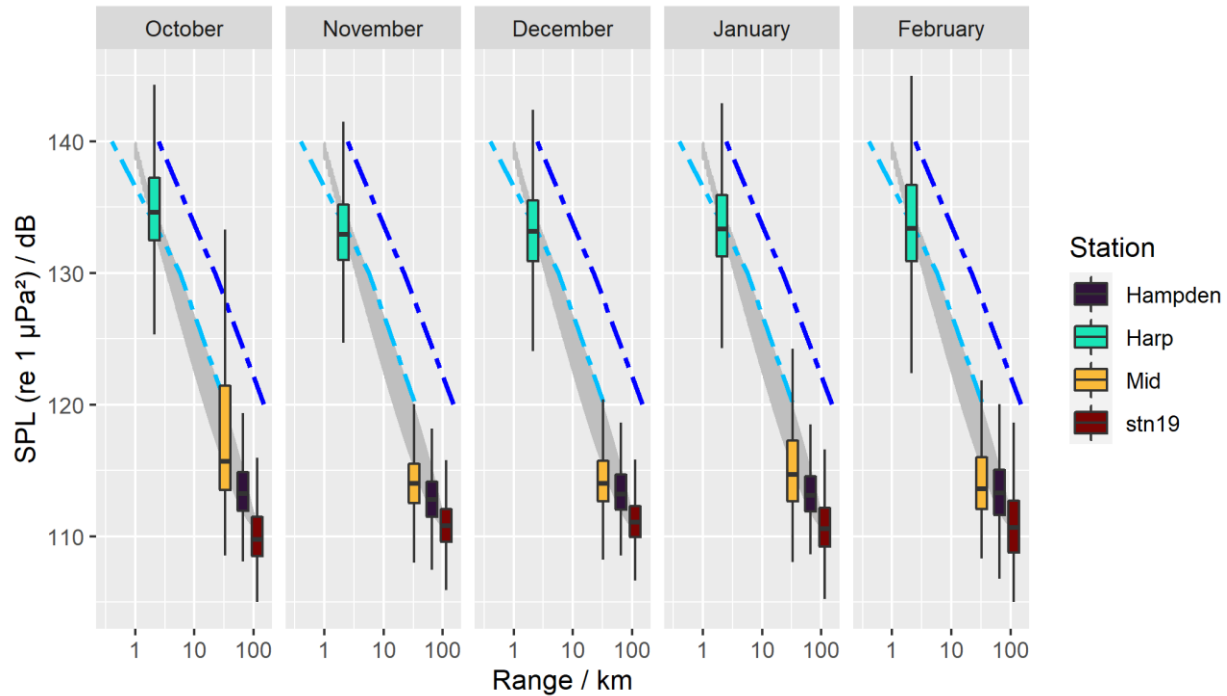


Figure 64. Comparison of broadband (10-16000 Hz) SPL for Oct 2019 - Feb 2020 as measured by the recorders at the seabed. The gray shape in the background is the prediction interval for the SPL as a function of range. The dark blue line shows the maximum range to the sound levels for an FPSO and support vessel in winter from Zykov (2016). The light blue line are the maximum range to the sound levels for the MODU and support vessel at a shallow water site near Harp from Zykov (2018).

4.5.2. Available Listening Range

As described in Section 2.4, the available listening range (ALR) for different types of marine mammal vocalizations were calculated (Figure 65 and Figure 66). ALR estimates the percentage of the best-case listening range that the animals have available for each day of the recordings. Due to the limited effects of human sounds at Stn 19, the ALR at this location may be taken as ‘normal’.

The presence of the MODU substantially reduced the ALR for the vocalizations analyzed. The effects are most prominent for the low-frequency cetaceans (Figure 65) where the ALR is reduced to less than 5% of the best case at the Harp (EL1165B) site when the MODU was present. Note that environmental conditions reduced the ALR to ~20-60% of the best case on most days. These results indicate a 10 to 100-fold decrease in distance in which the animals may hear each other. Interestingly, the fin whale chorus also reduced the ALR to ~5% of the best case at all stations at the peak of their vocalization season in January-February.

The ALR for mid-frequency cetaceans (Figure 66) depends on the frequency analyzed more than was the case for low-frequency cetaceans. Lower frequencies, which overlap to a greater degree with the MODU than higher frequencies, were more affected. The USBL transponders reduced the ALR for mid-frequency cetaceans’ echolocation clicks from ~50% of best case when the transponders were off to ~5% with them on, which equates to a 10-fold range reduction.

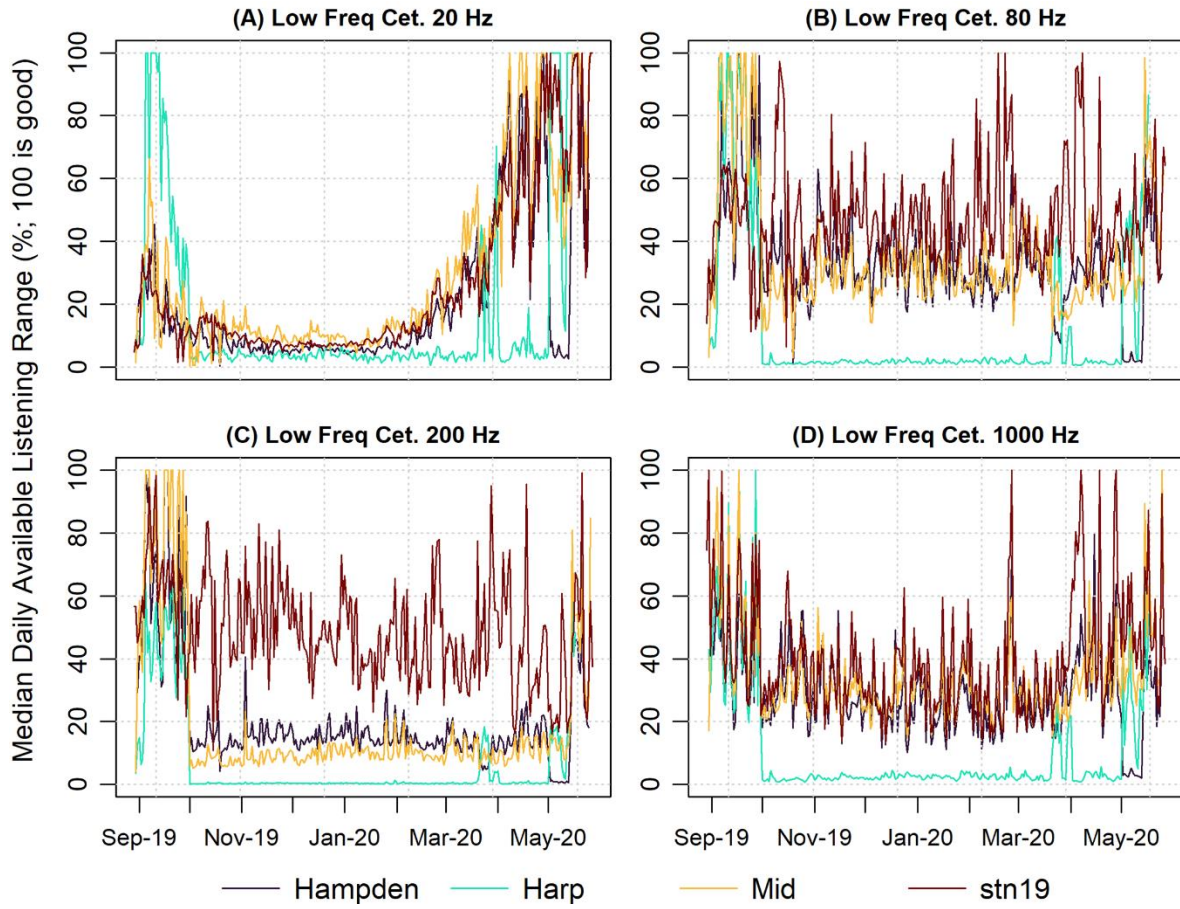


Figure 65. Available Listening Range for low-frequency cetaceans.

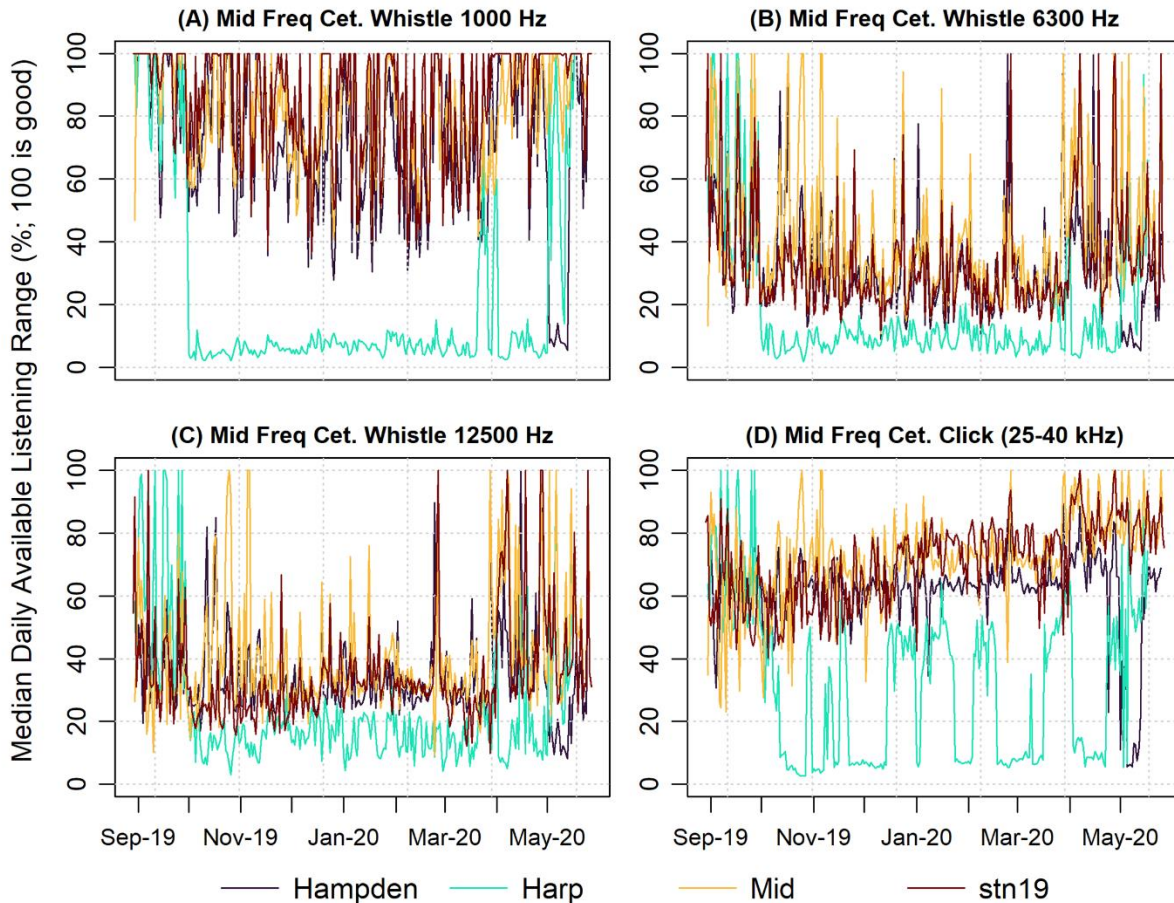


Figure 66. Available Listening Range for mid-frequency cetaceans.

4.6. Conclusion

The sound levels from the drilling operations of the West Aquarius MODU measured at the seabed in the Flemish Pass were well below the sound levels considered during the Environmental Assessment (Quijano et al. 2017). Those sound levels were based on the modeling performed for the Scotian Basin Exploration Project that took place in deep water off Nova Scotia (Zykov 2016). The measured sound levels closely matched the predictions for a MODU and support vessels operating in the Flemish Pass (Zykov 2018).

There was no clear evidence of changes in marine mammal distribution associated with the presence of the MODU at ranges of 32 km and beyond. At short range (2-5 km), the data provided evidence of avoidance of the Harp well site when the MODU was present in fin whale and harbour porpoise and avoidance or call masking in blue and pilot whales. Changes in distribution were one of the project's predicted effects in the Environmental Assessment.

Drilling operations were associated with prolonged periods of sound levels high enough to induce temporary hearing threshold shifts in low- and high-frequency cetaceans if avoidance behaviours were not initiated. Avoidance reactions most likely occurred to prevent auditory injuries, as marine mammals have been shown to react to sound sources, particularly at high sound exposure levels (Ellison et al. 2012). As received sound level generally decreases with distance from a source, avoidance behaviors can strongly influence the estimated maximum sound levels an animal is predicted to receive and significantly affects the probability of more pronounced direct or subsequent behavioral effects.

Additionally, animals are less likely to respond to sound levels distant from a source, even when those same levels elicit response at closer ranges; both proximity and received levels are important factors in aversive responses (Dunlop et al. 2017). Aversion reaction may also depend on an animal's behavior and previous exposures. While the onset of behavioural responses, including aversion, depends to some extent on received sound level, several contextual factors also influence response probability, including an animal's activity state, the type of sound, the relative positions of the source with respect to the receiving subject, the animal's gender, age and reproductive status of the receiving animal and whether it has been previously exposed to the type of sound (Ellison et al. 2012, DeRuiter et al. 2013, Goldbogen et al. 2013, Friedlaender et al. 2016, DeRuiter et al. 2017, Dunlop et al. 2018).

Even at sub-TTS sound pressure levels, marine mammals can experience chronic stress as a result of elevated ambient noise caused by vessel traffic (Rolland et al. 2012), the long-term consequences thereof being poorly understood. The consequences of displacement on the long-term fitness of affected individuals and populations is unknown but should be considered, particularly in the case of endangered species such as the blue whale (Atlantic population), or species displaying site fidelity to affected areas (Costa et al. 2016, Forney et al. 2017, Farmer et al. 2018).

Glossary

absorption

The reduction of acoustic pressure amplitude due to acoustic particle motion energy converting to heat in the propagation medium.

ambient noise

All-encompassing sound at a given place, usually a composite of sound from many sources near and far (ANSI S1.1-1994 R2004), e.g., shipping vessels, seismic activity, precipitation, sea ice movement, wave action, and biological activity.

attenuation

The gradual loss of acoustic energy from absorption and scattering as sound propagates through a medium.

audiogram

A graph of hearing threshold level (sound pressure levels) as a function of frequency, which describes the hearing sensitivity of an animal over its hearing range.

audiogram weighting

The process of applying an animal’s audiogram to sound pressure levels to determine the sound level relative to the animal’s hearing threshold (HT). Unit: dB re HT.

Auditory frequency weighting (auditory weighting function, frequency-weighting function)

The process of band-pass filtering sounds to reduce the importance of inaudible or less-audible frequencies for individual species or groups of species of aquatic mammals (ISO 2017a). One example is M-weighting introduced by Southall et al. (2007) to describe “Generalized frequency weightings for various functional hearing groups of marine mammals, allowing for their functional bandwidths and appropriate in characterizing auditory effects of strong sounds”.

background noise

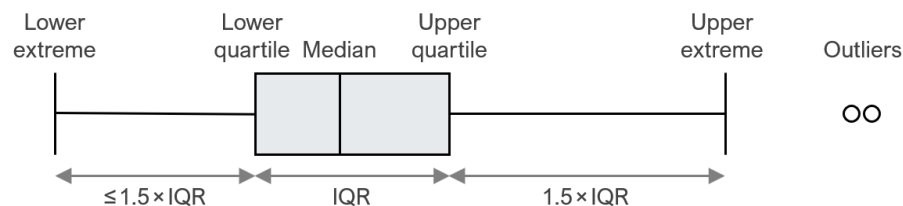
Total of all sources of interference in a system used for the production, detection, measurement, or recording of a signal, independent of the presence of the signal (ANSI S1.1-1994 R2004). Ambient noise detected, measured, or recorded with a signal is part of the background noise.

bandwidth

The range of frequencies over which a sound occurs. Broadband refers to a source that produces sound over a broad range of frequencies (e.g., seismic airguns, vessels) whereas narrowband sources produce sounds over a narrow frequency range (e.g., sonar) (ANSI/ASA S1.13-2005 R2010).

box-and-whisker plot

A plot that illustrates the centre, spread, and overall range of data from a visual 5-number summary. The box is the interquartile range (IQR), which shows the middle 50% of the data—from the lower quartile (25th percentile) to the upper quartile (75th percentiles). The line inside the box is the median (50th percentile). The whiskers show the lower and upper extremes excluding outliers, which are data points that fall more than $1.5 \times \text{IQR}$ beyond the upper and lower quartiles.



broadband sound level

The total sound pressure level measured over a specified frequency range. If the frequency range is unspecified, it refers to the entire measured frequency range.

cetacean

Any animal in the order Cetacea. These are aquatic, mostly marine mammals and include whales, dolphins, and porpoises.

continuous sound

A sound whose sound pressure level remains above ambient sound during the observation period (ANSI/ASA S1.13-2005 R2010). A sound that gradually varies in intensity with time, for example, sound from a marine vessel.

decade

Logarithmic frequency interval whose upper bound is ten times larger than its lower bound (ISO 2006).

decidecade

One tenth of a decade (ISO 2017a). Note: An alternative name for decidecade (symbol ddec) is “one-tenth decade”. A decidecade is approximately equal to one third of an octave ($1 \text{ ddec} \approx 0.3322 \text{ oct}$) and for this reason is sometimes referred to as a “one-third octave”.

decidecade band

Frequency band whose bandwidth is one decidecade. Note: The bandwidth of a decidecade band increases with increasing centre frequency.

decibel (dB)

One-tenth of a bel. Unit of level when the base of the logarithm is the tenth root of ten, and the quantities concerned are proportional to power (ANSI S1.1-1994 R2004).

delphinid

Family of oceanic dolphins, or Delphinidae, composed of approximately thirty extant species, including dolphins, pilot whales, and killer whales.

duty cycle

The time when sound is periodically recorded by an acoustic recording system.

fast Fourier transform (FFT)

A computationally efficient algorithm for computing the discrete Fourier transform.

frequency

The rate of oscillation of a periodic function measured in cycles-per-unit-time. The reciprocal of the period. Unit: hertz (Hz). Symbol: f . 1 Hz is equal to 1 cycle per second.

hearing group

Groups of marine mammal species with similar hearing ranges. Commonly defined functional hearing groups include low-, mid-, and high-frequency cetaceans, pinnipeds in water, and pinnipeds in air.

geoacoustic

Relating to the acoustic properties of the seabed.

hearing threshold

The sound pressure level for any frequency of the hearing group that is barely audible for a given individual in the absence of significant background noise during a specific percentage of experimental trials.

hertz (Hz)

A unit of frequency defined as one cycle per second.

high-frequency (HF) cetacean

The functional cetacean hearing group that represents those odontocetes (toothed whales) specialized for hearing high frequencies.

hydrophone

An underwater sound pressure transducer. A passive electronic device for recording or listening to underwater sound.

low-frequency (LF) cetacean

The functional cetacean hearing group that represents mysticetes (baleen whales) specialized for hearing low frequencies.

masking

Obscuring of sounds of interest by sounds at similar frequencies.

mean-square sound pressure spectral density

Distribution as a function of frequency of the mean-square sound pressure per unit bandwidth (usually 1 Hz) of a sound having a continuous spectrum (ANSI S1.1-1994 R2004). Unit: $\mu\text{Pa}^2/\text{Hz}$.

median

The 50th percentile of a statistical distribution.

mid-frequency (MF) cetacean

The functional cetacean hearing group that represents those odontocetes (toothed whales) specialized for mid-frequency hearing.

monopole source level (MSL)

A source level that has been calculated using an acoustic model that accounts for the effect of the sea-surface and seabed on sound propagation, assuming a point-like (monopole) sound source. Also see **radiated noise level**.

mysticete

Mysticeti, a suborder of cetaceans, use their baleen plates, rather than teeth, to filter food from water. They are not known to echolocate, but they use sound for communication. Members of this group include rorquals (Balaenopteridae), right whales (Balaenidae), and grey whales (*Eschrichtius robustus*).

non-impulsive sound

Sound that is broadband, narrowband or tonal, brief or prolonged, continuous or intermittent, and typically does not have a high peak pressure with rapid rise time (typically only small fluctuations in decibel level) that impulsive signals have (ANSI/ASA S3.20-1995 R2008). For example, marine vessels, aircraft, machinery, construction, and vibratory pile driving (NIOSH 1998, NOAA 2015).

octave

The interval between a sound and another sound with double or half the frequency. For example, one octave above 200 Hz is 400 Hz, and one octave below 200 Hz is 100 Hz.

odontocete

The presence of teeth, rather than baleen, characterizes these whales. Members of the Odontoceti are a suborder of cetaceans, a group comprised of whales, dolphins, and porpoises. The skulls of toothed whales are mostly asymmetric, an adaptation for their echolocation. This group includes sperm whales, killer whales, belugas, narwhals, dolphins, and porpoises.

percentile level, exceedance

The sound level exceeded $n\%$ of the time during a measurement.

permanent threshold shift (PTS)

A permanent loss of hearing sensitivity caused by excessive noise exposure. PTS is considered auditory injury.

phocid

A common term used to describe all members of the family Phocidae. These true/earless seals are more adapted to in-water life than are otariids, which have more terrestrial adaptations. Phocids use their hind flippers to propel themselves. Phocids are one of the three main groups in the superfamily Pinnipedia; the other two groups are otariids and walrus.

pinniped

A common term used to describe all three groups that form the superfamily Pinnipedia: phocids (true seals or earless seals), otariids (eared seals or fur seals and sea lions), and walrus.

point source

A source that radiates sound as if from a single point (ANSI S1.1-1994 R2004).

power spectrum density

Generic term, formally defined as power in W/Hz, but sometimes loosely used to refer to the spectral density of other parameters such as square pressure or time-integrated square pressure.

pressure, acoustic

The deviation from the ambient hydrostatic pressure caused by a sound wave. Also called overpressure. Unit: pascal (Pa). Symbol: p .

radiated noise level (RNL)

A source level that has been calculated assuming sound pressure decays geometrically with distance from the source, with no influence of the sea-surface and seabed. Also see **monopole source level**.

received level (RL)

The sound level measured (or that would be measured) at a defined location.

rms

root-mean-square.

sound

A time-varying pressure disturbance generated by mechanical vibration waves travelling through a fluid medium such as air or water.

sound exposure

Time integral of squared, instantaneous frequency-weighted sound pressure over a stated time interval or event. Unit: pascal-squared second ($\text{Pa}^2\cdot\text{s}$) (ANSI S1.1-1994 R2004).

sound exposure level (SEL)

A cumulative measure related to the sound energy in one or more pulses. Unit: dB re $1 \mu\text{Pa}^2\cdot\text{s}$. SEL is expressed over the summation period (e.g., per-pulse SEL [for airguns], single-strike SEL [for pile drivers], 24-hour SEL).

sound intensity

Sound energy flowing through a unit area perpendicular to the direction of propagation per unit time.

sound pressure level (SPL)

The decibel ratio of the time-mean-square sound pressure, in a stated frequency band, to the square of the reference sound pressure (ANSI S1.1-1994 R2004).

For sound in water, the reference sound pressure is one micropascal ($p_0 = 1 \mu\text{Pa}$) and the unit for SPL is dB re $1 \mu\text{Pa}^2$:

$$L_p = 10 \log_{10}(p^2/p_0^2) = 20 \log_{10}(p/p_0)$$

Unless otherwise stated, SPL refers to the root-mean-square (rms) pressure level. See also 90% sound pressure level and fast-average sound pressure level. Non-rectangular time window functions may be applied during calculation of the rms value, in which case the SPL unit should identify the window type.

sound speed profile

The speed of sound in the water column as a function of depth below the water surface.

source level (SL)

The sound level measured in the far-field and scaled back to a standard reference distance of 1 metre from the acoustic centre of the source. Unit: dB re $1 \mu\text{Pa}\cdot\text{m}$ (pressure level) or dB re $1 \mu\text{Pa}^2\cdot\text{s}\cdot\text{m}$ (exposure level).

spectral density level

The decibel level ($10\cdot\log_{10}$) of the spectral density of a given parameter such as SPL or SEL, for which the units are dB re $1 \mu\text{Pa}^2/\text{Hz}$ and dB re $1 \mu\text{Pa}^2\cdot\text{s}/\text{Hz}$, respectively.

spectrogram

A visual representation of acoustic amplitude compared with time and frequency.

spectrum

An acoustic signal represented in terms of its power, energy, mean-square sound pressure, or sound exposure distribution with frequency.

surface duct

The upper portion of a water column within which the sound speed profile gradient causes sound to refract upward and therefore reflect off the surface resulting in relatively long-range sound propagation with little loss.

temporary threshold shift (TTS)

Temporary loss of hearing sensitivity caused by excessive noise exposure.

transmission loss (TL)

The decibel reduction in sound level between two stated points that results from sound spreading away from an acoustic source subject to the influence of the surrounding environment. Also referred to as propagation loss.

Literature Cited

- [ISO] International Organization for Standardization. 2006. *ISO 80000-3:2006. Quantities and Units – Part 3: Space and time*. <https://www.iso.org/standard/31888.html>.
- [ISO] International Organization for Standardization. 2016. *ISO 17208-1:2016. Underwater acoustics – Quantities and procedures for description and measurement of underwater sound from ships – Part 1: Requirements for precision measurements in deep water used for comparison purposes*. <https://www.iso.org/standard/62408.html>.
- [ISO] International Organization for Standardization. 2017a. *ISO 18405:2017. Underwater acoustics – Terminology*. Geneva. <https://www.iso.org/standard/62406.html>.
- [ISO] International Organization for Standardization. 2017b. *ISO 18406:2017(E). Underwater acoustics— Measurement of radiated underwater sound from percussive pile driving*. Geneva. <https://www.iso.org/obp/ui/#iso:std:iso:18406:ed-1:v1:en>.
- [NIOSH] National Institute for Occupational Safety and Health. 1998. *Criteria for a recommended standard: Occupational noise exposure. Revised Criteria*. Document Number 98-126. US Department of Health and Human Services, NIOSH, Cincinnati, OH, USA. 122 p. <https://www.cdc.gov/niosh/docs/98-126/pdfs/98-126.pdf>.
- [NMFS] National Marine Fisheries Service (US) and [NOAA] National Oceanic and Atmospheric Administration (US). 1995. Small takes of marine mammals incidental to specified activities; offshore seismic activities in southern California: Notice of issuance of an incidental harassment authorization. *Federal Register* 60(200): 53753-53760.
- [NMFS] National Marine Fisheries Service (US). 2018. *2018 Revision to: Technical Guidance for Assessing the Effects of Anthropogenic Sound on Marine Mammal Hearing (Version 2.0): Underwater Thresholds for Onset of Permanent and Temporary Threshold Shifts*. US Department of Commerce, NOAA. NOAA Technical Memorandum NMFS-OPR-59. 167 p. <https://www.fisheries.noaa.gov/webdam/download/75962998>.
- [NOAA] National Oceanic and Atmospheric Administration (US). 2015. *Draft guidance for assessing the effects of anthropogenic sound on marine mammal hearing: Underwater acoustic threshold levels for onset of permanent and temporary threshold shifts*. NMFS Office of Protected Resources, Silver Spring, MD, USA. 180 p.
- [NOAA] National Oceanic and Atmospheric Administration (US). 2019. *ESA Section 7 Consultation Tools for Marine Mammals on the West Coast* (webpage), 27 Sep 2019. <https://www.fisheries.noaa.gov/west-coast/endangered-species-conservation/esa-section-7-consultation-tools-marine-mammals-west>. (Accessed 10 Mar 2020).
- [NRC] National Research Council (US). 2003. *Ocean Noise and Marine Mammals*. National Research Council (US), Ocean Studies Board, Committee on Potential Impacts of Ambient Noise in the Ocean on Marine Mammals. The National Academies Press, Washington, DC, USA. <https://www.nap.edu/read/10564/chapter/1>.
- Aerts, L.A.M., M. Bles, S.B. Blackwell, C.R. Greene, Jr., K.H. Kim, D.E. Hannay, and M.E. Austin. 2008. *Marine mammal monitoring and mitigation during BP Liberty OBC seismic survey in Foggy Island Bay, Beaufort Sea, July-August 2008: 90-day report*. Document Number P1011-1. Report by LGL Alaska Research Associates Inc., LGL Ltd., Greeneridge Sciences Inc., and JASCO Applied Sciences for BP Exploration Alaska. 199 p. ftp://ftp.library.noaa.gov/noaa_documents.lib/NMFS/Auke%20Bay/AukeBayScans/Removable%20Disk/P1011-1.pdf.

- Ainslie, M.A., J.L. Miksis-Olds, S.B. Martin, K. Heaney, C.A.F. de Jong, A.M. von Benda-Beckmann, and A.P. Lyons. 2018. *ADEON Underwater Soundscape and Modeling Metadata Standard*. Version 1.0. Technical report by JASCO Applied Sciences for ADEON Prime Contract No. M16PC00003.
- Andrew, R.K., B.M. Howe, and J.A. Mercer. 2011. Long-time trends in ship traffic noise for four sites off the North American West Coast. *Journal of the Acoustical Society of America* 129(2): 642-651. <https://doi.org/10.1121/1.3518770>.
- ANSI S1.1-1994. R2004. *American National Standard Acoustical Terminology*. American National Standards Institute, NY, USA.
- ANSI/ASA S1.13-2005. R2010. *American National Standard Measurement of Sound Pressure Levels in Air*. American National Standards Institute and Acoustical Society of America, NY, USA.
- ANSI/ASA S3.20-1995. R2008. *American National Standard Bioacoustical Terminology*. American National Standards Institute and Acoustical Society of America, NY, USA.
- Au, W.W. and D.L. Herzing. 2003. Echolocation signals of wild Atlantic spotted dolphin (*Stenella frontalis*). *The Journal of the Acoustical Society of America* 113(1): 598-604.
- Au, W.W.L., R.A. Kastelein, T. Rippe, and N.M. Schooneman. 1999. Transmission beam pattern and echolocation signals of a harbor porpoise (*Phocoena phocoena*). *Journal of the Acoustical Society of America* 106(6): 3699-3705. <https://doi.org/10.1121/1.428221>.
- Austin, M.E. and G.A. Warner. 2012. *Sound Source Acoustic Measurements for Apache's 2012 Cook Inlet Seismic Survey*. Version 2.0. Technical report by JASCO Applied Sciences for Fairweather LLC and Apache Corporation.
- Austin, M.E. and L. Bailey. 2013. *Sound Source Verification: TGS Chukchi Sea Seismic Survey Program 2013*. Document Number 00706, Version 1.0. Technical report by JASCO Applied Sciences for TGS-NOPEC Geophysical Company.
- Austin, M.E., A. McCrodon, C. O'Neill, Z. Li, and A.O. MacGillivray. 2013. *Marine mammal monitoring and mitigation during exploratory drilling by Shell in the Alaskan Chukchi and Beaufort Seas, July–November 2012: 90-Day Report*. In: Funk, D.W., C.M. Reiser, and W.R. Koski (eds.). *Underwater Sound Measurements*. LGL Rep. P1272D–1. Report from LGL Alaska Research Associates Inc. and JASCO Applied Sciences, for Shell Offshore Inc., National Marine Fisheries Service (US), and US Fish and Wildlife Service. 266 pp plus appendices.
- Austin, M.E. 2014. Underwater noise emissions from drillships in the Arctic. In: Papadakis, J.S. and L. Bjørnø (eds.). *UA2014 - 2nd International Conference and Exhibition on Underwater Acoustics*. 22-27 Jun 2014, Rhodes, Greece. pp. 257-263.
- Austin, M.E., H. Yurk, and R. Mills. 2015. *Acoustic Measurements and Animal Exclusion Zone Distance Verification for Furie's 2015 Kitchen Light Pile Driving Operations in Cook Inlet*. Version 2.0. Technical report by JASCO Applied Sciences for Jacobs LLC and Furie Alaska.
- Austin, M.E. and Z. Li. 2016. *Marine Mammal Monitoring and Mitigation During Exploratory Drilling by Shell in the Alaskan Chukchi Sea, July–October 2015: Draft 90-day report*. In: Ireland, D.S. and L.N. Bisson (eds.). *Underwater Sound Measurements*. LGL Rep. P1363D. Report from LGL Alaska Research Associates Inc., LGL Ltd., and JASCO Applied Sciences Ltd. For Shell Gulf of Mexico Inc, National Marine Fisheries Service, and US Fish and Wildlife Service. 188 pp + appendices.

- Bailey, H., G. Clay, E.A. Coates, D. Lusseau, B. Senior, and P.M. Thompson. 2010. Using T-PODs to assess variations in the occurrence of coastal bottlenose dolphins and harbour porpoises. *Aquatic Conservation: Marine and Freshwater Ecosystems* 20(2): 150-158. <https://doi.org/10.1002/aqc.1060>.
- Baumgartner, M.F., S.M. Van Parijs, F.W. Wenzel, C.J. Tremblay, H.C. Esch, and A.M. Warde. 2008. Low frequency vocalizations attributed to sei whales (*Balaenoptera borealis*). *Journal of the Acoustical Society of America* 124(2): 1339-1349. <https://doi.org/10.1121/1.2945155>.
- Becker, J.J., D.T. Sandwell, W.H.F. Smith, J. Braud, B. Binder, J. Depner, D. Fabre, J. Factor, S. Ingalls, et al. 2009. Global Bathymetry and Elevation Data at 30 Arc Seconds Resolution: SRTM30_PLUS. *Marine Geodesy* 32(4): 355-371. <https://doi.org/10.1080/01490410903297766>.
- Berchok, C.L., D.L. Bradley, and T.B. Gabrielson. 2006. St. Lawrence blue whale vocalizations revisited: Characterization of calls detected from 1998 to 2001. *Journal of the Acoustical Society of America* 120(4): 2340-2354. <https://doi.org/10.1121/1.2335676>.
- Carey, W.M. and R.B. Evans. 2011. *Ocean ambient noise: Measurement and Theory*. The Underwater Acoustics Series. Springer.
- Carnes, M.R. 2009. *Description and Evaluation of GDEM-V 3.0*. US Naval Research Laboratory, Stennis Space Center, MS. NRL Memorandum Report 7330-09-9165. 21 p. <https://apps.dtic.mil/dtic/tr/fulltext/u2/a494306.pdf>.
- Castellote, M., C.W. Clark, and M.O. Lammers. 2012. Acoustic and behavioural changes by fin whales (*Balaenoptera physalus*) in response to shipping and airgun noise. *Biological Conservation* 147(1): 115-122. <https://doi.org/10.1016/j.biocon.2011.12.021>.
- Cholewiak, D., S. Baumann-Pickering, and S.M. Van Parijs. 2013. Description of sounds associated with Sowerby's beaked whales (*Mesoplodon bidens*) in the western North Atlantic Ocean. *Journal of the Acoustical Society of America* 134(5): 3905-3912. <https://doi.org/10.1121/1.4823843>.
- Clark, C.W. 1990. Acoustic behaviour of mysticete whales. In Thomas, J. and R.A. Kastelein (eds.). *Sensory Abilities of Cetaceans*. Springer, Boston, MA. pp. 571-583. https://doi.org/10.1007/978-1-4899-0858-2_40.
- Collins, M.D. 1993. A split-step Padé solution for the parabolic equation method. *Journal of the Acoustical Society of America* 93(4): 1736-1742. <https://doi.org/10.1121/1.406739>.
- Collins, M.D., R.J. Cederberg, D.B. King, and S. Chin-Bing. 1996. Comparison of algorithms for solving parabolic wave equations. *Journal of the Acoustical Society of America* 100(1): 178-182. <https://doi.org/10.1121/1.415921>.
- Coppens, A.B. 1981. Simple equations for the speed of sound in Neptunian waters. *Journal of the Acoustical Society of America* 69(3): 862-863. <https://doi.org/10.1121/1.382038>.
- Costa, D.P., L.A. Hückstädt, L.K. Schwarz, A.S. Friedlaender, B.R. Mate, A.N. Zerbini, A. Kennedy, and N.J. Gales. 2016. Assessing the exposure of animals to acoustic disturbance: Towards an understanding of the population consequences of disturbance. *Proceedings of Meetings on Acoustics* 27: 010027. <https://doi.org/10.1121/2.0000298>.
- Croll, D.A., C.W. Clark, A. Acevedo-Gutiérrez, B. Tershy, S. Flores, J. Gedamke, and J. Urban. 2002. Only male fin whales sing loud songs. *Nature* 417(6891): 809. <http://www.nature.com/articles/417809a>.

- Davis, G.E. 2020. Using Passive Acoustic Data to Track Changes in Baleen Whale Distribution Throughout the Western North Atlantic Ocean.
- Deane, G.B. 2000. Long time-base observations of surf noise. *Journal of the Acoustical Society of America* 107(2): 758-770. <https://doi.org/10.1121/1.428259>.
- DeAngelis, A.I., J.E. Stanistreet, S. Baumann-Pickering, and D.M. Cholewiak. 2018. A description of echolocation clicks recorded in the presence of True's beaked whale (*Mesoplodon mirus*). *Journal of the Acoustical Society of America* 144(5): 2691-2700. <https://doi.org/10.1121/1.5067379>.
- Deecke, V.B., J.K.B. Ford, and P.J.B. Slater. 2005. The vocal behaviour of mammal-eating killer whales: Communicating with costly calls. *Animal Behaviour* 69(2): 395-405. <https://doi.org/10.1016/j.anbehav.2004.04.014>.
- Delarue, J., K.A. Kowarski, E.E. Maxner, J.T. MacDonnell, and S.B. Martin. 2018. *Acoustic Monitoring Along Canada's East Coast: August 2015 to July 2017*. Document Number 01279, Environmental Studies Research Funds Report Number 215, Version 1.0. Technical report by JASCO Applied Sciences for Environmental Studies Research Fund, Dartmouth, NS, Canada. 120 pp + appendices. https://static1.squarespace.com/static/52aa2773e4b0f29916f46675/t/5c784432e5e5f0533d5756f0/1551385685533/ESRF215_Delarue%2C+J+et+al_optimized.pdf.
- DeRuiter, S.L., B.L. Southall, J. Calambokidis, W.M. Zimmer, D. Sadykova, E.A. Falcone, Ari S. Friedlaender, J.E. Joseph, D. Moretti, et al. 2013. First direct measurements of behavioural responses by Cuvier's beaked whales to mid-frequency active sonar. *Biology Letters* 9(4): 1-5. <https://doi.org/10.1098/rsbl.2013.0223>.
- DeRuiter, S.L., R. Langrock, T. Skirbutas, J.A. Goldbogen, J. Calambokidis, A.S. Friedlaender, and B.L. Southall. 2017. A multivariate mixed hidden Markov model for blue whale behaviour and responses to sound exposure. *The Annals of Applied Statistics* 11(1): 362-392. <https://projecteuclid.org/443/euclid.aos/1491616885>.
- Deveau, T.J. 2018. *ESRF Transmission Loss Modelling: Predicted Received Levels, with M-weighting, for Offshore Airgun Surveys in Atlantic Canada*. Document Number 01620. Version 1.0. Technical report by JASCO Applied Sciences for Environmental Studies Research Fund.
- DFO. 2012. Recovery Strategy for the Beluga Whale (*Delphinapterus leucas*), St. Lawrence Estuary Population in Canada. *Species at Risk Act Recovery Strategy Series*. Fisheries and Oceans Canada, Ottawa. 88 pp + X pp.
- Di Iorio, L. and C.W. Clark. 2009. Exposure to seismic survey alters blue whale acoustic communication. *Biology Letters* 6(1): 51-54. <https://doi.org/10.1098/rsbl.2009.0967>.
- Ding, W., B. Würsig, and W. Evans. 1995. Comparisons of whistles among seven odontocete species. In Kastelein, R.A., J.A. Thomas, and P.E. Nachtigall (eds.). *Sensory Systems of Aquatic Mammals*. De Spil Publishers, The Netherlands. pp. 299-324.
- Dunlop, R.A., M.J. Noad, D.H. Cato, and D. Stokes. 2007. The social vocalization repertoire of east Australian migrating humpback whales (*Megaptera novaeangliae*). *Journal of the Acoustical Society of America* 122(5): 2893-2905. <https://doi.org/10.1121/1.2783115>.
- Dunlop, R.A., D.H. Cato, and M.J. Noad. 2008. Non-song acoustic communication in migrating humpback whales (*Megaptera novaeangliae*). *Marine Mammal Science* 24(3): 613-629. <https://doi.org/10.1111/j.1748-7692.2008.00208.x>

- Dunlop, R.A., M.J. Noad, R.D. McCauley, L. Scott-Hayward, E. Kniest, R. Slade, D. Paton, and D.H. Cato. 2017. Determining the behavioural dose–response relationship of marine mammals to air gun noise and source proximity. *Journal of Experimental Biology* 220(16): 2878-2886. <https://jeb.biologists.org/content/220/16/2878>.
- Dunlop, R.A., M.J. Noad, R.D. McCauley, E. Kniest, R. Slade, D. Paton, and D.H. Cato. 2018. A behavioural dose-response model for migrating humpback whales and seismic air gun noise. *Marine Pollution Bulletin* 133: 506-516.
- Edds-Walton, P.L. 1997. Acoustic communication signals of mysticetes whales. *Bioacoustics* 8(1-2): 47-60. <https://doi.org/10.1080/09524622.2008.9753759>.
- Ellison, W.T., B.L. Southall, C.W. Clark, and A.S. Frankel. 2012. A New Context-Based Approach to Assess Marine Mammal Behavioral Responses to Anthropogenic Sounds. *Conservation Biology* 26(1): 21-28. <https://doi.org/10.1111/j.1523-1739.2011.01803.x>.
- Erbe, C., C. Reichmuth, K. Cunningham, K. Lucke, and R. Dooling. 2016. Communication masking in marine mammals: A review and research strategy. *Marine Pollution Bulletin* 103(1): 15-38. <https://doi.org/10.1016/j.marpolbul.2015.12.007>.
- Eskesen, I.G., M. Wahlberg, M. Simon, and O.N. Larsen. 2011. Comparison of echolocation clicks from geographically sympatric killer whales and long-finned pilot whales. *Journal of the Acoustical Society of America* 130(1): 9-12. <https://doi.org/10.1121/1.3583499>.
- Farmer, N.A., K. Baker, D.G. Zeddies, S.L. Denes, D.P. Noren, L.P. Garrison, A. Machernis, E.M. Fougères, and M. Zykov. 2018. Population consequences of disturbance by offshore oil and gas activity for endangered sperm whales (*Physeter macrocephalus*). *Biological Conservation* 227: 189-204.
- Finneran, J.J. 2015. *Auditory weighting functions and TTS/PTS exposure functions for cetaceans and marine carnivores*. Technical report by SSC Pacific, San Diego, CA, USA.
- Finneran, J.J. 2016. *Auditory weighting functions and TTS/PTS exposure functions for marine mammals exposed to underwater noise*. Technical Report for Space and Naval Warfare Systems Center Pacific, San Diego, CA, USA. 49 p. <http://www.dtic.mil/dtic/tr/fulltext/u2/1026445.pdf>.
- Fisher, F.H. and V.P. Simmons. 1977. Sound absorption in sea water. *Journal of the Acoustical Society of America* 62(3): 558-564. <https://doi.org/10.1121/1.381574>.
- Ford, J.K.B. 1989. Acoustic behaviour of resident killer whales (*Orcinus orca*) off Vancouver Island, British Columbia. *Canadian Journal of Zoology* 67(3): 727-745. <https://doi.org/10.1139/z89-105>.
- Forney, K.A., B.L. Southall, E. Slooten, S. Dawson, A.J. Read, R.W. Baird, and R.L. Brownell Jr. 2017. Nowhere to go: Noise impact assessments for marine mammal populations with high site fidelity. *Endangered Species Research* 32: 391-413. <https://doi.org/10.3354/esr00820>.
- Freedman, D. and P. Diaconis. 1981. On the histogram as a density estimator: L_2 theory. *Probability theory* 57(4): 453-476. <https://doi.org/10.1007/BF01025868>.
- Friedlaender, A.S., E.L. Hazen, J.A. Goldbogen, A.K. Stimpert, J. Calambokidis, and B.L. Southall. 2016. Prey-mediated behavioral responses of feeding blue whales in controlled sound exposure experiments. *Ecological Applications* 26(4): 1075-1085. <https://doi.org/10.1002/15-0783>.
- Funk, D., D.E. Hannay, D.S. Ireland, R. Rodrigues, and W.R. Koski (eds.). 2008. *Marine mammal monitoring and mitigation during open water seismic exploration by Shell Offshore Inc. in the*

- Chukchi and Beaufort Seas, July–November 2007: 90-day report*. LGL Report P969-1. Prepared by LGL Alaska Research Associates Inc., LGL Ltd., and JASCO Research Ltd. for Shell Offshore Inc., National Marine Fisheries Service (U.S.), and U.S. Fish and Wildlife Service. 218 p.
- Gannier, A., S. Fuchs, P. Quèbre, and J.N. Oswald. 2010. Performance of a contour-based classification method for whistles of Mediterranean delphinids. *Applied Acoustics* 71(11): 1063-1069. <https://doi.org/10.1016/j.apacoust.2010.05.019>.
- Girola, E., M.J. Noad, R.A. Dunlop, and D.H. Cato. 2019. Source levels of humpback whales decrease with frequency suggesting an air-filled resonator is used in sound production. *The Journal of the Acoustical Society of America* 145(2): 869-880.
- Goldbogen, J.A., B.L. Southall, S.L. Deruiter, J. Calambokidis, A.S. Friedlaender, E.L. Hazen, E.A. Falcone, G.S. Schorr, A. Douglas, et al. 2013. Blue whales respond to simulated mid-frequency military sonar. *Proceedings of the Royal Society B* 280(1765): 1-8. <https://doi.org/10.1098/rspb.2013.0657>.
- Hannay, D.E. and R.G. Racca. 2005. *Acoustic Model Validation*. Document Number 0000-S-90-04-T-7006-00-E, Revision 02. Technical report by JASCO Research Ltd. for Sakhalin Energy Investment Company Ltd. 34 p.
- Hatch, L.T., C.W. Clark, S.M. Van Parijs, A.S. Frankel, and D.W. Ponirakis. 2012. Quantifying loss of acoustic communication space for right whales in and around a U.S. National Marine Sanctuary. *Conservation Biology* 26(6): 983-994. <https://doi.org/10.1111/j.1523-1739.2012.01908.x>.
- Holt, M.M., D.P. Noren, and C.K. Emmons. 2011. Effects of noise levels and call types on the source levels of killer whale calls. *Journal of the Acoustical Society of America* 130(5): 3100-3106. <https://doi.org/10.1121/1.3641446>.
- Hooker, S.K. and H. Whitehead. 2002. Click characteristics of northern bottlenose whales (*Hyperoodon ampullatus*). *Marine Mammal Science* 18(1): 69-80. <https://doi.org/10.1111/j.1748-7692.2002.tb01019.x>.
- Ireland, D.S., R. Rodrigues, D. Funk, W.R. Koski, and D.E. Hannay. 2009. *Marine mammal monitoring and mitigation during open water seismic exploration by Shell Offshore Inc. in the Chukchi and Beaufort Seas, July–October 2008: 90-Day Report*. Document Number P1049-1. 277 p.
- Janik, V.M. 2000. Source levels and the estimated active space of bottlenose dolphin (*Tursiops truncatus*) whistles in the Moray Firth, Scotland. *Journal of Comparative Physiology A* 186(7-8): 673-680. <https://doi.org/10.1007/s003590000120>.
- Jensen, F.B., W.A. Kuperman, M.B. Porter, and H. Schmidt. 2011. *Computational Ocean Acoustics*. 2nd edition. AIP Series in Modern Acoustics and Signal Processing. AIP Press - Springer, New York. 794 p.
- Kowarski, K.A., C. Evers, H. Moors-Murphy, B. Martin, and S.L. Denes. 2018. Singing through winter nights: Seasonal and diel occurrence of humpback whale (*Megaptera novaeangliae*) calls in and around the Gully MPA, offshore eastern Canada. *Marine Mammal Science* 34(1): 169-189. <https://doi.org/10.1111/mms.12447>.
- Kyhn, L.A., J. Tougaard, K. Beedholm, F.H. Jensen, E. Ashe, R. Williams, and P.T. Madsen. 2013. Clicking in a killer whale habitat: Narrow-band, high-frequency biosonar clicks of harbour porpoise (*Phocoena phocoena*) and Dall's porpoise (*Phocoenoides dalli*). *PLOS ONE* 8(5): e63763. <https://doi.org/10.1371/journal.pone.0063763>.

- Lammers, M.O. and W.W. Au. 2003. Directionality in the whistles of Hawaiian spinner dolphins (*Stenella longirostris*): A signal feature to cue direction of movement? *Marine Mammal Science* 19(2): 249-264.
- Lawson, J.W. and J.-F. Gosselin. 2009. *Distribution and preliminary abundance estimates for cetaceans seen during Canada's Marine Megafauna Survey-A component of the 2007 TNASS*. Document Number 2009/031. DFO Canadian Science Advisory Secretariat Research Document. © Her Majesty the Queen in Right of Canada. 28 p. <http://www.dfo-mpo.gc.ca/csas/>
- Lawson, J.W. and J.-F. Gosselin. 2018. *Estimates of cetacean abundance from the 2016 NAISS aerial surveys of eastern Canadian waters, with a comparison to estimates from the 2007 TNASS*. Document Number NAMMCO SC/25/AE/09. Report for the NAMMCO Secretariat. 40 p.
- MacGillivray, A.O. 2018. Underwater noise from pile driving of conductor casing at a deep-water oil platform. *Journal of the Acoustical Society of America* 143(1): 450-459. <https://doi.org/10.1121/1.5021554>.
- MacGillivray, A.O., Z. Li, D.E. Hannay, K.B. Trounce, and O. Robinson. 2019. Slowing deep-sea commercial vessels reduces underwater radiated noise. *Journal of the Acoustical Society of America* 146: 340-351. <https://doi.org/10.1121/1.5116140>.
- Madsen, P.T., I. Kerr, and R. Payne. 2004. Echolocation clicks of two free-ranging, oceanic delphinids with different food preferences: False killer whales *Pseudorca crassidens* and Risso's dolphins *Grampus griseus*. *Journal of Experimental Biology* 207(11): 1811-1823. <https://jeb.biologists.org/content/207/11/1811>.
- Malme, C.I., P.R. Miles, C.W. Clark, P.L. Tyack, and J.E. Bird. 1983. *Investigations of the Potential Effects of Underwater Noise from Petroleum Industry Activities on Migrating Gray Whale Behavior*. Report Number 5366. Report by Bolt Beranek and Newman Inc. for US Department of the Interior, Minerals Management Service, Alaska OCS Office. <http://www.boem.gov/BOEM-Newsroom/Library/Publications/1983/rpt5366.aspx>.
- Malme, C.I., P.R. Miles, C.W. Clark, P.L. Tyack, and J.E. Bird. 1984. *Investigations of the Potential Effects of Underwater Noise from Petroleum Industry Activities on Migrating Gray Whale Behavior. Phase II: January 1984 migration*. Report Number 5586. Report prepared by Bolt, Beranek and Newman Inc. for the US Department of the Interior, Minerals Management Service, Cambridge, MA, USA. 357 p. <https://www.boem.gov/BOEM-Newsroom/Library/Publications/1983/rpt5586.aspx>.
- Malme, C.I., B. Würsig, J.E. Bird, and P.L. Tyack. 1986. *Behavioral responses of gray whales to industrial noise: Feeding observations and predictive modeling*. Document Number 56. Final Reports of Principal Investigators. 393-600 p.
- Marten, K. 2000. Ultrasonic analysis of pygmy sperm whale (*Kogia breviceps*) and Hubb's beaked whale (*Mesoplodon carlhubbsi*) clicks. *Aquatic Mammals* 26(1): 45-48. https://www.aquaticmammalsjournal.org/share/AquaticMammalsIssueArchives/2000/AquaticMammals_26-01/26-01_Marten.pdf.
- Martin, B. 2013. Computing cumulative sound exposure levels from anthropogenic sources in large data sets. *Proceedings of Meetings on Acoustics* 19(1): 9. <https://doi.org/10.1121/1.4800967>.
- Martin, B., K. Bröker, M.-N.R. Matthews, J.T. MacDonnell, and L. Bailey. 2015. Comparison of measured and modeled air-gun array sound levels in Baffin Bay, West Greenland. *OceanNoise 2015*. 11-15 May 2015, Barcelona, Spain.

- Martin, B., J.T. MacDonnell, and K. Bröker. 2017a. Cumulative sound exposure levels—Insights from seismic survey measurements. *Journal of the Acoustical Society of America* 141(5): 3603-3603. <https://doi.org/10.1121/1.4987709>.
- Martin, S.B. and A.N. Popper. 2016. Short- and long-term monitoring of underwater sound levels in the Hudson River (New York, USA). *Journal of the Acoustical Society of America* 139(4): 1886-1897. <https://doi.org/10.1121/1.4944876>.
- Martin, S.B., M.-N.R. Matthews, J.T. MacDonnell, and K. Bröker. 2017b. Characteristics of seismic survey pulses and the ambient soundscape in Baffin Bay and Melville Bay, West Greenland. *Journal of the Acoustical Society of America* 142(6): 3331-3346. <https://doi.org/10.1121/1.5014049>.
- Martin, S.B., K.A. Kowarski, E.E. Maxner, and C.C. Wilson. 2019a. *Acoustic Monitoring During Scotian Basin Exploration Project: Summer 2018*. Document Number 01687, Version 2.0. Technical report by JASCO Applied Sciences for BP Canada Energy Group ULC. https://www.bp.com/content/dam/bp-country/en_ca/canada/documents/NS_Drilling_Pgm/Acoustic-Monitoring-During-Scotian-Basin-Exploration-Project-Summer-2018.pdf.
- Martin, S.B., C. Morris, K. Bröker, and C. O'Neill. 2019b. Sound exposure level as a metric for analyzing and managing underwater soundscapes. *Journal of the Acoustical Society of America* 146(1): 135-149. <https://doi.org/10.1121/1.5113578>.
- Mathias, D., A.M. Thode, J. Straley, and R.D. Andrews. 2013. Acoustic tracking of sperm whales in the Gulf of Alaska using a two-element vertical array and tags. *Journal of the Acoustical Society of America* 134(3): 2446-2461. <https://doi.org/10.1121/1.4816565>.
- Matthews, M.-N.R. and A.O. MacGillivray. 2013. Comparing modeled and measured sound levels from a seismic survey in the Canadian Beaufort Sea. *Proceedings of Meetings on Acoustics* 19(1): 1-8. <https://doi.org/10.1121/1.4800553>
- Maxner, E.E., B. Martin, and K.A. Kowarski. 2017. *Marine Mammals and Ambient Sound Sources in the Flemish Pass: Analysis from 2014 and 2015 Acoustic Recordings*. Document Number 01456, Version 1.0. Technical report by JASCO Applied Sciences for Statoil Canada Ltd.
- McCrodan, A., C.R. McPherson, and D.E. Hannay. 2011. *Sound Source Characterization (SSC) Measurements for Apache's 2011 Cook Inlet 2D Technology Test*. Version 3.0. Technical report by JASCO Applied Sciences for Fairweather LLC and Apache Corporation. 51 p.
- McDonald, M.A., J. Calambokidis, A.M. Teranishi, and J.A. Hildebrand. 2001. The acoustic calls of blue whales off California with gender data. *Journal of the Acoustical Society of America* 109(4): 1728-1735. <https://doi.org/10.1121/1.1353593>.
- McKenna, M.F., D. Ross, S.M. Wiggins, and J.A. Hildebrand. 2012. Underwater radiated noise from modern commercial ships. *Journal of the Acoustical Society of America* 131(1): 92-103. <https://doi.org/10.1038/srep01760>.
- McPherson, C.R. and G.A. Warner. 2012. *Sound Sources Characterization for the 2012 Simpson Lagoon OBC Seismic Survey 90-Day Report*. Document Number 00443, Version 2.0. Technical report by JASCO Applied Sciences for BP Exploration (Alaska) Inc. http://www.nmfs.noaa.gov/pr/pdfs/permits/bp_openwater_90dayreport_appendices.pdf.
- McPherson, C.R., K. Lucke, B.J. Gaudet, B.S. Martin, and C.J. Whitt. 2018. *Pelican 3-D Seismic Survey Sound Source Characterisation*. Document Number 001583. Version 1.0. Technical report by JASCO Applied Sciences for RPS Energy Services Pty Ltd.

- McPherson, C.R. and B. Martin. 2018. *Characterisation of Polarcus 2380 in³ Airgun Array*. Document Number 001599, Version 1.0. Technical report by JASCO Applied Sciences for Polarcus Asia Pacific Pte Ltd.
- Melcon, M.L., A.J. Cummins, S.M. Kerosky, L.K. Roche, S.M. Wiggins, and J.A. Hildebrand. 2012. Blue whales respond to anthropogenic noise. *PLOS ONE* 7(2): 1-6. <https://doi.org/10.1371/journal.pone.0032681>.
- Mellinger, D.K. and C.W. Clark. 2003. Blue whale (*Balaenoptera musculus*) sounds from the North Atlantic. *Journal of the Acoustical Society of America* 114(2): 1108-1119. <https://doi.org/10.1121/1.1593066>.
- Miksis-Olds, J.L. and S.M. Nichols. 2016. Is low frequency ocean sound increasing globally? *Journal of the Acoustical Society of America* 139(1): 501-511. <https://doi.org/10.1121/1.4938237>.
- Miksis-Olds, J.L., D.V. Harris, and K.D. Heaney. 2019. Comparison of estimated 20-Hz pulse fin whale source levels from the tropical Pacific and Eastern North Atlantic Oceans to other recorded populations. *The Journal of the Acoustical Society of America* 146(4): 2373-2384.
- Møhl, B., M. Wahlberg, P.T. Madsen, L.A. Miller, and A. Surlykke. 2000. Sperm whale clicks: Directionality and source level revisited. *Journal of the Acoustical Society of America* 107(1): 638-648. <https://doi.org/10.1121/1.428329>.
- Møhl, B., M. Wahlberg, P.T. Madsen, A. Heerfordt, and A. Lund. 2003. The monopulsed nature of sperm whale clicks. *Journal of the Acoustical Society of America* 114(2): 1143-1154. <https://doi.org/10.1121/1.1586258>.
- Nedwell, J.R. and A.W. Turnpenny. 1998. The use of a generic frequency weighting scale in estimating environmental effect. *Workshop on Seismics and Marine Mammals*. 23–25 Jun 1998, London, UK.
- Nedwell, J.R., A.W. Turnpenny, J. Lovell, S.J. Parvin, R. Workman, J.A.L. Spinks, and D. Howell. 2007. *A validation of the dB_{HL} as a measure of the behavioural and auditory effects of underwater noise*. Document Number 534R1231 Report prepared by Subacoustech Ltd. for the UK Department of Business, Enterprise and Regulatory Reform under Project No. RDCZ/011/0004. 74 p. <https://tethys.pnnl.gov/sites/default/files/publications/Nedwell-et-al-2007.pdf>.
- Nemiroff, L. and H. Whitehead. 2009. Structural characteristics of pulsed calls of long-finned pilot whales *Globicephala melas*. *Bioacoustics* 19(1-2): 67-92. <https://doi.org/10.1080/09524622.2009.9753615>.
- Newhall, A.E., Y.-T. Lin, J.F. Lynch, M.F. Baumgartner, and G.G. Gawarkiewicz. 2012. Long distance passive localization of vocalizing sei whales using an acoustic normal mode approach. *The Journal of the Acoustical Society of America* 131(2): 1814-1825.
- Nieukirk, S.L., K.M. Stafford, D.K. Mellinger, R.P. Dziak, and C.G. Fox. 2004. Low-frequency whale and seismic airgun sounds recorded in the mid-Atlantic Ocean. *Journal of the Acoustical Society of America* 115(4): 1832-1843. <https://doi.org/10.1121/1.1675816>.
- O'Neill, C., D. Leary, and A. McCrodan. 2010. Sound Source Verification. (Chapter 3) In Blees, M.K., K.G. Hartin, D.S. Ireland, and D.E. Hannay (eds.). *Marine mammal monitoring and mitigation during open water seismic exploration by Statoil USA E&P Inc. in the Chukchi Sea, August-October 2010: 90-day report*. LGL Report P1119. Prepared by LGL Alaska Research Associates Inc., LGL Ltd., and JASCO Applied Sciences Ltd. for Statoil USA E&P Inc., National Marine Fisheries Service (US), and US Fish and Wildlife Service. pp. 1-34.

- Oleson, E.M., J. Calambokidis, W.C. Burgess, M.A. McDonald, C.A. Leduc, and J.A. Hildebrand. 2007. Behavioral context of call production by eastern North Pacific blue whales. *Marine Ecology Progress Series* 330: 269-284. <https://www.int-res.com/abstracts/meps/v330/p269-284/>.
- Oswald, J.N., J. Barlow, and T.F. Norris. 2003. Acoustic identification of nine delphinid species in the eastern tropical Pacific Ocean. *Marine Mammal Science* 19(1): 20-37. <https://doi.org/10.1111/j.1748-7692.2003.tb01090.x>.
- Parks, S.E., P.K. Hamilton, S.D. Kraus, and P.L. Tyack. 2005. The gunshot sound produced by male North Atlantic right whales (*Eubalaena glacialis*) and its potential function in reproductive advertisement. *Marine Mammal Science* 21(3): 458-475. <https://doi.org/10.1111/j.1748-7692.2005.tb01244.x>
- Parks, S.E. and P.L. Tyack. 2005. Sound production by North Atlantic right whales (*Eubalaena glacialis*) in surface active groups. *Journal of the Acoustical Society of America* 117(5): 3297-3306. <https://doi.org/10.1121/1.1882946>.
- Pine, M.K., D.E. Hannay, S.J. Insley, W.D. Halliday, and F. Juanes. 2018. Assessing vessel slowdown for reducing auditory masking for marine mammals and fish of the western Canadian Arctic. *Marine Pollution Bulletin* 135: 290-302. <https://doi.org/10.1016/j.marpolbul.2018.07.031>.
- Pine, M.K., K. Nikolich, B. Martin, C. Morris, and F. Juanes. 2020. Assessing auditory masking for management of underwater anthropogenic noise. *Journal of the Acoustical Society of America* 147(5): 3408-3417. <https://doi.org/10.1121/10.0001218>.
- Porter, M.B. and Y.-C. Liu. 1994. Finite-element ray tracing. In: Lee, D. and M.H. Schultz (eds.). *International Conference on Theoretical and Computational Acoustics*. Volume 2. World Scientific Publishing Co. pp. 947-956.
- Quijano, J.E., M.-N.R. Matthews, and B. Martin. 2017. *Eastern Newfoundland Drilling Noise Assessment: Qualitative Assessment of Radiated Sound Levels and Acoustic Propagation Conditions*. Document Number 01366. Technical report by JASCO Applied Sciences for Stantec Consulting Ltd.
- Racca, R.G., A.N. Rutenko, K. Bröker, and M.E. Austin. 2012a. A line in the water - design and enactment of a closed loop, model based sound level boundary estimation strategy for mitigation of behavioural impacts from a seismic survey. *11th European Conference on Underwater Acoustics*. Volume 34(3), Edinburgh, UK.
- Racca, R.G., A.N. Rutenko, K. Bröker, and G. Gailey. 2012b. Model based sound level estimation and in-field adjustment for real-time mitigation of behavioural impacts from a seismic survey and post-event evaluation of sound exposure for individual whales. In: McMinn, T. (ed.). *Acoustics 2012 Fremantle: Acoustics, Development and the Environment. Proceedings of the Annual Conference of the Australian Acoustical Society*. Fremantle, Australia. http://www.acoustics.asn.au/conference_proceedings/AAS2012/papers/p92.pdf.
- Racca, R.G., M.E. Austin, A.N. Rutenko, and K. Bröker. 2015. Monitoring the gray whale sound exposure mitigation zone and estimating acoustic transmission during a 4-D seismic survey, Sakhalin Island, Russia. *Endangered Species Research* 29(2): 131-146. <https://doi.org/10.3354/esr00703>.
- Rendell, L.E., J.N. Matthews, A. Gill, J.C.D. Gordon, and D.W. MacDonald. 1999. Quantitative analysis of tonal calls from five odontocete species, examining interspecific and intraspecific variation. *Journal of Zoology* 249(4): 403-410. <https://doi.org/10.1111/j.1469-7998.1999.tb01209.x>.

- Richardson, W.J., B. Würsig, and C.R. Greene, Jr. 1990. Reactions of bowhead whales, *Balaena mysticetus*, to drilling and dredging noise in the Canadian Beaufort Sea. *Marine Environmental Research* 29(2): 135-160. [https://doi.org/10.1016/0141-1136\(90\)90032-J](https://doi.org/10.1016/0141-1136(90)90032-J).
- Richardson, W.J., G.W. Miller, and C.R. Greene, Jr. 1999. Displacement of migrating bowhead whales by sounds from seismic surveys in shallow waters of the Beaufort Sea. *Journal of the Acoustical Society of America* 106(4): 2281-2281. <https://doi.org/10.1121/1.427801>.
- Risch, D., C.W. Clark, P.J. Corkeron, A. Elepfandt, K.M. Kovacs, C. Lydersen, I. Stirling, and S.M. Van Parijs. 2007. Vocalizations of male bearded seals, *Erignathus barbatus*: Classification and geographical variation. *Animal Behaviour* 73(5): 747-762. <https://doi.org/10.1016/j.anbehav.2006.06.012>.
- Risch, D., C.W. Clark, P.J. Dugan, M. Popescu, U. Siebert, and S.M. Van Parijs. 2013. Minke whale acoustic behavior and multi-year seasonal and diel vocalization patterns in Massachusetts Bay, USA. *Marine Ecology Progress Series* 489: 279-295. <https://doi.org/10.3354/meps10426>.
- Rolland, R.M., S.E. Parks, K.E. Hunt, M. Castellote, P.J. Corkeron, D.P. Nowacek, S.K. Wasser, and S.D. Kraus. 2012. Evidence that ship noise increases stress in right whales. *Proceedings of the Royal Society B*. <https://doi.org/10.1098/rspb.2011.2429>.
- Ross, D. 1976. *Mechanics of Underwater Noise*. Pergamon Press, NY, USA.
- Samarra, F.I.P., V.B. Deecke, K. Vinding, M.H. Rasmussen, R.J. Swift, and P.J.O. Miller. 2010. Killer whales (*Orcinus orca*) produce ultrasonic whistles. *Journal of the Acoustical Society of America* 128(5): EL205-EL210. <https://doi.org/10.1121/1.3462235>.
- Shaffer, J.W., D. Moretti, S. Jarvis, P. Tyack, and M. Johnson. 2013. Effective beam pattern of the Blainville's beaked whale (*Mesoplodon densirostris*) and implications for passive acoustic monitoring. *The Journal of the Acoustical Society of America* 133(3): 1770-1784.
- Simard, Y., N. Roy, C. Gervaise, and S. Giard. 2016. Analysis and modeling of 255 source levels of merchant ships from an acoustic observatory along St. Lawrence Seaway. *Journal of the Acoustical Society of America* 140(3): 2002-2018. <https://doi.org/10.1121/1.4962557>.
- Simon, M., K.M. Stafford, K. Beedholm, C.M. Lee, and P.T. Madsen. 2010. Singing behavior of fin whales in the Davis Strait with implications for mating, migration and foraging. *Journal of the Acoustical Society of America* 128(5): 3200-3210. <https://doi.org/10.1121/1.3495946>.
- Smith, W.H.F. and D.T. Sandwell. 1997. Global sea floor topography from satellite altimetry and ship depth soundings. *Science* 277(5334): 1956-1962. <https://science.sciencemag.org/content/277/5334/1956>.
- Southall, B.L., A.E. Bowles, W.T. Ellison, J.J. Finneran, R.L. Gentry, C.R. Greene, Jr., D. Kastak, D.R. Ketten, J.H. Miller, et al. 2007. Marine Mammal Noise Exposure Criteria: Initial Scientific Recommendations. *Aquatic Mammals* 33(4): 411-521. <https://doi.org/10.1080/09524622.2008.9753846>.
- Southall, B.L., S.L. DeRuiter, A. Friedlaender, A.K. Stimpert, J.A. Goldbogen, E. Hazen, C. Casey, S. Fregosi, D.E. Cade, et al. 2019a. Behavioral responses of individual blue whales (*Balaenoptera musculus*) to mid-frequency military sonar. *Journal of Experimental Biology* 222(5).
- Southall, B.L., J.J. Finneran, C. Reichmuth, P.E. Nachtigall, D.R. Ketten, A.E. Bowles, W.T. Ellison, D.P. Nowacek, and P.L. Tyack. 2019b. Marine Mammal Noise Exposure Criteria: Updated Scientific

- Recommendations for Residual Hearing Effects. *Aquatic Mammals* 45(2): 125-232. <https://doi.org/10.1578/AM.45.2.2019.125>.
- Stafford, K.M., D.K. Mellinger, S.E. Moore, and C.G. Fox. 2007. Seasonal variability and detection range modeling of baleen whale calls in the Gulf of Alaska, 1999–2002. *Journal of the Acoustical Society of America* 122(6): 3378-3390. <https://doi.org/10.1121/1.2799905>.
- Steiner, W.W. 1981. Species-specific differences in pure tonal whistle vocalizations of five western North Atlantic dolphin species. *Behavioral Ecology and Sociobiology* 9(4): 241-246. <https://doi.org/10.1007/BF00299878>.
- Teague, W.J., M.J. Carron, and P.J. Hogan. 1990. A comparison between the Generalized Digital Environmental Model and Levitus climatologies. *Journal of Geophysical Research* 95(C5): 7167-7183. <https://doi.org/10.1029/JC095iC05p07167>.
- Terhune, J.M. 1994. Geographical variation of harp seal underwater vocalizations. *Canadian Journal of Zoology* 72(5): 892-897. <https://doi.org/10.1139/z94-121>.
- Thode, A.M., G.L. D'Spain, and W.A. Kuperman. 2000. Matched-field processing, geoacoustic inversion, and source signature recovery of blue whale vocalizations. *Journal of the Acoustical Society of America* 107(3): 1286-1300. <https://doi.org/10.1121/1.428417>.
- Tyack, P.L. and C.W. Clark. 2000. Communication and acoustic behavior of dolphins and whales. *In Hearing by whales and dolphins*. Springer, New York. pp. 156-224.
- Wahlberg, M., F.H. Jensen, N. Aguilar Soto, K. Beedholm, L. Bejder, C. Oliveira, M. Rasmussen, M. Simon, A. Villadsgaard, et al. 2011. Source parameters of echolocation clicks from wild bottlenose dolphins (*Tursiops aduncus* and *Tursiops truncatus*). *The Journal of the Acoustical Society of America* 130(4): 2263-2274.
- Wahlberg, M., K. Beedholm, A. Heerfordt, and B. Møhl. 2012. Characteristics of biosonar signals from the northern bottlenose whale, *Hyperoodon ampullatus*. *Journal of the Acoustical Society of America* 130(5): 3077-3084. <https://doi.org/10.1121/1.3641434>.
- Wang, D., W. Huang, H. Garcia, and P. Ratilal. 2016. Vocalization source level distributions and pulse compression gains of diverse baleen whale species in the Gulf of Maine. *Remote Sensing* 8(11): 881.
- Warner, G.A., C. Erbe, and D.E. Hannay. 2010. Underwater Sound Measurements. (Chapter 3) *In* Reiser, C.M., D. Funk, R. Rodrigues, and D.E. Hannay (eds.). *Marine Mammal Monitoring and Mitigation during Open Water Shallow Hazards and Site Clearance Surveys by Shell Offshore Inc. in the Alaskan Chukchi Sea, July-October 2009: 90-Day Report*. LGL Report P1112-1. Report by LGL Alaska Research Associates Inc. and JASCO Applied Sciences for Shell Offshore Inc., National Marine Fisheries Service (US), and Fish and Wildlife Service (US). pp. 1-54.
- Warner, G.A., M.E. Austin, and A.O. MacGillivray. 2017. Hydroacoustic measurements and modeling of pile driving operations in Ketchikan, Alaska. *Journal of the Acoustical Society of America* 141(5): 3992. <https://doi.org/10.1121/1.4989141>.
- Watkins, W.A. 1981. Activities and underwater sounds of fin whales. *Scientific Reports of the Whales Research Institute* 33: 83-117.
- Watkins, W.A., P.L. Tyack, K.E. Moore, and J.E. Bird. 1987. The 20-Hz signals of finback whales (*Balaenoptera physalus*). *Journal of the Acoustical Society of America* 82(6): 1901–1912. <https://doi.org/10.1121/1.395685>.

- Weirathmueller, M.J., W.S.D. Wilcock, and D.C. Soule. 2013. Source levels of fin whale 20 Hz pulses measured in the Northeast Pacific Ocean. *Journal of the Acoustical Society of America* 133(2): 741-749. <https://doi.org/10.1121/1.4773277>.
- Wenz, G.M. 1962. Acoustic Ambient Noise in the Ocean: Spectra and Sources. *Journal of the Acoustical Society of America* 34(12): 1936-1956. <https://doi.org/10.1121/1.1909155>.
- Zhang, Z.Y. and C.T. Tindle. 1995. Improved equivalent fluid approximations for a low shear speed ocean bottom. *Journal of the Acoustical Society of America* 98(6): 3391-3396. <https://doi.org/10.1121/1.413789>.
- Zimmer, W.M.X., M.P. Johnson, P.T. Madsen, and P.L. Tyack. 2005. Echolocation clicks of free-ranging Cuvier's beaked whales (*Ziphius cavirostris*). *Journal of the Acoustical Society of America* 117(6): 3919-3927. <https://doi.org/10.1121/1.1910225>.
- Zykov, M.M. and J.T. MacDonnell. 2013. *Sound Source Characterizations for the Collaborative Baseline Survey Offshore Massachusetts Final Report: Side Scan Sonar, Sub-Bottom Profiler, and the R/V Small Research Vessel experimental*. Document Number 00413, Version 2.0. Technical report by JASCO Applied Sciences for Fugro GeoServices, Inc. and the (US) Bureau of Ocean Energy Management.
- Zykov, M.M. 2016. *Modelling Underwater Sound Associated with Scotian Basin Exploration Drilling Project: Acoustic Modelling Report*. Document Number 01112, Version 2.0. Technical report by JASCO Applied Sciences for Stantec Consulting Ltd. <https://www.ceaa.gc.ca/050/documents/p80109/116305E.pdf>.
- Zykov, M.M. 2018. *Underwater Sound Modelling of Seismic Survey and Development Activities Off-shore Newfoundland: Equinor's Bay Du Nord Development Project*. Document Number 01664, Version 2.0. Technical report by JASCO Applied Sciences for Wood PLC.

Appendix A. Sound Level Terminology

A.1. Acoustic Metrics

Underwater sound pressure amplitude is measured in decibels (dB) relative to a fixed reference pressure of $p_0 = 1 \mu\text{Pa}$. Because the perceived loudness of sound, especially pulsed sound such as from seismic airguns, pile driving, and sonar, is not generally proportional to the instantaneous acoustic pressure, several sound level metrics are commonly used to evaluate sound and its effects on marine life. Here we provide specific definitions of relevant metrics used in the accompanying report. Where possible, we follow International Organization for Standardization definitions and symbols for sound metrics (e.g., ISO 2017a).

The zero-to-peak sound pressure, or peak sound pressure (PK or $L_{p,pk}$; dB re $1 \mu\text{Pa}$), is the decibel level of the maximum instantaneous acoustic pressure in a stated frequency band attained by an acoustic pressure signal, $p(t)$:

$$L_{p,pk} = 10 \log_{10} \frac{\max|p^2(t)|}{p_0^2} = 20 \log_{10} \frac{\max|p(t)|}{p_0} \quad (\text{A-1})$$

PK is often included as a criterion for assessing whether a sound is potentially injurious; however, because it does not account for the duration of an acoustic event, it is generally a poor indicator of perceived loudness.

The peak-to-peak sound pressure (PK-PK or $L_{p,pk-pk}$; dB re $1 \mu\text{Pa}$) is the difference between the maximum and minimum instantaneous sound pressure, possibly filtered in a stated frequency band, attained by an impulsive sound, $p(t)$:

$$L_{p,pk-pk} = 10 \log_{10} \frac{[\max(p(t)) - \min(p(t))]^2}{p_0^2} \quad (\text{A-2})$$

The sound pressure level (SPL or L_p ; dB re $1 \mu\text{Pa}$) is the root-mean-square (rms) pressure level in a stated frequency band over a specified time window (T ; s). It is important to note that SPL always refers to an rms pressure level and therefore not instantaneous pressure:

$$L_p = 10 \log_{10} \left(\frac{1}{T} \int_T g(t) p^2(t) dt / p_0^2 \right) \text{ dB} \quad (\text{A-3})$$

where $g(t)$ is an optional time weighting function. In many cases, the start time of the integration is marched forward in small time steps to produce a time-varying SPL function. For short acoustic events, such as sonar pulses and marine mammal vocalizations, it is important to choose an appropriate time window that matches the duration of the signal. For in-air studies, when evaluating the perceived loudness of sounds with rapid amplitude variations in time, the time weighting function $g(t)$ is often set to a decaying exponential function that emphasizes more recent pressure signals. This function mimics the leaky integration nature of mammalian hearing. For example, human-based fast time-weighted SPL ($L_{p,fast}$) applies an exponential function with time constant 125 ms. A related simpler approach used in underwater acoustics sets $g(t)$ to a boxcar (unity amplitude) function of width 125 ms; the results can be referred to as $L_{p,boxcar 125ms}$. Another approach, historically used to evaluate SPL of impulsive signals underwater, defines $g(t)$ as a boxcar function with edges set to the times corresponding to 5% and 95% of the cumulative square pressure function encompassing the duration of an impulsive acoustic event. This calculation is applied individually to each impulse signal, and the results have been referred to as 90% SPL ($L_{p,90\%}$).

The sound exposure level (SEL or L_E ; dB re 1 $\mu\text{Pa}^2\cdot\text{s}$) is the time-integral of the squared acoustic pressure over a duration (T):

$$L_E = 10 \log_{10} \left(\int_T p^2(t) dt / T_0 p_0^2 \right) \text{ dB} \quad (\text{A-4})$$

where T_0 is a reference time interval of 1 s. SEL continues to increase with time when non-zero pressure signals are present. It is a dose-type measurement, so the integration time applied must be carefully considered for its relevance to impact to the exposed recipients.

SEL can be calculated over a fixed duration, such as the time of a single event or a period with multiple acoustic events. When applied to pulsed sounds, SEL can be calculated by summing the SEL of the N individual pulses. For a fixed duration, the square pressure is integrated over the duration of interest. For multiple events, the SEL can be computed by summing (in linear units) the SEL of the N individual events:

$$L_{E,N} = 10 \log_{10} \left(\sum_{i=1}^N 10^{\frac{L_{E,i}}{10}} \right) \text{ dB} \quad (\text{A-5})$$

Because the $\text{SPL}(T_{90})$ and SEL are both computed from the integral of square pressure, these metrics are related numerically by the following expression, which depends only on the duration of the time window T :

$$L_p = L_E - 10 \log_{10}(T) \quad (\text{A-6})$$

$$L_{p90} = L_E - 10 \log_{10}(T_{90}) - 0.458 \quad (\text{A-7})$$

where the 0.458 dB factor accounts for the 10% of pulse SEL missing from the $\text{SPL}(T_{90})$ integration time window.

Energy equivalent SPL (L_{eq} ; dB re 1 μPa) denotes the SPL of a stationary (constant amplitude) sound that generates the same SEL as the signal being examined, $p(t)$, over the same time period, T :

$$L_{eq} = 10 \log_{10} \left(\frac{1}{T} \int_T p^2(t) dt / p_0^2 \right) \quad (\text{A-8})$$

The equations for SPL and the energy-equivalent SPL are numerically identical. Conceptually, the difference between the two metrics is that the SPL is typically computed over short periods (typically of 1 s or less) and tracks the fluctuations of a non-steady acoustic signal, whereas the L_{eq} reflects the average SPL of an acoustic signal over time periods typically of 1 min to several hours.

If applied, the frequency weighting of an acoustic event should be specified, as in the case of weighted SEL (e.g., $L_{E,LF,24h}$; see Appendix Appendix B) or auditory-weighted SPL ($L_{p,ht}$). The use of fast, slow, or impulse exponential-time-averaging or other time-related characteristics should also be specified.

A.2. Deci-Decade-Band Analysis

The distribution of a sound’s power with frequency is described by the sound’s spectrum. The sound spectrum can be split into a series of adjacent frequency bands. Splitting a spectrum into 1 Hz wide bands, called passbands, yields the power spectral density of the sound. These values directly compare to the Wenz curves, which represent typical deep ocean sound levels (Wenz 1962). This splitting of the spectrum into passbands of a constant width of 1 Hz, however, does not represent how animals perceive sound.

Because animals perceive exponential increases in frequency rather than linear increases, analyzing a sound spectrum with passbands that increase exponentially in size better approximates real-world scenarios. In underwater acoustics, a spectrum is commonly split into decidecade bands, which are approximately one-tenth of a decade wide (historically these have also been referred to as 1/3-octave-bands, base 10). Each octave represents a doubling in sound frequency. The centre frequency of the *i*th band, $f_c(i)$, is defined as:

$$f_c(i) = 10^{\frac{i}{10}} \text{ kHz} \tag{A-9}$$

and the low (f_{lo}) and high (f_{hi}) frequency limits of the *i*th decade band are defined as:

$$f_{lo,i} = 10^{\frac{-1}{20}} f_c(i) \quad \text{and} \quad f_{hi,i} = 10^{\frac{1}{20}} f_c(i) \tag{A-10}$$

The decidecade bands become wider with increasing frequency, and on a logarithmic scale the bands appear equally spaced (Figure A-1).

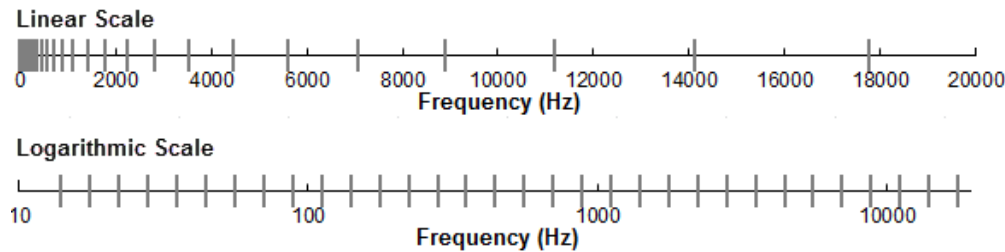


Figure A-1. Decidecade frequency bands (vertical lines) shown on a linear frequency scale and a logarithmic scale.

The sound pressure level in the *i*th band ($L_{p,i}$) is computed from the spectrum $S(f)$ between $f_{lo,i}$ and $f_{hi,i}$:

$$L_{p,i} = 10 \log_{10} \int_{f_{lo,i}}^{f_{hi,i}} S(f) df \tag{A-7}$$

Summing the sound pressure level of all the bands yields the broadband sound pressure level:

$$\text{Broadband SPL} = 10 \log_{10} \sum_i 10^{\frac{L_{p,i}}{10}} \tag{A-8}$$

Figure A-2 shows an example of how the decidecade band sound pressure levels compare to the power spectrum of an ambient noise signal. Because the decidecade bands are wider with increasing frequency, the decidecade band SPL is higher than the power spectrum, at higher frequencies. Decidecade band analysis is applied to both continuous and impulsive noise sources. For impulsive sources, the decidecade band SEL is typically reported.

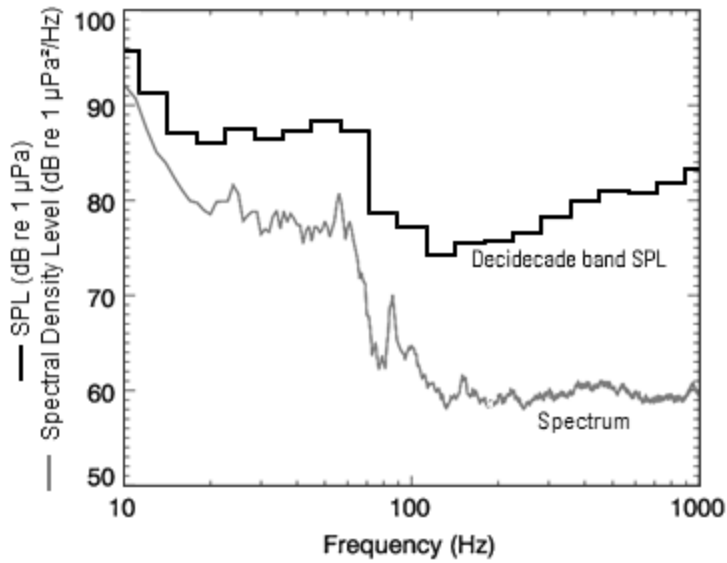


Figure A-2. A power spectrum and the corresponding decidecade sound pressure levels of example ambient noise shown on a logarithmic frequency scale. Because the decibands are wider with increasing frequency, their SPL is higher than the power spectrum.

Table A-1. Decidecade band frequencies (Hz).

Band	Lower frequency	Nominal centre frequency	Upper frequency
10	8.9	10.0	11.2
11	11.2	12.6	14.1
12	14.1	15.8	17.8
13	17.8	20.0	22.4
14	22.4	25.1	28.2
15	28.2	31.6	35.5
16	35.5	39.8	44.7
17	44.7	50.1	56.2
18	56.2	63.1	70.8
19	70.8	79.4	89.1
20	89.1	100.0	112.2
21	112	126	141
22	141	158	178
23	178	200	224
24	224	251	282
25	282	316	355
26	355	398	447
27	447	501	562
28	562	631	708
29	708	794	891

30	891	1000	1122
31	1122	1259	1413
32	1413	1585	1778
33	1778	1995	2239
34	2239	2512	2818
35	2818	3162	3548
36	3548	3981	4467
37	4467	5012	5623
38	5623	6310	7079
39	7079	7943	8913
40	8913	10000	11220
41	11220	12589	14125
42	14260	16000	17952
43	17825	20000	22440
44	22281	25000	28050
45	28074	31500	35344
46	35650	40000	44881
47	44563	50000	56101
48	56149	63000	70687
49	71300	80000	89761
50	89125	100000	112202
51	111406	125000	140252
52	142600	160000	179523
53	178250	200000	224404
54	222813	250000	280505

Table A-2. Decade-band frequencies (Hz).

Decade band	Lower frequency	Nominal centre frequency	Upper frequency
A	10	50	100
B	100	500	1,000
C	1,000	5,000	10,000
D	10,000	50,000	100,000

Appendix B. Marine Mammal Auditory Frequency Weighting

The potential for noise to affect animals depends on how well the animals can hear it. Noises are less likely to disturb or injure an animal if they are at frequencies that the animal cannot hear well. An exception occurs when the sound pressure is so high that it can physically injure an animal by non-auditory means (i.e., barotrauma). For sound levels below such extremes, the importance of sound components at particular frequencies can be scaled by frequency weighting relevant to an animal's sensitivity to those frequencies (Nedwell and Turnpenny 1998, Nedwell et al. 2007).

B.1.1. NMFS (2018) Frequency Weighting Functions

In 2015, a US Navy technical report by Finneran (2015) recommended new auditory weighting functions. The auditory weighting functions for marine mammals are applied in a similar way as A-weighting for noise level assessments for humans. The new frequency-weighting functions are expressed as:

$$G(f) = K + 10 \log_{10} \left\{ \frac{(f/f_1)^{2a}}{[1 + (f/f_1)^2]^a [1 + (f/f_2)^2]^b} \right\} \quad (\text{B-1})$$

Finneran (2015) proposed five functional hearing groups for marine mammals in water: low-, mid- and high-frequency cetaceans (LF, MF, and HF cetaceans, respectively), phocid pinnipeds, and otariid pinnipeds. The parameters for these frequency-weighting functions were further modified the following year (Finneran 2016) and were adopted in NOAA's technical guidance that assesses acoustic impacts on marine mammals (NMFS 2018). The updates did not affect the content related to either the definitions of M-weighting functions or the threshold values. Table B-1 lists the frequency-weighting parameters for each hearing group. Figure B-1 shows the resulting frequency-weighting curves.

Table B-1. Parameters for the auditory weighting functions recommended by NMFS (2018) and Temporary Threshold Shift (TTS) onset thresholds.

Functional hearing group	<i>a</i>	<i>b</i>	<i>f</i> ₁ (Hz)	<i>f</i> ₂ (Hz)	<i>K</i> (dB)	Weighted TTS onset threshold (SEL _{cum})
Low-frequency cetaceans	1.0	2	200	19,000	0.13	179 dB
Mid-frequency cetaceans	1.6	2	8,800	110,000	1.20	178 dB
High-frequency cetaceans	1.8	2	12,000	140,000	1.36	153 dB
Phocid pinnipeds in water	1.0	2	1,900	30,000	0.75	181 dB
Otariid pinnipeds in water	2.0	2	940	25,000	0.64	199 dB

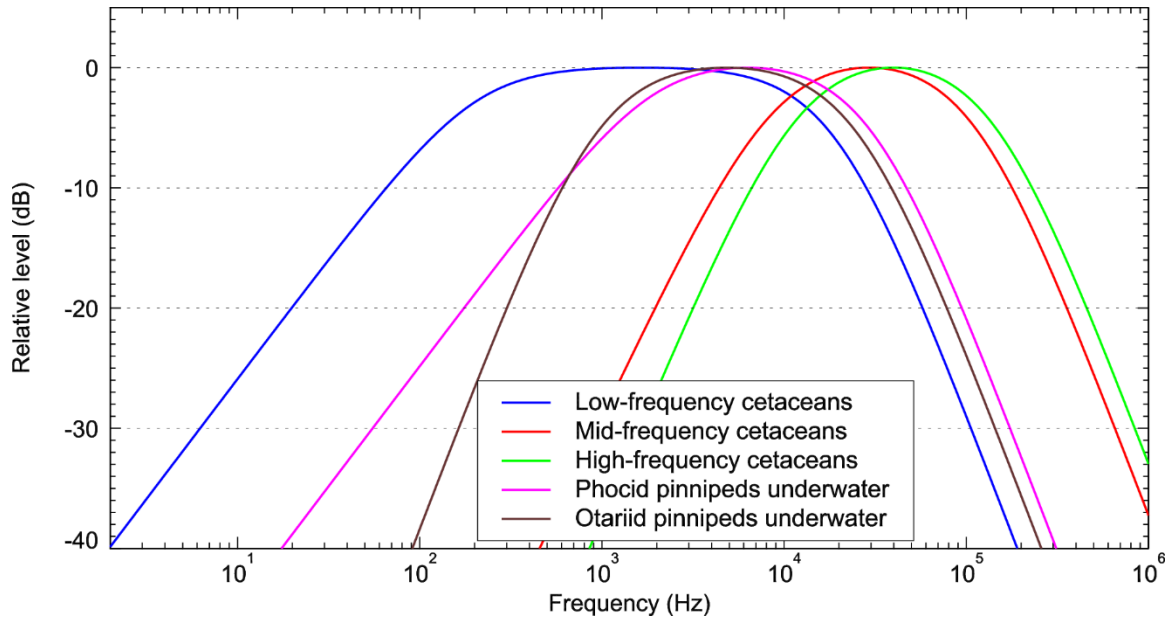


Figure B-1. Auditory weighting functions for the functional marine mammal hearing groups as recommended by NMFS (2018).

Appendix C. Detection Range Modelling

C.1. Sound Propagation Models: MONM-BELLHOP

Long-range sound fields were computed using JASCO’s Marine Operations Noise Model (MONM). MONM is well suited for effective longer-range estimation but less accurately predicts steep-angle propagation for environments with higher shear speed. This model computes sound propagation at frequencies of 10 Hz to 2 kHz via a wide-angle parabolic equation solution to the acoustic wave equation (Collins 1993) based on a version of the U.S. Naval Research Laboratory’s Range-dependent Acoustic Model (RAM), which has been modified to account for a solid seabed (Zhang and Tindle 1995). For this project, MONM computes sound propagation at frequencies above 2 kHz via the BELLHOP Gaussian beam acoustic ray-trace model (Porter and Liu 1994).

The parabolic equation method has been extensively benchmarked and is widely employed in the underwater acoustics community (Collins et al. 1996). MONM accounts for the additional reflection loss at the seabed, which results from partial conversion of incident compressional waves to shear waves at the seabed and sub-bottom interfaces, and it includes wave attenuations in all layers. MONM incorporates the following site-specific environmental properties: a bathymetric grid of the modelled area, underwater sound speed as a function of depth, and a geoacoustic profile based on the overall stratified composition of the seafloor.

MONM accounts for sound attenuation due to energy absorption through ion relaxation and viscosity of water in addition to acoustic attenuation due to reflection at the medium boundaries and internal layers (Fisher and Simmons 1977). The former type of sound attenuation is significant for frequencies higher than 5 kHz and cannot be neglected without noticeably affecting the model results.

MONM computes acoustic fields in three dimensions by modelling transmission loss within two-dimensional (2-D) vertical planes aligned along radials covering a 360° swath from the source, an approach commonly referred to as Nx2-D. These vertical radial planes are separated by an angular step size of $\Delta\theta$, yielding $N = 360^\circ/\Delta\theta$ number of planes (Figure C-1).

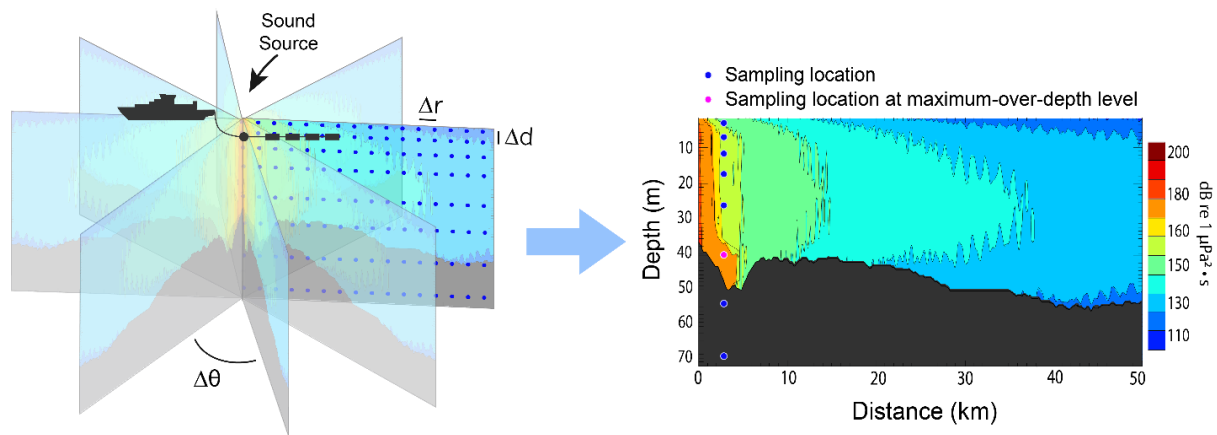


Figure C-1. The Nx2-D and maximum-over-depth modelling approach used by MONM.

MONM treats frequency dependence by computing acoustic transmission loss at the centre frequencies of decidecade bands. Sufficiently many decidecade bands, starting at 10 Hz, are modelled to include most of the acoustic energy emitted by the source. At each centre frequency, the transmission loss is modelled within each of the N vertical planes as a function of depth and range from the source.

C.2. Marine Mammal Parameters

The parameters used as inputs to the detection range modelling (see Section 2.3) are summarized in Figure C-1.

Table C-1. Marine mammal input parameters. The detection threshold refers to the threshold of the relevant detectors.

Species	Frequency range (Hz)	Mean source level (dB)	Source level standard deviation	Source depth range (m)	Detection threshold	References
<i>Mysticetes</i>						
Blue whale A-B calls	16	182	3	5–25	4	Thode et al. (2000), McDonald et al. (2001)
Fin Whale 20-Hz calls	20–25	185	5	10–30	4	Weirathmueller et al. (2013), Wang et al. (2016), Miksis-Olds et al. (2019)
Sei whale downsweeps	32–80	179	4	5–25	3.5	Newhall et al. (2012)
Humpback Whale moans	50–1000	171.5	5.7	10–30	3	Girola et al. (2019)
<i>Odontocetes</i>						
Sperm Whale clicks	2000–16000	186	5	100–1000	14	Mathias et al. (2013)
Killer whale tonal signals	700–5000	155	6.5	5–50	3	Holt et al. (2011)
Delphinid whistles	5000–12500	155	5	5–50	3	Janik (2000), Lammers and Au (2003)
Delphinid Clicks	16000–63000	185	5	5–100	14	Au and Herzing (2003), Madsen et al. (2004), Eskesen et al. (2011), Wahlberg et al. (2011)
Northern bottlenose clicks	20000–50000	186	9	50–1000	14	Wahlberg et al. (2012)
Sowerby's beaked whale clicks	50000–100000	190	10	50–1000	14	Shaffer et al. (2013)
Harbour Porpoise	100000–150000	172	5	1–50	14	Kyhn et al. (2013)

C.3. Environmental Parameters

C.3.1. Bathymetry

Water depths throughout the modelled area were extracted from the SRTM15+ grid (Smith and Sandwell 1997, Becker et al. 2009).

C.3.2. Sound speed profile

The sound speed profiles for the modelled site were derived from temperature and salinity profiles from the U.S. Naval Oceanographic Office's Generalized Digital Environmental Model V 3.0 (GDEM; Teague et al. 1990, Carnes 2009). GDEM provides an ocean climatology of temperature and salinity for the world's oceans on a latitude-longitude grid with 0.25° resolution, with a temporal resolution of one month, based on global historical observations from the U.S. Navy's Master Oceanographic Observational Data Set (MOODS). The climatology profiles include 78 fixed depth points to a maximum depth of 6800 m (where the ocean is that deep). The GDEM temperature-salinity profiles were converted to sound speed profiles according to Coppens (1981).

Sound speed profiles for September and March were used as inputs to the sound propagation modelling. These two months had the most extreme profiles during the study period. Figure C-2 illustrates these differences for station Hampden (EL 1165A).

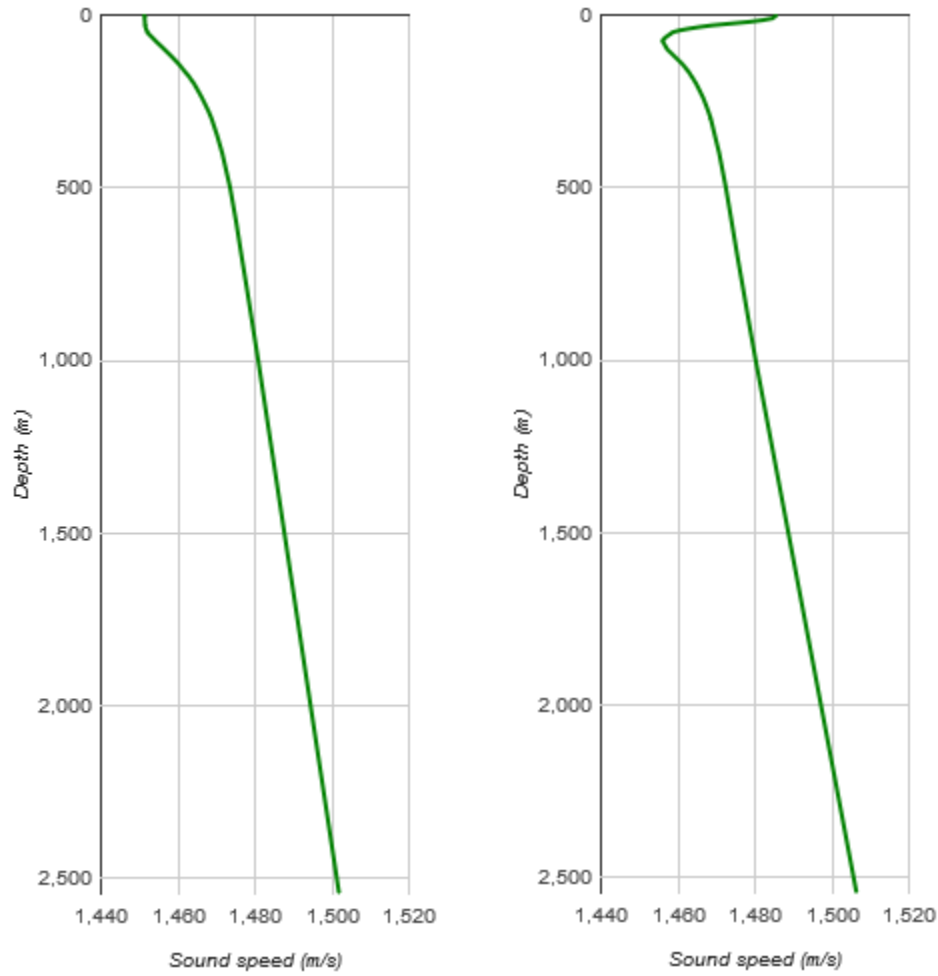


Figure C-2. The sound speed profiles for March (left) and September (right) at Hampden (EL 1165A). The profile was calculated from temperature and salinity profiles from GDEM V 3.0 (GDEM; Teague et al. 1990, Carnes 2009).

C.3.3. Geoacoustics

The geoacoustic properties of the modelled area were derived from previous sound propagation modelling projects by JASCO in the same area (Quijano et al. 2017, Zykov 2018). We used a profile for the shallowest site (Harp (EL 1165B), 300 m) and another, single profile for the three deep sites (depth from 800 to 1600 m).

Table 23. Geacoustic parameters for the transmission loss modelling at the shallow station (Harp (EL 1165B)).

Depth	P-wave velocity (m/s)	Density (g/cm ³)	P-wave attenuation (dB/lambda)	S-wave velocity (m/s)	S-wave attenuation (dB/lambda)
0	1518	1.51	0.3	150	3.65
1	1559	1.52	0.4		
5	1646	1.7	0.64		
50	1912	1.95	1.16		
500	2436	2.07	1.98		

Table 24. Geacoustic parameters for the transmission loss modelling at the deep stations (Hampden (EL 1165A), Mid and Stn 19).

Depth	P-wave velocity (m/s)	Density (g/cm ³)	P-wave attenuation (dB/lambda)	S-wave velocity (m/s)	S-wave attenuation (dB/lambda)
0	1518	1.51	0.25	150	3.65
1	1526	1.52	0.26		
5	1588	1.7	0.42		
50	1778	1.95	0.77		
500	2103	2.07	1.41		

C.4. Model Validation Information

Predictions from JASCO’s propagation models (e.g., MONM) have been validated against experimental data from a number of underwater acoustic measurement programs conducted by JASCO globally, including the United States and Canadian Arctic, Canadian and southern United States waters, Greenland, Russia and Australia (Hannay and Racca 2005, Aerts et al. 2008, Funk et al. 2008, Ireland et al. 2009, O’Neill et al. 2010, Warner et al. 2010, Racca et al. 2012a, Racca et al. 2012b, Matthews and MacGillivray 2013, Martin et al. 2015, Racca et al. 2015, Martin et al. 2017a, Martin et al. 2017b, Warner et al. 2017, MacGillivray 2018, McPherson et al. 2018, McPherson and Martin 2018).

In addition, JASCO has conducted measurement programs associated with a significant number of anthropogenic activities which have included internal validation of the modelling that supported the detection range assessment (including McCrodan et al. 2011, Austin and Warner 2012, McPherson and Warner 2012, Austin and Bailey 2013, Austin et al. 2013, Zykov and MacDonnell 2013, Austin 2014, Austin et al. 2015, Austin and Li 2016, Martin and Popper 2016).

C.5. Results

C.5.1. Detection Range Tables

Table C-2. Detection ranges associated with three ambient noise percentile and three probability of detection (Pd) at Stn 19 in March.

Species	Noise percentile	Pd=0.1	Pd=0.5	Pd=0.9
Sperm whale click	NL10	9.2 - 13.1	4.8 - 5.9	1.9 - 2.9
	NL50	6.4 - 7.5	3.0 - 3.9	1.1 - 1.9
	NL90	4.5 - 5.4	1.7 - 2.8	0.7 - 1.0
Blue whale A-B call	NL10	6.1 - 76.4	5.4 - 48.5	4.8 - 27.6
	NL50	5.0 - 29.4	4.4 - 20.0	3.8 - 9.3
	NL90	4.1 - 14.7	3.7 - 8.1	3.1 - 6.1
Fin whale 20-Hz call	NL10	5.4 - 78.5	4.8 - 28.1	3.7 - 9.9
	NL50	5.2 - 46.8	4.1 - 17.2	3.4 - 5.3
	NL90	4.6 - 24.8	3.7 - 9.5	2.8 - 4.3
Sei whale downsweep	NL10	3.0 - 5.6	2.5 - 3.9	2.2 - 3.1
	NL50	2.6 - 4.1	2.2 - 3.3	1.7 - 2.7
	NL90	2.3 - 3.6	1.8 - 2.8	1.2 - 2.2
Humpback whale song note	NL10	0.9 - 2.2	0.0 - 0.1	0.0 - 0.1
	NL50	0.0 - 0.1	0.0 - 0.1	0.0 - 0.1
	NL90	0.0 - 0.1	0.0 - 0.1	0.0 - 0.1
Delphinid whistles	NL10	1.0 - 1.9	0.0 - 0.2	0.0 - 0.1
	NL50	0.0 - 0.6	0.0 - 0.1	0.0 - 0.1
	NL90	0.0 - 0.1	0.0 - 0.1	0.0 - 0.1
Killer whale tonal call	NL10	0.0 - 0.5	0.0 - 0.1	0.0 - 0.1
	NL50	0.0 - 0.1	0.0 - 0.1	0.0 - 0.1
	NL90	0.0 - 0.1	0.0 - 0.1	0.0 - 0.1
Northern bottlenose whale	NL10	6.0 - 6.6	3.8 - 4.1	2.0 - 2.1
	NL50	5.5 - 6.0	3.4 - 3.7	1.6 - 1.8
	NL90	3.9 - 4.2	2.0 - 2.1	0.7 - 0.8
Sowerby's beaked whale	NL10	2.5 - 2.7	1.8 - 2.0	1.1 - 1.2
	NL50	2.5 - 2.7	1.8 - 2.0	1.1 - 1.2
	NL90	2.4 - 2.7	1.8 - 2.0	1.0 - 1.1
Delphinid click	NL10	5.0 - 5.2	3.6 - 3.7	2.5 - 2.5
	NL50	4.4 - 4.6	3.1 - 3.3	2.0 - 2.1
	NL90	2.7 - 2.9	1.6 - 1.7	0.6 - 0.8

Table C-3. Detection ranges associated with three ambient noise percentile and three probability of detection (Pd) at Stn 19 in September.

Species	Noise percentile	Pd=0.1	Pd=0.5	Pd=0.9
Sperm whale click	NL10	13.9 - 17.7	7.0 - 7.9	3.3 - 4.1
	NL50	7.6 - 8.6	3.6 - 4.4	1.5 - 2.0
	NL90	4.9 - 5.8	2.0 - 2.7	0.8 - 1.4
Blue Whale A-B call	NL10	6.0 - 76.8	5.5 - 41.6	5.0 - 29.1
	NL50	5.1 - 36.8	4.6 - 20.9	3.9 - 11.2
	NL90	3.9 - 9.3	3.3 - 6.9	2.8 - 4.1
Fin Whale 20-Hz call	NL10	6.1 - 81.1	5.1 - 40.3	4.1 - 17.6
	NL50	4.6 - 23.8	3.7 - 8.6	2.8 - 4.3
	NL90	3.8 - 10.1	3.1 - 4.7	2.3 - 3.3
Sei whale downsweep	NL10	2.9 - 4.6	2.5 - 3.9	2.1 - 3.1
	NL50	2.6 - 4.0	2.2 - 3.2	1.4 - 2.7
	NL90	2.2 - 3.4	1.6 - 2.7	1.1 - 1.9
Humpback Whale Song note	NL10	0.9 - 2.4	0.0 - 0.1	0.0 - 0.1
	NL50	0.0 - 1.4	0.0 - 0.1	0.0 - 0.1
	NL90	0.0 - 0.1	0.0 - 0.1	0.0 - 0.1
Delphinid whistles	NL10	2.3 - 2.9	0.0 - 0.9	0.0 - 0.1
	NL50	0.4 - 1.3	0.0 - 0.1	0.0 - 0.1
	NL90	0.0 - 0.2	0.0 - 0.1	0.0 - 0.1
Killer whale tonal call	NL10	0.7 - 1.4	0.0 - 0.1	0.0 - 0.1
	NL50	0.0 - 0.1	0.0 - 0.1	0.0 - 0.1
	NL90	0.0 - 0.1	0.0 - 0.1	0.0 - 0.1
Northern bottlenose whale click	NL10	6.4 - 6.9	4.2 - 4.5	2.3 - 2.6
	NL50	5.5 - 5.9	3.3 - 3.7	1.7 - 2.0
	NL90	4.2 - 4.5	2.3 - 2.6	0.9 - 1.1
Sowerby's beaked whale click	NL10	2.6 - 2.8	1.9 - 2.0	1.1 - 1.6
	NL50	2.5 - 2.7	1.9 - 2.0	1.1 - 1.6
	NL90	2.3 - 2.6	1.6 - 1.9	0.9 - 1.1
Delphinid click	NL10	5.7 - 6.7	4.4 - 4.9	2.9 - 3.1
	NL50	4.6 - 5.4	3.2 - 3.4	2.1 - 2.2
	NL90	3.2 - 3.5	2.1 - 2.3	1.1 - 1.3

Table C-4. Detection ranges associated with three ambient noise percentile and three probability of detection (Pd) at Hampden (EL 1165A) in March.

Species	Noise percentile	Pd=0.1	Pd=0.5	Pd=0.9
Sperm whale click	NL10	13.9 - 19.2	7.3 - 7.8	3.6 - 4.3
	NL50	7.7 - 8.3	3.9 - 4.4	1.9 - 3.4
	NL90	5.3 - 5.8	2.7 - 3.7	1.2 - 2.3
Blue whale A-B call	NL10	46.5 - 100.0	40.9 - 99.7	36.0 - 90.6
	NL50	39.3 - 99.2	34.0 - 83.9	26.1 - 55.7
	NL90	32.1 - 69.9	24.9 - 53.7	16.5 - 32.8
Fin whale 20-Hz call	NL10	47.7 - 100.0	41.9 - 100.0	29.3 - 71.4
	NL50	44.4 - 100.0	35.4 - 86.7	23.5 - 48.0
	NL90	38.3 - 100.0	25.1 - 56.6	15.9 - 27.6
Sei whale downsweep	NL10	30.0 - 76.2	21.3 - 39.9	9.0 - 16.1
	NL50	24.4 - 54.9	12.1 - 22.1	7.4 - 7.7
	NL90	12.1 - 22.3	7.4 - 7.8	1.9 - 2.3
Humpback whale song note	NL10	4.9 - 5.3	0.0 - 0.1	0.0 - 0.1
	NL50	0.0 - 0.1	0.0 - 0.1	0.0 - 0.1
	NL90	0.0 - 0.1	0.0 - 0.1	0.0 - 0.1
Delphinid whistles	NL10	2.6 - 3.0	0.7 - 1.1	0.0 - 0.1
	NL50	0.8 - 1.1	0.0 - 0.1	0.0 - 0.1
	NL90	0.0 - 0.1	0.0 - 0.1	0.0 - 0.1
Killer whale tonal call	NL10	0.4 - 0.6	0.0 - 0.1	0.0 - 0.1
	NL50	0.0 - 0.1	0.0 - 0.1	0.0 - 0.1
	NL90	0.0 - 0.1	0.0 - 0.1	0.0 - 0.1
Northern bottlenose whale click	NL10	6.4 - 6.6	4.2 - 4.4	2.3 - 2.6
	NL50	5.6 - 5.8	3.6 - 3.7	1.8 - 2.0
	NL90	5.3 - 5.5	3.2 - 3.4	1.7 - 1.8
Sowerby's beaked whale click	NL10	2.6 - 2.8	1.9 - 2.1	1.1 - 1.3
	NL50	2.6 - 2.8	1.9 - 2.1	1.1 - 1.3
	NL90	2.6 - 2.8	1.8 - 2.0	1.1 - 1.3
Delphinid click	NL10	5.7 - 5.9	4.0 - 4.0	2.7 - 2.8
	NL50	4.4 - 4.8	3.1 - 3.2	2.0 - 2.2
	NL90	4.0 - 4.1	2.7 - 2.9	1.7 - 1.9

Table C-5. Detection ranges associated with three ambient noise percentile and three probability of detection (Pd) at Hampden (EL 1165A) in September.

Species	Noise percentile	Pd=0.1	Pd=0.5	Pd=0.9
Sperm whale click	NL10	19.3 - 31.1	10.8 - 12.5	4.9 - 7.4
	NL50	11.3 - 14.2	7.5 - 8.1	2.7 - 4.0
	NL90	8.4 - 9.1	3.2 - 4.1	1.7 - 2.5
Blue whale A-B call	NL10	45.9 - 100.0	40.1 - 100.0	35.6 - 91.0
	NL50	38.0 - 100.0	33.4 - 85.3	23.7 - 55.5
	NL90	24.1 - 55.7	17.1 - 34.9	12.6 - 20.9
Fin whale 20-Hz call	NL10	45.6 - 100.0	38.8 - 99.7	25.3 - 57.6
	NL50	39.4 - 99.8	27.9 - 61.7	17.5 - 32.0
	NL90	31.3 - 64.1	19.4 - 39.5	7.6 - 15.8
Sei whale downsweep	NL10	34.2 - 100.0	24.1 - 57.6	13.2 - 28.7
	NL50	24.6 - 59.2	14.4 - 32.1	6.8 - 7.0
	NL90	13.3 - 28.8	6.6 - 6.9	2.8 - 3.1
Humpback whale song note	NL10	18.5 - 34.3	7.7 - 7.9	0.0 - 0.1
	NL50	8.3 - 8.6	0.0 - 0.1	0.0 - 0.1
	NL90	4.3 - 6.7	0.0 - 0.1	0.0 - 0.1
Delphinid whistles	NL10	7.1 - 7.4	1.6 - 2.1	0.0 - 0.1
	NL50	1.6 - 2.1	0.0 - 0.1	0.0 - 0.1
	NL90	0.5 - 0.6	0.0 - 0.1	0.0 - 0.1
Killer whale tonal call	NL10	1.9 - 2.3	0.0 - 0.1	0.0 - 0.1
	NL50	0.2 - 0.5	0.0 - 0.1	0.0 - 0.1
	NL90	0.0 - 0.1	0.0 - 0.1	0.0 - 0.1
Northern bottlenose whale click	NL10	6.7 - 7.9	4.4 - 4.5	2.5 - 2.7
	NL50	5.5 - 5.9	3.5 - 3.7	1.8 - 2.0
	NL90	4.5 - 4.7	2.6 - 2.8	1.2 - 1.3
Sowerby's beaked whale click	NL10	2.6 - 2.7	1.8 - 2.0	1.1 - 1.3
	NL50	2.6 - 2.7	1.8 - 2.0	1.1 - 1.3
	NL90	2.4 - 2.6	1.7 - 1.8	1.0 - 1.1
Delphinid click	NL10	7.3 - 7.6	4.4 - 4.9	2.9 - 3.1
	NL50	5.2 - 5.7	3.2 - 3.5	2.1 - 2.2
	NL90	3.5 - 3.7	2.3 - 2.5	1.4 - 1.5

Table C-6. Detection ranges associated with three ambient noise percentile and three probability of detection (Pd) at Harp (EL 1165B) in March. ND: not detectable.

Species	Noise percentile	Pd=0.1	Pd=0.5	Pd=0.9
Sperm whale click	NL10	13.6 - 19.5	5.7 - 7.7	2.2 - 2.5
	NL50	2.8 - 3.1	1.1 - 1.4	0.5 - 0.9
	NL90	1.3 - 1.5	0.6 - 1.0	0.4 - 0.8
Blue whale A-B call	NL10	52.0 - 100.0	41.0 - 100.0	27.4 - 100.0
	NL50	10.3 - 26.5	9.0 - 16.8	6.3 - 10.8
	NL90	3.6 - 4.6	2.2 - 2.7	1.1 - 1.4
Fin whale 20-Hz call	NL10	67.1 - 100.0	50.3 - 100.0	24.1 - 100.0
	NL50	15.1 - 32.2	9.6 - 18.5	5.9 - 10.2
	NL90	8.0 - 15.9	5.0 - 7.6	3.1 - 3.4
Sei whale downsweep	NL10	19.0 - 79.2	12.4 - 21.8	7.5 - 13.1
	NL50	3.8 - 5.1	1.8 - 2.2	0.6 - 0.7
	NL90	1.9 - 2.5	0.7 - 0.9	0.2 - 0.2
Humpback whale song note	NL10	3.8 - 4.6	1.4 - 1.6	0.0 - 0.0
	NL50	0.0 - 0.0	0.0 - 0.0	0.0 - 0.0
	NL90	0.0 - 0.0	0.0 - 0.0	0.0 - 0.0
Delphinid whistles	NL10	1.8 - 2.0	0.7 - 0.9	0.2 - 0.2
	NL50	0.6 - 0.7	0.0 - 0.1	0.0 - 0.0
	NL90	0.1 - 0.1	0.0 - 0.0	0.0 - 0.0
Killer Whale Tonal call	NL10	0.8 - 1.1	0.0 - 0.0	0.0 - 0.0
	NL50	0.0 - 0.0	0.0 - 0.0	0.0 - 0.0
	NL90	0.0 - 0.0	0.0 - 0.0	0.0 - 0.0
Northern Bottlenose Whale click	NL10	6.5 - 6.9	4.1 - 4.4	2.2 - 2.4
	NL50	4.5 - 4.7	2.4 - 2.6	1.1 - 1.3
	NL90	3.2 - 3.4	1.5 - 1.7	0.6 - 1.1
Sowerby's beaked whale click	NL10	2.8 - 3.0	2.1 - 2.4	1.4 - 2.0
	NL50	2.8 - 2.9	1.9 - 2.3	1.3 - 1.9
	NL90	2.6 - 2.7	1.8 - 2.3	1.1 - 1.7
Delphinid click	NL10	5.2 - 5.9	4.0 - 4.1	2.5 - 2.8
	NL50	3.4 - 3.6	2.1 - 2.4	1.3 - 1.6
	NL90	2.3 - 2.5	1.4 - 1.8	0.9 - 1.1
Harbour porpoise Click	NL10	0.8 - 1.4	0.7 - 1.2	0.5 - 1.0
	NL50	0.8 - 1.3	0.6 - 1.1	0.5 - 0.9
	NL90	0.8 - 1.3	0.6 - 1.1	0.5 - 0.9

Table C-7. Detection ranges associated with three ambient noise percentile and three probability of detection (Pd) at Harp (EL 1165B) in September. ND: not detectable.

Species	Noise percentile	Pd=0.1	Pd=0.5	Pd=0.9
Sperm whale click	NL10	44.2 - 50.0	26.3 - 33.6	14.5 - 18.4
	NL50	20.8 - 27.9	11.4 - 16.4	4.7 - 7.1
	NL90	12.8 - 17.2	5.4 - 7.5	3.0 - 3.1
Blue whale A-B call	NL10	77.3 - 100.0	64.7 - 100.0	62.0 - 100.0
	NL50	61.5 - 100.0	43.6 - 100.0	29.0 - 100.0
	NL90	8.8 - 18.7	6.5 - 11.4	4.8 - 7.4
Fin whale 20-Hz call	NL10	82.2 - 100.0	66.9 - 100.0	46.8 - 100.0
	NL50	62.2 - 100.0	39.1 - 100.0	18.9 - 94.3
	NL90	19.8 - 96.4	10.5 - 26.1	7.6 - 15.3
Sei whale downsweep	NL10	46.8 - 100.0	26.3 - 100.0	13.5 - 36.0
	NL50	26.3 - 100.0	13.5 - 73.2	9.4 - 23.6
	NL90	8.0 - 17.2	6.0 - 9.9	3.8 - 4.8
Humpback whale song note	NL10	9.8 - 24.1	5.8 - 9.8	2.1 - 2.3
	NL50	7.8 - 14.3	3.1 - 5.6	1.7 - 1.8
	NL90	2.2 - 2.4	1.3 - 1.5	0.0 - 0.0
Delphinid whistles	NL10	9.1 - 15.7	6.4 - 9.5	3.3 - 5.6
	NL50	3.8 - 6.0	2.3 - 2.4	0.6 - 0.9
	NL90	2.5 - 2.8	0.7 - 1.0	0.0 - 0.2
Killer whale tonal call	NL10	5.7 - 6.5	2.3 - 2.4	0.2 - 0.4
	NL50	2.5 - 2.6	0.5 - 0.6	0.0 - 0.0
	NL90	0.8 - 1.1	0.0 - 0.1	0.0 - 0.0
Northern bottlenose whale click	NL10	8.7 - 9.3	6.1 - 6.6	3.8 - 4.0
	NL50	6.9 - 7.4	4.4 - 4.7	2.6 - 2.7
	NL90	6.2 - 6.7	3.8 - 4.1	2.1 - 2.3
Sowerby's beaked whale click	NL10	3.0 - 3.1	2.2 - 2.3	1.4 - 1.8
	NL50	2.9 - 3.0	2.2 - 2.2	1.3 - 1.8
	NL90	2.8 - 3.0	2.1 - 2.2	1.3 - 1.8
Delphinid click	NL10	8.8 - 9.7	6.5 - 8.0	5.3 - 5.8
	NL50	6.3 - 7.8	5.1 - 5.6	3.3 - 3.6
	NL90	5.5 - 6.2	3.9 - 4.9	2.8 - 3.0
Harbour porpoise click	NL10	1.0 - 1.5	0.9 - 1.3	0.8 - 1.1
	NL50	1.0 - 1.5	0.9 - 1.2	0.8 - 1.0
	NL90	1.0 - 1.4	0.9 - 1.2	0.7 - 1.0

Table C-8. Detection ranges associated with three ambient noise percentile and three probability of detection (Pd) at Mid in March. ND: not detectable.

Species	Noise percentile	Pd=0.1	Pd=0.5	Pd=0.9
Sperm whale click	NL10	14.7 - 28.0	7.2 - 10.2	3.6 - 4.4
	NL50	9.5 - 13.4	4.4 - 5.4	2.2 - 2.7
	NL90	6.0 - 7.1	2.9 - 3.7	1.3 - 1.7
Blue whale A-B call	NL10	49.6 - 100.0	46.2 - 100.0	41.9 - 100.0
	NL50	45.1 - 100.0	40.2 - 100.0	33.8 - 85.6
	NL90	35.5 - 98.0	27.4 - 62.6	16.4 - 48.0
Fin whale 20-Hz call	NL10	51.7 - 100.0	42.3 - 100.0	34.8 - 100.0
	NL50	47.2 - 100.0	39.1 - 100.0	29.1 - 100.0
	NL90	41.4 - 100.0	32.0 - 100.0	16.7 - 33.2
Sei whale downsweep	NL10	32.9 - 99.7	23.6 - 48.5	12.3 - 19.1
	NL50	26.7 - 71.7	15.6 - 25.4	6.8 - 10.8
	NL90	16.3 - 26.4	7.9 - 11.5	3.4 - 4.2
Humpback whale song note	NL10	3.5 - 4.5	0.4 - 0.7	0.0 - 0.0
	NL50	2.0 - 2.6	0.0 - 0.0	0.0 - 0.0
	NL90	0.0 - 0.0	0.0 - 0.0	0.0 - 0.0
Delphinid whistles	NL10	2.6 - 2.7	1.2 - 1.3	0.0 - 0.1
	NL50	1.4 - 1.5	0.0 - 0.3	0.0 - 0.0
	NL90	0.5 - 0.6	0.0 - 0.0	0.0 - 0.0
Killer whale tonal call	NL10	0.7 - 0.8	0.0 - 0.0	0.0 - 0.0
	NL50	0.0 - 0.2	0.0 - 0.0	0.0 - 0.0
	NL90	0.0 - 0.0	0.0 - 0.0	0.0 - 0.0
Northern bottlenose whale click	NL10	6.8 - 7.4	4.5 - 5.0	2.6 - 2.9
	NL50	5.9 - 6.3	3.7 - 4.1	2.0 - 2.2
	NL90	5.1 - 5.4	3.0 - 3.6	1.5 - 1.7
Sowerby's beaked whale click	NL10	2.6 - 3.0	1.9 - 2.3	1.3 - 1.7
	NL50	2.6 - 2.9	1.9 - 2.3	1.3 - 1.7
	NL90	2.5 - 2.9	1.8 - 2.2	1.2 - 1.6
Delphinid click	NL10	5.8 - 6.5	4.4 - 4.9	3.0 - 3.4
	NL50	4.8 - 5.2	3.3 - 3.7	2.2 - 2.4
	NL90	3.5 - 4.1	2.5 - 2.6	1.6 - 1.7
Harbour porpoise click	NL10	0.4 - 1.1	0.2 - 0.7	0.1 - 0.6
	NL50	0.4 - 1.0	0.1 - 0.7	0.1 - 0.6
	NL90	0.4 - 1.0	0.1 - 0.7	0.1 - 0.6

Table C-9. Detection ranges associated with three ambient noise percentile and three probability of detection (Pd) at Mid in September. ND: not detectable.

Species	Noise percentile	Pd=0.1	Pd=0.5	Pd=0.9
Sperm whale click	NL10	20.9 - 44.2	13.0 - 16.2	6.6 - 7.6
	NL50	12.5 - 16.1	6.5 - 7.5	3.0 - 3.6
	NL90	8.0 - 10.2	3.7 - 4.5	1.8 - 2.2
Blue whale A-B call	NL10	46.3 - 100.0	41.7 - 100.0	36.3 - 99.9
	NL50	30.3 - 90.7	23.6 - 59.5	12.8 - 32.3
	NL90	1.9 - 2.3	1.4 - 1.6	0.8 - 0.9
Fin whale 20-Hz call	NL10	51.6 - 100.0	41.5 - 100.0	30.9 - 74.2
	NL50	41.7 - 100.0	31.1 - 74.3	15.5 - 30.6
	NL90	18.1 - 46.5	8.1 - 13.3	2.8 - 3.4
Sei whale downsweep	NL10	41.0 - 100.0	32.3 - 99.9	22.1 - 47.0
	NL50	31.9 - 99.8	20.7 - 31.6	9.7 - 16.3
	NL90	9.7 - 16.2	4.2 - 5.0	2.0 - 2.9
Humpback whale song note	NL10	22.2 - 59.1	8.0 - 16.0	2.3 - 2.8
	NL50	10.3 - 17.3	3.0 - 4.7	0.0 - 0.0
	NL90	4.5 - 7.2	0.0 - 0.0	0.0 - 0.0
Delphinid whistles	NL10	6.0 - 7.6	2.0 - 2.1	0.7 - 0.8
	NL50	1.9 - 2.0	0.6 - 0.6	0.0 - 0.0
	NL90	0.9 - 1.0	0.0 - 0.0	0.0 - 0.0
Killer Whale Tonal call	NL10	2.4 - 2.6	0.3 - 0.4	0.0 - 0.0
	NL50	1.1 - 1.3	0.0 - 0.0	0.0 - 0.0
	NL90	0.0 - 0.3	0.0 - 0.0	0.0 - 0.0
Northern bottlenose whale click	NL10	7.2 - 7.6	4.6 - 5.1	2.8 - 2.9
	NL50	5.9 - 6.2	3.6 - 3.9	1.9 - 2.1
	NL90	3.9 - 4.2	2.2 - 2.4	1.0 - 1.2
Sowerby's beaked whale click	NL10	2.7 - 3.0	2.0 - 2.2	1.3 - 1.5
	NL50	2.6 - 3.0	2.0 - 2.2	1.3 - 1.5
	NL90	2.2 - 2.5	1.5 - 1.8	0.9 - 1.2
Delphinid click	NL10	7.3 - 7.8	5.6 - 6.1	3.4 - 5.0
	NL50	5.6 - 6.2	3.5 - 5.1	2.2 - 2.4
	NL90	3.0 - 3.4	1.9 - 2.0	1.1 - 1.2
Harbour porpoise clicks	NL10	0.5 - 1.2	0.3 - 1.0	0.2 - 0.8
	NL50	0.5 - 1.2	0.3 - 1.0	0.2 - 0.8
	NL90	0.4 - 1.2	0.3 - 1.0	0.1 - 0.7

Appendix D. Marine Mammal Detection Methods

D.1. Automated Click Detector for Odontocetes

We applied an automated click detector/classifier to detect clicks from porpoise and dolphins (Figure D-1.). This detector/classifier is based on the zero-crossings in the acoustic time series. Zero-crossings are the rapid oscillations of a click's pressure waveform above and below the signal's normal level (e.g., Figure D-1.). Clicks are detected by the following steps (Figure D-1.):

1. The raw data is high-pass filtered to remove all energy below 5 kHz. This removes most energy from other sources such as shrimp, vessels, wind, and cetacean tonal calls, yet allows the energy from all marine mammal click types to pass.
2. The filtered samples are summed to create a 0.334 ms rms time series. Most marine mammal clicks have a 0.1–1 ms duration.
3. Possible click events are identified with a split-window normalizer that divides the 'test' bin of the time series by the mean of the 6 'window' bins on either side of the test bin, leaving a 1-bin wide 'notch'.
4. A Teager-Kaiser energy detector identifies possible click events.
5. The high-pass filtered data is searched to find the maximum peak signal within 1 ms of the detected peak.
6. The high-pass filtered data is searched backwards and forwards to find the time span where the local data maxima are within 9 dB of the maximum peak. The algorithm allows for two zero-crossings to occur where the local peak is not within 9 dB of the maximum before stopping the search. This defines the time window of the detected click.
7. The classification parameters are extracted. The number of zero crossings within the click, the median time separation between zero crossings, and the slope of the change in time separation between zero crossings are computed. The slope parameter helps to identify beaked whale clicks, as beaked whales can be identified by the increase in frequency (upsweep) of their clicks.
8. The Mahalanobis distance between the extracted classification parameters and the templates of known click types is computed. The covariance matrices for the known click types, computed from thousands of manually identified clicks for each species, are stored in an external file. Each click is classified as a type with the minimum Mahalanobis distance, unless none of them are less than the specified distance threshold.

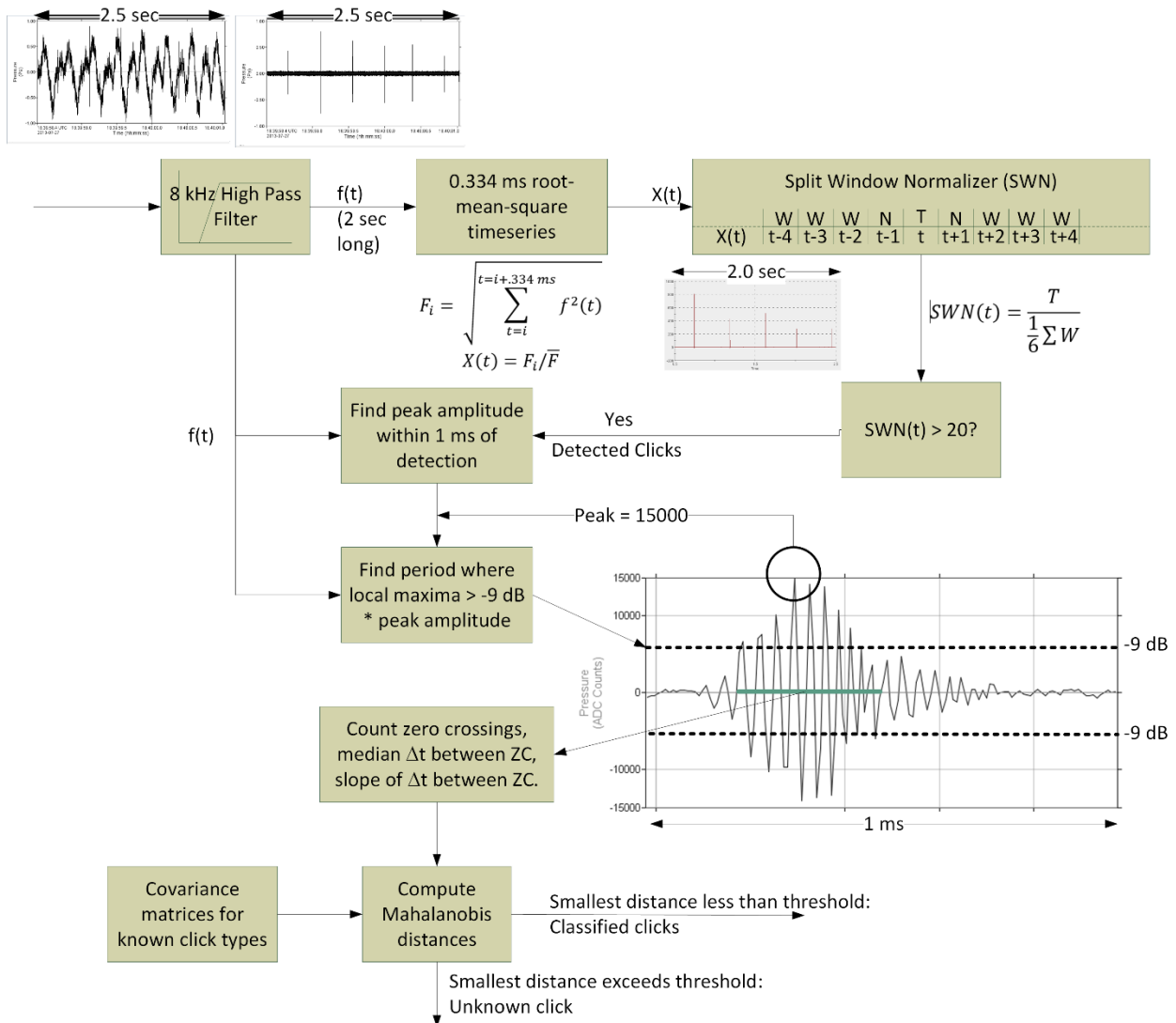


Figure D-1. The click detector/classifier block diagram.

Odontocete clicks occur in groups called click trains. Each species has a characteristic inter-click-interval (ICI) and number of clicks per train. The click detector includes a second stage that associates individual clicks into trains (Figure D-2). The steps of the click train associator algorithm are:

1. Queue clicks for N seconds, where N is twice the maximum number of clicks per train times the maximum ICI.
2. Search for all clicks within the window that have Mahalanobis distances less than 11 for the species of interest (this gets 99% of all clicks for the species as defined by the template).
3. Create a candidate click train if:
 - a. the number of clicks is greater or equal to the minimum number of clicks in a train;
 - b. the maximum time between any two clicks is less than twice the maximum ICI, and
 - c. the smallest Mahalanobis distance for all clicks in the candidate train is less than 4.1.
4. Create a new 'time-series' that has a value of 1 at the time of arrival of each clicks and zeroes everywhere else.

5. Apply a Hann window to the timeseries then compute the cepstrum.
6. A click train is classified if a peak in the cepstrum with amplitude > 5 times the standard deviation of the cepstrum occurs at a quefreny between the minimum maximum ICI.
7. Queue clicks for N seconds
8. Search for all clicks within the window that have Malahanobis distances less than 10 (equal to the extent of the variance in the training data set).
9. If the number of clicks is greater than or equal to 3 and dT is less than $2 * \max ICI$, make a new time-series at the 0.333 ms rate; where the value is 1 when the clicks occurred and 0 for all other time bins. Perform the following processing on this time series:
 - a. Compute cepstrum
 - b. ICI is the peak of the cepstrum with amplitude > $5 * stdev$ and searching for quefreny between $minICI$ and $maxICI$.
 - c. For each click related to the previous N cepstrum, create a new time series and compute ICI; if we get a good match, extend the click train; find a mean ICI and variance.
10. If the click features, total clicks and mean ICI match the species, output a species_click_train detection.

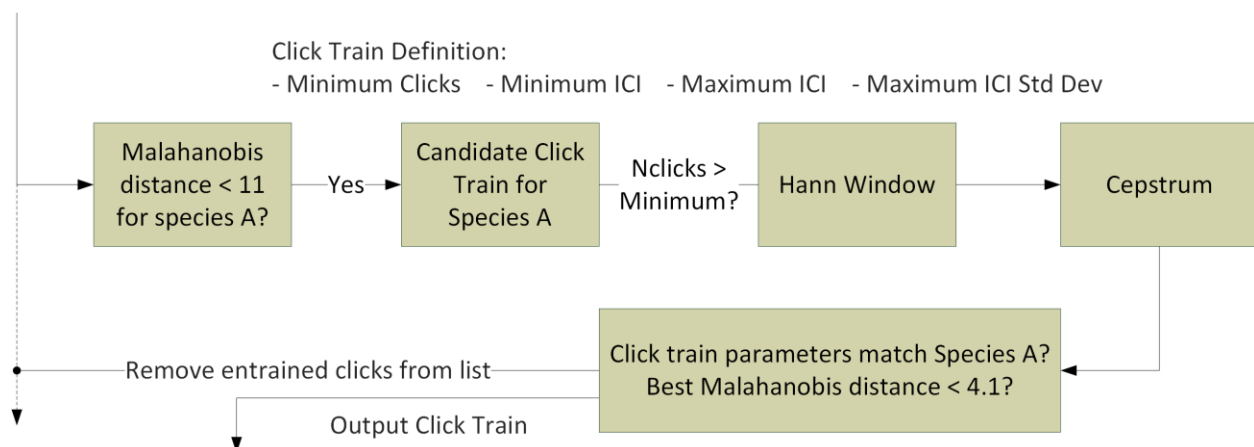


Figure D-2. The click train detector/classifier block diagram.

D.2. Tonal Signal Detection

Marine mammal tonal acoustic signals are detected by the following steps:

1. Spectrograms of the appropriate resolution for each mammal vocalization type that were normalized by the median value in each frequency bin for each detection window (Table D-1.) were created.
2. Adjacent bins were joined, and contours were created via a contour-following algorithm (Figure D-3.).
3. A sorting algorithm determined if the contours match the definition of a marine mammal vocalization (Table D-2.).

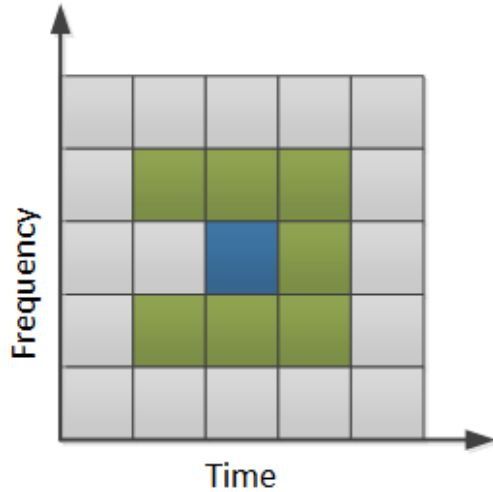


Figure D-3. Illustration of the search area used to connect spectrogram bins. The blue square represents a bin of the binary spectrogram equalling 1 and the green squares represent the potential bins it could be connected to. The algorithm advances from left to right so grey cells left of the test cell need not be checked.

Table D-1. Fast Fourier Transform (FFT) and detection window settings for all contour-based detectors used to detect tonal vocalizations of marine mammal species expected in the data. Values are based on JASCO’s experience and empirical evaluation on a variety of data sets.

Detector	FFT			Detection window (s)	Detection threshold
	Resolution (Hz)	Frame length (s)	Timestep (s)		
Atl_BlueWhale_GL_IM	0.125	2	0.5	40	4
Atl_BlueWhale_IM	0.125	2	0.5	40	4
Atl_BlueWhale_IM2	0.125	2	0.5	120	4
Atl_FinWhale_130	2	0.2	0.05	5	3
Atl_FinWhale_21.2	1	0.2	0.05	5	1.7
Atl_FinWhale_21.2	1	0.2	0.05	5	4
MinkePulseTrain	8	0.1	0.025	1	40
N_RightWhale_Up1	4	0.128	0.032	8	2.5
N_RightWhale_Up2	4	0.128	0.032	8	3
N_RightWhale_Up3	7	0.17	0.025	10	3
SeiWhale	3.25	0.2	0.035	5	3.5
VLFMoan	2	0.2	0.05	15	4
LFMoan	2	0.25	0.05	10	3
ShortLow	7	0.17	0.025	10	3
MFMoanLow	4	0.2	0.05	5	3
MFMoanHigh	8	0.125	0.05	5	3
WhistleLow	16	0.03	0.015	5	3
WhistleHigh	64	0.015	0.005	5	3

Table D-2. A sample of vocalization sorter definitions for the tonal vocalizations of cetacean species expected in the area. N/A: Not applicable.

Detector	Target species	Frequency (Hz)	Duration (s)	Bandwidth (B; Hz)	Other detection parameters
Atl_BlueWhale_GL_IM	Blue whales	14–22	8.00–30.00	1<B<5	minSweepRate= -500 Hz/s; minF<18 Hz 16.5<PeakF<17.5 Hz
Atl_BlueWhale_IM	Blue whales	14–22	8.00–30.00	1<B<5	minSweepRate= -500 Hz/s; minF<18 Hz 16.5<FrequencyOfPeakIntensity<18 Hz
Atl_BlueWhale_IM2	Blue whales	15–22	8.00–30.00	1<B<5	N/A
Atl_FinWhale_130	Fin whales	110–150	0.30–1.50	>6	minF<125 Hz
Atl_FinWhale_21.2	Fin whales	10–40	0.40–3.00	>6	-100<SweepRate<0 Hz/s; minF<17 Hz 20<FrequencyOfPeakIntensity<22 Hz
Atl_FinWhale_21.2	Fin whales	8–40	0.30–3.00	>6	-100<SweepRate<0 Hz/s; minF<17 Hz
MinkePulseTrain	Minke whales	50–500	0.025–0.3		0.25<PulseGap<2 s; 10<TrainLength<100 s
N_RightWhale_Up1	Right whales	65–260	0.60–1.20	70<B<195	minF<75 Hz 30<SweepRate<290 Hz/s
N_RightWhale_Up2	Right whales	65–260	0.50–1.20	B>25	30<SweepRate<290 Hz/s
N_RightWhale_Up3	Right whales	30–400	0.50–10.00		10<SweepRate<500 Hz/s
SeiWhale	Sei whales	20–150	0.50–1.70	19<B<120	-100<SweepRate<-6 Hz/s InstantaneousBandwidth<100 Hz
VLFMoan	Blue/fin/sei whales	10–100	0.30–10.00	>10	minF<40 Hz
LFMoan	Blue/right/sei whales	40–250	0.50–10.00	>15	InstantaneousBandwidth<50 Hz
ShortLow	Fin/baleen whales	30–400	0.08–0.60	>25	N/A
MFMoanLow	Humpback whales	100–700	0.50–5.00	>50	minF<450 Hz InstantaneousBandwidth<200 Hz
MFMoanHigh	Humpback whales	500–2500	0.50–5.00	>150	minF<1500 Hz InstantaneousBandwidth<300 Hz
WhistleLow	Pilot/killer whales	1000–10000	0.50–5.00	>300	Max Instantaneous Bandwidth = 1000 Hz minF<5000 Hz
WhistleHigh	Other delphinid	4000–20000	0.30–3.00	>700	Max Instantaneous Bandwidth = 5000 Hz

D.3. File Selection Process for Validating Detections

To standardize the file selection process, we developed an algorithm that automatically selects a sample of files for review. The selection process starts by computing the distribution of three variables that describe the detections in the full data set: the diversity of detected species per file, the number of detections per file (per species), and the temporal distribution of each species. The algorithm iteratively removes files from the data set by computing the difference between the original distribution and the distribution without each file—the file whose removal brings the new distribution closest to the original distribution is removed. The process is repeated until the sample size is reduced to N , which was set to 1 or 2% of the total duration of acoustic data. In this description, the term ‘species’ identifies a marine mammal detector whose performance needs to be assessed. The three variables used by the algorithm are described further below:

1. **Diversity:** Select files representative of the range of species diversity (number of detected species in a file). The diversity of the full data set is log transformed to reduce the skew of the data. After being logged, the histogram bin size of the full data set is calculated using the Freedman-Diaconis rule (Freedman and Diaconis 1981), with a maximum of 20 bins. Sample files are selected such that the distribution of diversity within the sample matches the distribution of logged diversity in the full data set.
2. **Counts:** Select files representative of the range of detection counts (number of detections per file for each species). For each species, the detection counts of the full data set are log transformed to manage the skew of the data. After being logged, the histogram bin size of the full data set is calculated using the Freedman-Diaconis rule (Freedman and Diaconis 1981), with a maximum of 20 bins. Sample files are selected such that the distribution of detection counts within the sample matches the distribution of logged detection counts in the full data set. Files with no detections are not included in the calculation for each species (0-detection count files for a species will naturally be included in files selected for other species).
3. **Temporal distribution:** Select files representative of the temporal range of files containing detections for each species. The time frame of the full data set is divided into 12 equally sized bins. If the bin size is greater than 30 days, then the time frame is divided into 30-day bins. File counts per species for each bin are log transformed to reduce the skew of the data. Sample files are selected such that the distribution of files containing detections for each species within the sample matches the distribution of files containing detections for each species in the full data set.

In each iteration, we remove the file whose omission minimizes the Total Variation (v_T). The v_T is the sum of the following:

- Diversity Variation (v_D),
- Count Variation (v_C), which is the average of the per species count variations (v_{C_s}), and
- Temporal Distribution Variation (v_{TD}), which is the average of the per species temporal variations (v_{TD_s}).

$$v_T = v_D + v_C + v_{TD}$$

$$\Delta = \sum_{b=1}^B |Pf_b - Ps_b|$$

$$v_D = \Delta_D$$

$$v_{C_s} = \Delta_{C_s}$$

$$v_C = \frac{\sum_{s=1}^S v_{C_s}}{S}$$

$$v_{TD_s} = \Delta_{TD_s}$$

$$v_{TD} = \frac{\sum_{s=1}^S v_{TD_s}}{S}$$

where Pf_b is proportion of bin 'b' within the full data set, Ps_b is the proportion of bin 'b' within subset 's', Δ is difference between distributions, B is the total number of bins in the distribution, and S is the number of species. Two final constraints on the algorithm are preserving at least 10 files per species and attempting to have the files for each species at least 6 h apart.

Once the sample size has been reduced to N , the two files with the highest detection counts for each species are added back into the sample, if they were not already included. This can result in the final sample being trivially greater than N .

D.4. Divergence Curves

In order to assess whether the selected validation effort was appropriate to produce accurate detector performance metrics, we calculated the variation of the three variables used to score validation file samples (i.e., Diversity, Counts and Temporal Distribution; see Appendix D.3) plus an aggregate score (labelled 'Overall' in Figure D-4) from the full data set for decreasing sample sizes (N), where low variation (denoted Divergence in Figure D-4) indicates little difference between the sample and the full data set. The N at which the average variation of the three variables and aggregate score is minimal (distribution of sample does not get closer to that of full data set with further decreases in sample size) can be determined. This N_{ideal} represents the minimum proportion of files to be validated. N_{ideal} can vary across data sets depending on the acoustic environments encountered throughout the data sets and the automated detectors employed.

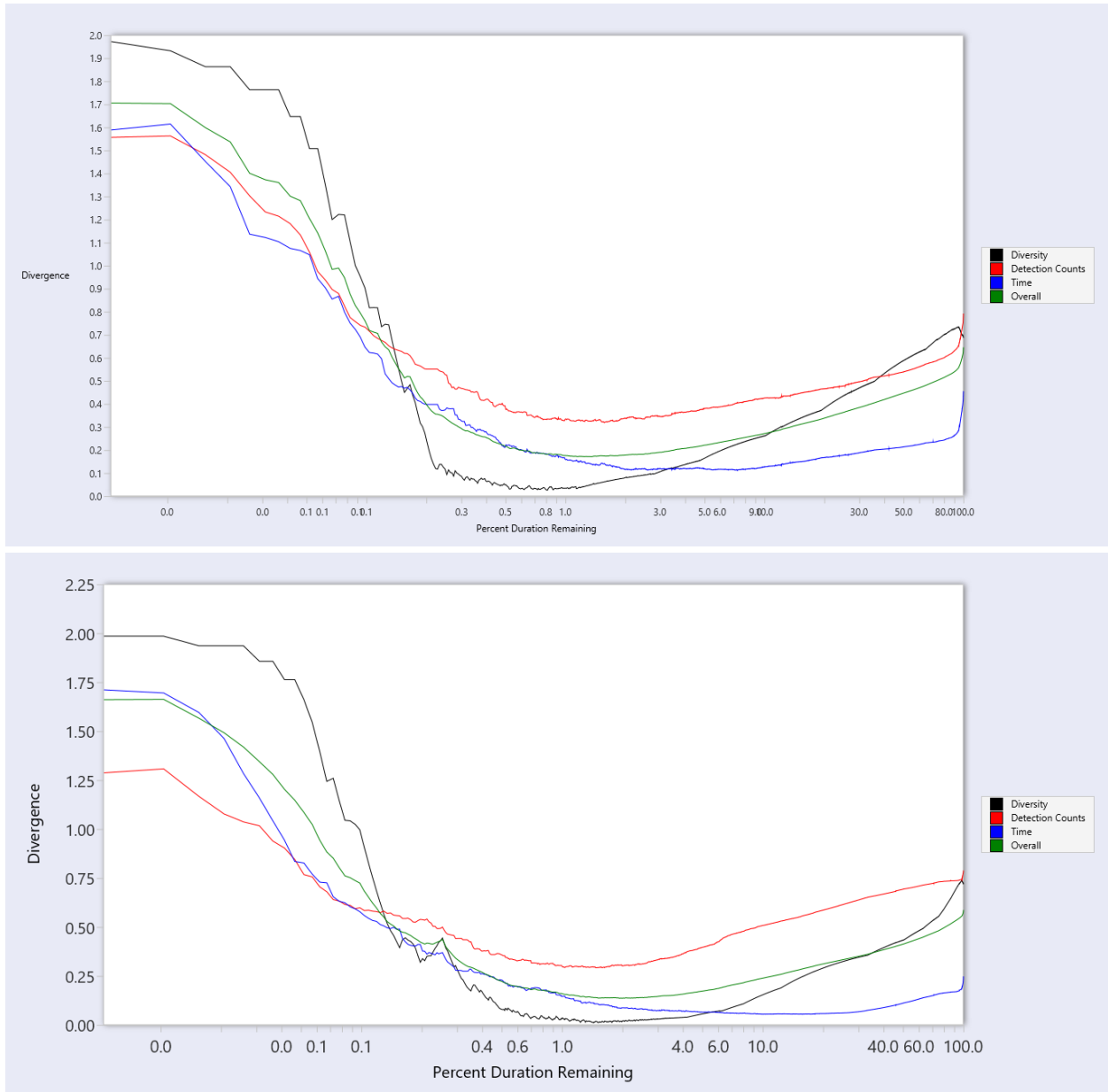


Figure D-4. Divergence curves for Hampden (EL 1165A), 32 kHz data (top) and 512 kHz data (bottom).

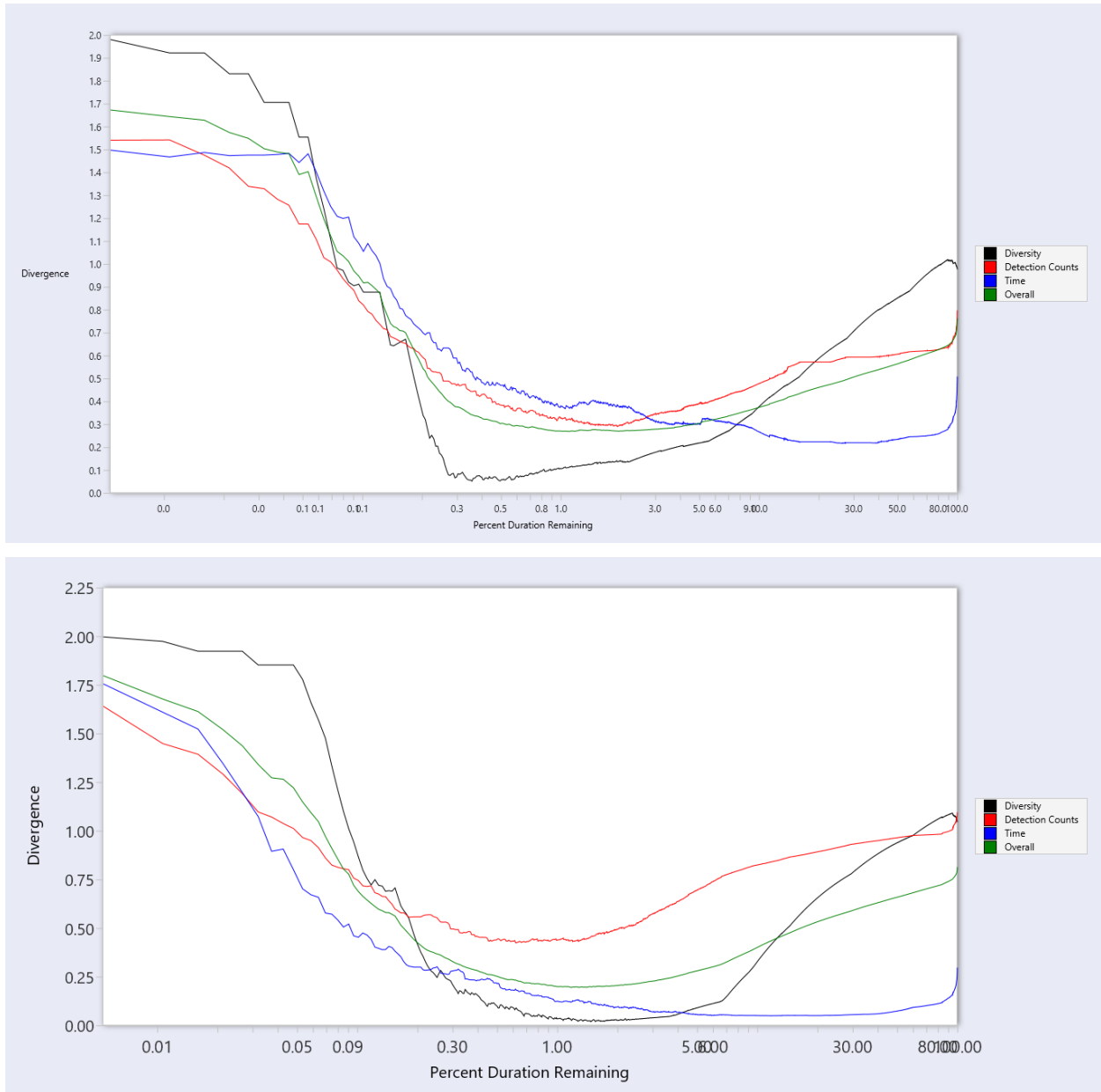


Figure D-5. Divergence curves for Harp (EL 1165B), 32 kHz data (top) and 512 kHz data (bottom).

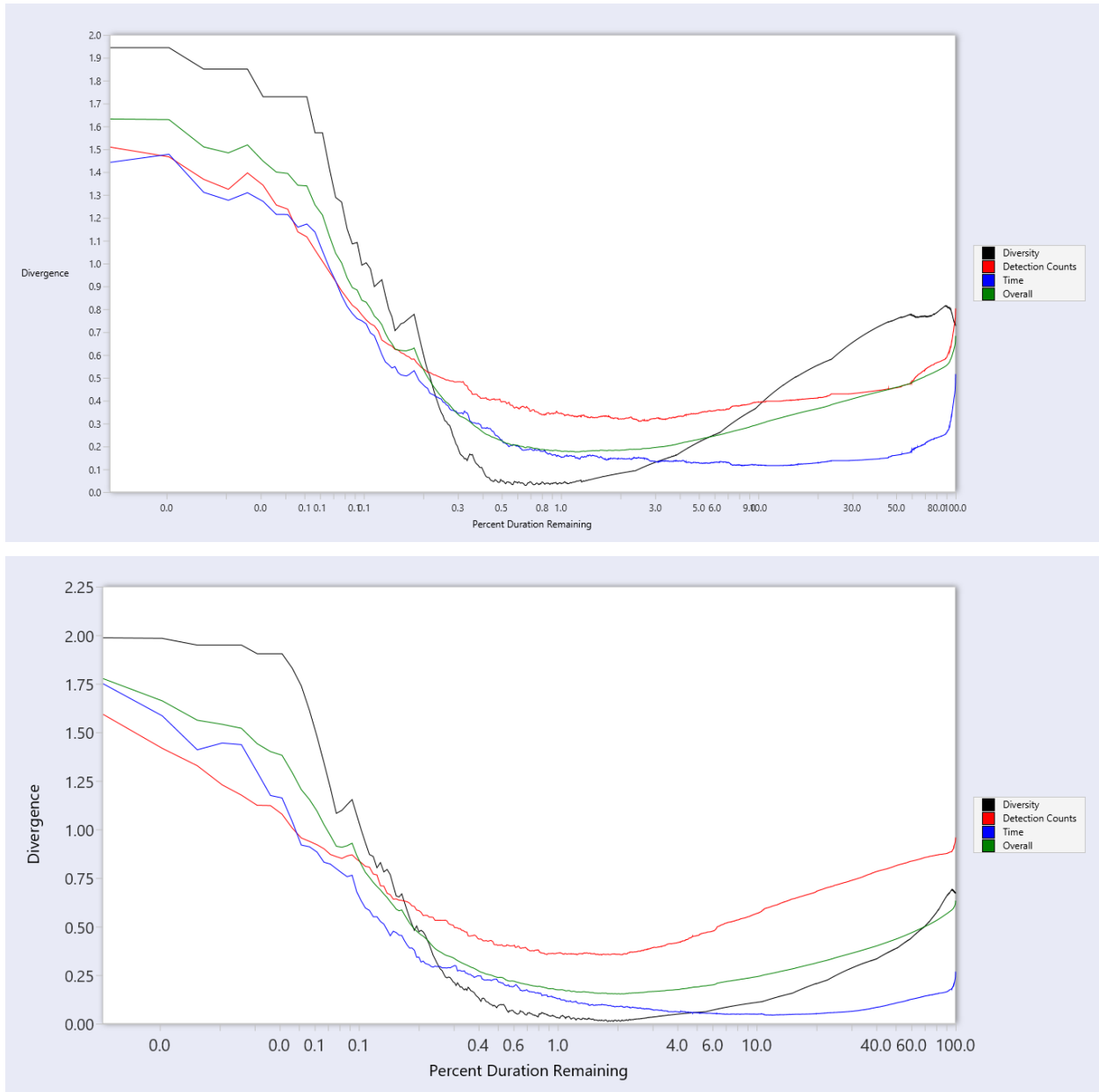


Figure D-6. Divergence curves for Mid, 32 kHz data (top) and 512 kHz data (bottom).

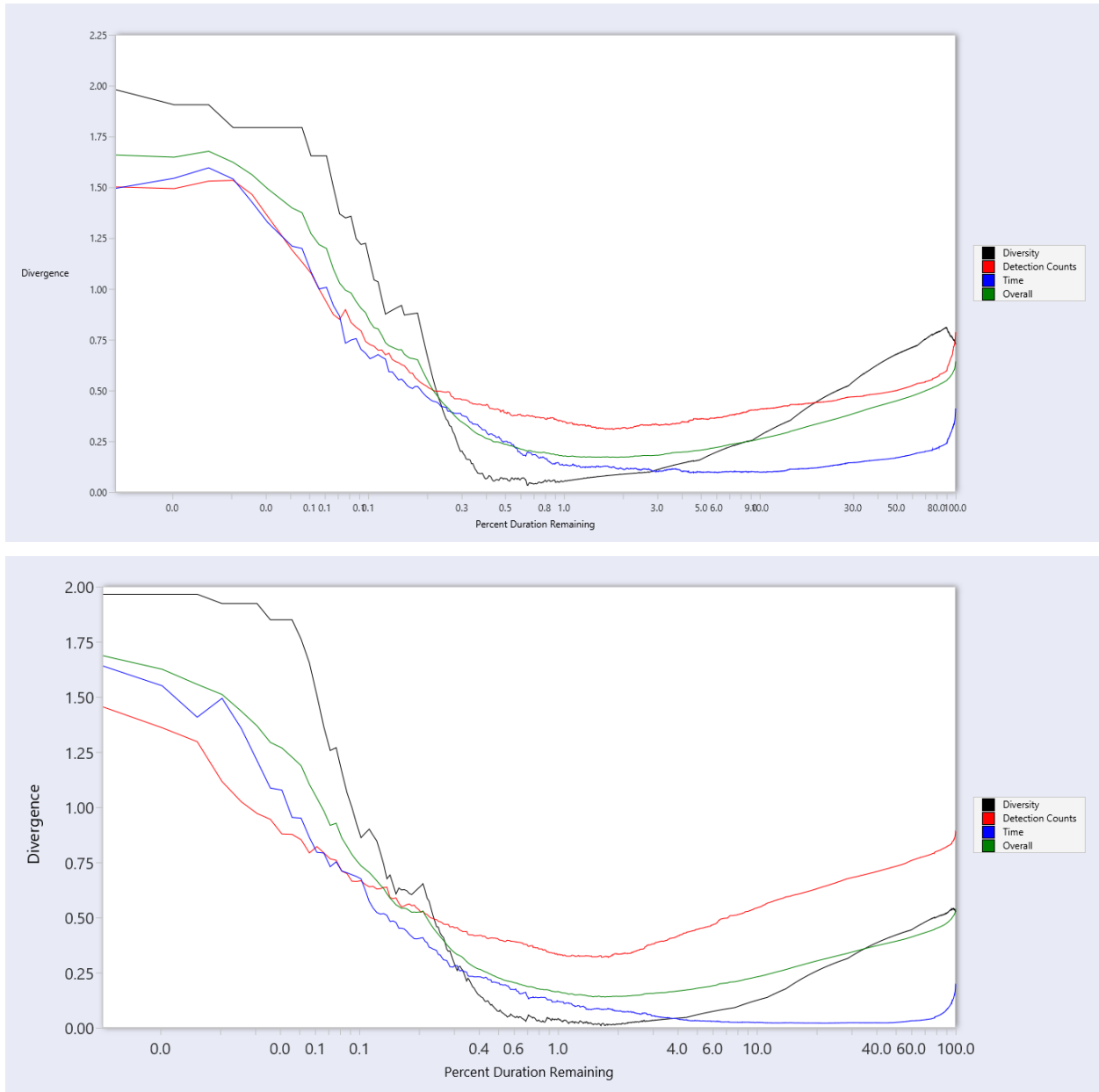


Figure D-7. Divergence curves for Stn 19, 32 kHz data (top) and 512 kHz data (bottom).

D.5. Detector Performance Calculation and Optimization

All files selected for manual validation were reviewed by one of two experienced analysts using JASCO's PAMlab software to determine the presence or absence of every species, regardless of whether a species was automatically detected in the file. Although the detectors classify specific signals, we validated the presence/absence of species at the file level, not the detection level. Acoustic signals were only assigned to a species if the analyst was confident in their assessment. When unsure, analysts would consult one another, peer-reviewed literature, and other experts in the field. If certainty could not be reached, the file of concern would be classified as possibly containing the species in question or containing an unknown acoustic signal. A sample of manually validated vocalizations were reviewed by a senior analyst for all stations to look for erroneous records or assign unidentified signals to a known species. Next, the validated results were compared to the raw detector results in three phases to refine the results and ensure they accurately represent the occurrence of each species in the study area.

In phase 1, the validated versus detector results were plotted as time series and critically reviewed to determine when and where automated detections should be excluded. Questionable detections that overlap with the detection period of other species were scrutinized. By restricting detections spatially and temporally where appropriate, we can maximize the reliability of the results. The following restrictions were applied to our detector results:

1. If a species was automatically detected at a location, but was never manually validated, all automated detections were considered false and the species was considered absent.
2. If a species was automatically detected over a specific timeframe, but manual validation revealed all detections to be falsely triggered by another sound source or species, all automated detections during that period were excluded. Any time frame restrictions employed are described in the results section.

In phase 2, the performance of the detectors was calculated based on the phase 1 restrictions and optimized for each species using a threshold, defined as the number of detections per file at and above which detections of species were considered valid.

To determine the performance of each detector and any necessary thresholds, the automated and validated results (excluding files where an analyst indicated uncertainty in species occurrence) were fed to a maximum likelihood estimation algorithm that maximizes the probability of detection and minimizes the number of false alarms using the MCC:

$$MCC = \frac{TP \times TN - FP \times FN}{\sqrt{(TP + FP)(TP + FN)(TN + FP)(TN + FN)}}$$

$$P = \frac{TP}{TP + FP}; R = \frac{TP}{TP + FN}$$

where TP (true positive) is the number of correctly detected files, FP (false positive) is the number of files that are false detections, and FN (false negatives) is the number of files with missed detections.

Where the number of validated files was too low, and/or the overlap between manual and automated detections was too limited for the calculation of P , R , and MCC , automated detections were ignored, and only validated results were used to describe the acoustic occurrence of a species